Study of the Effects of Ageing and Steam Oxidation on Sintered Iron Alloys and Steels Containing Phosphorus

ABSTRACT

A THESIS SUBMITTED FOR THE DEGREE OF

Doctor of Philosophy

IN

CHEMISTRY

NADEEM AHMAD SIDDIQI

M. Sc., M. Phil (Alig.)

DEPARTMENT OF CHEMISTRY
ALIGARH MUSLIM UNIVERSITY
ALIGARH (INDIA)

August 1986

ABSTRACT

Sintered iron and steel components are frequently subjected to post-sintering treatments like steam oxidation with a view to seal at least the surface pores and make it wear and corrosion resistant due to a thin, tenaceous and adherent bluish oxide layer. There is no reported work in the literature on the effects of alloying elements except Cu on steam treatment of sintered iron and steel. The main objective of the present work is to study the influence of various alloying elements on the steam oxidation behaviour of iron and steels containing various percentages of phosphorus. Further, some of the alloying elements e.g. copper, phosphorus and molybdenum are capable of causing appreciable age-hardening in ferrite. Fortunately, the age-hardening temperature required due to the presence of the above alloying elements is around the steam oxidation temperature of sintered iron and steels. Thus, the twin function of age-hardening and steam oxidation is possible in a single operation improving hardness and wear resistance of sintered ferrous components. Further, phosphorus, because of liquid phase sintering and ferrite stabilization spheroidizes the pores and reduces the amount of interconnected porosity yielding Fe-P sintered compacts at a

density of more than 7.2 Mg m^{-3}, a potential alloy for making gas tight components. Thus, the present work is a systematic investigation of effect of alloying elements on steam oxidation of P-containing iron. The premixes which have been studied in this investigation are as follows :

PNC30 -1 to 4 % Cu or 1 to 4 % MCM

PNC45 - 1 to 4 % Cu or 1 to 4 % MCM

PNC60 - 1 to 4 % Cu or 1 to 4 % MCM

Fe-P (0 to 0.6 wt. %)

PNC30-Mo (1-4 wt. %)

PNC60-MO (1-4 wt. %)

PNC60-Ni (2 and 4 wt.%) - Cu (1 and 4 wt. %)

PNC45-Mo (1 and 2 wt. %) - Cu (1 and 4 wt. %)

PNC60-Mo (2 and 4 wt. %) - Cu (1 and 4 wt. %)

PNC60-MCM (2 and 4 wt. %) - Cu (1 and 4 wt.%)

Fe-P (0.3 and 0.8 %)

PASC30-0.3 and 0.6 % C - 1 and 2 % Cu

PASC30-0.3 and 0.6 % C - 1 and 2 % Ni

PASC30-0.3 and 0.6 % C - 1 and 2 % Mo

PASC30-0.3 and 0.6 % C - 1 and 2 % MCM

PASC30-0.3 and 0.6 % C - 1 and 2 % MVM

PASC80-0.3 and 0.6 % C - 1 and 2 % Cu

PASC80-0.3 and 0.6 % C - 1 and 2 % Ni

PASC80-0.3 and 0.6 % C - 1 and 2 % Mo

PASC80-0.3 and 0.6 % C - 1 and 2 % MCM

PASC80-0.3 and 0.6 % C - 1 and 2 % MVM

PNC is phosphorus-containing iron based on normal compressibility sponge iron powder grade NC100.24 while PASC is P-containing iron based on super compressibility atomized iron grade ASC100.29. Content of P is expressed in hundredth of percentage e.g. PNC30 means containing 0.3 % P and so on.

Various premixes were made by mannual mixing for 1 hour using small amount of acetone as medium. No lubricant was added during mixing. In case of PNC based powder premixes, green compacts were made in a single action compression machine at a pressure of 600 MPa while those based on PASC powders, MPIF (Metal Powder Industries Federation) standard tensile test bars were made at 691 MPa pressure. Green dimensions and weight of all specimens were measured and green density was calculated.

Green compacts made from NC100.24 and PNC based powders were sintered at 1120°C for 30 minutes in hydrogen atmosphere (dew point 233 K) in the Globar tubular furnace.

MPIF test pieces made from PASC based powders were sintered in Pusher type industrial furnace at 1120°C for 30 minutes in cracked ammonia atmosphere (dew point 240 K).

Sintered density, densification parameter, lateral and axial linear dimensional change percentages, sintered hardness were determined and tensile testing was carried out. Scanning electron fractography of surfaces of fractured tensile test pieces was determined.

For PNC based sintered powder compacts, steam treatment was carried out at 500°C for times varying between 5 and 120 minutes. For PASC powder compacts, steam treatment was carried out at 450, 500, 527, 550 and 600°C, for times varying between 45 to 120 minutes.

After steam treatment, samples were weighed and dimensions were measured. Weight gain per unit area of oxidized surface was determined. Weight gain and hardness versus treatment times for different composition of the alloys are plotted. Metallographic studies of oxidized plus non-oxidized layers were carried out. Scanning electron picture

at the transition region between scale and matrix was taken. X-ray diffraction studies of the steam oxidized samples were carried out.

In case of PNC-Cu sintered compacts weight gain and hardness increased with increase in steam oxidation time upto 30 minutes after which it remained constant. With increasing copper content oxidation resistance was less. Phosphorus increased the oxidation resistance and acted as a barrier for diffusion of oxygen by reducing the amount of interconnected porosity and spheroidizing the pores due to liquid and the α-phase sintering. Increase in hardness was attributed to combined action of magnetite formation and precipitation hardening.

In case of PNC-MCM sintered compact, weight gain increased with increasing steam oxidation period upto 60 minutes while hardness increased with increased treatment time upto 90 minutes after which it either remained constant or marginally increased. Increasing MCM content increased porosity making the alloy less oxidation resistant. Phosphorus again reduced the amount of interconnected porosity at the sintering stage and decreased oxidation. The improvement in hardness was considered to be due to oxidation of iron and other easily oxidizable alloying elements.

In case of PNC-Ni/Mo/MCM-Cu, sintered compacts, increase in hardness and weight gain upon steam oxidation was generally similar to those observed in case of PNC-Cu system. However, weight gain increased in the order Mo → Ni → MCM system while hardness in the order Ni → Mo → MCM. This was attributed to higher hardness due to oxides of alloying elements in MCM and more precipitation hardening effect in case of Mo- containing compacts. Microhardness values showed that increase in hardness was mainly due to effect of oxidation but marginally due to age-hardening effect of Cu, Mo and P. X-ray diffraction studies showed that major constituents in oxide were Fe_3O_4 and P, Mo or Cu did not oxidize at the temperature of 500°C for times of oxidation used.

Sintering of PASC-C-X (where X stands for 1-2 % Cu, Ni, Mo, MCM or MVM) compacts sintered under dissociated ammonia at 1120°C for 30 minutes shows that addition or increase in P- content generally, improved densification and mechanical properties of sintered test pieces. However, presence of carbon changed the role of alloying elements on sintered properties of PASC premixes. For example C in PASC-Cu premixes decreased growth while in PASC-Ni premixes decreased shrinkage upon sintering which was attributed to

effect of C in affecting solubility and dihedral angle.

Improvement in tensile properties of Cu- containing compacts was better than those of others. Other alloying elements were found to be of almost equal value in affecting mechanical properties of PASC based sintered steels. Higher amount of phosphorus was more effective in enhancing ultimate tensile and yield strengths and ductility of MCM,MVM, and Ni- containing sintered test pieces than those of the remaining two systems which was explained on the basis of effectiveness of liquid phase sintering in such systems.

In general, shrinkage or growth of the specimens was anisotropic but reasonably low and it was possible to achieve a UTS, YS and El % values of 330-650 MPa, 200-450 MPa and 3 to 12 % respectively depending upon the alloy systems and specific composition.

Improvement in strength properties are due to solid solution hardening effect, formation of pearlitic phase due to C and modification of pore morphology due to α- and liquid phase sintering.

In case of sintered PASC-C-X compacts, gain in weight upon steam oxidation was generally lower which was reasoned to be partly due to higher sintered density due to higher

compaction pressure and also due to higher compressibility of atomized powders, but mainly due to smoother and regular morphology of atomized powders which persisted in sintered structures. Gain in hardness after steam treatment of PASC- based sintered compact was generally higher which was attributed to larger contribution due to precipitation hardening effect and/or transformation products because of larger amount of elements retained in solid solution due to faster rate of cooling employed in industrial furnaces.

Increase in oxidation period generally increased hardness and weight gain upto generally 45-60 minutes which was dependent upon alloy systems and its specific composition and steam treatment temperature.

Out of the various alloy systems used for steam oxidation in the PASC- based systems, weight gain was Mo → Ni → Cu → MVM → MCM systems in increasing order. Hardness benefit was Ni → Cu → Mo → MVM → MCM in the increasing order. Sharpness and definition of oxide decreased in the order Mo → Cu → Ni → MCM → MVM. The optimum steam oxidation temperature in respect of hardness benefit, sharpness and definition of oxide layer, appears to be generally 527°C with occasional variation to 500 or 550°C. Generally,

saturation time required from consideration of weight gain and maximum hardness achieved, decreased with increase in steam oxidation temperature. Kinetic curves for all systems studied were parabolic in nature and was attributed to be mainly due to dense and non-porous magnetite as the main constituent in oxide. Precipitation hardening was found to be effective mainly in case of Mo- and Cu-containing compacts and this phenomena appeared to increase with increase in temperature. This was explained as retention of these elements into solid solution and probable consequent precipitation as hard phases at the temperature of steam treatment used. The higher hardness of MCM and MVM containing compacts was attributed to transformation hardening and hard oxides of alloying elements. The slightly lower hardness of MVM-containing compacts as compared to MCM- containing compacts was probably due to loss of vanadium forming oxides.

Carbon was generally found to be ineffective in forming oxides and giving any contribution to hardness upon steam treatment. However, in case of MCM- and MVM-containing compacts, higher carbon content generally increased steam treated hardness which was attributed to contribution due to transformation products.

It is concluded that it is possible to seal the surface pores of PASC-C-X sintered compacts by steam oxidation at a temperature of 450-600°C for short time of 45 to 60 minutes and the optimum results being obtained at around 527 ± 25°C.

Study of the Effects of Ageing and Steam Oxidation on Sintered Iron Alloys and Steels Containing Phosphorus

A THESIS SUBMITTED FOR THE DEGREE OF

Doctor of Philosophy

NADEEM AHMAD SIDDIQI

M. Sc., M. Phil (Alig.)

DEPARTMENT OF CHEMISTRY

ALIGARH MUSLIM UNIVERSITY

ALIGARH (INDIA)

August 1986

DEDICATED TO THE MEMORY

OF MY GRAND FATHER

Md. Hamiuddin
B.Sc. Engg.(Met.), M. Tec.(Mat. Sc.),
Ph.D.(Met. Engg), MIIM, MPMAI.
Member, APMI.

READER

PHONE : 5399
DEPARTMENT OF MECHANICAL ENGG.
Z. H. COLLEGE OF ENGG. & TECH.
ALIGARH MUSLIM UNIVERSITY
ALIGARH-202001, INDIA

Date August, 1986

This is to certify that this work, "**STUDY OF THE EFFECTS OF AGEING AND STEAM OXIDATION ON SINTERED IRON ALLOYS AND STEELS CONTAINING PHOSPHORUS**" has been carried out by Mr. **Nadeem Ahmad Siddiqi** under my supervision and is an original piece of research. It has not been submitted elsewhere for a degree.

Md. Hamiuddin

(Md. Hamiuddin)

ACKNOWLEDGEMENTS

I have no words to express my gratitude to my guide Dr. Md. Hamiuddin, Reader, Department of Mechanical Engineering, Z.H. College of Engineering and Technology, Aligarh Muslim University, Aligarh, without whose invaluable suggestions able guidance and lively discussions this work would not have emerged in its present form.

I shall be failing in my duty if I do not acknowledge my gratefulness to Professor A.U. Malik, Chairman, Chemistry Section, Z.H. College of Engg. and Tech., A.M.U., Aligarh who motivate me to do research in the field of Powder Metallurgy under Dr. Hamiuddin and provided all the necessary facilities.

I am thankful to Prof.(Dr.) S.R. Khan, Chairman, Department of Mechanical Engineering, Z.H. College of Engg. and Tech., A.M.U. Aligarh for providing laboratory facilities.

Grateful acknowledgements are due to M/S Höganas, AB, Sweden, Mahindra Sintered Products, Pune, INCO Europe Ltd., London, U.K., Sinter metallwerk, Krebsöge, W.G. for the supply of various powders and for some of the sintering facilities provided. Thanks are also due to Advance Centre

of Materials Science, I.I.T. Kanpur, National Botanical Research Institute, Lucknow and Regional Sophisticated Instrumentation Centre, Bose Institute, Calcutta for carrying out Scanning Electron Microscopy and other studies.

I would like to thank my research colleagues M/S Mohd. Arif Siddiqui and Abdul Jabbar Khan, friends especially S. Aslam Shaheer and Farhat N. Siddiqui, room mates Imran Ahmad and M. Ishraq and well wishers for their cooperation and encouragement.

My thanks are also due to Mr. Masood Alam for typing the manuscript. The financial assistance from Council of Scientific and Industrial Research, New Delhi is gratefully acknowledged.

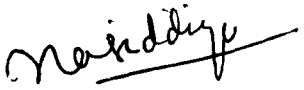

(Nadeem Ahmad Siddiqi)

C O N T E N T S

Page

. . . .

LIST OF TABLES

CHAPTER 1

REVIEW OF LITERATURE

1.1 INTRODUCTION

Steam oxidation as a surface finishing technique has been in use for many years to improve the appearance of small mechanical components produced from steel or cast iron and to improve their resistance to wear and corrosion. Examples of components which are steam treated are gears, cams, chains, pinions, compressor parts, bearings, pulleys, sprockets etc. Typically, all exterior surfaces react to form a very thin skin (2.5 to 5 μm) of oxide.

These days, there is considerable interest in Powder Metallurgy (PM) as a manufacturing technique for fabrication of small structural components. The technology has shown the highest rate of growth during the last three decades, i.e. 6-7 % on an average in the world. This is mainly due to (i) saving in material and machining cost, (ii) high productivity method yielding products exactly or very close to final dimensions requiring very little or no machining afterwards, (iii) simple and automated method of manufacture and (iv) its being energetically favourable process.

However, conventional PM products are less hard and strong as compared to their wrought or cast counterparts having identical chemistry. This is due to inherent porosity (10-25 %) present in them which may be isolated or interconnected. The interconnected porosity in PM parts may constitute upto 97 % of the pores or voids in the part. Thus, PM parts require some type of treatment to seal, at least the surface pores particularly for corrosion resistance. Various methods of closing the pores are as follow :

1.1.1 Alloy infiltration

In this method, a low melting alloy slug is placed on the part which is then put through the sintering furnace at a temperature which is above the melting point of the alloy. The molten alloy then wicks through the part, effectively sealing off the porosity. This process greatly increases the strength of the part and improves machinability.

1.1.2 Wax impregnation

This is a less common method of sealing, primarily because it is difficult to get rid of surplus wax on the surface and because use of the part at elevated temperatures can cause the wax to melt.

1.1.3 Plastic impregnation

This is presently the most prevalent method used for sealing PM parts. It is usually applied under vacuum and uses relatively fast curing resins. Unless there are unusual cracks or very large voids in the part, resin impregnation will seal against high pressure of hydrogen as well as hydraulic pressure.

1.1.4 Steam treatment

This is possibly the least expensive method of sealing pores. When sintered ferrous components are exposed to steam at elevated temperature, a layer of oxide upto 5 μm thick forms on all exterior surfaces and also within the interconnected pore net work to an extent which is dependent on the steam treatment conditions (1). Following advantages have been claimed for steam treatment of sintered ferrous parts :

(i) Magnetic iron oxide formed improves wear resistance of the surface to abrasive wear during service. The oxide formed within the pore network provides wear resistance (2,3) after surface layer is wornout.

(ii) The oxide layer formed is extremely adherent (4,5)

and is less prone to defects such as cracks and blisters than oxide coating formed in air.

(iii) Compressive strength of the part increases (3).

(iv) The oxide layer becomes impermeable at thickness of about 5 μm (6) and resistance to rusting of treated component is improved. The danger of local corrosion cells being created within pores is reduced.

(v) In case of high density sintered parts, surface pores can be completely closed. Impregnation and consequent entrapment of electrolyte during subsequent electroplating operations is prevented but conductivity remains sufficiently high for direct plating to be carried out. When surface pores are completely closed the parts can withstand high gas pressures (7).

(vi) The small dimensional increase (about 10 μm), after treatment does not create problems (4).

(vii) The treatment is economic (8) and it has been claimed that the cost of pore sealing by steam treatment is about 15 % of that arising during infiltration with copper and about 30 % of that

incurred during plastic impregnation (5).

(viii) The blue-black colour developed during treatment is pleasant in appearance especially after subsequent oil dipping.

Additional reported works (9-20) on the effects of steam oxidation on porosity andproperties of sintered iron also claim one or more of the above benefits.

1.2 STEAM TREATMENT OF Fe-Cu SINTERED ALLOYS

Effect of copper on steam treatment of sintered iron has also been studied quite extensively (17, 21-31).

Sunter and Cosh (17) after studying steam treatment of sintered iron and iron 1.1 wt % Cu alloy found that corrosion rates were considerably reduced. They have claimed superior surface finish and corrosion resistance to that of a similarly shaped wrought and machined part.

Hammer and Vannerberg (21) found that small additions of copper had little effect on the oxidation of solid iron at 500°C in oxygen or oxygen-argon atmosphere.

Phadke and Davies (25) carried out ageing treatment at 500°C in nitrogen or vacuum of Fe-2 to 6 wt. % Cu powder compacts sintered at 1150°C for 1 hr. and found

significant increase in hardness of quenched as well as furnace cooled (25°C/min) specimens after precipitation hardening treatment. Massive martensite was found in some regions of 4 and 6 wt % Cu alloy after water quenching but it was absent from the 2 wt % Cu alloy. Solution treated peak hardness values increased with copper percentages. However, the 2 wt. % Cu alloy showed maximum percentage increase in hardness although the magnitude of hardness increase over the solution treated values was nearly the same in the three alloys.

The above observations led to the authors (26) to prepare Fe-2 % Cu compact from elemental powders and sinter for 1 hr. at 1150°C and cool at an average rate of 75°C/min in an industrial sintering furnace. The resulting alloy was aged at 500°C in an inert atmosphere and also in steam. The hardness increase during ageing in an inert atmosphere was about 22 %. However, ageing in steam resulted in an additional gain in hardness due to simultaneous precipitation of copper and also formation of Fe_3O_4 by void filling. The hardness values obtained during ageing in steam were compared with the values calculated from data obtained on steam oxidized pure iron compacts and results of ageing in inert atmosphere. The

result showed that degree of hardness increase due to steam oxidation was found to be nearly the same in pure iron and in the Fe-Cu alloy studied. This preliminary study appeared attractive from the point of eliminating separate solution and ageing treatments in Fe-Cu sintered alloys. Later on Phadke (27) carried out ageing of iron-copper compacts containing 2,4,6 and 8 wt % Cu at 500°C and observed that hardness increased after furnace cooling but the response to subsequent ageing decreased as the copper content increased. The magnitude of increase in peak hardness was detected in Fe-8 Cu alloy. The size of the precipitates which could be resolved at a magnification of 20000 X was above about 25 nm in all the alloys. Similar results were found in a further study (28) by simultaneous ageing and steam oxidation. The results indicate that the oxidation rate decreases with copper addition.

The response to simultaneous ageing and steam oxidation decreases with increasing copper content. For maximum benefit, it is necessary that maximum mass gain due to formation of Fe_3O_4 should occur before or concurrently with peak hardness due to precipitation of copper. This condition was fulfilled only in the case of Fe-2 % Cu alloy.

Razavizadeh and Davies (29) selected sponge and atomized - two types of iron powders and after compaction to densities of 6.0, 6.4 and 6.8 Mg/m^3 and after sintering under standard conditions subjected sintered compacts to steam oxidation at 450, 525 and 600°C. Kinetics of oxidation were always faster for sponge iron than for atomized iron and there was a corresponding increase in the rate of pore closure and in surface hardness. It was concluded that for effective sealing of surface pores components should be of high density and be steam treated at 600°C but for attainment of maximum hardness components should be of high density and be steam treated at 525°C. After certain time, dependent on initial density and steam treatment temperature, surface pores became sealed and steam could no longer permeate through the internal pore net-work. Open porosity decreased to an apparently low level.

Razavizadeh and Davies (29), have summarized the previous work on theoretical and kinetic aspects of steam oxidation. It has been shown (6) that Fe_3O_4 is the only oxide formed when the ratio P_{H_2O} / P_{H_2} lies between 0.1 and 1 when the temperature of reaction falls between 400-600°C. At low temperatures, (25°C), the only product formed when iron reacts with water vapour free from oxygen

is $Fe(OH)_2$. However, if air is present, some Fe_3O_4 also forms (32). At temperatures above 60°C Fe_3O_4 is formed. FeO does not form at temperatures less than 570°C but within the range 570-700°C both FeO and Fe_3O_4 form and the proportion of FeO produced increases with temperature. The phase diagram for the Fe/O_2 system shows that at 570°C, FeO decomposes eutectoidally to α-Fe and Fe_3O_4.

The initial rate of steam oxidation, as measured by weight gain, is very rapid and more than 50 % of the total weight gain occurs within 10 min. (30 and 32). The reaction rate decreases markedly after about 1 hr. Franklin and Davies (1) examined the influence of treatment at 520 and 650°C and demonstrated that at 650°C very rapid oxidation occured, but because of surface sealing, a lower total oxide content is achieved after long treatment times than is normal at the lower temperature. It was suggested that treatment at the higher temperature might be appropriate as a preliminary to electroplating. In a further study (30) of Fe-2 to 8 wt % in alloy compacted to a density of 6.8 Mg/m^3 and sintered for 1 hr. at 1120°C and steam treated at 525°C, it was observed that wear resistance of sintered iron were improved by steam treatment and by addition of copper in amounts upto 8 wt %. However, steam treatment of sintered Fe-Cu alloys has

adverse effects on wear resistance. An increase in hardness was associated with an increase in wear resistance. They (30) used atomized iron powders grade ASC with admixed copper as well as pre-alloyed iron powder which were compacted to 6.8 Mg/m^3 density and sintered at 1120°C for 1 hr. in dissociated ammonia atmosphere and half of the specimens were steam treated at 525°C for 100 minutes. By X-ray examination of Fe-2 to 8 wt. % Cu powder compacts sintered at 1120°C for 1 hr. at 6.4 to 6.8 Mg/m^3 and steam treated at 525°C, it was confirmed (31) that the principal product formed during steam treatment was Fe_3O_4 and that copper was not oxidized by steam. It has been concluded (33) that, precipitation treatment in a steam atmosphere, as opposed to in an inert atmosphere, increases the hardness of the sintered Fe-2Cu alloy.

In alloys containing more than 2 % Cu, precipitation treatment in an inert atmosphere promotes greater hardening than that in a steam atmosphere.

Steam treatment increases the radial crushing stress (RCS) of sintered iron but decreases the RCS of all iron copper alloys.

In a recent work (33) effects of steam treatment and time were studied on the air tightness and oxide formation

characteristics of sintered Fe-0.5 % graphite steels of different densities. Results showed that surface oxidation rate increased above treatment temperature of 600°C and that there was a maximum in the total amount of oxide produced at temperature between 500 and 550°C. The amount of total oxide decreased with an increase in density of the specimen. Metallographic observations showed that different oxide layers predominated over the range of steam treatment temperature used. The effects of the different oxide formation on air tightness were discussed. It was shown that the air tightness of the steam treated steels was closely related to the total amount of oxide produced, regardless of specimen density.

Steam oxidation in a fluidized bed (34) were studied for Fe- based PM parts containing 1.1 % carbon, 2.7 % Cu, 0.32 % Mn, 0.09 % Si, 0.01 % P, 0.001 % S, 0.08 % Nitrogen, 0.025 % Al, 0.015 % Mg, oxidized in fluidized bed of 120 μm white corrundum floated with saturated steam at 2000 mm Hg and 550-600°C. The use of this method significantly increased the oxidation rate and results in strength and corrosion characteristics exceeding those obtained by conventional oxidation techniques. In fluidized bed oxidation micro-voids characteristics of PM products become completely sealed by dense oxide layer.

In a recent study (35), thermochemical equilibria that governs the oxidation of Fe in steam are examined, with particular reference to the treatment of sintered steel parts, in which open or interconnected porosity plays a role. The parameters required to regulate the amount of steam in accordance with the surface to be oxidized and the characteristics of furnace are shown in simple graphic form. The range of operating temperature is defined by the properties of water and the equilibrium diagram of Fe-O. The thermal balance resulting from the dissociation of H_2O and the formation of Fe_3O_4 is calculated and the possible influence of these phenomena on control of the furnace temperature is taken into consideration. The formation of very hard layers on the surface of porous parts communicating with the external atmosphere induces a considerable increase in apparent surface hardness. If the evaluation is not hampered by microstructural transformation, it is possible to establish a relation between increase in weight and increase in hardness (HV-30 scale) which is consistent with the experimental results. Since steam treatment of sintered steel parts is often used to make them impermeable, a method of calculation suitable for estimating the changes in porosity and permeability in treated material is shown. This

method can be applied as a theoretical basis for an easily used experimental methodology.

The oxidation kinetic study of iron was carried out (36) at 773 K under the total pressure of 10^5 Pa with the precise control of oxygen partial pressure from log (P_{O_2} / Pa) = -0.7 to 5.0. The kinetics nearly obeyed the parabolic rate law except between log (P_{O_2} / Pa) = 0.0 and 0.5. The oxidation kinetics at 773 K were studied by many investigators (32, 37-41) only in air or oxygen atmosphere and most of their results fairly agreed with the results of Sakai et al (36) in air and oxygen. However, Hussey et al (42, 43) who only studied on the oxidation under reduced pressures at 773 K, indicated that the oxidation kinetics did not obey the simple rate law in the range from log (P_{O_2} / Pa) = -1.88 to 5.0. The enhanced blistering of the oxide film under the reduced pressure may be one of the main reasons for the disagreement between their results and Sakai et al (36).

Below log (P_{O_2} /Pa) = 0.0 the oxidation provided was parabolic mainly by the growth of magnetite.

The deviation from the parabolic rate law was related to the decrease of the oxidation rate with increasing oxygen partial pressure in the range log (P_{O_2} / Pa) = 0.0

to 0.5. This may be explained by the formation of dense hematite on the surface of magnetite which occurred more quickly at higher oxygen partial pressures. The similar tendency was also reported by Hussey et al (42, 43) at a little lower oxygen partial pressures.

The oxidation rate increased with increasing oxygen partial pressure from log (P_{O_2} / Pa) = 0.5 to 1.8 due to the formation of crack in the oxide film which allowed the growth of magnetite.

Above log (P_{O_2} / Pa) = 1.8, the parabolic rate constants were almost constant independent of the oxygen partial pressure, although the increase of the oxidation rate with increasing oxygen partial pressure in this range was reported previously (14,19), which may be explained by the effect of blistering introduced by the use of the reduced pressure technique.

1.3 SCOPE OF THE PRESENT WORK

The existing literature contains little reference to the influence of alloying additions (except copper) on the response of sintered ferrous alloys to steam oxidation and this was the principal subject of the present investigation. Further, some of the alloying elements, e.g.

phosphorus and molybdenum are capable of causing appreciable age-hardening in ferrite (44). Hörnbogen (45) showed that phosphorus could produce appreciable age-hardening in Fe-P alloys containing 0.15 % C and 1.5 % Mn. Age-hardening occurred in temperature range 400-550°C, but the maximum effect was observed at 450°C. The intensity of age-hardening increased with increasing phosphorus content. At phosphorus content above 0.5 wt. % , increasing amount of ferrite were observed at the solution treatment temperature with increasing phosphorus contents. At 2 % P, the steel was virtually ferrite at room temperature. The precipitating phase was Fe_3P but the details of age-hardening process have not been investigated. Also, phosphorus because of liquid phase sintering and ferrite stabilization, spheroidizes the pores and reduces the amount of interconnected porosity (46) yielding Fe-P sintered compacts at a density of more than 7.2 Mg/m^3 a potential alloy for making gas tight components.

The most commonly used alloying additions in sintered ferrous alloys are Cu, Ni and/or Mo in the decreasing order due to their low affinity to oxygen and/or cost.

The difficulty of adding high hardenability but easily oxidizable alloying elements, Mn, Cr and V have been

overcome (47,48) by adding these elements in the form of master alloy carbides MCM and MVM (containing approximately 20-23 % each of Mn, Cr or V, Mo, 6-7 % C and balance Fe). These additions result into better mechanical properties and make sintered steels amenable to transformation hardening after addition of carbon. Apart from this, literature contains little reference regarding the effect of Ni, and Mo on the sintering behaviour of iron with or without phosphorus (32,46,49-54).

Thus the present work is a preliminary but systematic investigation of the effect of alloying elements Cu, Ni, Mo, MCM and MVM - 1 or 2 wt. % with 0.3 and 0.6 wt. % C on the steam treatment of P-containing atomized iron powders. Mechanical properties of sintered compacts of Atomized iron powders have also been determined since with the exception of copper mechanical properties of Ni, Mo and MCM containing iron compacts with phosphorus and carbon are hardly reported in literature (50-54).

Apart from this effect of 1-4 wt. % Cu or MCM on steam oxidation of sintered sponge iron powder containing 0 to 0.6 wt. % P sintered compacts have been studied. Other premixes which have been used for the present investigation are as follows :

Fe-P (0 to 0.6 wt. %)

Fe-0.3P-Mo (1-4 wt. %)

Fe-0.6P-Mo (1-4 wt. %)

Fe-0.6P-Ni (2 and 4 wt. %) - Cu (1 and 4 wt. %)

Fe-0.45P-Mo (1 and 2 wt. %) - Cu (1 and 4 wt. %)

Fe-0.6P-Mo (2 and 4 wt. %) - Cu (1 and 4 wt. %)

Fe-0.6P-MCM (2 and 4 wt. %) - Cu (1 and 4 wt. %)

The above premixes have been selected to show the effect of phosphorus alone and also the effect of quantity, nature and distribution of pores on the steam treatment behaviour. Apart from this, influence of ternary alloying elements on steam treatment behaviour of sintered ferrous alloys can be evaluated with the above premixes.

CHAPTER 2

EXPERIMENTAL

2.1 PROCEDURE

Following raw materials were used for the present investigation.

2.1.1 Iron powder

High compressibility sponge iron powder, grade NC 100.24, obtained from Höganäs AB, Sweden, was selected as base material. Characteristics of this powder are :

Carbon content	0.01 %
SiO_2	0.22 %
H_2 loss	0.20 %
Apparent density	2.4 Mg/m^3
Flow rate (Hall flow meter)	31 secs/50 gms.
Compressibility	6.4 Mg/m^3 at 420 MPa
Particle size	+100 mesh ... 0.5 % approx.
	-325 mesh ... 21.5 % approx.

2.1.2 *P-containing sponge iron powder*

PNC30, PNC45 and PNC60 supplied by Höganäs AB,

Sweden were used for 0.3, 0.45 and 0.6 pct, P-containing iron powder, respectively. These powders are based on NC100.24 with admixed ferrophosphorus (Fe_3P) containing 15.6 % phosphorus. Characteristics of these powders are :

Carbon content	0.01 %
SiO_2	0.16 %
H_2 loss	0.20 %
Apparent density	2.6 Mg/m^3
Flow rate (Hall flow meter)	31 secs/50 gms.
Compressibility	6.4 Mg/m^3 at 420 MPa
Particle size	+100 mesh ... 1 % maximum
	-325 mesh ... 20 %

2.1.3 P-containing atomized iron powder

PASC30 and PASC80 powders obtained from Höganäs AB, Sweden were used for 0.3 and 0.8 % P-containing iron respectively. These powders are based on very pure and super compressibility iron powder grade ASC100.29. Characteristics of these powders are :

Carbon content	0.01 %
H_2 loss	0.1 %
Apparent density	3.0 Mg/m^3

Flow rate	27 secs/50 gms.
(Hall flow meter)	
Compressibility	6.70 Mg/m^3 at 420 MPa
	and 7.00 Mg/m^3 at 600 MPa
Particle size	+65 mesh 0 %
	+100 mesh ... 10 % maximum
	-325 mesh ... 20 %

2.1.4 Copper powder

Copper powder used was reduced one and obtained from M/S Mahindra Sintered Products, Pune, Characteristics of this powder are :

Copper content	99.5 %
H_2 loss	0.11 %
Apparent density	2.25 Mg/m^3
Flow rate	26 secs/50 gms.
(Hall flow meter)	
Particle size	+100 mesh 1.0 %
	+150 mesh 25.7 %
	+200 mesh 14.9 %
	+250 mesh 19.4 %
	+325 mesh 2.4 %
	-325 mesh 36.5 %

2.1.5 MCM and MVM powder

MCM and MVM are transition metal carbide master alloys. MCM contains manganese, chromium and molybdenum while MVM contains Vanadium instead of chromium and carbon and iron as balance. These powders of average particle size 5 μm FSSS were obtained from Sinter metallwerk, GmbH, Krebsöge, W.G. and have the following composition:

	% Mn	Cr	V	Mo	Cu	C	Si
MCM	20	20	-	20	0.22	7	0.35
MVM	20	-	20	20	0.22	5	0.40

2.1.6 Molybdenum powder

Molybdenum powder used was obtained from metallwerk, Plansee, Austria of particle size 4-6 μm which was measured on Fischer subsieve sizer.

2.1.7 Nickel powder

Nickel powder used was type 255, obtained from INCO Europe Ltd., London, U.K., the characteristics of this powder are as follows :

Chemical composition

Ni	Balance

C	0.2 %
Fe	0.005 %
Co	0.0003 %
N	0.0002 %
O	0.07 %
S	0.0002 %

Other trace elements < 0.001 %

Apparent density measured by Scott-Volumeter - 0.50-0.65 Mg/m^3.

Typical specific surface area m^2/g - 0.7

Average particle size µm = 2.2-2.8 FSSS

2.1.8 Graphite

Graphite powder grade UF_4 of average particle size 4 µm FSSS was obtained from Sintermetallwerk, Krebsöge, W.G.

2.2 PREMIX PREPARATION

In sponge iron powder, phosphorus content was varied as 0, 0.30, 0.45 and 0.6 wt. %. Alloying additions, Cu and MCM were varied at an interval of 1 wt. % and upto 4 wt. %. In case of ternary premixes, i.e. PNC60-Ni-Cu, PNC45-Mo-Cu or PNC60-Mo-Cu and PNC60-MCM-Cu, copper content was 1 and 4 wt. %.

In case of super compressibility atomized iron powder, the phosphorus content was varied as 0, 0.30 and 0.8 wt. % with 0.3 or 0.6 % carbon (Actually, the graphite addition for C was 0.5 and 1.0 % to compensate for loss during sintering which was evaluated after preliminary experiments), and 1 or 2 % each of Cu, Ni, Mo, MCM or MVM. Various premixes were prepared by mannual mixing for 1 hour using acetone as medium. No lubricant was added during mixing.

2.3 COMPACTION

Green compacts of the dimension 5 mm x 5 mm x 20 mm were made in a single action compression machine at a pressure of 600 MPa. The die made of special K steel, cleaned with acetone, lubricated with zinc stearate and filled with powder premix, was subjected to the required load at an approximate rate of loading of 1000 kg/minute. MPIF (Metal Powders Industries Federation) standard tensile test bars, the details of which are given in Fig. 2.1 and having a thickness of approximately 5.7 mm were made on Bussmann Demag hydraulic press of 200 tons capacity at 691 MPa pressure. The die wall was lubricated with kenulube 11. Green density of the compacts were determined by dimensional measurement and is summarized in table III.3.1.

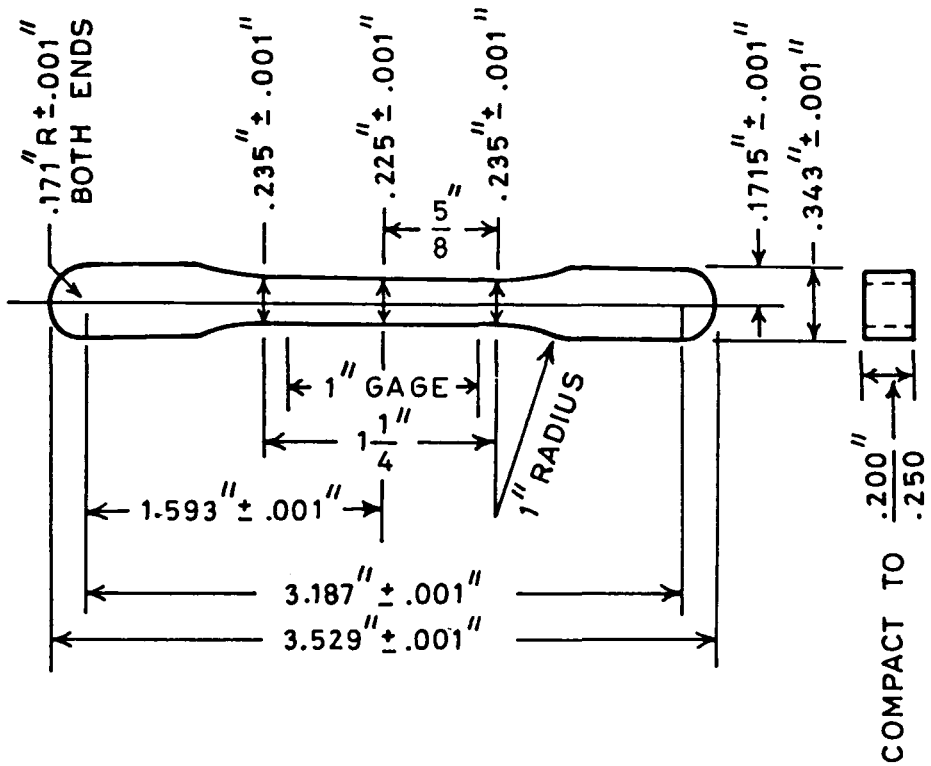

Fig. 2·1 MPIF tensile test piece; green dimension, when in the die.

2.4 SINTERING

2.4.1 Hydrogen atmosphere sintering

Green pellets were sintered in a globar tubular furnace under dry hydrogen atmosphere at 1120°C for 30 min. The furnace tube had ID of 6.26 cms. and capable of attaining a maximum temperature of 1300°C with a control of ± 10°C over a length of 10 cms. at the centre. The temperature profile of the furnace is shown in Fig. 2.2. The rate of heating to sintering temperature was 7 K/min. The rate of cooling from sintering temperature was 13 K/min. in case of Fe-P-Cu compacts while in other, it was 16 K/min.

2.4.2 Dissociated ammonia atmosphere sintering

MPIF tensile test bars made from PASC powders were sintered in pusher type Industrial furnace at 1120°C for 30 minutes in cracked ammonia atmosphere (dew point 240 K) of M/S Mahindra Sintered Products Ltd., Pune.

2.5 SINTERING PARAMETERS

2.5.1 Linear dimensional change

Linear dimensional change of MPIF tensile test bars was calculated by measuring the difference between

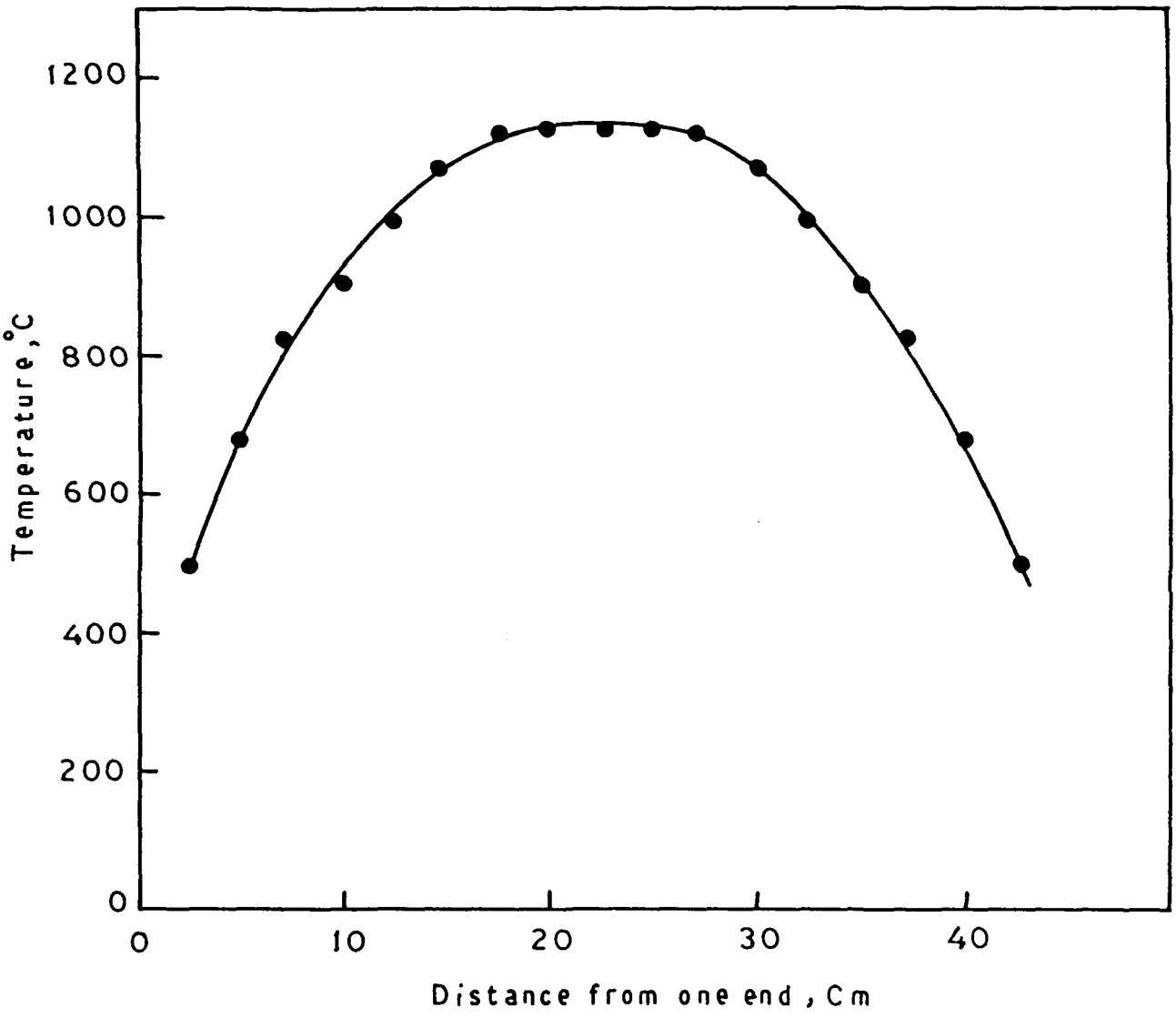

Fig. 2.2 TEMPERATURE PROFILE OF THE SINTERING FURNACE AT 1120 °C

sintered and green length as follows :

$$\text{Pct. Linear dimensional change} = \frac{\text{Sintered length} - \text{Green length}}{\text{Green length}} \times 100$$

In case of cylindrical compacts, radial dimensional change was also determined as above. Shrinkage ratio was calculated whereever it was possible as follows :

$$\text{Shrinkage ratio} = \frac{\text{Radial dimensional change}}{\text{Axial dimensional change}}$$

Volumetric shrinkage or growth was also derived as follows:

$$\frac{\Delta V}{V}\,\% = \frac{V_s - V_g}{V_g}$$

where $\frac{\Delta V}{V}\,\%$ is volumetric change, V_s and V_g are sintered and green volumes respectively.

2.5.2 Sintered density

Sintered density was calculated from the mass of the samples and dimensional measurements of the MPIF tensile test bars immediately after sintering. The mass of the compacts were determined on an electrical balance of capacity 100 gms. The balance had a measurement

accuracy of ±0.0005 gms. Sintered density of few compacts were also measured by Archmedis principle by first dipping in silicone oil to close open porosity and then usual measurement of mass of samples in air and water. The variation in sintered densities between these two methods were not more than 2 %.

2.5.3 Densification parameter

Densification parameter (ΔD) was calculated from the formula :

$$\Delta D = \frac{\text{Sintered density - Green density}}{\text{Theoretical density - Green density}}$$

Theoretical density of iron was taken as 7.86 Mg/m^3. Theoretical density of each composition was calculated from rule of mixture taking the theoretical density of the various elements at room temperature as follows :

Density	Phosphorus	Graphite	Copper	Nickel
Mg/m^3	1.82	2.25	8.92	8.91

Molybdenum	MCM	MVM
10.2	7.4	7.4

Theoretical density of the various premixes for evaluation of sintered properties are shown in table 2.1

Table 2.1 Theoretical density of various premixes used.

Alloy	Theoretical density	Alloy	Theoretical density
Fe	7.86	PNC45-1Cu	7.843
PNC30	7.842	PNC45-2Cu	7.854
PNC45	7.833	PNC45-3Cu	7.865
PNC60	7.824	PNC45-4Cu	7.875
NC-1Cu	7.871	PNC60-1Cu	7.834
NC-2Cu	7.881	PNC60-2Cu	7.845
NC-3Cu	7.892	PNC60-3Cu	7.856
NC-4Cu	7.902	PNC60-4Cu	7.866
PNC30-1Cu	7.852	PNC30-1Mo	7.865
PNC30-2Cu	7.863	PNC30-2Mo	7.889
PNC30-3Cu	7.874	PNC30-3Mo	7.912
PNC30-4Cu	7.889	PNC30-4Mo	7.935

Continued ....

Table 2.1 continued

Alloy	Theoretical density	Alloy	Theoretical density
PNC60-1Mo	7.847	PNC45-1MCM	7.828
PNC60-2Mo	7.870	PNC45-2MCM	7.824
PNC60-3Mo	7.894	PNC45-3MCM	7.819
PNC60-4Mo	7.917	PNC45-4MCM	7.814
NC-1MCM	7.855	PNC60-1MCM	7.827
NC-2MCM	7.851	PNC60-2MCM	7.814
NC-3MCM	7.846	PNC60-3MCM	7.810
NC-4MCM	7.842	PNC60-4MCM	7.805
PNC30-1MCM	7.837	PNC45-1Mo-1Cu	7.867
PNC30-2MCM	7.833	PNC45-1Mo-4Cu	7.897
PNC30-3MCM	7.828	PNC45-2Mo-1Cu	7.890
PNC30-4MCM	7.825	PNC45-2Mo-4Cu	7.922

Continued ....

Table 2.1 continued

Alloy	Theoretical density	Alloy	Theoretical density
PNC60-2Mo-1Cu	7.881	PNC60-4MCM-1Cu	7.816
PNC60-2Mo-4Cu	7.913	PNC60-4MCM-1Cu	7.848
PNC60-4Mo-1Cu	7.928	PNC60-2Ni-1Cu	7.855
PNC60-4Mo-4Cu	7.960	PNC60-2Ni-4Cu	7.887
PNC60-2MCM-1Cu	7.825	PNC60-4Ni-1Cu	7.876
PNC60-2MCM-4Cu	7.857	PNC60-4Ni-4Cu	7.908
PASC30	7.842	PASC80	7.812
PASC30-0.3C-1Cu	7.824	PASC80-0.3C-1Cu	7.794
PASC30-0.3C-2Cu	7.835	PASC80-0.3C-2Cu	7.805
PASC30-0.6C-1Cu	7.953	PASC80-0.6C-1Cu	7.766
PASC30-0.6C-2Cu	7.807	PASC80-0.6C-2Cu	7.777

Continued ....

Table 2.1 continued

Alloy	Theoretical density	Alloy	Theoretical density
PASC30-0.3C-1Ni	7.824	PASC80-0.3C-1Ni	7.794
PASC30-0.3C-2Ni	7.935	PASC80-0.3C-2Ni	7.805
PASC30-0.6C-1Ni	7.953	PASC80-0.6C-1Ni	7.766
PASC30-0.6C-2Ni	7.807	PASC80-0.6C-2Ni	7.777
PASC30-0.3C-1Mo	7.837	PASC80-0.3C-1Mo	7.807
PASC30-0.3C-2Mo	7.861	PASC80-0.3C-2Mo	7.830
PASC30-0.6C-1Mo	7.809	PASC80-0.6C-1Mo	7.779
PASC30-0.6C-2Mo	7.832	PASC80-0.6C-2Mo	7.802
PASC30-0.3C-1MCM	7.809	PASC80-0.3C-1MCM	7.787
PASC30-0.3C-2MCM	7.805	PASC80-0.3C-2MCM	7.774
PASC30-0.6C-1MCM	7.789	PASC80-0.6C-1MCM	7.751
PASC30-0.6C-2MCM	7.776	PASC80-0.6C-2MCM	7.746

Continued ....

Table 2.1 continued

Alloy	Theoretical density	Alloy	Theoretical density
PASC30-0.3C-1MVM	7.809	PASC80-0.3C-1MVM	7.787
PASC30-0.3C-2MVM	7.805	PASC80-0.3C-2MVM	7.774
PASC30-0.6C-1MVM	7.789	PASC80-0.6C-1MVM	7.751
PASC30-0.6C-2MVM	7.776	PASC80-0.6C-2MVM	7.746

2.6 STEAM TREATMENT EXPERIMENTS

After determining sintered density from weight and dimensional measurements and Vickers hardness determination at a load of 5 or 10 kg, 3 mm thick slices were cut and ground with silicon carbide paper of grit size 180 and 320. The slices were cleaned with trichloro ethylene and acetone and weighed on a microbalance having an accuracy of $\pm$ 0.0005 gm. They were then put in a previously weighed silica boat and inserted into Nichrome wound tubular furnace having temperature control of $\pm$ 10°C. Temperature profile of the furnace is shown in Fig. 2.3. Steam is generated in a retort and preheated in a heated copper coil to the approximate treatment temperature. The steam was then passed at atmospheric pressure through the tube furnace and finally vented to the atmosphere. Specimens were introduced into the furnace tube with steam already flowing and with the furnace at the temperature.

Coldest part of furnace charge must be at a temperature greater than 100°C before steam is admitted to the treatment furnace, otherwise hydroxide of iron is formed which subsequently changes to red rust according to the reaction.

$$2Fe(OH)_3 \rightarrow Fe_2O_3 + 3H_2O$$

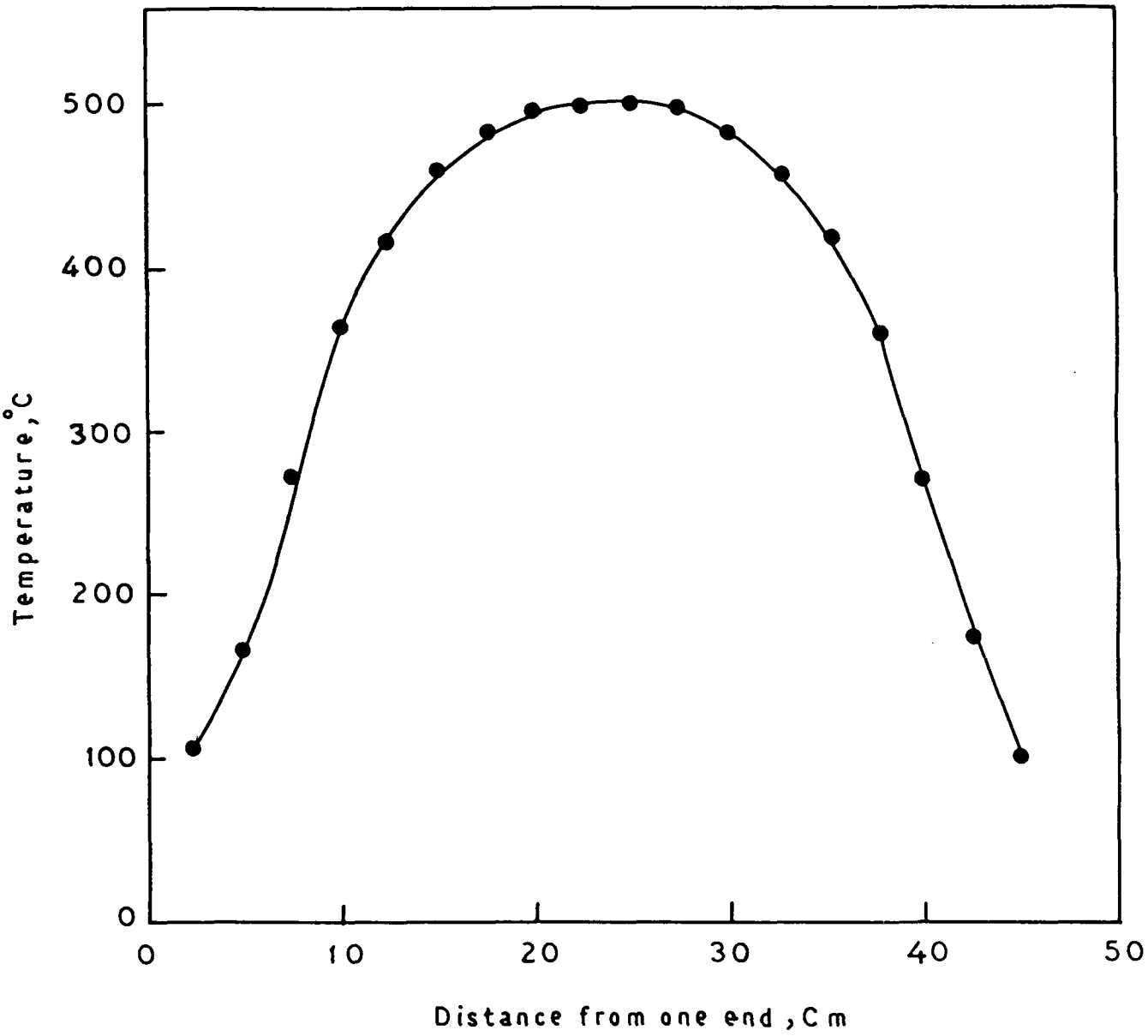

Fig. 2.3 TEMPERATURE PROFILE OF TUBULAR FURNACE AT 500°C

If air is present in the furnace, Fe_2O_3 may form. During short time of about 30 or 50 seconds, there is little chance of air entering into the furnace since the furnace tube is at positive steam pressure.

For PNC compacts the treatment was carried out at 500°C for times varying between 5 to 120 mins. and for PASC compacts the treatment was carried out at 450, 500, 527, 550 and 600°C for times of 45, 60, 90, and 120 minutes.

Specimens after steam treatment were weighed and dimensions were measured. The area of steam oxidised surface A_s was calculated as follows :

$$A_s = 2(l \times b + b \times t + l \times t)$$

where l is length, b the breadth and t thickness of oxidized slices. Weight gain or loss per unit oxidized area was calculated and weight gain vs. treatment time was plotted.

2.7 STRUCTURAL STUDIES

2.7.1 Optical microscopy

Oxidized sintered specimens are among the most difficult ones to prepare for metallographic examination. The oxide skin should be retained. They were mounted in

Araldite and ground on SiC paper of grit sizes 180, 320, 400, 500 and 600 μm. They were then polished on CENSICO single disc polishing machine using short napped sylvet or velvet cloth to avoid relief. The machine had a relatively low speed of 500 rpm. Polishing was done using 1 micron alumina powder suspension in distilled water. Preparation of the specimen was found difficult. Some times free copper occasionally present in sintered and steam treated alloys smeared over the surface and frequently oxide layer was broken up and smeared and embeded in araldite which shall be evident in third chapter.

Dilute solution of nitric acid in alcohol was used for etching of the polished specimens.

2.7.2 Scanning electron microscopy

Scanning electron microscopy studies were carried out on Cambridge Stereoscan Electron Microscope for which the facilities of Metallurgical Engg. Department of Banaras Hindu University, Varanasi were used, and Jeol model JSM-35C for which the facilities of National Botanical Research Institute, Lucknow were used. Scanning electron picture of fractured surfaces was taken on Philips Videoscan model PSCM 500 Electron Microscope with a tilt

angle of 33.50 at 30 KVA, for which the facilities of RSIC, Bose Institute Calcutta, were used.

2.8 HARDNESS MEASUREMENTS

Hardness of the steam treated specimens were determined on Vickers hardness testing machine at a load of 10 kg. The scatter in hardness reading was ± 15 HV10. Each value is an average of at least six readings.

2.8.1 Microhardness determination

Microhardness of oxide was determined on Buehler Microhardness tester at a load of 100 gms. Visible pores and unoxidized area were avoided as far as possible. The indentor impressions at lower load were sometimes obscure probably because of pore and/or matrix area being covered by the indentor. In such cases hardness readings were discarded and fresh readings were taken. Each micro-hardness value is an average of at least four readings.

2.9 TENSILE TEST

Tensile testing was done on an Instron machine Model 1195, with a chart speed of 10 mm/min., cross head speed of 0.5 mm/min. and full scale of load 2000 kg for which the facilities of Advance Centre for Material Science,

I.I.T. Kanpur were used.

2.10 X-RAY STUDIES

X-ray diffraction studies of oxidized samples were carried out for which the facilities of Advance Centre for Material Science, I.I.T. Kanpur were used.

CHAPTER 3

RESULTS

Experimental results are described in three parts. Part I describes the results of steam treatment studies on PNC powder compacts. Part II describes the sintered properties of PASC powder compacts since mechanical properties of such sintered compacts in conjunction with the various alloying elements are hardly available in literature as already discussed in Chapter I. Part III describes the results of steam oxidation experiments on sintered PASC powder compacts.

Part I

3.1 STEAM TREATMENT OF PNC POWDER COMPACTS

Few specimens of Fe-P, Fe-P-Cu and Fe-P-MCM were subjected to air oxidation for 30 to 90 minutes at 500-600°C. It was observed that oxide layers formed were inhomogenous, non-adherent and peeled off during handling. Air oxidation was not continued any further.

Table III.1.1 shows the per cent porosity and hardness of sintered compacts. The appearance of oxide layer formed was generally bluish grey to black and visual observation showed that oxide layers were generally uniform.

Table III.1.1 Per cent porosity and Hardness of compacts sintered at 1120°C for 30 minutes in H_2 ; compaction pressure 600 MPa.

Alloy	per cent porosity	Hardness HV5	Alloy	Per cent porosity	Hardness HV5
NC100.24	14.504	49.0	PNC45-1Cu	13.553	84.0
PNC30	14.180	85.0	PNC45-2Cu	14.184	88.0
PNC45	11.400	91.0	PNC45-3Cu	15.448	110.0
PNC60	8.998	110.0	PNC45-4Cu	15.937	96.0
NC-1Cu	14.242	64.5	PNC60-1Cu	11.667	70.0
NC-2Cu	14.985	76.5	PNC60-2Cu	12.811	80.0
NC-3Cu	15.864	81.2	PNC60-3Cu	13.438	98.0
NC-4Cu	16.223	72.0	PNC60-4Cu	13.806	93.0
PNC30-1Cu	14.671	112.5	PNC30-1Mo	13.287	92.0
PNC30-2Cu	14.791	100.0	PNC30-2Mo	12.790	94.0
PNC30-3Cu	15.672	107.0	PNC30-3Mo	12.285	106.0
PNC30-4Cu	16.339	100.6	PNC30-4Mo	11.531	108.0

Continued ....

Table III.1.1 continued

Alloy	Per cent porosity	Hardness HV5	Alloy	Per cent porosity	Hardness HV5
PNC60-1Mo	10.412	131.0	PNC45-1MCM	13.260	110.0
PNC60-2Mo	9.403	143.0	PNC45-2MCM	14.494	122.0
PNC60-3Mo	8.158	153.0	PNC45-3MCM	14.823	124.0
PNC60-4Mo	7.115	157.0	PNC45-4MCM	14.512	127.0
NC-1MCM	13.304	61.0	PNC60-1MCM	12.137	120.0
NC-2MCM	14.151	65.0	PNC60-2MCM	12.137	124.0
NC-3MCM	14.606	70.0	PNC60-3MCM	12.932	125.0
NC-4MCM	15.583	76.0	PNC60-4MCM	13.389	130.0
PNC30-1MCM	12.722	93.0	PNC45-1Mo-1Cu	13.436	100.0
PNC30-2MCM	14.209	100.0	PNC45-1Mo-4Cu	15.664	126.0
PNC30-3MCM	14.921	105.0	PNC45-2Mo-1Cu	11.787	136.0
PNC30-4MCM	15.099	107.0	PNC45-2Mo-4Cu	13.106	152.0

Continued ....

Table III.1.1 continued

Alloy	Per cent porosity	Hardness HV5
PNC60-2Mo-1Cu	10.291	133.0
PNC60-2Mo-4Cu	12.296	172.0
PNC60-4Mo-1Cu	10.192	187.0
PNC60-4Mo-4Cu	13.317	200.0
PNC60-2MCM-1Cu	12.843	150.0
PNC60-2MCM-4Cu	15.108	165.0
PNC60-4MCM-1Cu	14.406	158.0
PNC60-4MCM-4Cu	17.176	158.0
PNC60-2Ni-1Cu	12.412	139.0
PNC60-2Ni-4Cu	14.416	160.0
PNC60-4Ni-1Cu	12.138	119.0
PNC60-4Ni-4Cu	16.414	161.0

3.1.1 Kinetic Studies

3.1.1.1 Fe-P compacts

Weight gain increases with increasing treatment times upto 60 minutes (Fig. 3.1). With increasing phosphorus content, weight gain generally decreases.

3.1.1.2 Fe-P-Cu compacts

In case of Fe-Cu and Fe-0.3 P-Cu sintered compacts, weight gain increases with increasing steam treatment times (Fig. 3.2a and 3.2b). For higher (0.45 and 0.6 %) P-containing compacts, weight gain increases upto 60 minutes of oxidation after which it remains constant (Figs. 3.2c and 3.2d). In general, with increasing copper content, weight gain increases while with increasing phosphorus content, it usually decreases (Fig. 3.2).

3.1.1.3 Fe-P-Mo compacts

Weight gain increases with increase in steam treatment times similar to that of Fe-P-Cu compacts (Fig. 3.3). However, upto about 45 minutes of treatment times, the variation of weight gain with times and increase in molybdenum content is not regular (Fig. 3.3a and 3.3b). After 45 minutes of treatment times, weight gain, generally,

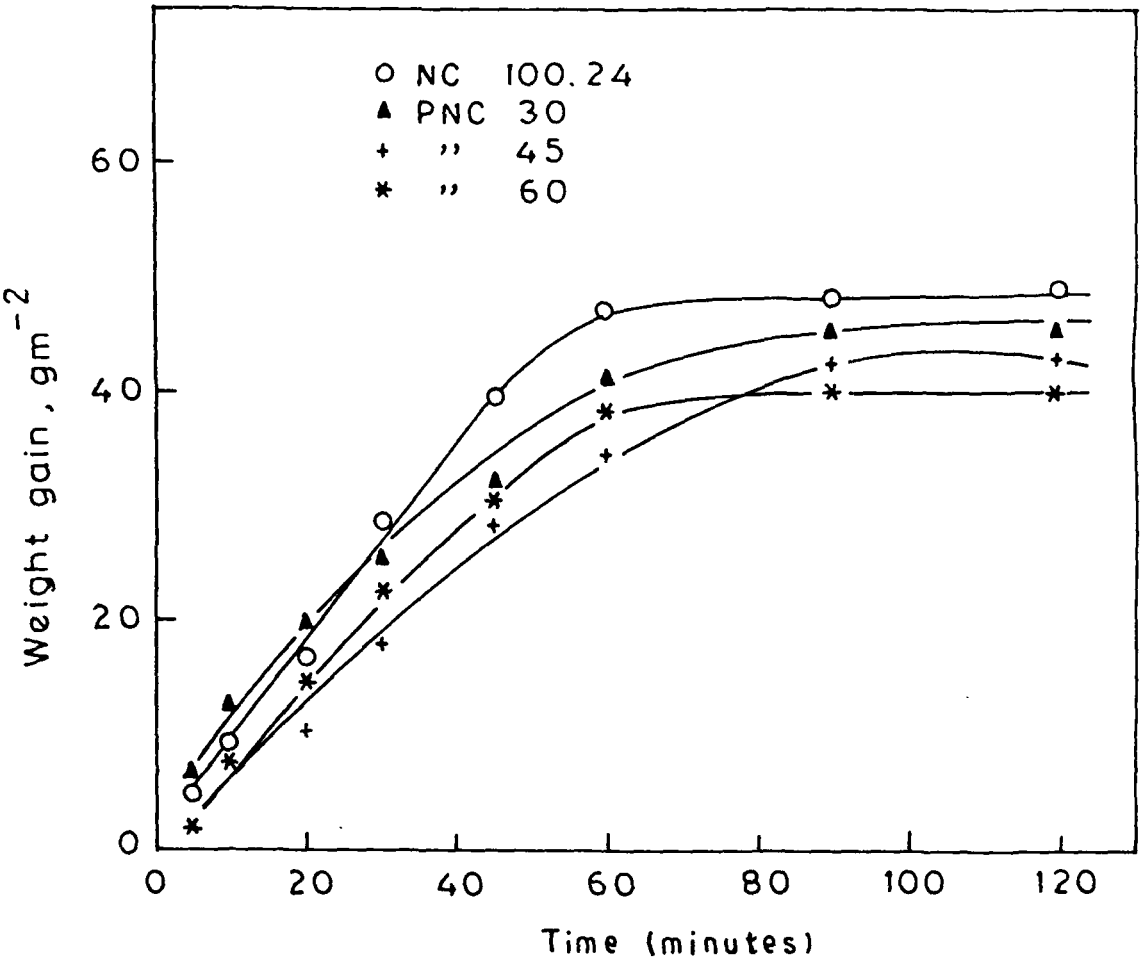
NC 100.24
PNC 30
" 45
" 60
Weight gain, gm^{-2}
Time (minutes)
0
20
40
60
80
100
120

Fig. 3.1

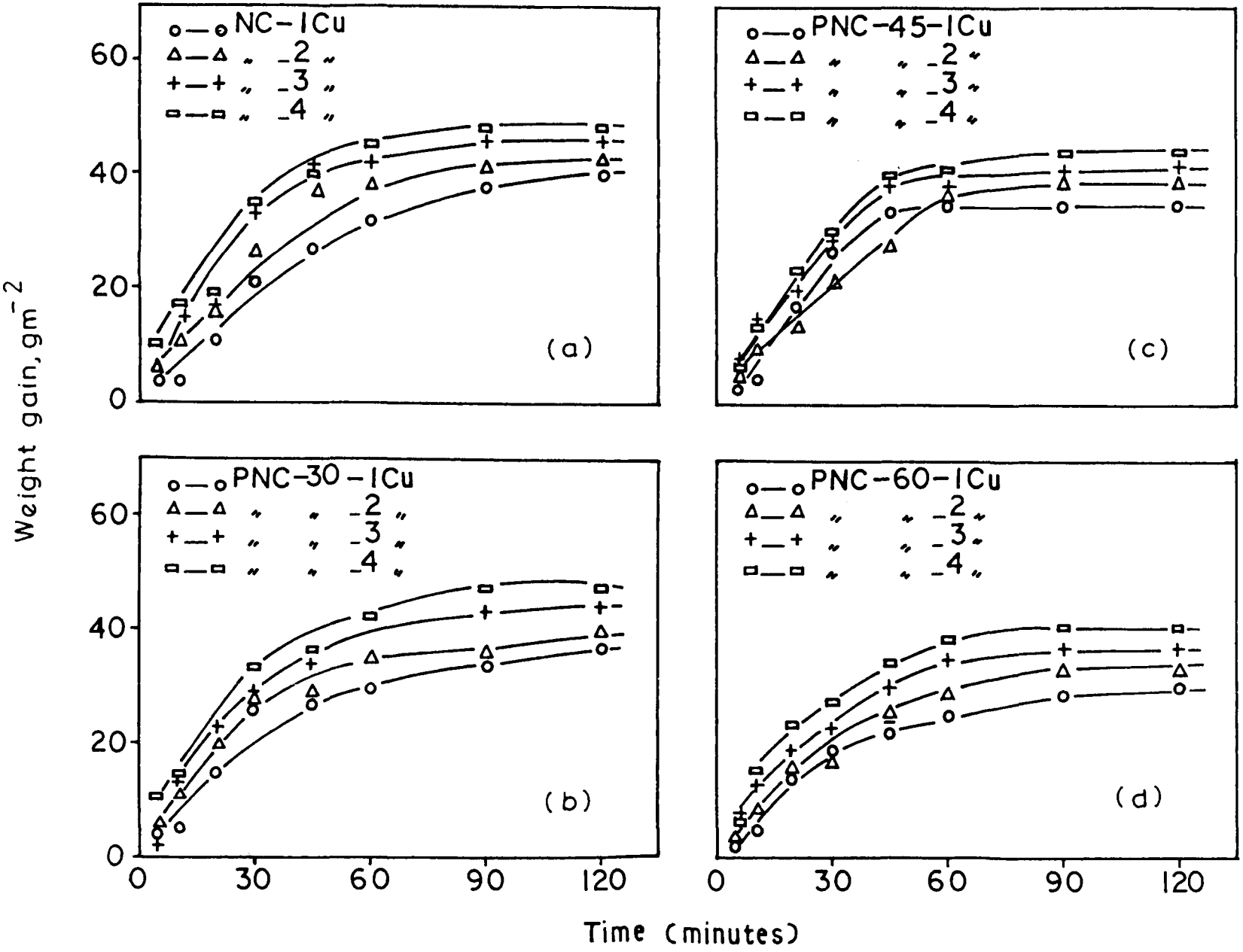
o—o NC-1Cu
Δ—Δ " -2 "
+—+ " -3 "
□—□ " -4 "
(a)
o—o PNC-45-1Cu
Δ—Δ " -2 "
+—+ " -3 "
□—□ " -4 "
(c)
o—o PNC-30-1Cu
Δ—Δ " -2 "
+—+ " -3 "
□—□ " -4 "
(b)
o—o PNC-60-1Cu
Δ—Δ " -2 "
+—+ " -3 "
□—□ " -4 "
(d)
Weight gain, gm^{-2}
0
20
40
60
0
30
60
90
120
Time (minutes)

Fig 3·2

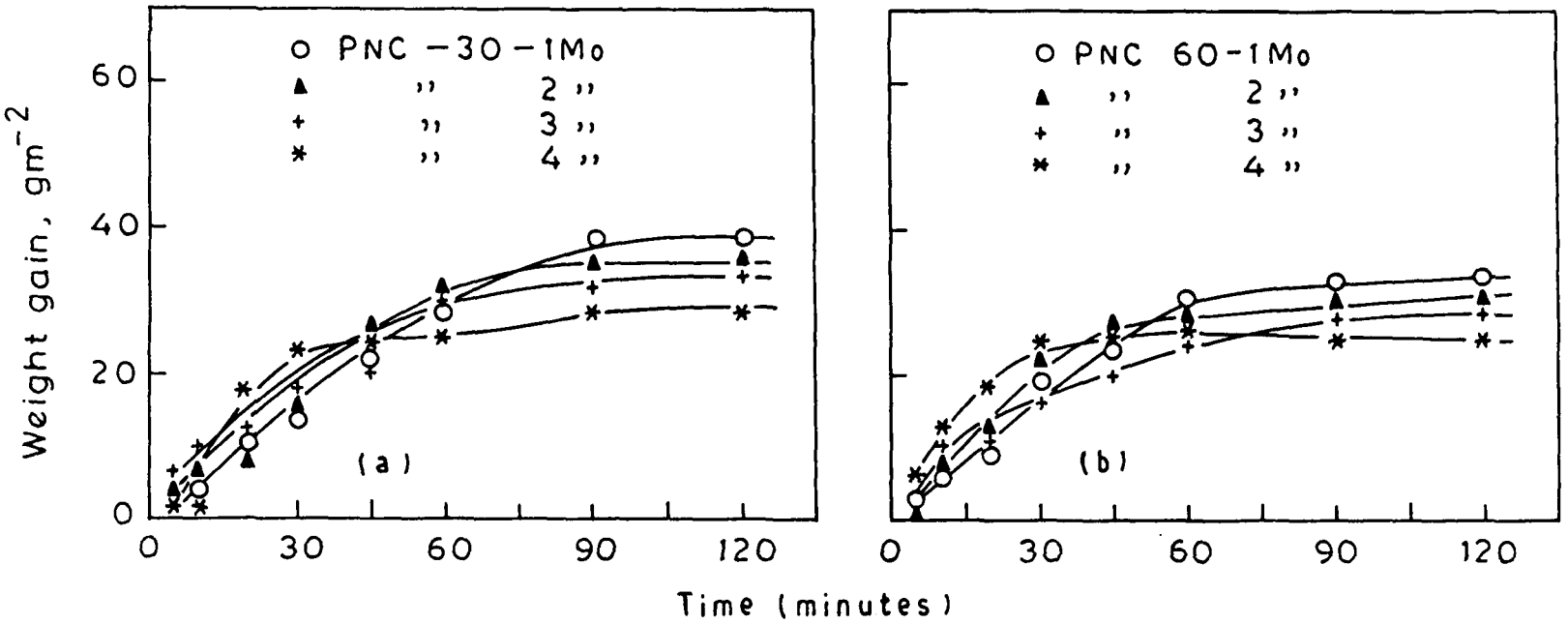
o PNC −30−1Mo
▲ ,, 2 ,,
+ ,, 3 ,,
* ,, 4 ,,
(a)
o PNC 60-1Mo
▲ ,, 2 ,,
+ ,, 3 ,,
* ,, 4 ,,
(b)
Weight gain, gm^{-2}
0
20
40
60
0
30
60
90
120
Time (minutes)

Fig. 3.3

decreases with increasing Mo content. With increasing P-content, there occurs a decrease in weight gain. Level of weight gain is slightly lower in Mo containing compacts as compared to that of Cu-containing compacts (Fig. 3.2 and 3.3). The variation of weight gain with time levels off at about 60-90 minutes of treatment times (Fig. 3.3).

3.1.1.4 Fe-P-MCM compacts

Variation of weight gain with increasing steam treatment times and increasing phosphorus content in sintered compacts is similar to that in case of Cu-containing compacts (Figs. 3.4a to 3.4d). With increasing MCM contents, weight gain invariably increases. At lower phosphorus levels, weight gain in MCM-containing compacts is higher than that in case of Cu-containing compacts (Fig. 3.2 and 3.4) but at higher phosphorus contents, weight gain in MCM and Cu-containing compacts are comparable.

3.1.1.5 Ternay powder premixes

In case of ternary powder compacts, the variation of weight gain with treatment times and copper contents are similar to that observed in case of binary premixes (Fig. 3.5a and 3.5d). The order of increase of weight

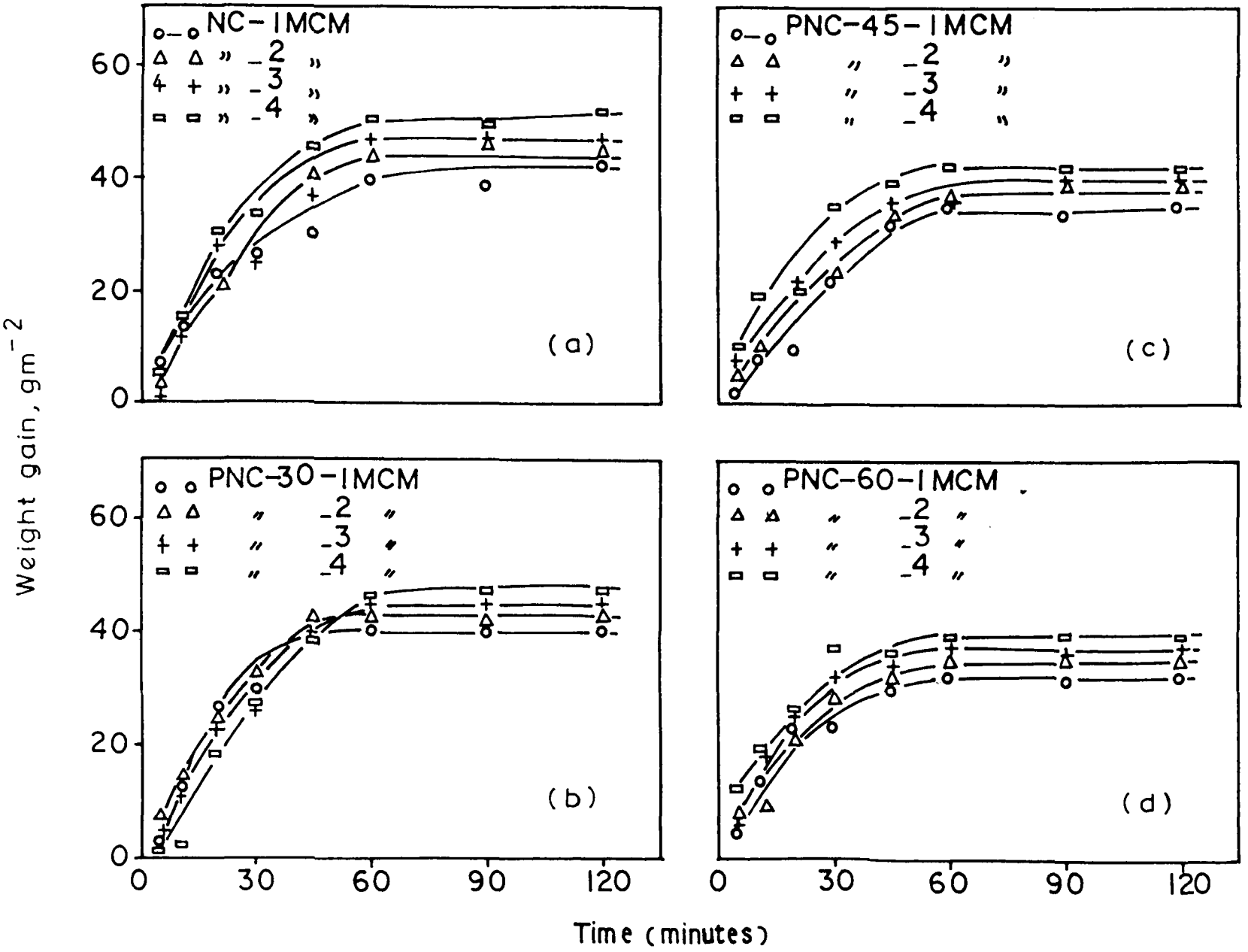
NC-1MCM
PNC-45-1MCM
PNC-30-1MCM
PNC-60-1MCM
(a)
(b)
(c)
(d)
Weight gain, gm^{-2}
Time (minutes)
0
20
40
60
30
90
120

Fig. 3·4

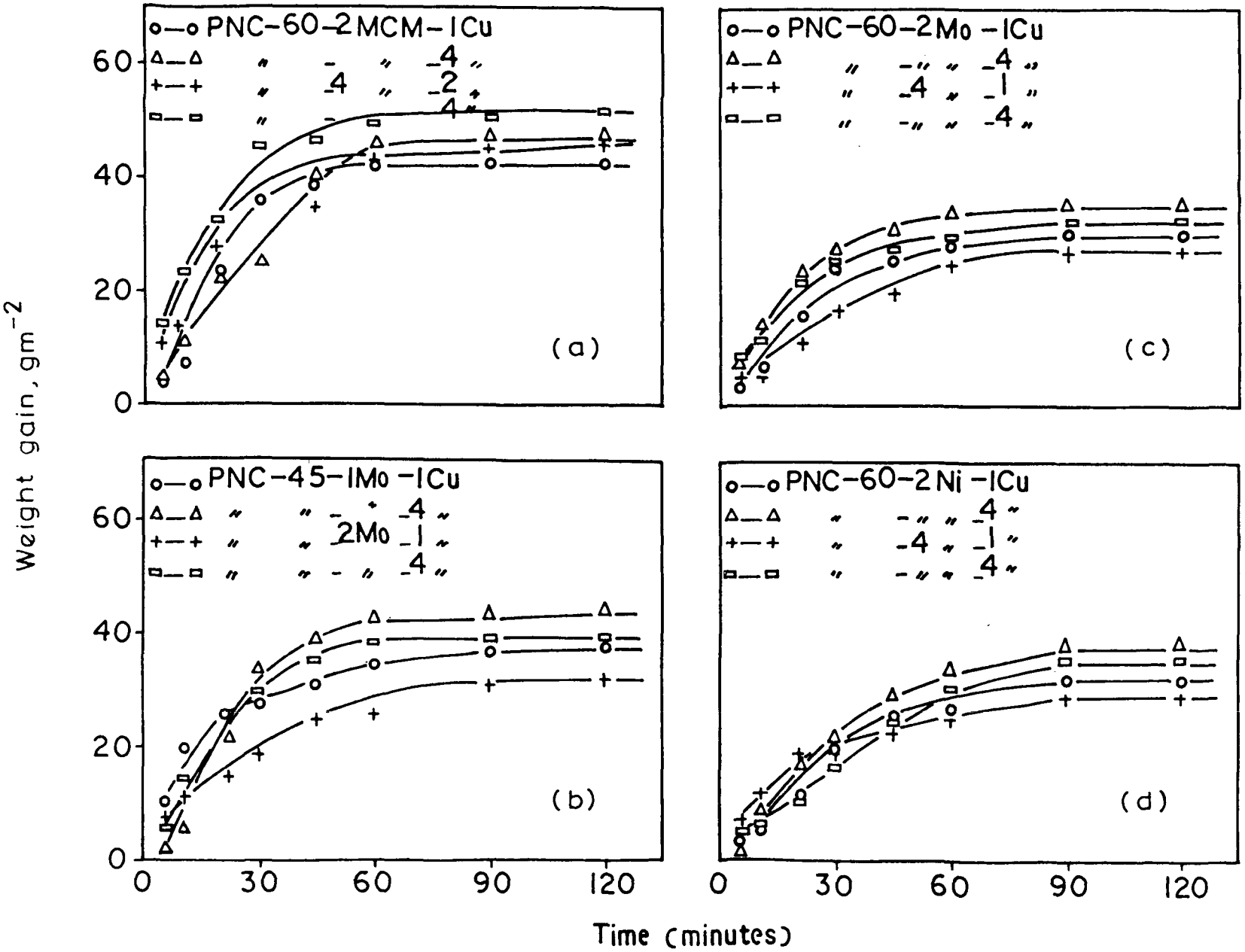
o—o PNC-60-2MCM-1Cu
Δ—Δ " - " -4 "
+—+ " -4 " -2 "
□—□ " - " -4 "
(a)
o—o PNC-60-2Mo-1Cu
Δ—Δ " -" " -4 "
+—+ " -4 " -1 "
□—□ " -" " -4 "
(c)
o—o PNC-45-1Mo-1Cu
Δ—Δ " " - " -4 "
+—+ " " -2Mo -1 "
□—□ " " - " -4 "
(b)
o—o PNC-60-2Ni-1Cu
Δ—Δ " -" " -4 "
+—+ " -4 " -1 "
□—□ " -" " -4 "
(d)
Weight gain, gm^{-2}
Time (minutes)
0
20
40
60
0
30
60
90
120

Fig. 3·5

gain in case of MCM containing compacts is highest. Higher Mo and P decrease the level of weight gain (Fig. 3.5b and 3.5c).

3.1.2 Hardness

3.1.2.1 Fe-P compacts

Hardness increases with increasing treatment times upto 30 minutes after which there occurs a marginal decrease in it (Fig. 3.6). With increase in phosphorus content from 0 to 0.45 wt. %, there is a small increase in hardness while when P content is increased from 0.45 to 0.6 wt. %, hardness increases significantly. With increasing P contents, maximum in hardness is achieved at shorter treatment times.

3.1.2.2 Fe-P-Cu compacts

Maximum hardness was found after steam oxidation for 30 minutes (Figs. 3.7 and 3.8). After 30 minutes of treatment, hardness either remains constant or there is a marginal decrease. However, there occurs a significant increase in hardness of the oxidized samples over that of as sintered specimens (Figs. 3.7 and 3.8 and Table III.1.1). The level of increase in hardness of Fe-Cu oxidized

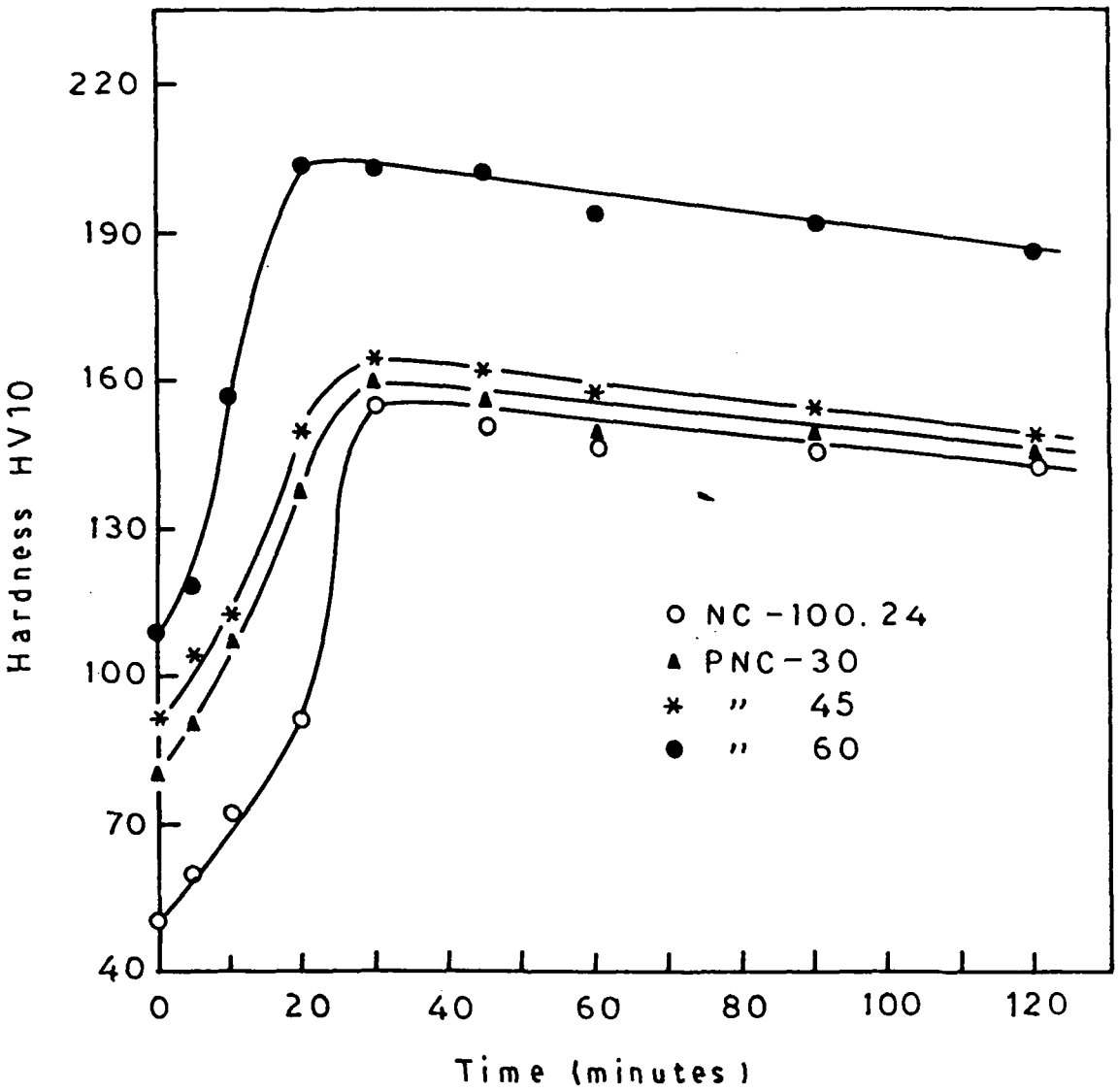
220
190
160
130
100
70
40
Hardness HV10
0
20
40
60
80
100
120
Time (minutes)
o NC -100.24
▲ PNC-30
* " 45
● " 60

Fig. 3.6

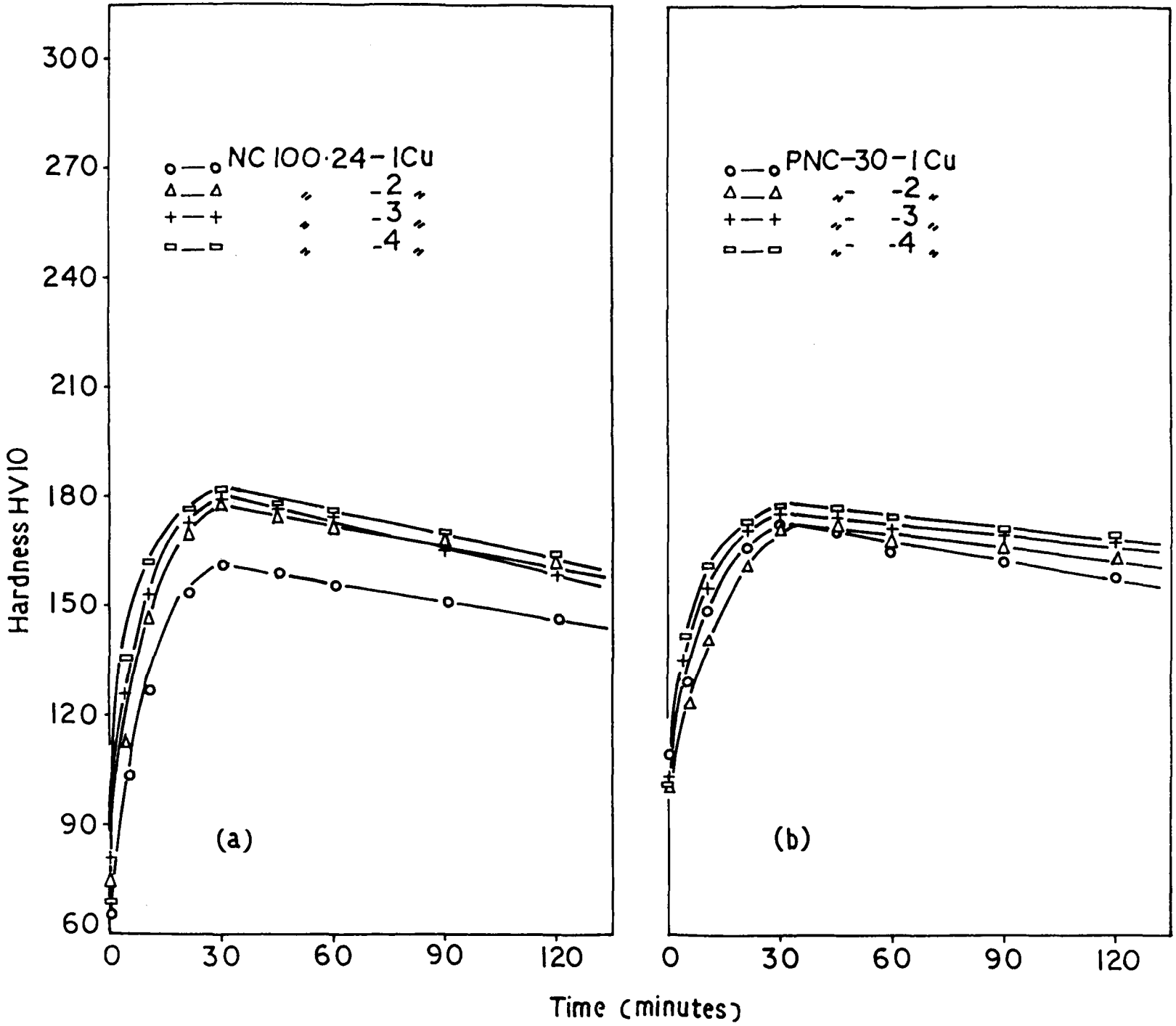
300
270
240
210
180
150
120
90
60
Hardness HV10
o—o NC 100·24-1Cu
Δ—Δ " -2 "
+—+ " -3 "
□—□ " -4 "
(a)
0
30
60
90
120
o—o PNC-30-1Cu
Δ—Δ " -2 "
+—+ " -3 "
□—□ " -4 "
(b)
0
30
60
90
120
Time (minutes)

Fig. 3·7

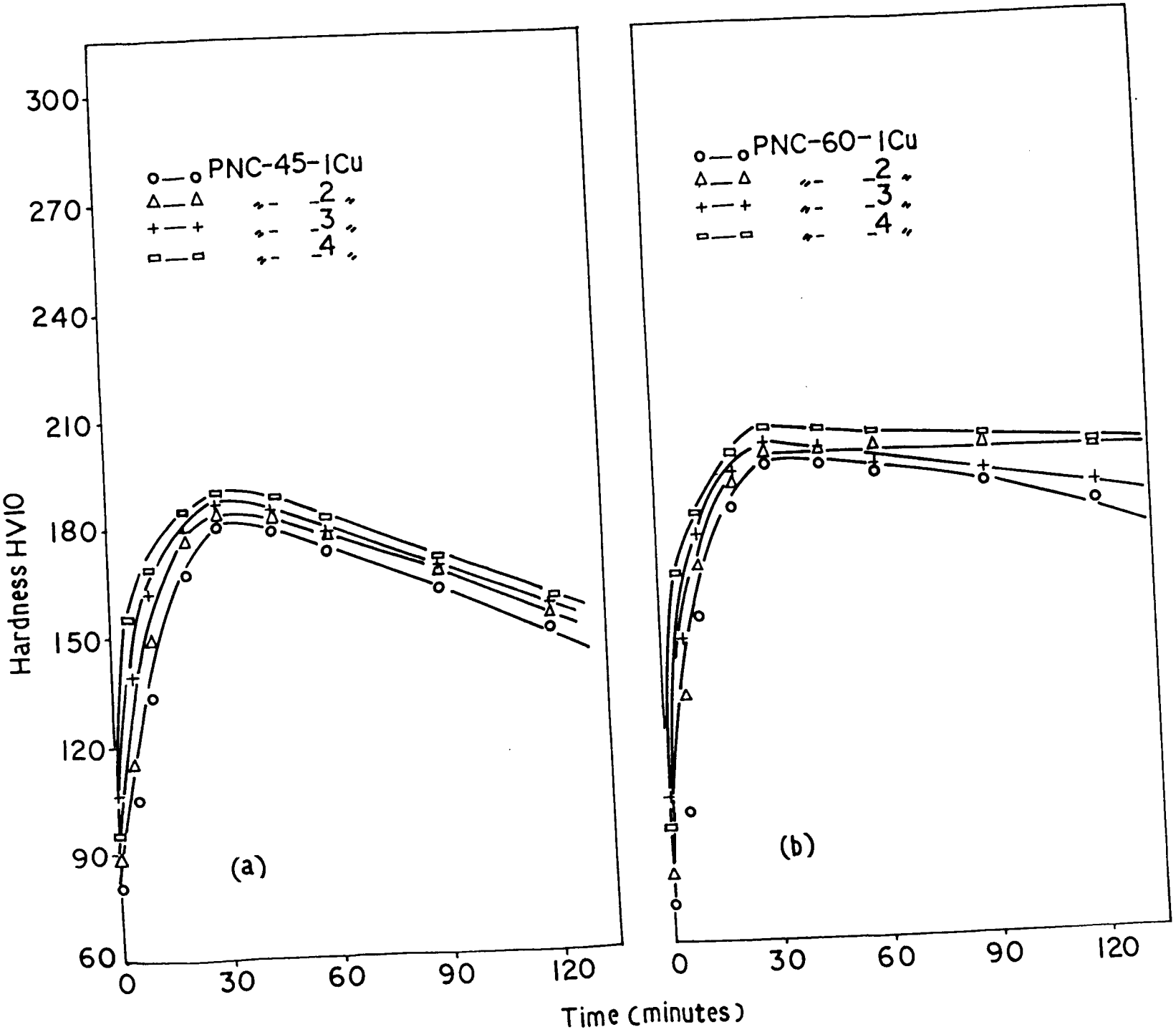
PNC-45-1Cu
-2 "
-3 "
-4 "
PNC-60-1Cu
-2 "
-3 "
-4 "
Hardness HV10
300
270
240
210
180
150
120
90
60
0
30
60
90
120
(a)
(b)
Time (minutes)

specimen (Fig. 3.7a) is higher than that in case of Fe-0.3 P-Cu specimens (Fig. 3.7b). After 0.3 wt. % P level hardness in general increases with increasing P content (Figs. 3.8a and 3.8b). In general, hardness increases with increasing copper content (Figs. 3.7 and 3.8).

3.1.2.3 Fe-P-Mo compacts

The variation of hardness with steam treatment times is similar to that of Fe-P or Fe-P-Cu compacts (Fig. 3.9) except that maximum in hardness is achieved at around 60 minutes of treatment times. With increase in P content from 0.3 to 0.6 wt. % the hardness increase is of the order of 60 HV10 while with increase in Mo content from 1 to 4 wt. %, hardness increase is upto 30 HV10 only. However, with steam treatment, hardness increase of upto over 100 % is obtained over that of as sintered compacts.

3.1.2.4 Fe-P-MCM compacts

The variation of hardness with steam oxidation time with increasing MCM or P content is in general similar to that of other systems (Figs. 3.10 and 3.11). However, one important point to note is that no maximum in hardness is observed. Hardness regularly increases with increasing treatment times. This trend of regular increases in hard-

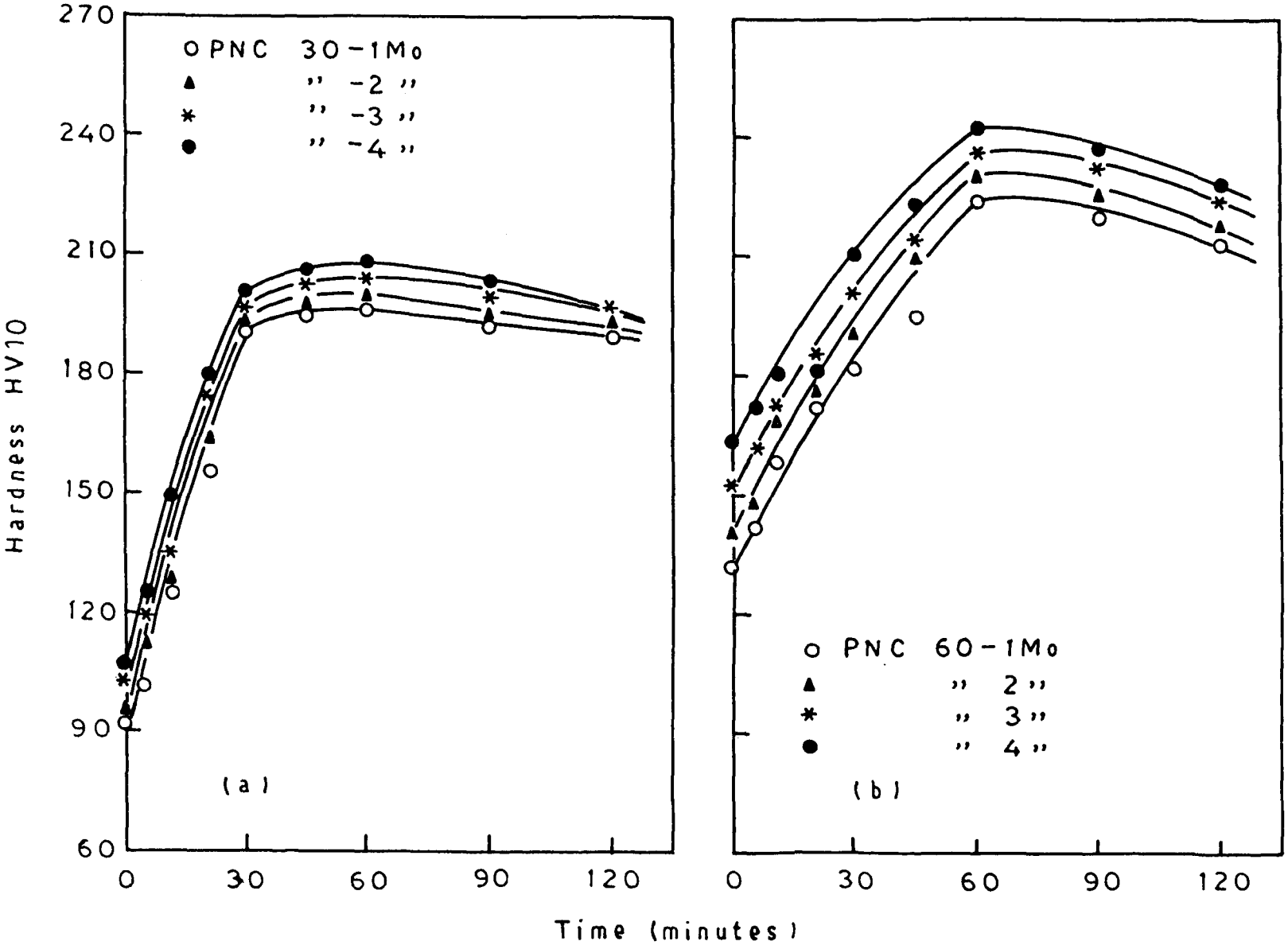
270
240
210
180
150
120
90
60
Hardness HV10
○ PNC 30-1Mo
▲ " -2 "
* " -3 "
● " -4 "
(a)
○ PNC 60-1Mo
▲ " 2 "
* " 3 "
● " 4 "
(b)
0
30
60
90
120
Time (minutes)

Fig. 3.9

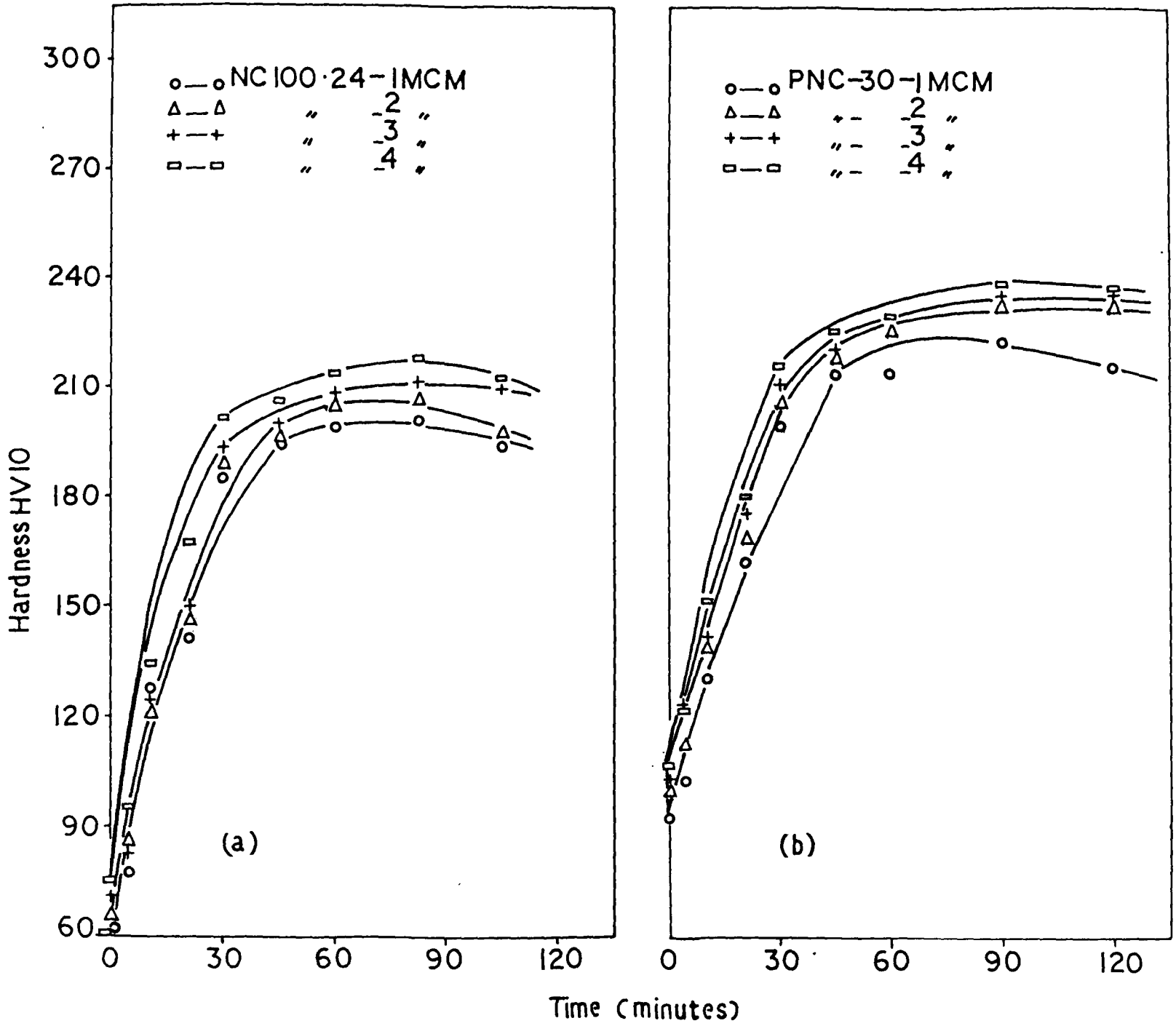
NC 100·24-1MCM
" -2 "
" -3 "
" -4 "
PNC-30-1MCM
" -2 "
" -3 "
" -4 "
Hardness HV10
300
270
240
210
180
150
120
90
60
0
30
60
90
120
(a)
(b)
Time (minutes)

Fig. 3·10

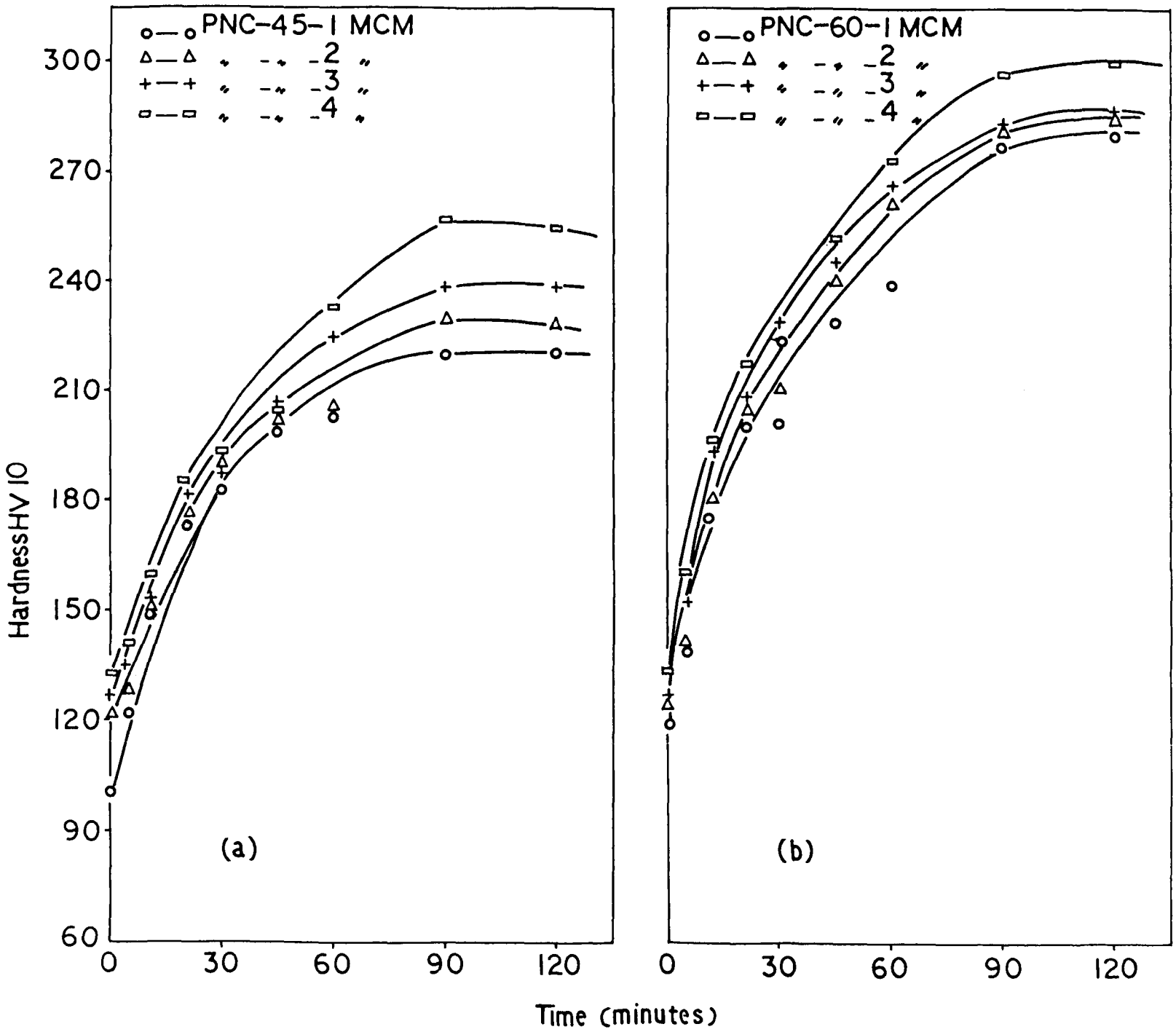
PNC-45-1 MCM
2
3
4
PNC-60-1 MCM
2
3
4
300
270
240
210
180
150
120
90
60
Hardness HV 10
0
30
60
90
120
(a)
(b)
Time (minutes)

Fig. 3·11

ness with increasing treatment times goes on becoming more and more evident with increasing phosphorus content. The increase in hardness of as steam treated samples over that of as sintered ones is upto 120 %.

3.1.2.5 Ternary powder compacts

In case of Mo-containing sintered ternary premixes, with increase in treatment times, the variation of hardness is generally similar to that of other binary premixes (Figs. 3.12a and 3.12b). However, maximum in hardness in case of PNC45-Mo-Cu compacts is achieved at 45 minutes of treatment times. With increasing Mo content hardness generally increases but with increasing Cu contents hardness generally decreases (Figs. 3.12a and 3.12b).

In MCM containing compacts, increasing MCM contents increases hardness but increasing copper addition decreases hardness (Fig. 3.13a). Variation of hardness with increasing treatment times is similar to other ternary systems.

In case of Ni-containing compacts hardness increases upto 60 minutes of treatment times after which there is a fall (Fig. 3.13b). However, variation with increasing Ni or Cu content does not give any conclusive result.

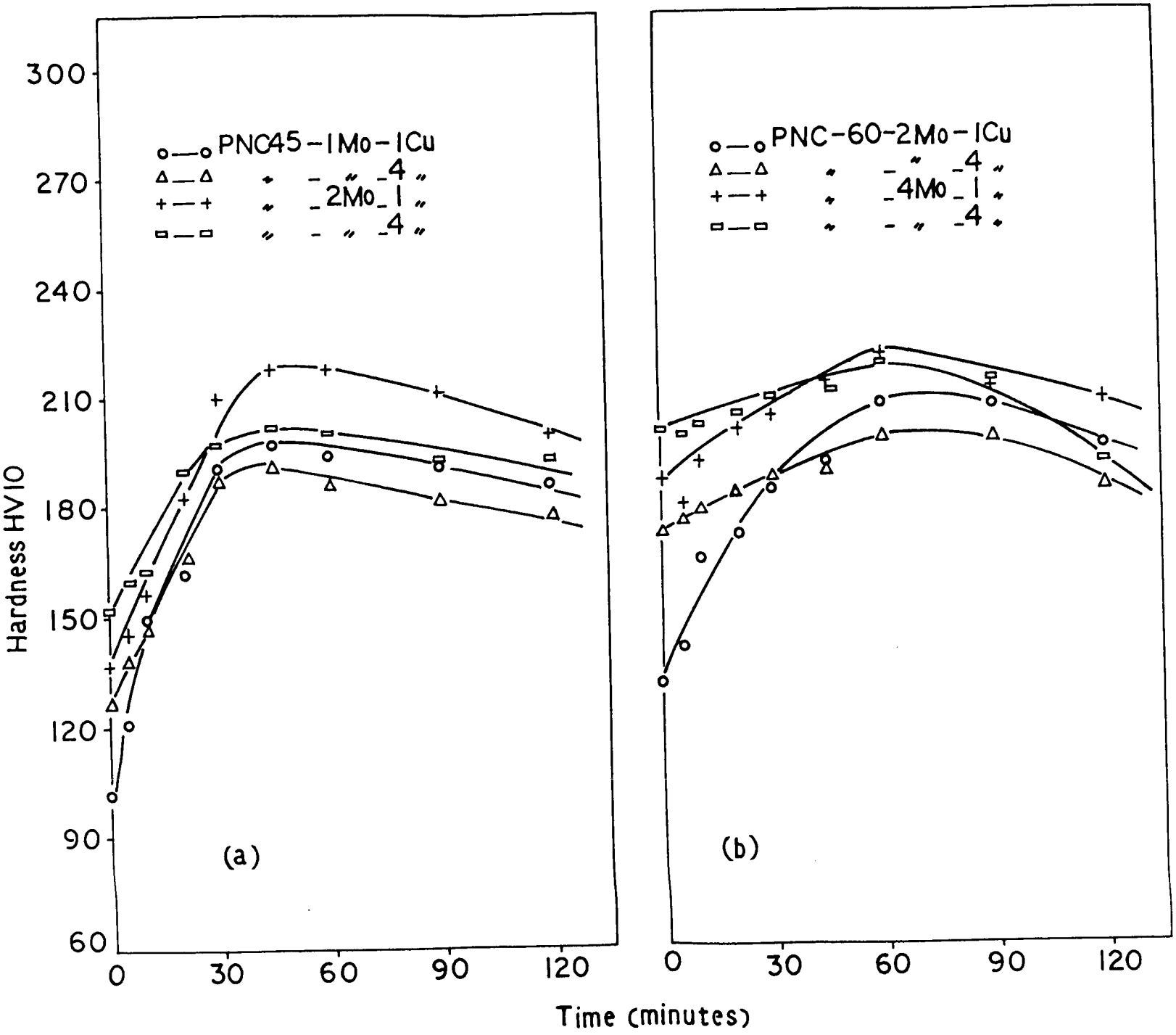
300
270
240
210
180
150
120
90
60
Hardness HV10
PNC45-1Mo-1Cu
4 "
2Mo 1 "
4 "
(a)
PNC-60-2Mo-1Cu
4 "
4Mo 1 "
4 "
(b)
0
30
60
90
120
Time (minutes)

Fig. 3·12

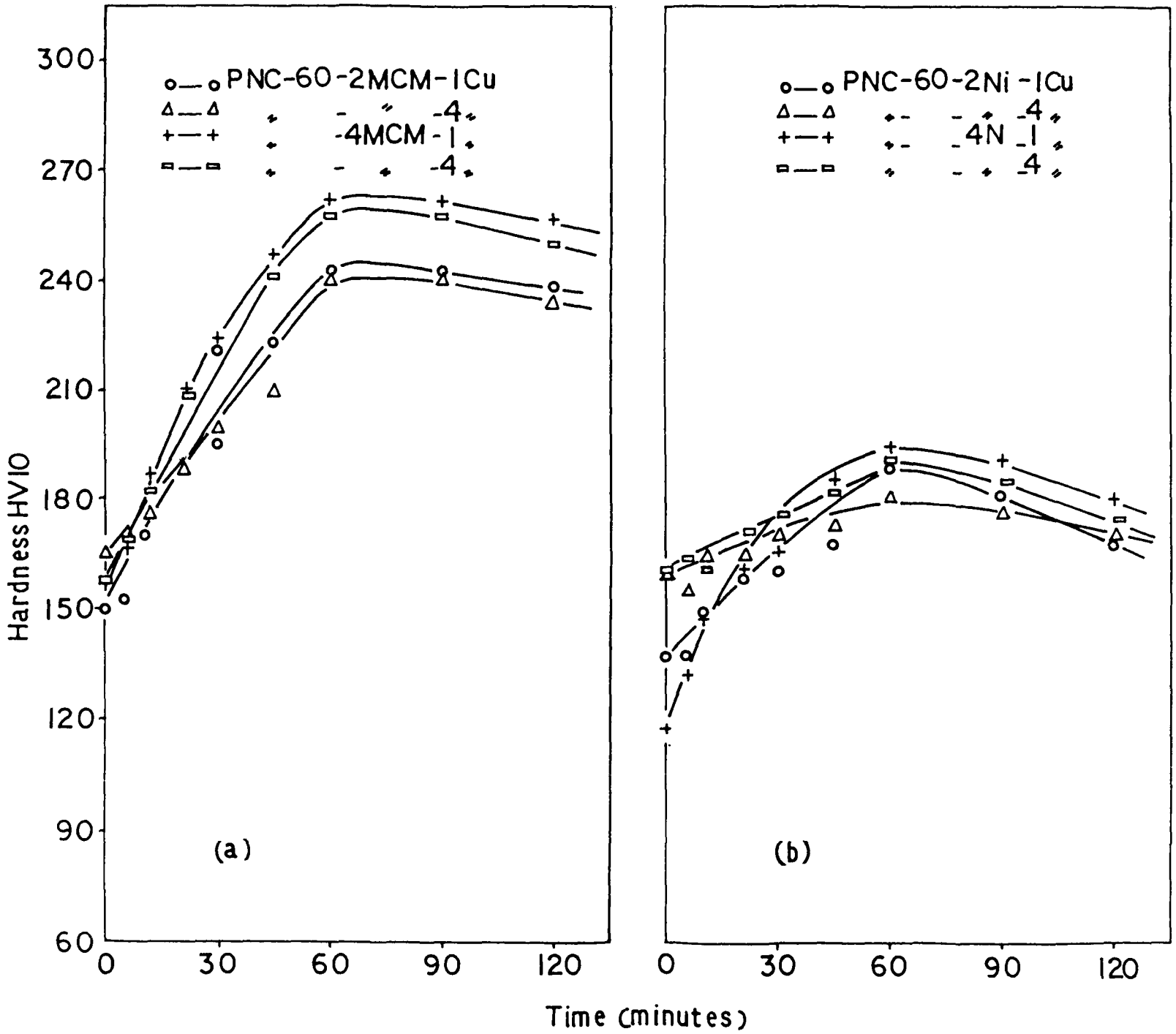
PNC-60-2MCM-1Cu
-4MCM-1
PNC-60-2Ni-1Cu
-4N-1
Hardness HV10
300
270
240
210
180
150
120
90
60
0
30
60
90
120
(a)
(b)
Time (minutes)

Fig. 3·13

3.1.3 Structural studies

3.1.3.1 Fe-P compacts

In general, with increase in steam treatment times, oxide layer was found to be thicker and slightly diffused. In case of plain iron, the oxide layer seems to have broken during grinding and polishing and smeared over the surface. With increasing P content oxide layer is relatively sharp (Figs. 3.14a to 3.14d).

3.1.3.2 Fe-P-Cu compacts

Microstructural examination shows that with increasing treatment times, oxygen diffuses deeper into the matrix (Figs. 3.15a to 3.15f). When the copper content was increased, oxidation increases (Figs. 3.15a and 3.15c or 3.15b and 3.15d). Higher amount of phosphorus decreases the rate of oxidation (Figs. 3.15e and 3.15f). The above observations are more evident through scanning electron pictures of oxide plus matrix regions (Figs. 3.16 to 3.19). Longer treatment time increases the thickness of oxide layer (Figs. 3.16 and 3.17). In case of P-containing specimens, oxide thickness does not appear to have increased with increasing treatment time (Figs. 3.18 and 3.19).

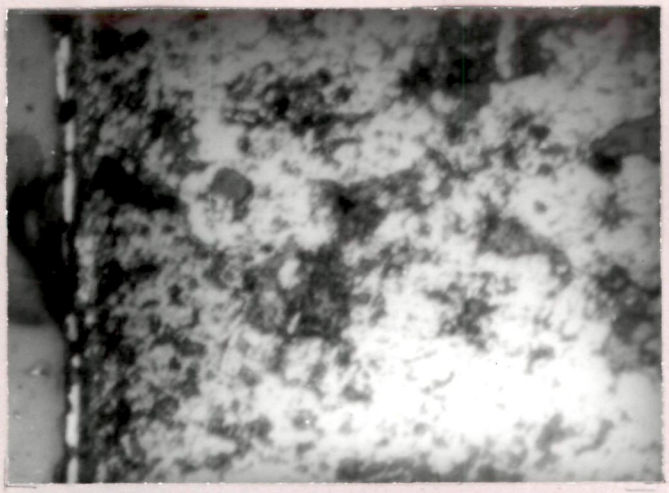

(a) NC100·24

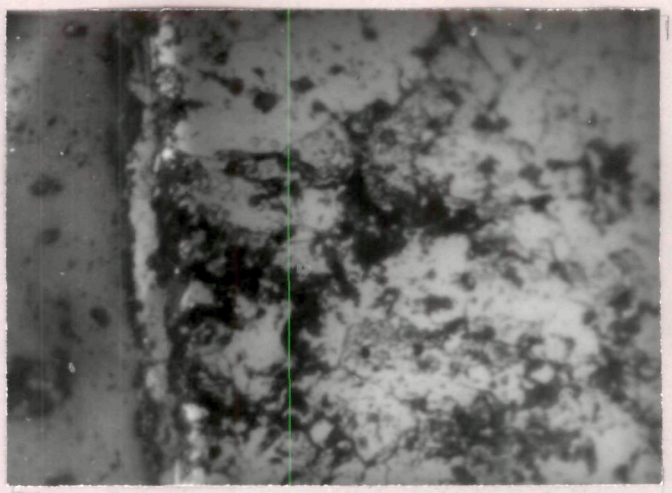

(b) PNC30

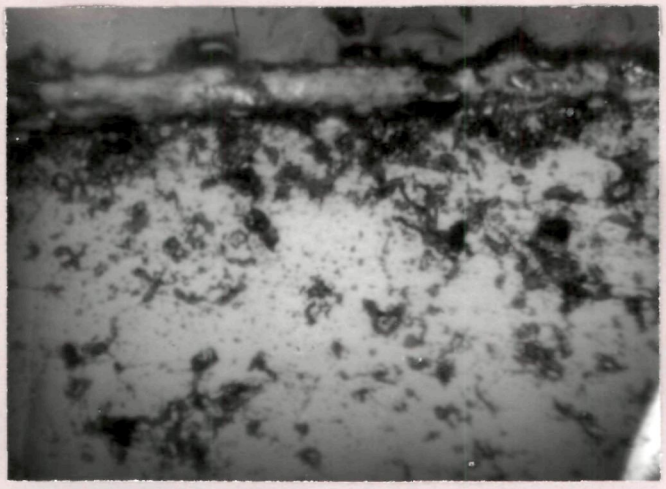

(c) PNC45

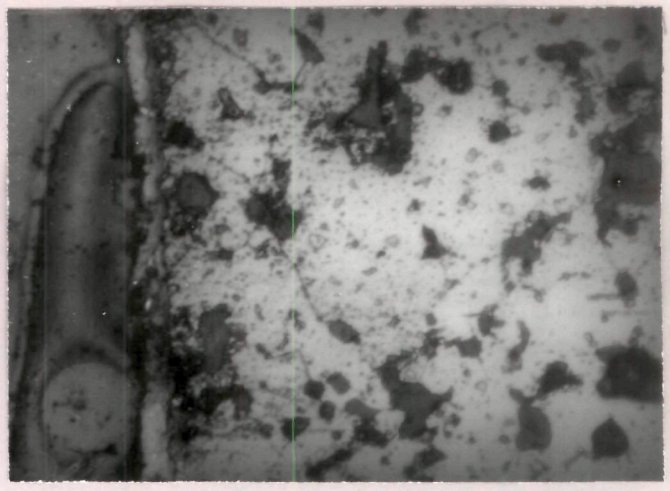

(d) PNC60

Fig. 3·14

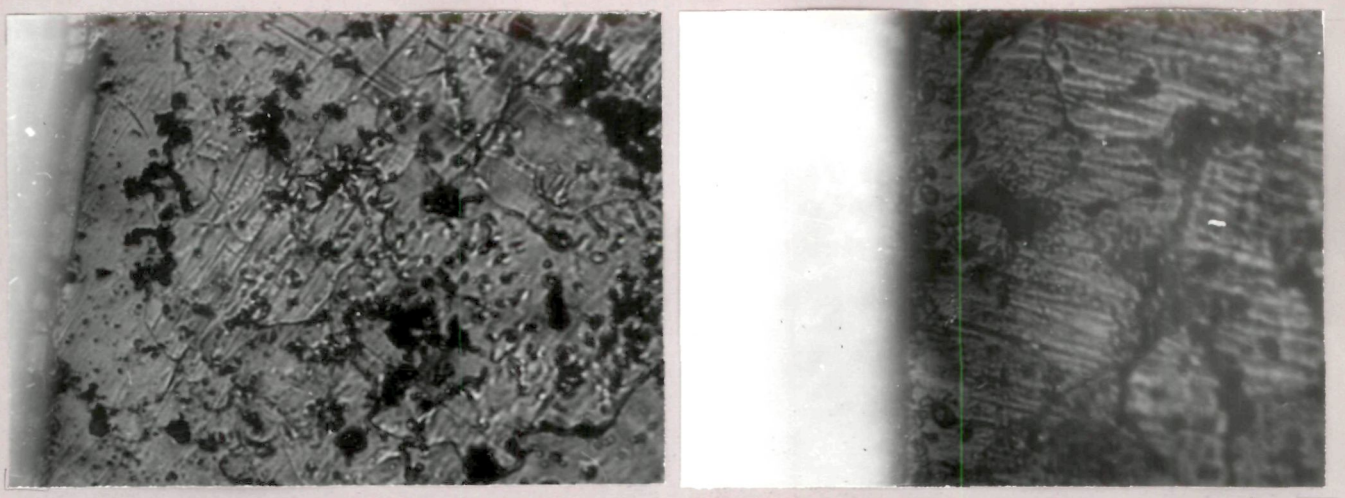

(a) NC - 1Cu (b)

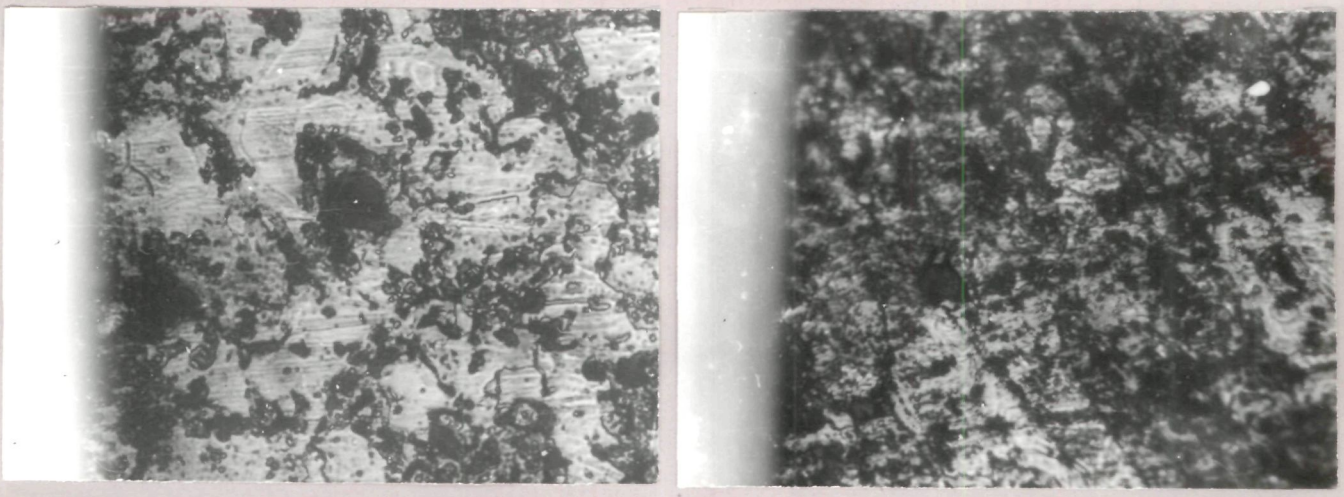

(c) NC - 4Cu (d)

Fig. 3·15

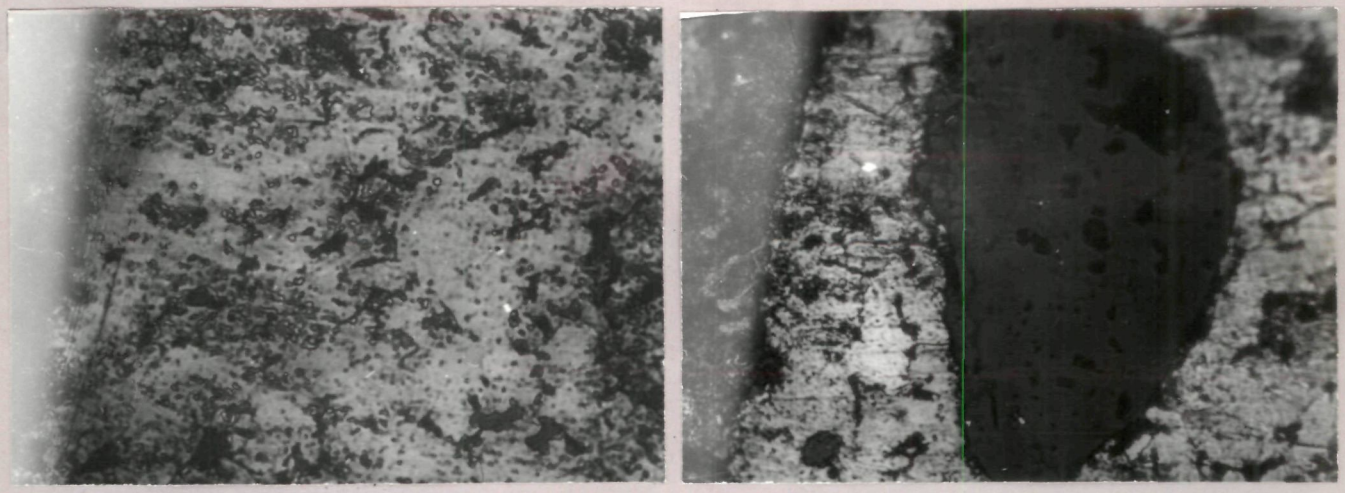

(e) PNC60 - 4Cu (f)

Fig. 3·15

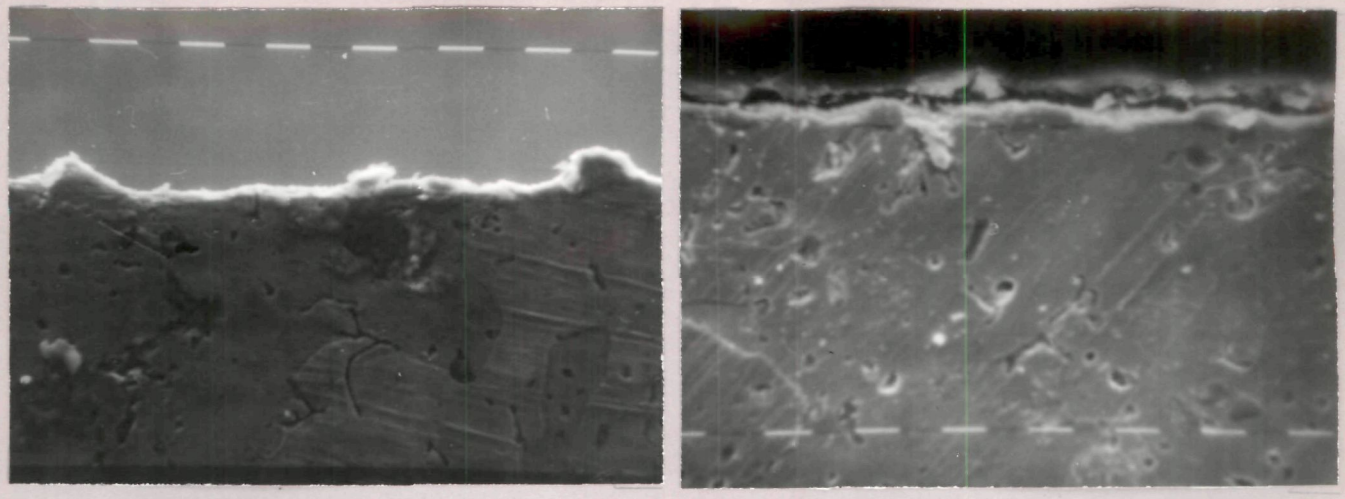

(a) 640X (b)

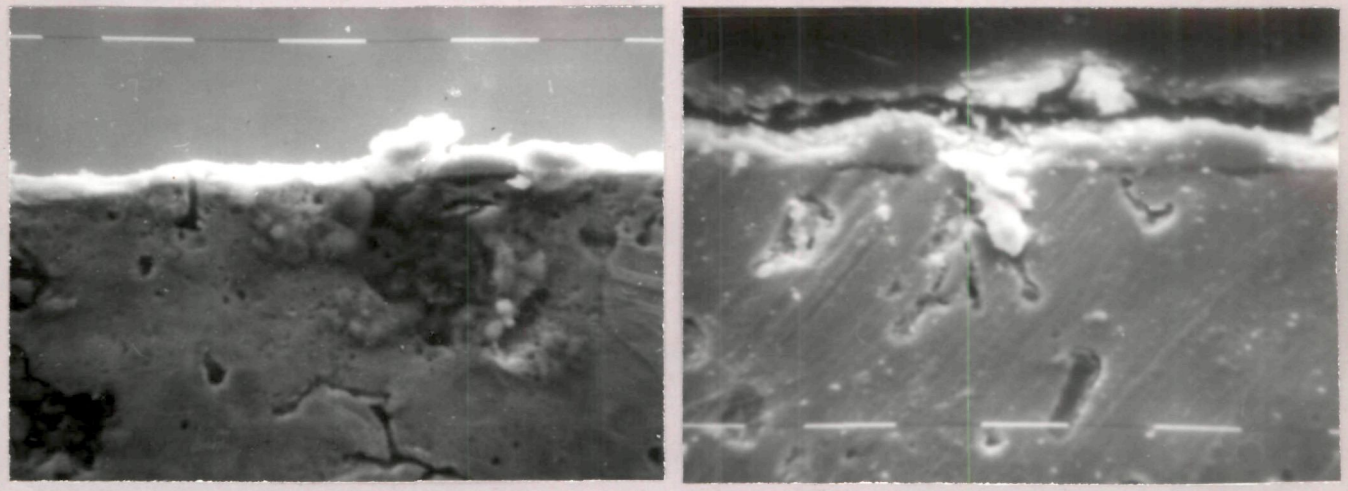

(c) 1250X (d)

NC-1Cu

Fig. 3·16

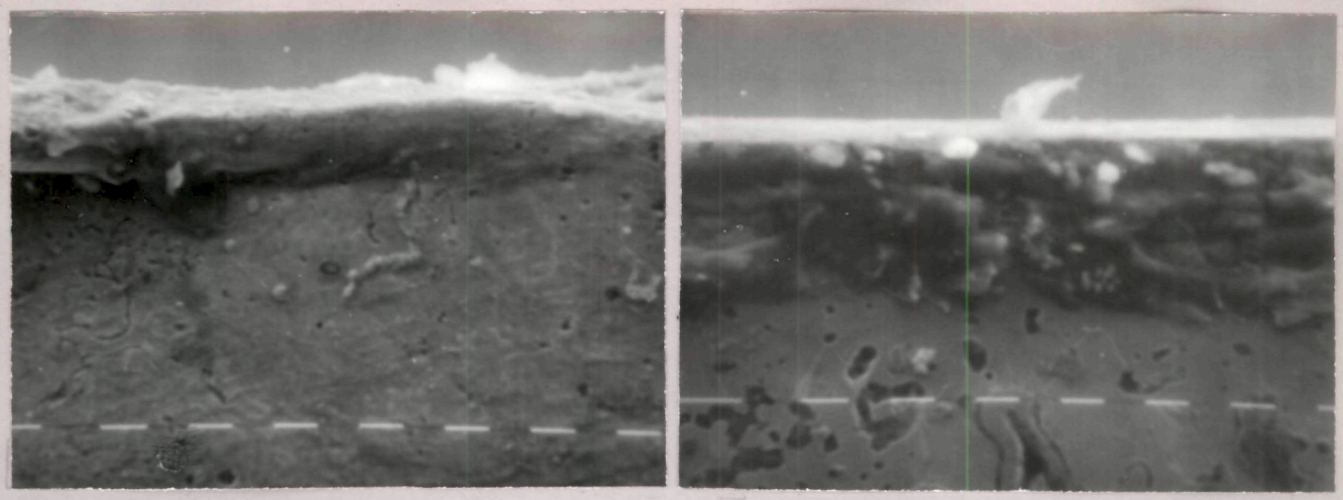

(a) 640X (b)

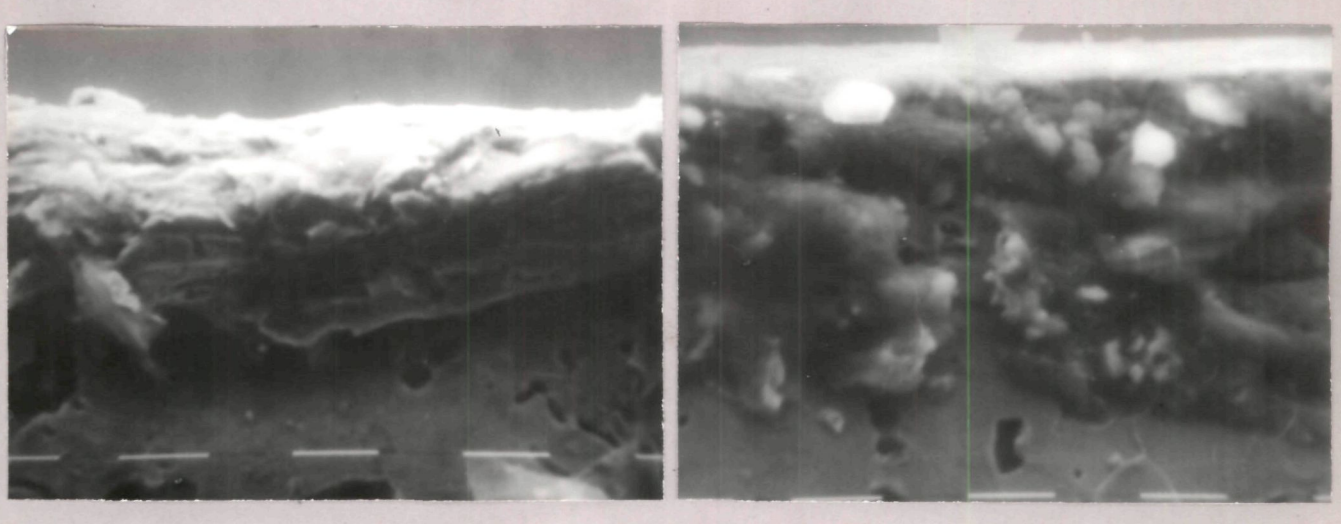

(c) 1250X (d)

NC - 4Cu

Fig. 3·17

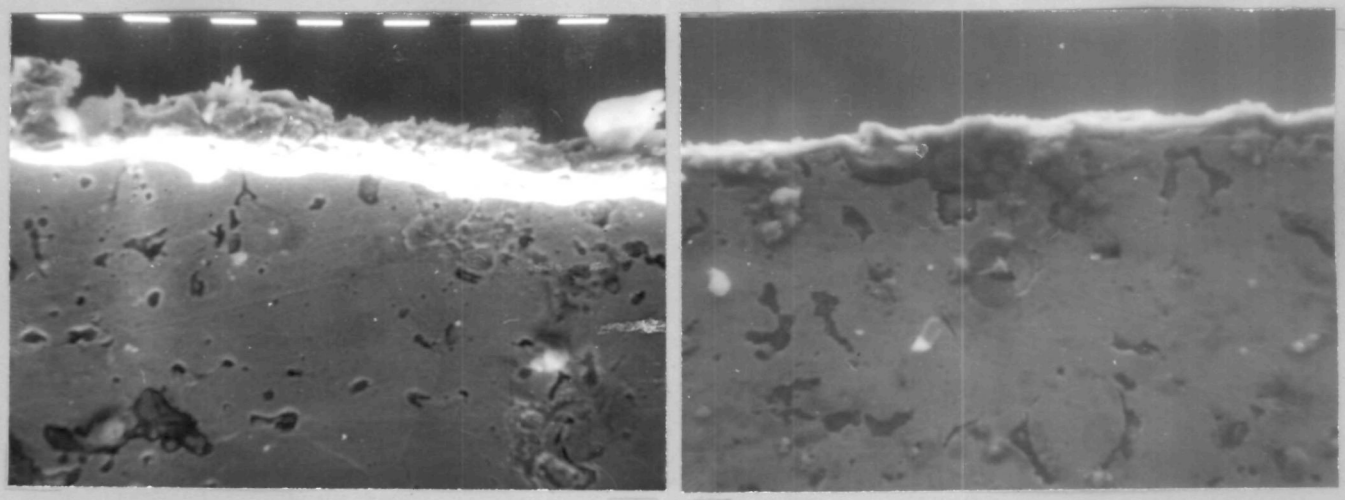

(a) 640X (b)

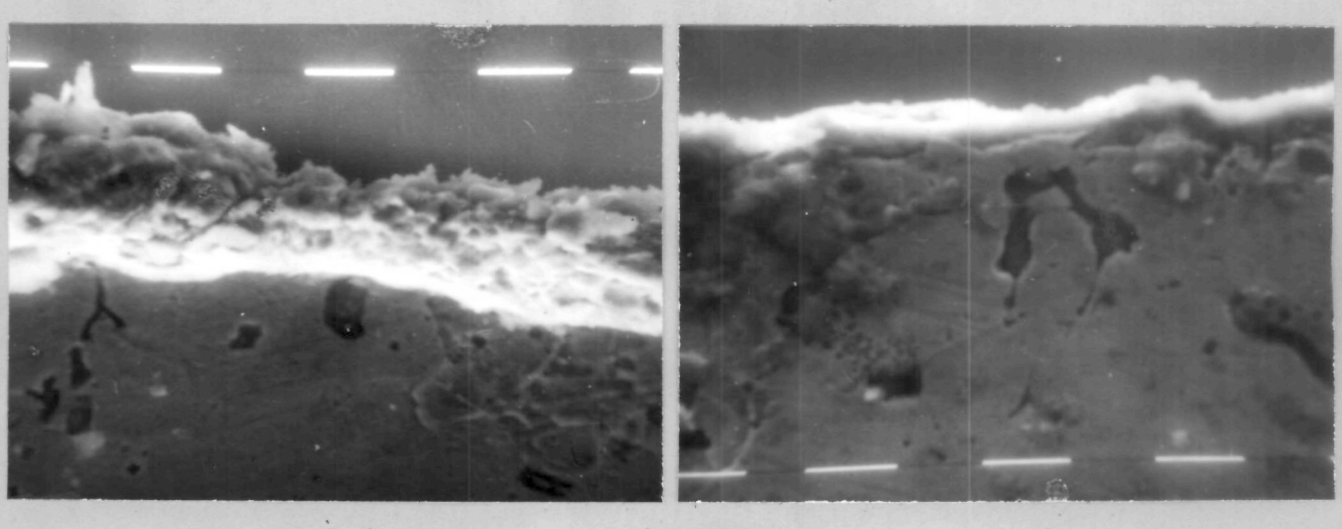

(c) 1250X (d)

PNC60 - 1Cu

Fig. 3·18

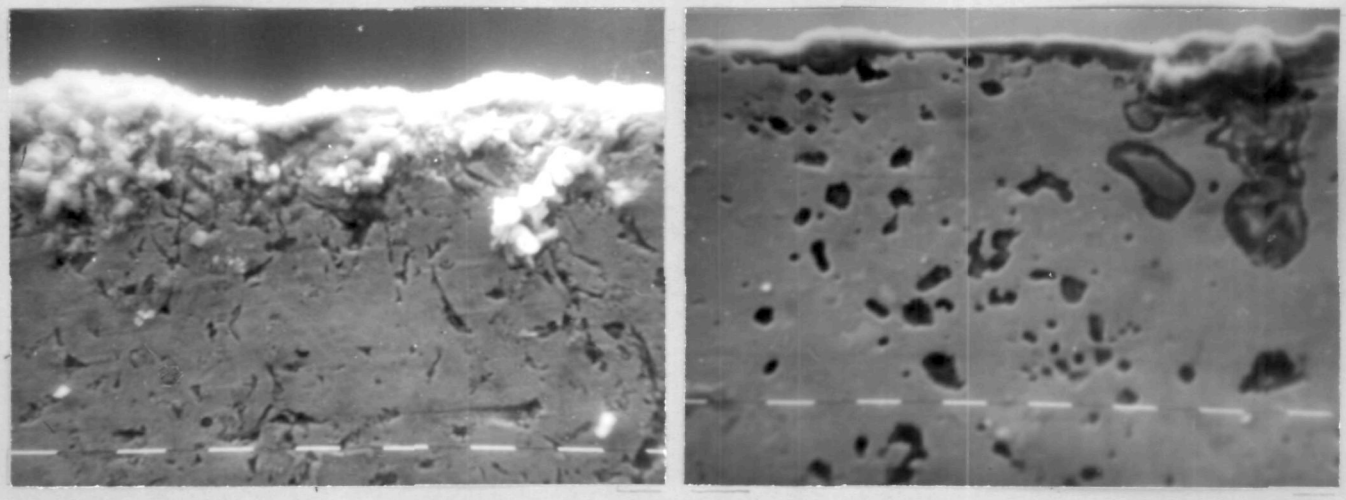

(a) 640 X (b)

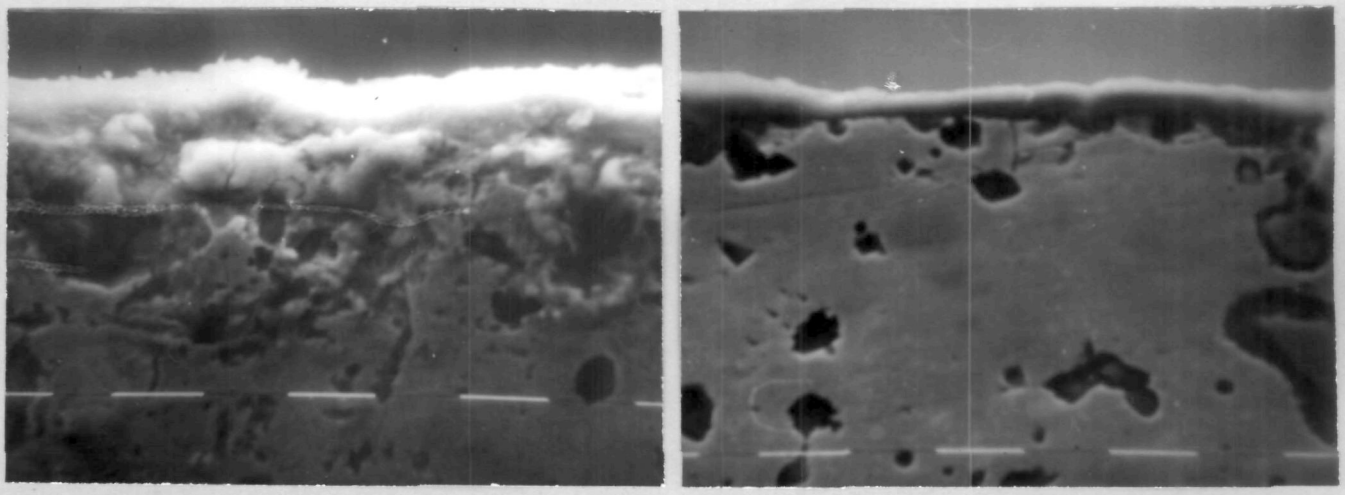

(c) 1250 X (d)

PNC60 - 4Cu

Fig. 3·19

3.1.3.3 Fe-P-Mo compacts

At lower treatment times, the oxide layer formed is thin and diffuse (Fig. 3.20). Some selective oxide patches near pores have been shown in various compacts. In case of Fe-0.3P-3Mo compacts, steam treated for 90 minutes, relatively well defined oxide layers have been obtained (Fig. 3.20c). Such layers have been found in higher Mo and/or higher P-containing compacts (Figs. 3.20 and 3.21). Higher Mo and/or higher P-containing compacts show sharp, well defined and large grains (Figs. 3.20d and 3.21). Pores are smaller and rounded ones. During specimen preparation oxide particles frequently smeared over araldite and vice-versa as shown in Fig. 3.21.

3.1.3.4 Fe-P-MCM compacts

With increasing treatment times in case of PNC-I MCM compacts, thickness of oxide layer increases (Figs. 3.22 and 3.23). With increasing MCM contents, the definition of oxide layer decreases. For higher P-containing Fe-MCM compacts the oxide layer was frequently broken. However, the oxide layers are diffuse (Figs. 3.24 and 3.25) contrary to the effect of P on other systems.

3.1.3.5 Ternary powder compacts

In case of Mo-containing compacts, the effect of

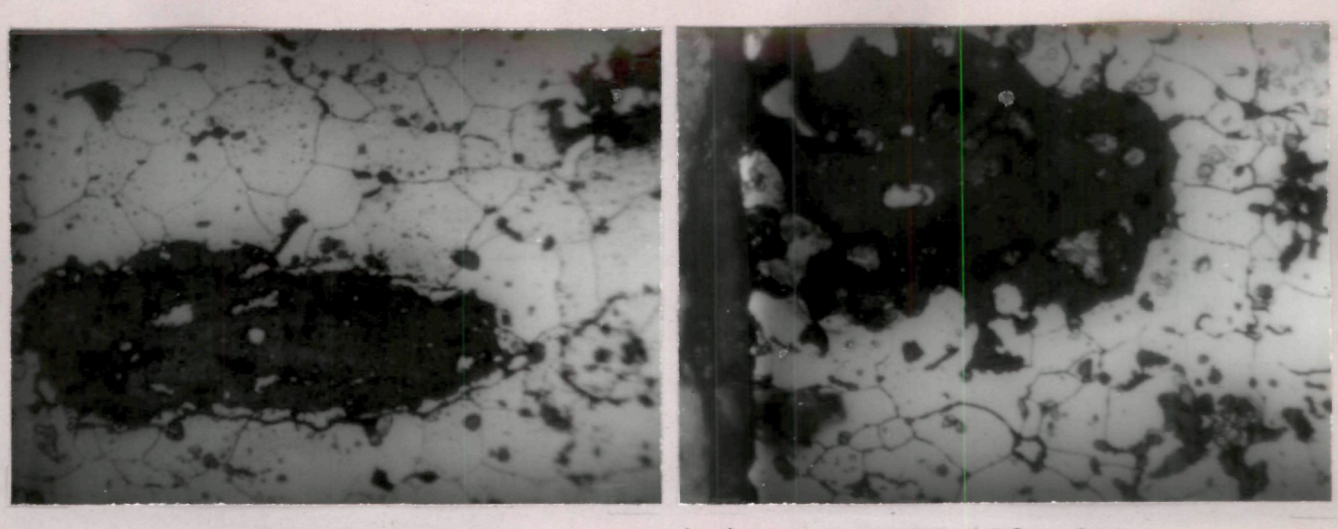

(a) PNC30 - 2Mo (b) PNC30 - 3Mo

(c) PNC30 - 3Mo (d) PNC30 - 4Mo

Fig. 3·20

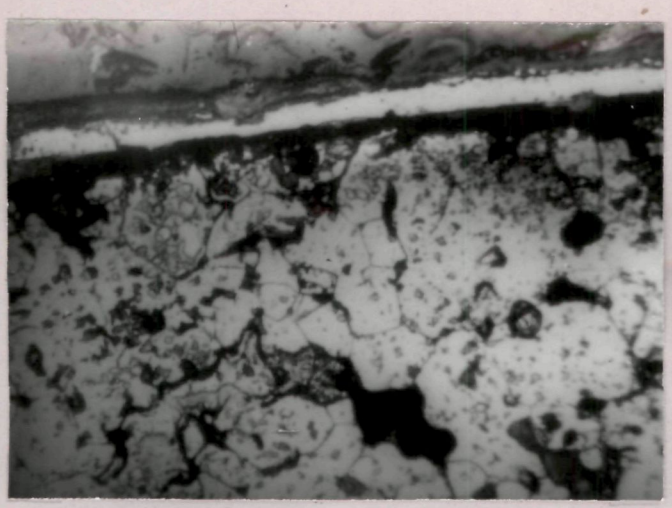

(a) PNC60 - 1Mo

(b) PNC60 - 2Mo

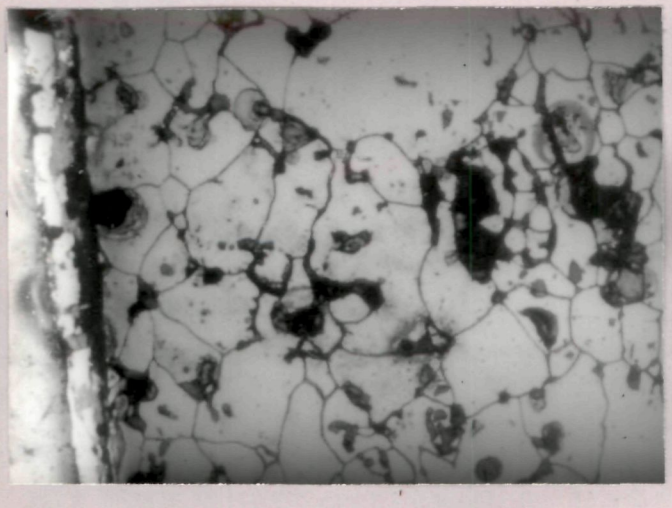

(c) PNC60 - 3Mo

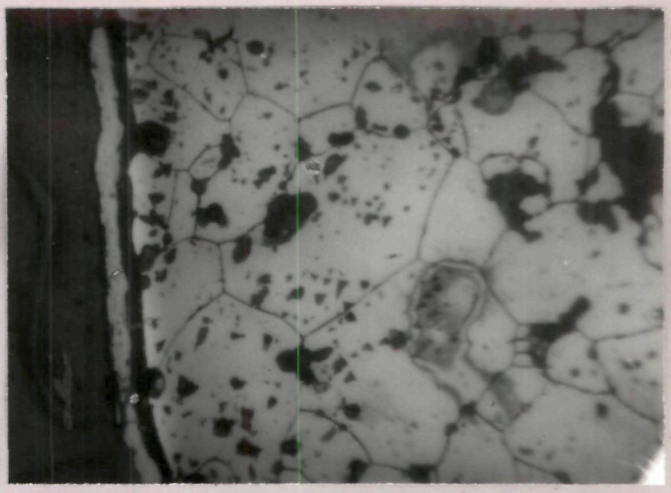

(d) PNC60 - 4Mo

Fig. 3·21

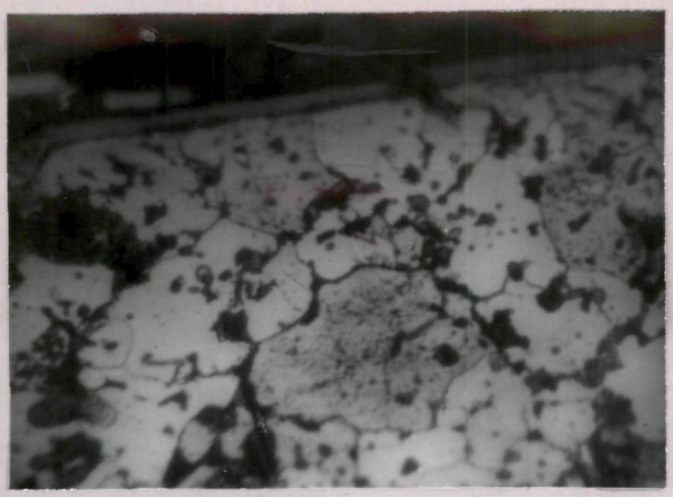

(a) NC - 1MCM

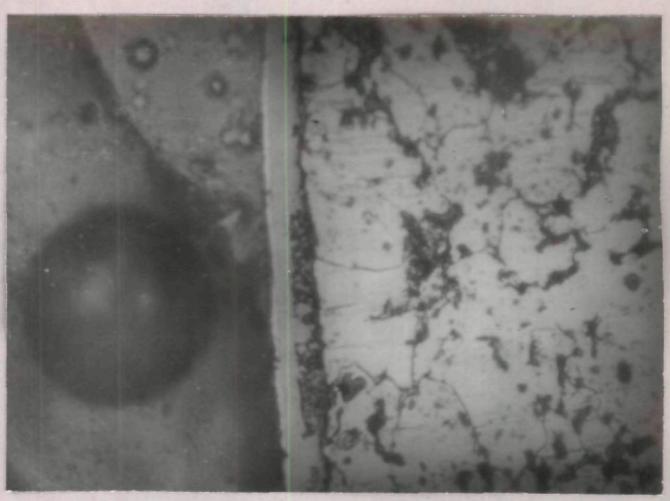

(b) NC - 1MCM

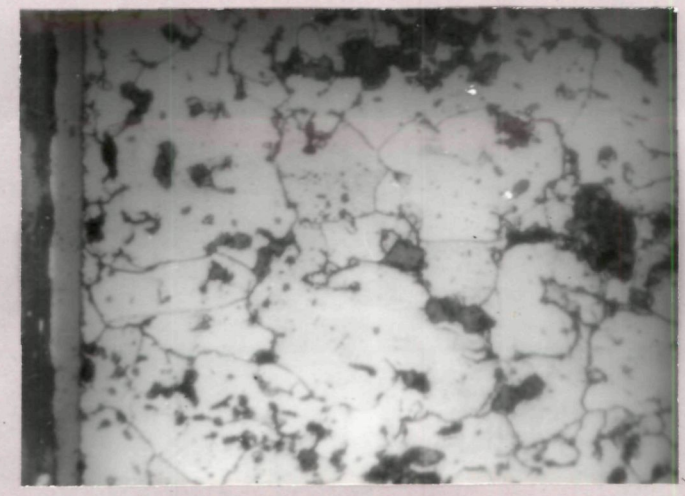

(c) NC - 2MCM

Fig. 3·22

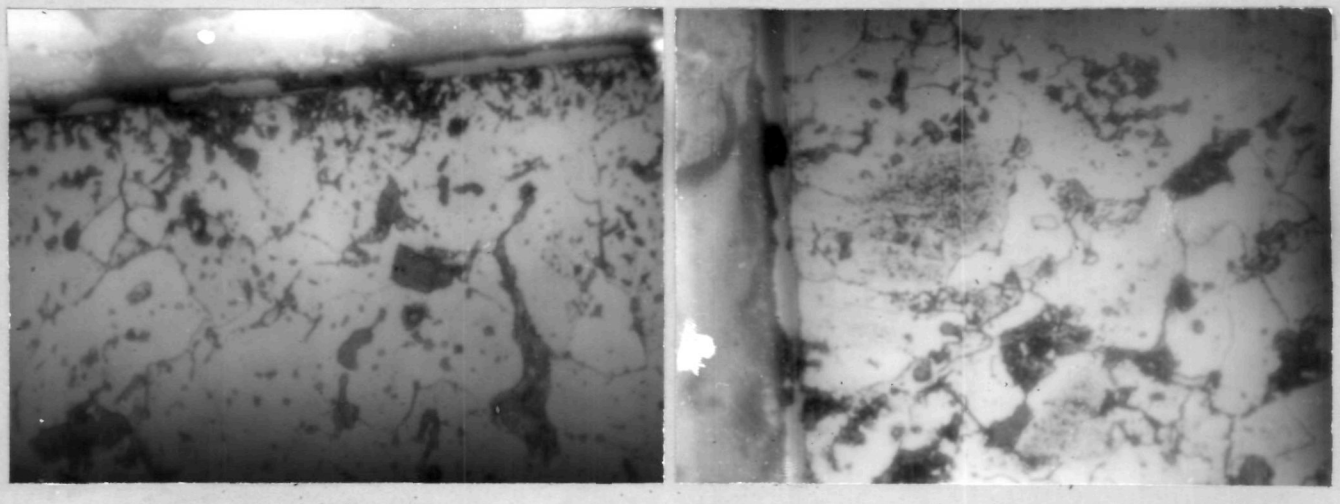

(d) NC - 3MCM (e)

Fig.3·22

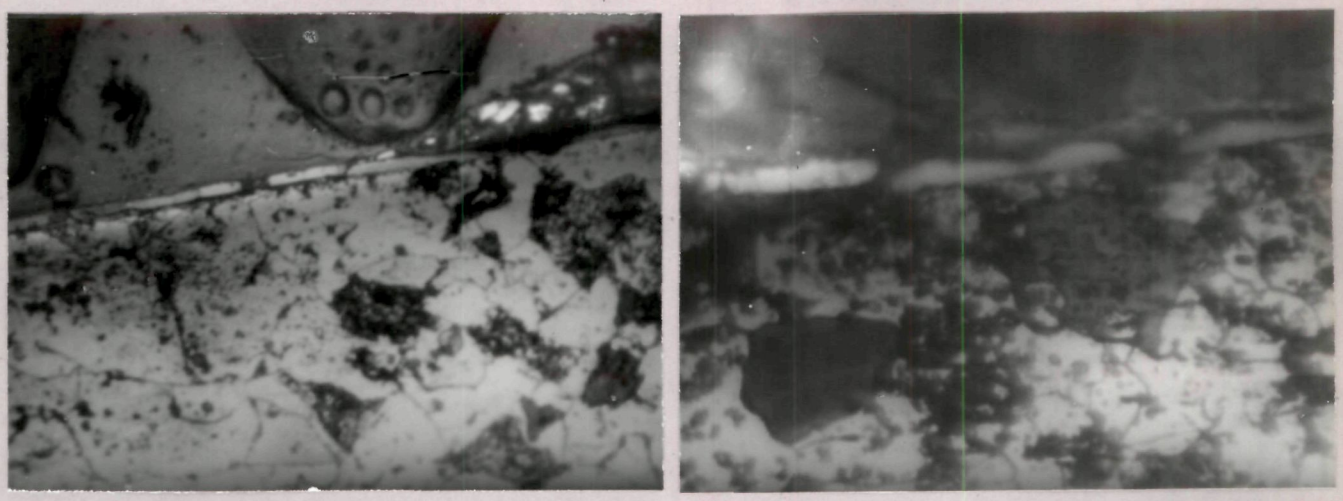

(a) NC - 4MCM (b)

Fig. 3·23

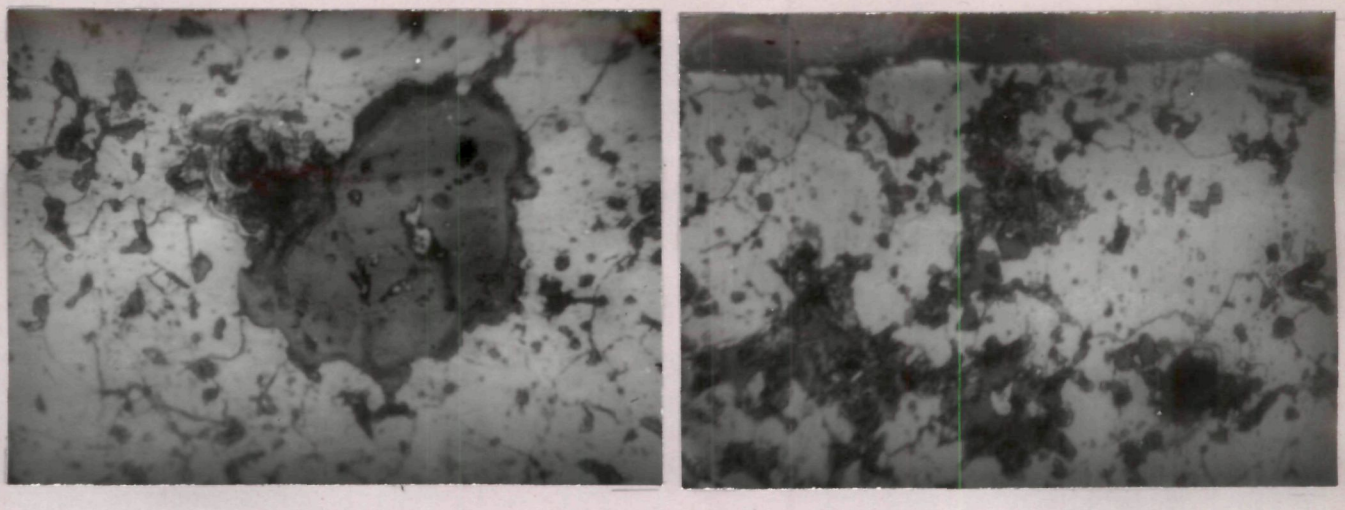

(a) PNC45 - 1MCM (b)

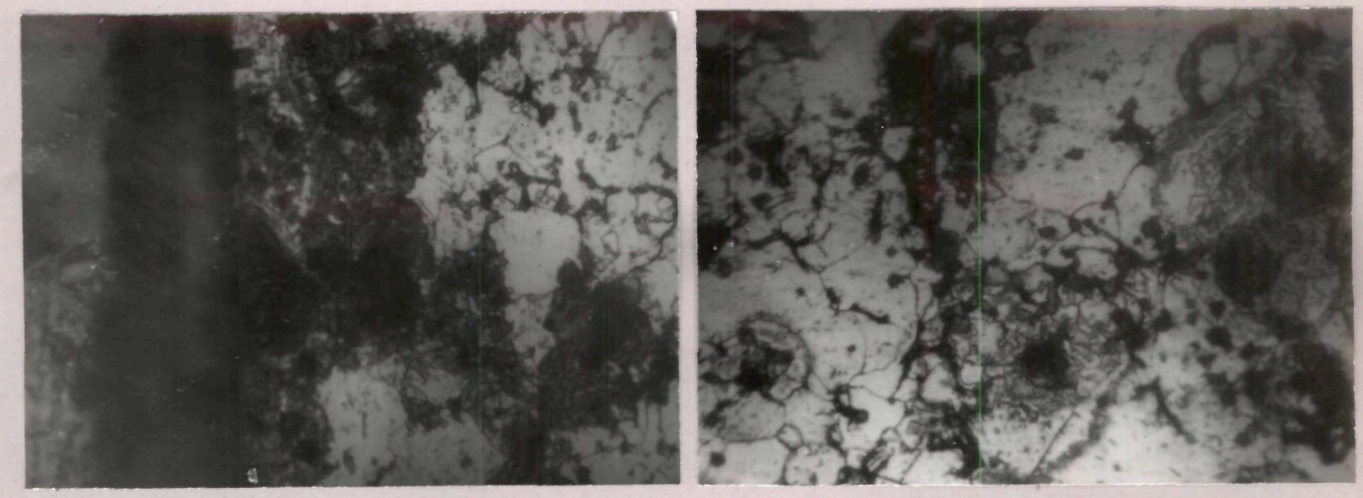

(c) PNC45 - 4MCM (d)

Fig. 3·24

(a) PNC 60 - 2MCM (b)

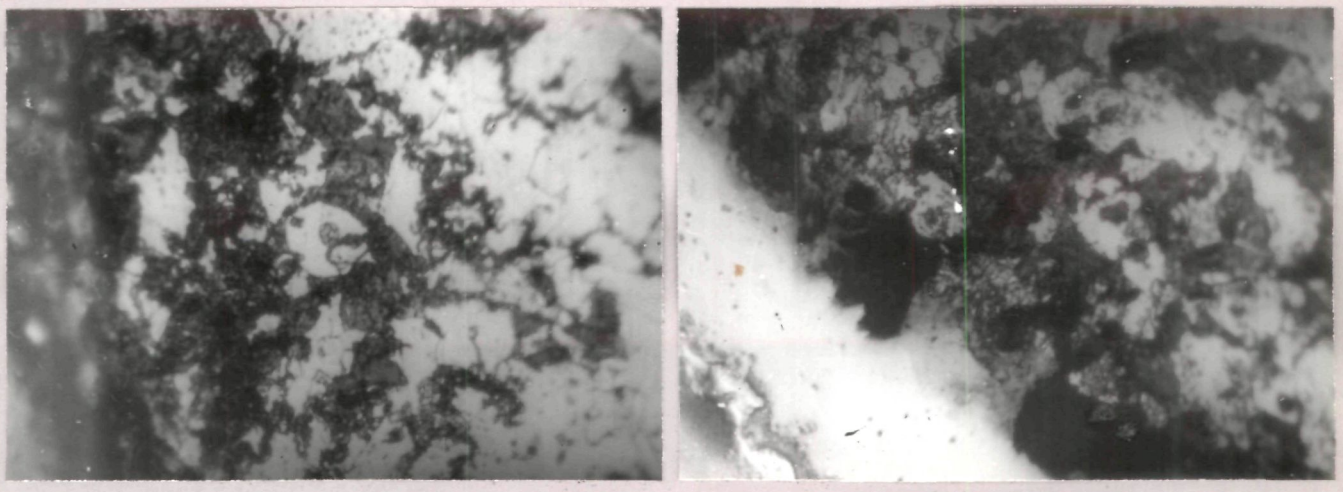

(c) PNC60 - 3MCM (d)

Fig. 3·25

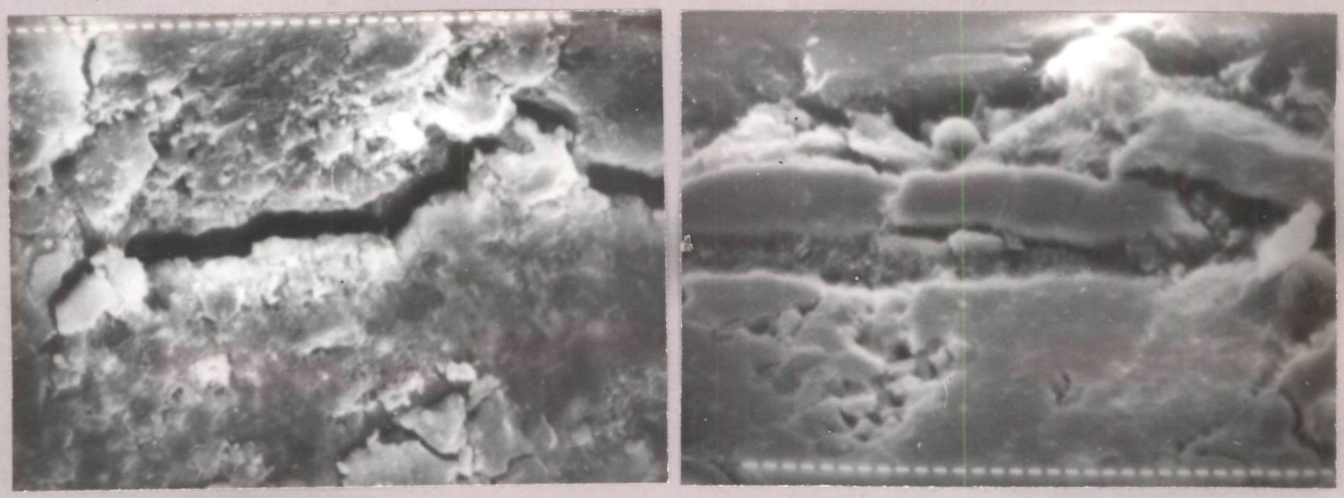

(a) PNC60-1MCM (b) PNC60-4MCM

1280X

Fig. 3·26

increasing Cu content on sharpness and definition of oxide layer is marginal (Fig. 3.27a and 3.27b). The oxide layer obtained is relatively sharp. Sharpness of oxide layer is improved but thickness is reduced by increasing P content to 0.6 wt. % and Mo content to 2 % (Fig. 3.27c).

In case of MCM-containing compacts, increasing MCM content and increasing treatment times increases the rate of oxidation (Fig. 3.28). Increasing copper content increases oxidation and yields diffuse oxide layer (Fig. 3.28c).

In case of Ni-containing compacts, the oxide layer formed is very thin at 10 minutes of treatment times while with higher treatment times and higher copper contents no well defined oxide layers are formed. (Figs. 3.29a and 3.29b). Microstructural observation does not give any conclusive result. The structures are heterogenous.

3.1.4 Microhardness determination

Microhardness values (Table III.1.2) show that with increase in P content, there is significant increase in microhardness values. An increase in hardness values of about 100-150 HV0.1 is observed when P content is increased

(a) PNC45 - 1Mo - 1Cu

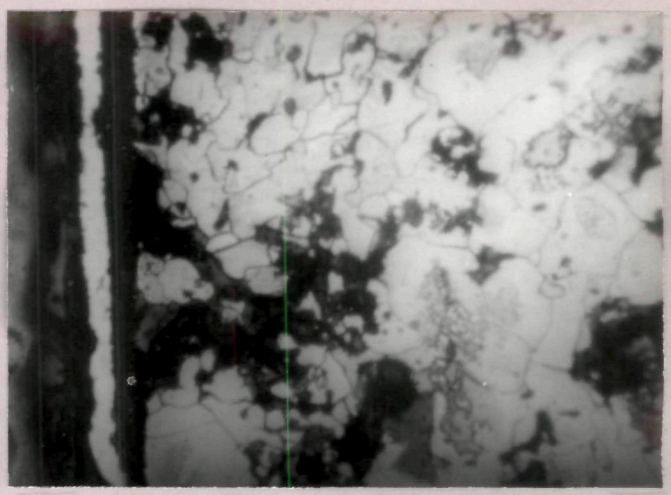

(b) PNC45 - 1Mo - 4Cu

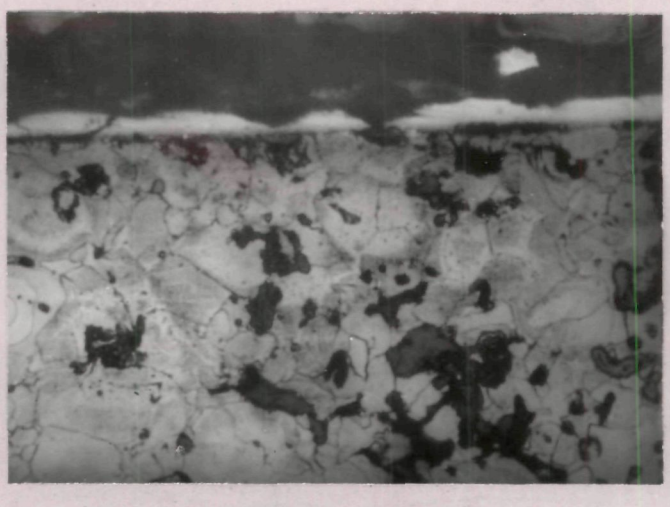

(c) PNC60 - 2Mo - 4Cu

Fig. 3·27

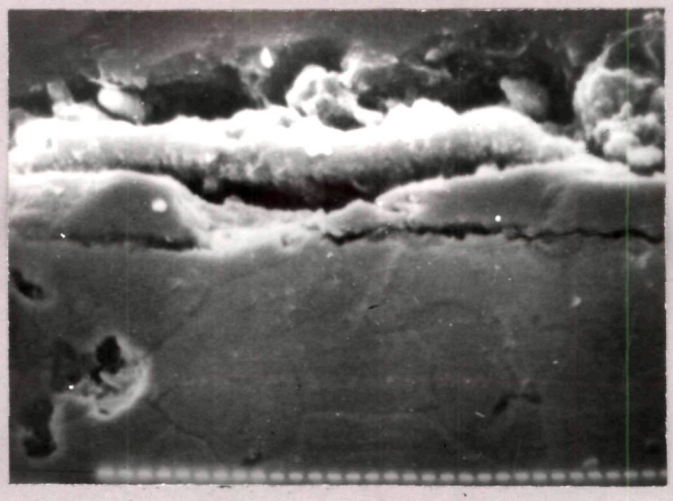

(d) PNC60-2Mo-4Cu

1280X

Fig. 3·27

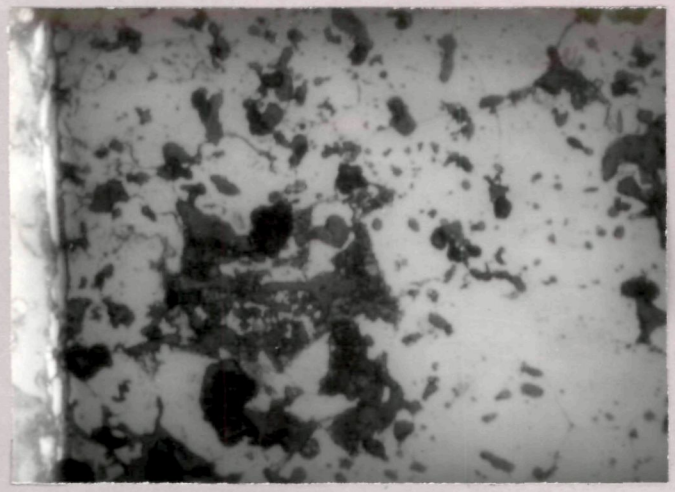

(a) PNC60 - 2MCM - 1Cu

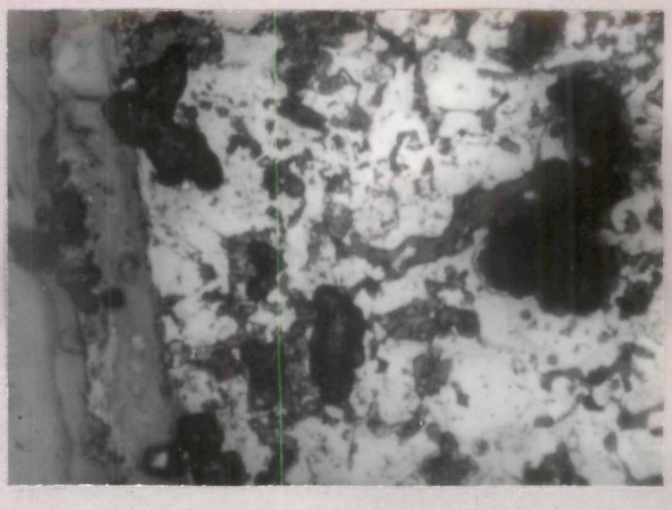

(b) PNC60 - 4MCM - 4Cu

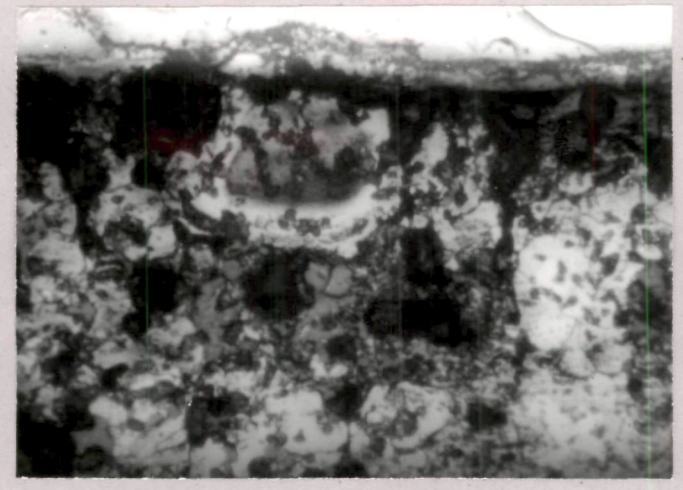

(c) PNC60 - 4MCM - 4Cu

Fig. 3·28

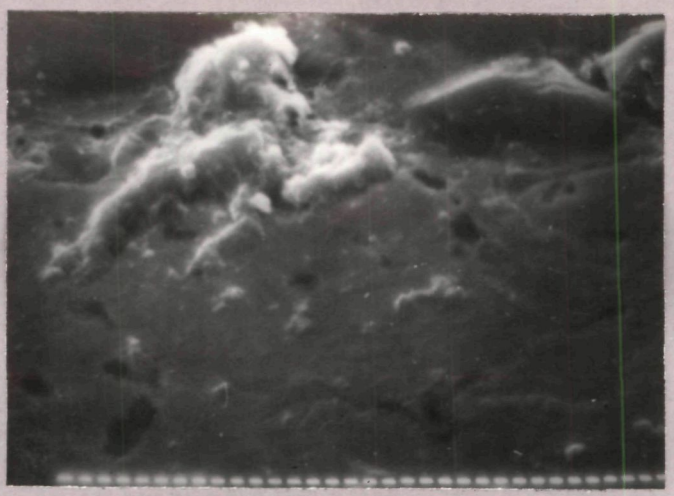

(d) PNC60 - 4MCM - 4Cu

1280X

Fig. 3·28

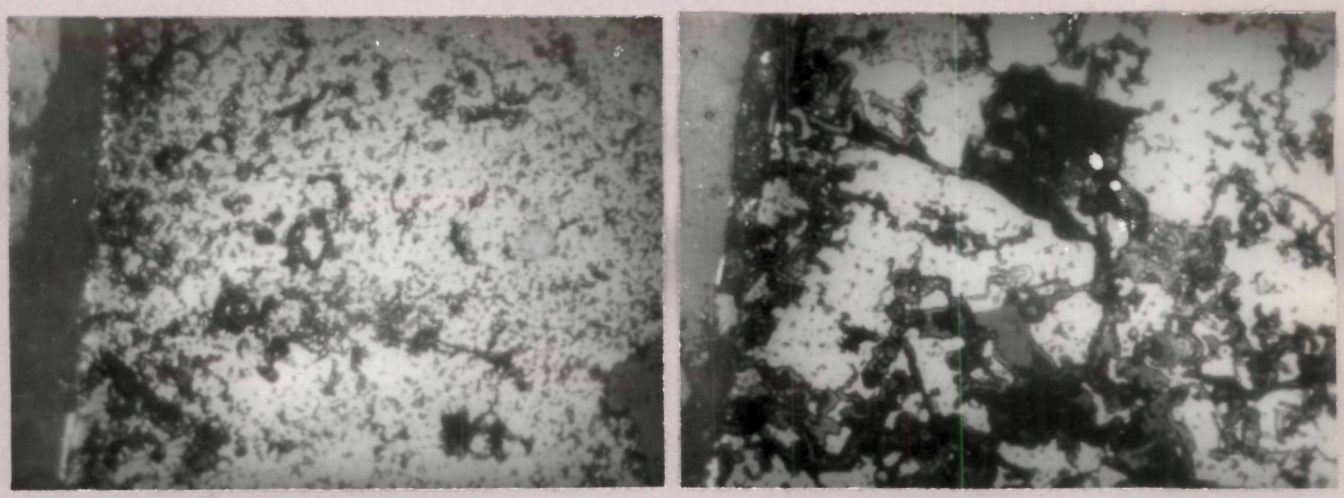

(a) PNC60 - 4Ni - 1Cu (b) PNC60 - 4Ni - 4Cu

Fig. 3·29

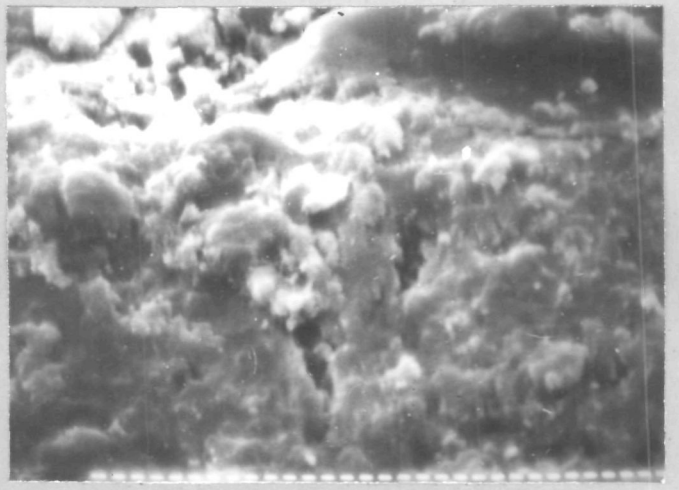

(c) PNC 60 - 4Ni - 4Cu

1280 X

Fig. 3·29

Table III.1.2 Microhardness values of the Steam Oxidized Samples

Alloy	Time in minutes	Hardness HV0.1	Alloy	Time in minutes	Hardness HV0.1
NC100.24	30	183.0	NC-1Cu	30	259.0
NC100.24	60	186.0	NC-1Cu	60	262.0
NC100.24	90	206.3	NC-1Cu	90	265.0
PNC30	30	193.0	NC-2Cu	30	262.0
PNC30	60	236.6	NC-2Cu	60	266.0
PNC30	90	240.6	NC-2Cu	90	270.0
PNC45	30	285.0	NC-3Cu	30	270.0
PNC45	60	290.0	NC-3Cu	60	272.0
PNC45	90	292.0	NC-3Cu	90	279.0
PNC60	30	309.0	NC-4Cu	30	276.0
PNC60	60	330.0	NC-4Cu	60	278.0
PNC60	90	351.3	NC-4Cu	90	286.0

Continued ....

Table III.1.2 continued

Alloy	Time in minutes	Hardness HV0.1	Alloy	Time in minutes	Hardness HV0.1
PNC30-1Cu	30	267.0	PNC45-1Cu	30	288.0
PNC30-1Cu	60	268.0	PNC45-1Cu	60	295.0
PNC30-1Cu	90	277.0	PNC45-1Cu	90	299.0
PNC30-2Cu	30	270.0	PNC45-2Cu	30	289.0
PNC30-2Cu	60	272.0	PNC45-2Cu	60	295.0
PNC30-2Cu	90	278.0	PNC45-2Cu	90	301.0
PNC30-3Cu	30	273.0	PNC45-3Cu	30	290.0
PNC30-3Cu	60	279.0	PNC45-3Cu	60	299.0
PNC30-3Cu	90	284.0	PNC45-3Cu	90	309.0
PNC30-4Cu	30	279.0	PNC45-4Cu	30	300.0
PNC30-4Cu	60	283.0	PNC45-4Cu	60	305.0
PNC30-4Cu	90	290.0	PNC45-4Cu	90	325.0

Continued ....

Table III.1.2 continued

Alloy	Time in minutes	Hardness HV0.1	Alloy	Time in minutes	Hardness HV0.1
PNC60-1Cu	30	326.0	PNC30-1Mo	30	309.0
PNC60-1Cu	60	333.0	PNC30-1Mo	60	311.0
PNC60-1Cu	90	345.0	PNC30-1Mo	90	323.0
PNC60-2Cu	30	341.0	PNC30-2Mo	30	308.0
PNC60-2Cu	60	346.0	PNC30-2Mo	60	311.0
PNC60-2Cu	90	353.0	PNC30-2Mo	90	325.0
PNC60-3Cu	30	360.0	PNC30-3Mo	30	313.0
PNC60-3Cu	60	366.0	PNC30-3Mo	60	317.0
PNC60-3Cu	90	371.0	PNC30-3Mo	90	327.0
PNC60-4Cu	30	370.0	PNC30-4Mo	30	318.0
PNC60-4Cu	60	379.0	PNC30-4Mo	60	321.0
PNC60-4Cu	90	385.0	PNC30-4Mo	90	339.0

Continued ....

Table III.1.2 continued

Alloy	Time in minutes	Hardness HV0.1	Alloy	Time in minutes	Hardness HV0.1
PNC60-1Mo	30	341.0	NC-1MCM	30	407.6
PNC60-1Mo	60	347.0	NC-1MCM	60	419.0
PNC60-1Mo	90	356.0	NC-1MCM	90	439.0
PNC60-2Mo	30	344.6	NC-2MCM	30	408.0
PNC60-2Mo	60	355.6	NC-2MCM	60	427.0
PNC60-2Mo	90	369.0	NC-2MCM	90	442.0
PNC60-3Mo	30	353.0	NC-3MCM	30	411.0
PNC60-3Mo	60	367.0	NC-3MCM	60	427.0
PNC60-3Mo	90	379.0	NC-3MCM	90	445.0
PNC60-4Mo	30	357.0	NC-4MCM	30	421.0
PNC60-4Mo	60	381.0	NC-4MCM	60	461.0
PNC60-4Mo	90	399.0	NC-4MCM	90	488.0

Continued ....

Table III.1.2 continued

Alloy	Time in minutes	Hardness HV0.1	Alloy	Time in minutes	Hardness HV0.1
PNC30-1MCM	30	430.0	PNC45-1MCM	30	405.0
PNC30-1MCM	60	442.0	PNC45-1MCM	60	461.0
PNC30-1MCM	90	444.0	PNC45-1MCM	90	463.0
PNC30-2MCM	30	431.0	PNC45-2MCM	30	405.0
PNC30-2MCM	60	445.0	PNC45-2MCM	60	450.0
PNC30-2MCM	90	451.0	PNC45-2MCM	90	465.0
PNC30-3MCM	30	455.0	PNC45-3MCM	30	425.0
PNC30-3MCM	60	460.0	PNC45-3MCM	60	451.0
PNC30-3MCM	90	477.0	PNC45-3MCM	90	470.0
PNC30-4MCM	30	454.0	PNC45-4MCM	30	459.0
PNC30-4MCM	60	478.0	PNC45-4MCM	60	488.0
PNC30-4MCM	90	496.0	PNC45-4MCM	90	521.0

Continued ....

Table III.1.2 continued

Alloy	Time in minutes	Hardness HV0.1	Alloy	Time in minutes	Hardness HV0.1
PNC60-1MCM	30	491.0	PNC45-1Mo-1Cu	30	355.0
PNC60-1MCM	60	521.0	PNC45-1Mo-1Cu	60	369.0
PNC60-1MCM	90	542.0	PNC45-1Mo-1Cu	90	373.0
PNC60-2MCM	30	501.0	PNC45-1Mo-4Cu	30	351.0
PNC60-2MCM	60	524.0	PNC45-1Mo-4Cu	60	363.0
PNC60-2MCM	90	541.0	PNC45-1Mo-4Cu	90	370.0
PNC60-3MCM	30	515.0	PNC45-2Mo-1Cu	30	401.0
PNC60-3MCM	60	535.0	PNC45-2Mo-1Cu	60	409.0
PNC60-3MCM	90	541.0	PNC45-2Mo-1Cu	90	421.0
PNC60-4MCM	30	588.6	PNC45-2Mo-4Cu	30	350.0
PNC60-4MCM	60	605.0	PNC45-2Mo-4Cu	60	359.0
PNC60-4MCM	90	622.6	PNC45-2Mo-4Cu	90	366.0

Continued ....

Table III.1.2 continued

Alloy	Time in minutes	Hardness HV0.1	Alloy	Time in minutes	Hardness HV0.1
PNC60-2Mo-1Cu	30	385.0	PNC60-2MCM-1Cu	30	378.0
PNC60-2Mo-1Cu	60	389.0	PNC60-2MCM-1Cu	60	381.0
PNC60-2Mo-1Cu	90	400.0	PNC60-2MCM-1Cu	90	385.0
PNC60-2Mo-4Cu	30	379.0	PNC60-2MCM-4Cu	30	380.0
PNC60-2Mo-4Cu	60	383.0	PNC60-2MCM-4Cu	60	386.0
PNC60-2Mo-4Cu	90	397.0	PNC60-2MCM-4Cu	90	389.0
PNC60-4Mo-1Cu	30	435.0	PNC60-4MCM-1Cu	30	520.0
PNC60-4Mo-1Cu	60	451.6	PNC60-4MCM-1Cu	60	523.0
PNC60-4Mo-1Cu	90	465.3	PNC60-4MCM-1Cu	90	540.0
PNC60-4Mo-4Cu	30	391.0	PNC60-4MCM-4Cu	30	405.0
PNC60-4Mo-4Cu	60	393.0	PNC60-4MCM-4Cu	60	420.0
PNC60-4Mo-4Cu	90	410.0	PNC60-4MCM-4Cu	90	433.0

Continued ....

Table III.1.2 continued

Alloy	Time in minutes	Hardness HV0.1
PNC60-2Ni-1Cu	30	310.6
PNC60-2Ni-1Cu	60	339.0
PNC60-2Ni-1Cu	90	364.0
PNC60-2Ni-4Cu	30	281.0
PNC60-2Ni-4Cu	60	283.0
PNC60-2Ni-4Cu	90	290.0
PNC60-4Ni-1Cu	30	343.0
PNC60-4Ni-1Cu	60	351.0
PNC60-4Ni-1Cu	90	355.0
PNC60-4Ni-4Cu	30	311.0
PNC60-4Ni-4Cu	60	341.0
PNC60-4Ni-4Cu	90	368.0

from 0 to 0.6 wt. %.

In case of PNC60 compacts, increase of treatment time also shows marginal increase in hardness values.

In case of Fe-P-Cu compacts, there occurs a very slight increase in microhardness values with increasing Cu or P content. Increasing treatment time also does not increase microhardness value to any significant degree.

In case of Fe-P-Mo compacts, effect of increasing Mo, P or treatment time is in general similar to that mentioned above in case of Fe-P-Cu compacts. The microhardness values obtained in case of Fe-P, Fe-P-Cu or Fe-P-Mo compacts does not exceed 400 HV0.1.

In case of Fe-P-MCM compacts, microhardness values generally increase with increasing P content and also with increasing MCM content at a particular level of phosphorus. Microhardness values obtained in this system range between 400 to 622 HV0.1.

In ternary compacts microhardness values obtained are in the order MCM → Mo → Ni in decreasing magnitude.

FIGURE CAPTIONS

Fig. 3.1 Weight gain with respect to time of steam treatment at 500°C for sintered Fe-P alloys.

Fig. 3.2 Weight gain with respect to time of steam treatment at 500°C for sintered Fe-P-Cu alloys.

Fig. 3.3 Weight gain with respect to time of steam treatment at 500°C for sintered Fe-P-Mo alloys.

Fig. 3.4 Weight gain with respect to time of steam treatment at 500°C for sintered Fe-P-MCM alloys.

Fig. 3.5 Weight gain with respect to time of steam treatment at 500°C for sintered (a) Fe-P-MCM-Cu, (b) and (c) Fe-P-Mo-Cu and (d) Fe-P-Ni-Cu.

Fig. 3.6 Variation of hardness with time of steam treatment at 500°C for sintered Fe-P alloys.

Fig. 3.7 Variation of hardness with time of steam treatment at 500°C for sintered Fe-P-Cu alloys.

Fig. 3.8 Variation of hardness with time of steam treatment at 500°C for sintered Fe-P-Cu alloys.

Fig. 3.9 Variation of hardness with time of steam treatment at 500°C for sintered Fe-P-Mo alloys.

Fig. 3.10 Variation of hardness with time of steam treatment at 500°C for sintered Fe-P-MCM alloys.

Fig. 3.11 Variation of hardness with time of steam treatment at 500°C for sintered Fe-P-MCM alloys.

Fig. 3.12 Variation of hardness with time of steam treatment at 500°C for sintered Fe-P-Mo-Cu alloys.

Fig. 3.13 Variation of hardness with time of steam treatment at 500°C for sintered (a) Fe-P-MCM-Cu, (b) Fe-P-Ni-Cu.

Fig. 3.14 Microstructures of sintered and steam treated ferrous alloys showing oxidized layer and matrix region, treated for 90 minutes. Magnification 200X, Nital etched.

Fig. 3.15 Microstructures of sintered and steam treated ferrous alloys showing oxidized layer and matrix region (a), (c) and (e) treated for 30 minutes; (b), (d) and (f) treated for 90 minutes. Magnification 200X, Nital etched.

Fig. 3.16 Scanning electron microstructures of steam treated alloy, (a) and (c) treated for 30 minutes; (b) and (d) treated for 90 minutes.

Fig. 3.17 Scanning electron microstructures of steam treated alloy, (a) and (c) treated for 30 minutes; (b) and (d) treated for 90 minutes.

Fig. 3.18 Scanning electron microstructures of steam treated alloy, (a) and (c) treated for 30 minutes; (b) and (d) treated for 90 minutes.

Fig. 3.19 Scanning electron microstructures of steam treated alloy, (a) and (c) treated for 30 minutes; (b) and (d) treated for 90 minutes.

Fig. 3.20 Microstructures of sintered and steam treated ferrous alloys; (a) and (b) treated for 10 minutes; (c) and (d) treated for 90 minutes. Magnification 200X, Nital etched.

Fig. 3.21 Microstructures of sintered at steam treated ferrous alloys, treated for 90 minutes. Magnification 200X, Nital etched.

Fig. 3.22 Microstructures of sintered and steam treated ferrous alloys, (a) and (d) treated for 10 minutes; (b), (c) and (e) treated for 90 minutes. Magnification 200X, Nital etched.

Fig. 3.23 Microstructures of sintered and steam treated ferrous alloy, (a) and (b) treated for 10 and 90 minutes, respectively. Magnification 200X, Nital etched.

Fig. 3.24 Microstructures of sintered and steam treated ferrous alloys, (a) and (c) treated for 10 minu-

tes; (b) and (d) treated for 90 minutes. Magnification 200X, Nital etched.

Fig. 3.25 Microstructures of sintered and steam treated ferrous alloys, (a) and (c) treated for 10 minutes; (b) and (d) treated for 90 minutes. Magnification 200X, Nital etched.

Fig. 3.26 Scanning electron microstructures of steam treated alloys, treated for 90 minutes.

Fig. 3.27 Microstructures (a), (b), (c) and SEM (d) of sintered and steam treated ferrous alloys, treated for 90 minutes.

Fig. 3.28 Microstructures (a), (b), (d) and SEM (d) of sintered and steam treated ferrous alloys, (a), (b) and (d) treated for 90 minutes, (c) treated for 10 minutes.

Fig. 3.29 Microstructures (a), (b) and SEM (c) of sintered and steam treated ferrous alloys, treated for 90 minutes.

Part II

3.2 PROPERTIES OF PASC POWDER COMPACTS

3.2.1 Densification

In case of both PASC30 and PASC80 powder compacts, at 0.3 % carbon level, copper addition upto 2 % decreases sintered density (Fig. 3.30a) while at 0.6 % C level, there is an improvement in densification (Figs. 3.30a and 3.31a). However, linear dimensional change in radial direction is small i.e. -0.1 to +0.2 %.

At 0.3 % C level, 1 % of nickel addition decreases sintered density after which effect of either carbon or nickel increase on sintered density and densification parameter is marginal (Figs. 3.30b and 3.31b) in PASC30- as well as PASC80 powder compacts. Linear dimensional change increases regularly with increase in either Ni or C content (Figs. 3.30b and 3.31b). Increase in P content from 0.3 to 0.8 % increases growth of Fe-C-Ni sintered test pieces (Figs. 3.30b and 3.31b).

At 0.3 % C content, increasing molybdenum content improves sintered density while at 0.6 % C level, the role of molybdenum on densification changes (Figs. 3.30c and 3.31c). With a change from PASC30 to PASC80 powder compacts,

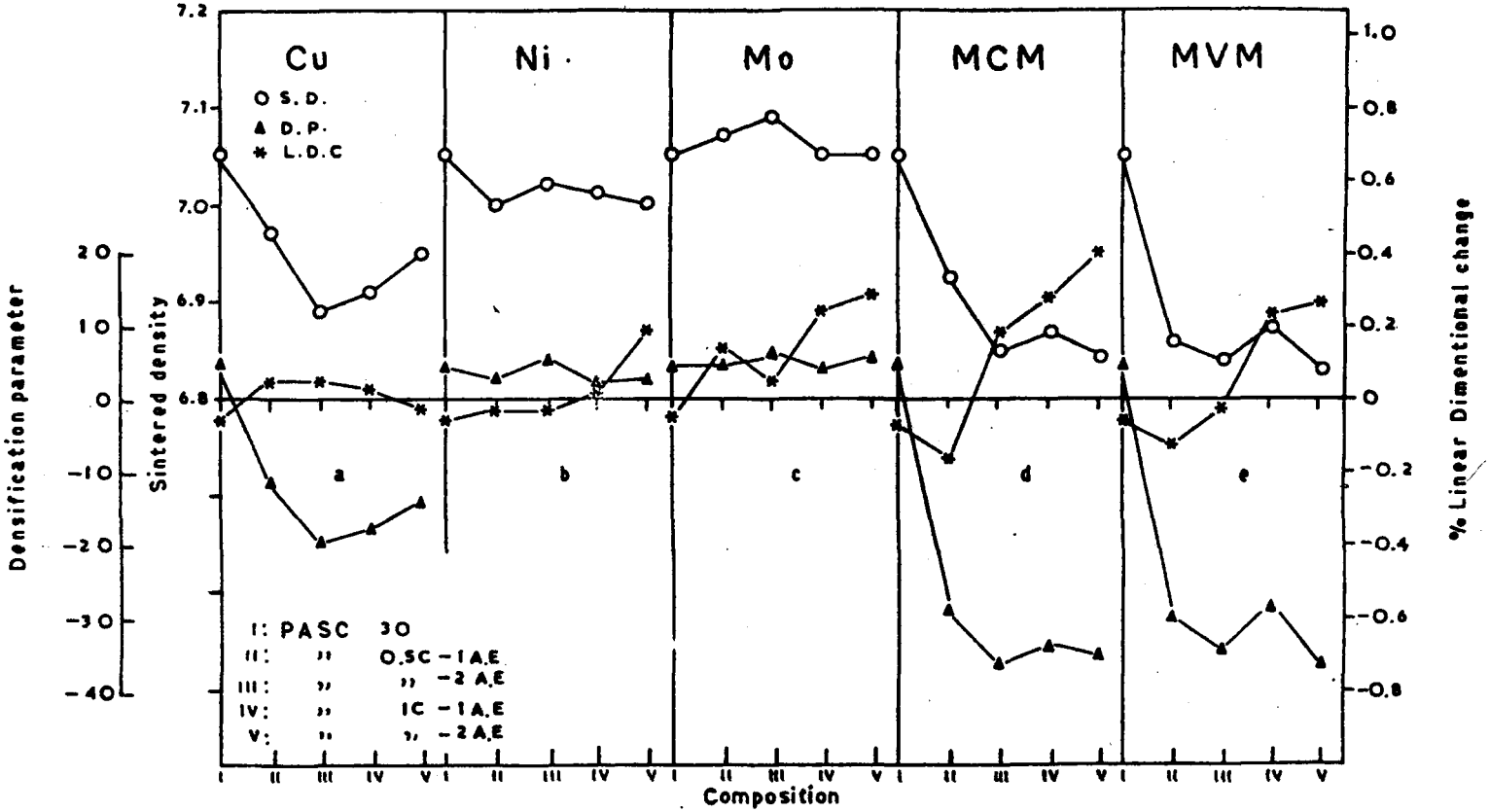
Cu
Ni
Mo
MCM
MVM
O S.D.
▲ D.P.
* L.D.C
Densification parameter
Sintered density
% Linear Dimentional change
Composition
a
b
c
d
e
I: PASC 30
II: " O.5C - 1A.E
III: " " - 2 A.E
IV: " 1C - 1A.E
V: " " - 2A.E

Fig. 3.30

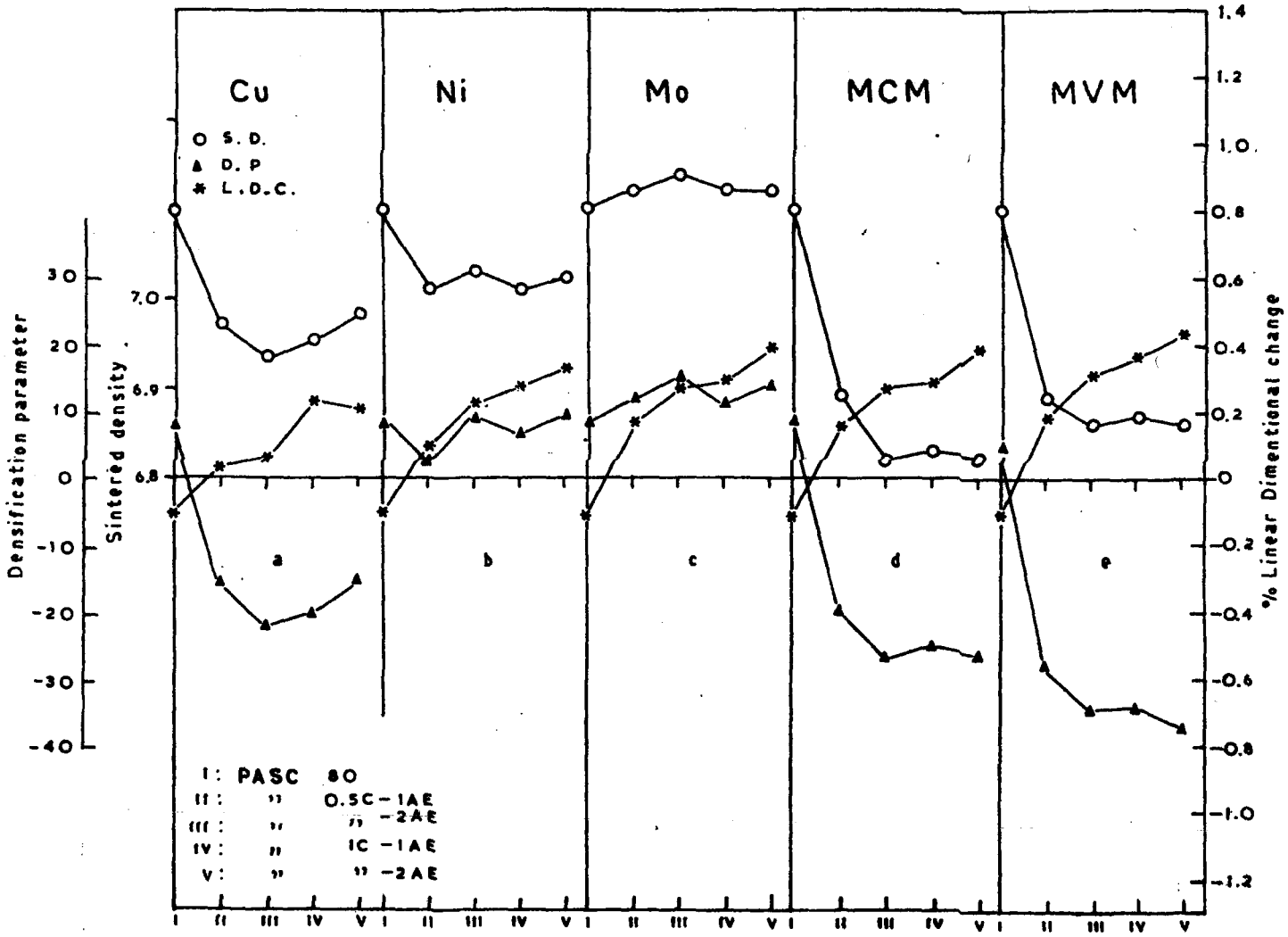
Cu
Ni
Mo
MCM
MVM
S. D.
D. P
L.D.C.
Densification parameter
Sintered density .
% Linear Dimentional change
a
b
c
d
e
I : PASC 80
II : " 0.5C-1AE
III : " " -2AE
IV : " 1C -1AE
V : " " -2AE

Fig. 3.31

magnitude of growth in Fe-C-Mo system increases (Figs. 3.30c and 3.31c).

At 0.3 % C level, MCM addition upto 2 % sharply decreases sintered density and densification parameter of both PASC30 as well as PASC80 powder compacts while at 0.6 % C level, the effect of equal amount of MCM addition on such sintered properties is marginal (Figs. 3.30d and 3.31d). The trend of linear dimensional change variation in case of PASC-C-MCM compacts is similar to that of sintered density or densification parameter variation.

The effect of MVM addition of densification and linear dimensional change of sintered PASC-C compacts is generally similar to that of MCM addition (Figs. 3.30e and 3.31e). Increase in P-content from 0.3 to 0.8 % improves densification of Fe-C-MCM/MVM compacts (Figs. 3.30d and e, 3.31d and e).

3.2.2 Tensile properties

Both ultimate tensile and yield strengths increase with increasing copper and/or carbon contents in case of sintered PASC30 powder compacts (Fig. 3.32a). However, ductility, in general, decreases with increasing copper contents at both C-levels of 0.3 and 0.6 % (Fig. 3.32a).

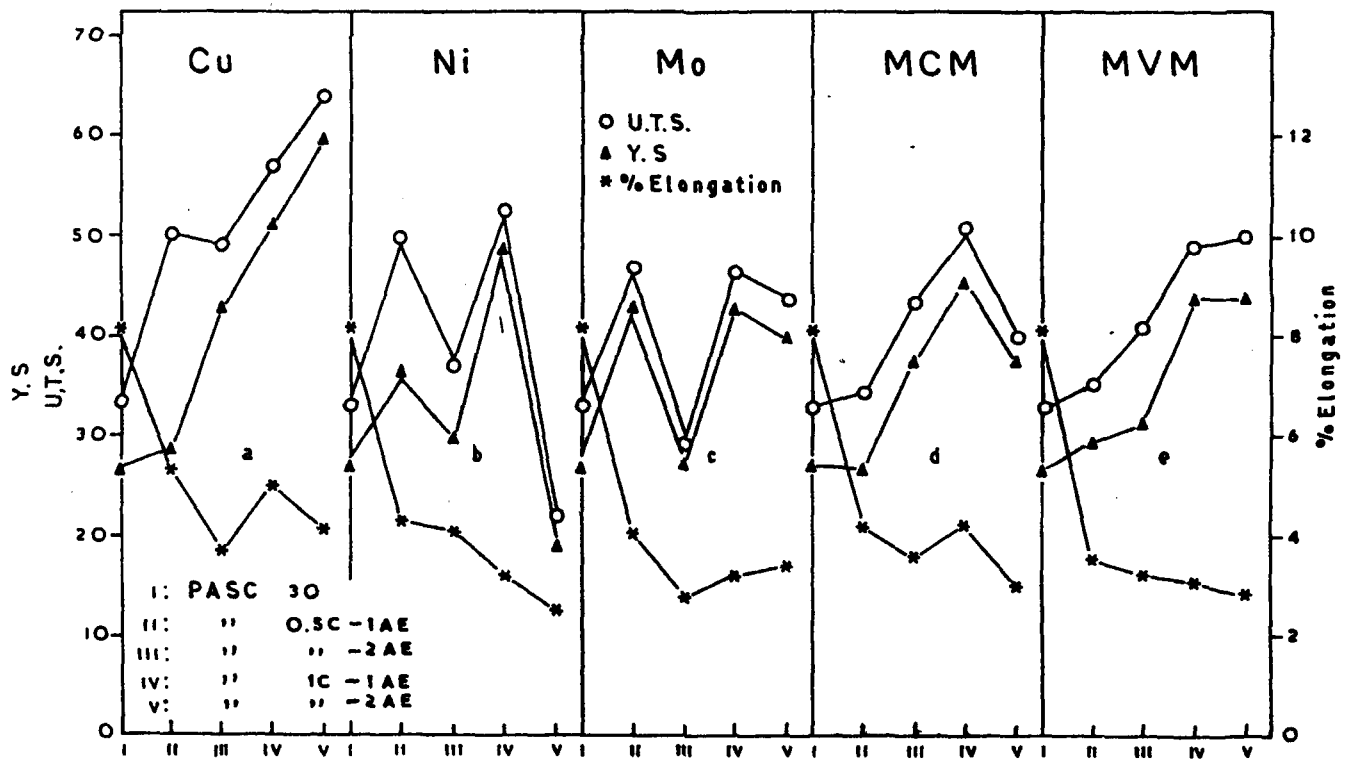
Cu
Ni
Mo
MCM
MVM
O U.T.S.
▲ Y.S
* % Elongation
Y.S
U.T.S.
% Elongation
I: PASC 30
II: " 0.5C-1AE
III: " " -2AE
IV: " 1C-1AE
V: " " -2AE
a
b
c
d
e

Fig. 3.32

When phosphorus content was increased from 0.3 to 0.8 %, UTS and Y.S. decrease initially with 1 % Cu addition at 0.3 % C level and then increase at either C contents (Fig. 3.33a). The variation of ductility in case of PASC80 powder compacts is similar to that of PASC30 powder compacts (Figs. 3.32a and 3.33a). The difference between UTS and YS of sintered PASC-0.3C-1 to 2 Cu powder compacts is relatively large which is narrowed down at higher C and/or P levels (Figs. 3.32a and 3.33a). The magnitude of UTS and YS in case of PASC80 sintered powder compacts is smaller than that in case of PASC30 premixes (Figs. 3.32a and 3.33).

In case of PASC30 premixes, at 0.3 % as well as 0.6 % C level, when nickel content was increased from 1 to 2 %, UTS and YS decrease (Fig. 3.32b). Ductility regularly falls with C and/or Ni addition keeping either element constant (Fig. 3.32b). When P-content was increased, both UTS and YS increase upto 0.6 C and 1 % Ni after which there is a fall (Fig. 3.33b). Initial addition of 0.3 % C and 1 % Ni to PASC80 premixes, decreases ductility to a very significant extent after which the change in elongation percentage is marginal (Fig. 3.33b).

Variation of tensile properties in case of Mo-

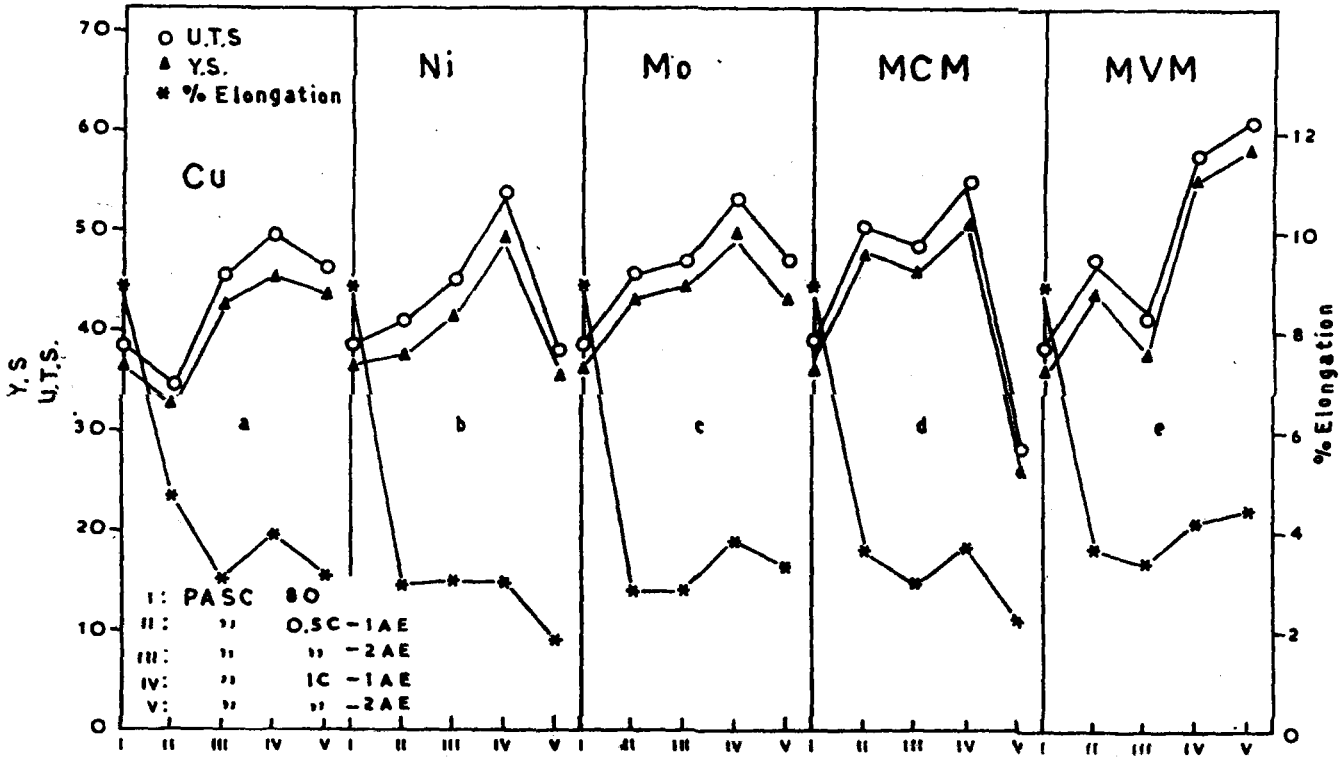
o U.T.S
▲ Y.S.
* % Elongation
Cu
Ni
Mo
MCM
MVM
a
b
c
d
e
I: PASC 80
II: " O.SC-1AE
III: " " -2AE
IV: " IC -1AE
V: " " -2AE
Y.S
U.T.S.
% Elongation
0
10
20
30
40
50
60
70
2
4
6
8
10
12
I II III IV V

Fig.3.33

containing compacts, is in general, similar to that of Ni-containing compacts (Figs. 3.32c and 3.33c). However, the magnitude of strengths is slightly higher at higher P-content but the effect of phosphorus on ductility is insignificant (Fig. 3.33c).

In case of PASC30 premixes, strength properties improve upto 0.3 % C and 2 % MCM while ductility, in general decreases (Fig. 3.32d). Generally, similar trend in tensile properties variation is noticed at higher P-level of 0.8 % (Fig. 3.33d).

In case of PASC30 compacts, strength properties improve with either C and/or MVM additions while ductility decreases with such additions (Fig. 3.32e). In general, a similar trend in tensile properties variation is observed when P-content was increased from 0.3 to 0.8 %

3.2.3 Anisotropic dimensional change

In order to have an idea about isotropy of growth or shrinkage, shrinkage ratio defined as radial dimensional change divided by axial dimensional change (with respect to direction of pressing) after sintering have been plotted in Fig. 3.34. Side by side, volume shrinkage with similar additions of alloying elements have been plotted. It can

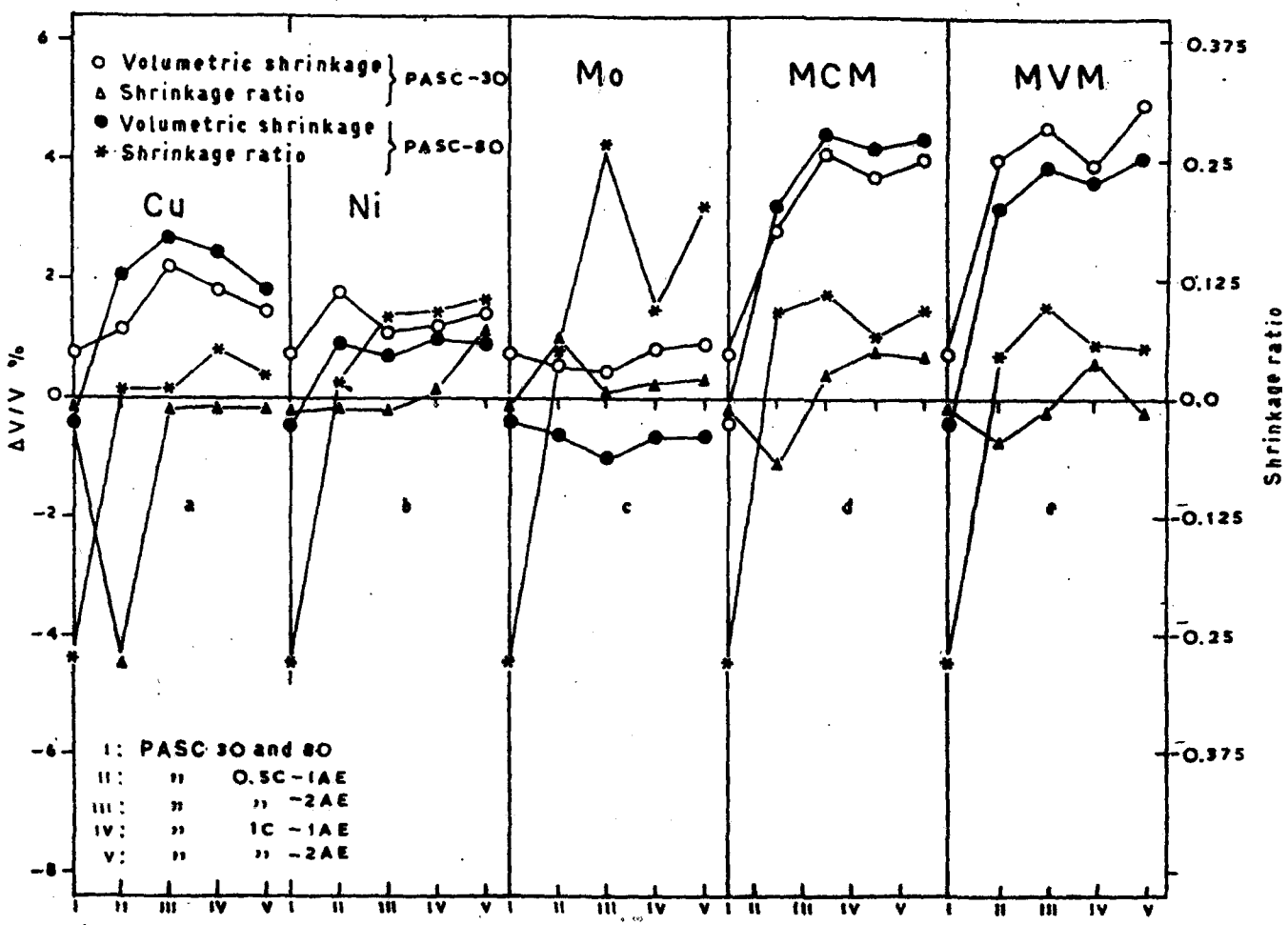
Volumetric shrinkage
Shrinkage ratio
PASC-30
Volumetric shrinkage
Shrinkage ratio
PASC-80
Cu
Ni
Mo
MCM
MVM
ΔV/V %
Shrinkage ratio
a
b
c
d
e
I: PASC 30 and 80
II: " 0.5C-1AE
III: " " -2AE
IV: " 1C -1AE
V: " " -2AE

Fig. 3.34

be observed (Fig. 3.34a to e) that the variation of volume shrinkage, is in general, similar to that of densification parameter variation. However, volume shrinkage does not vary similar to that of linear dimensional change (Figs. 3.30, 3.31 and 3.34). This is because of an isotropic shrinkage or growth.

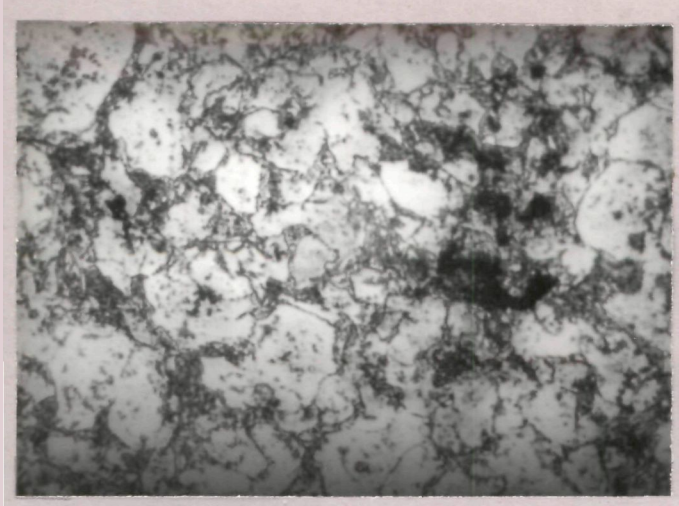

(a) PASC30 - 0·3C - 2Cu

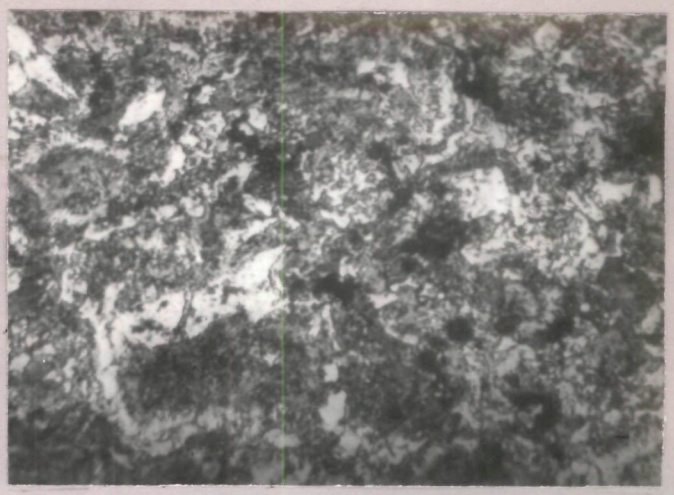

(b) PASC30 - 0·6C - 2Cu

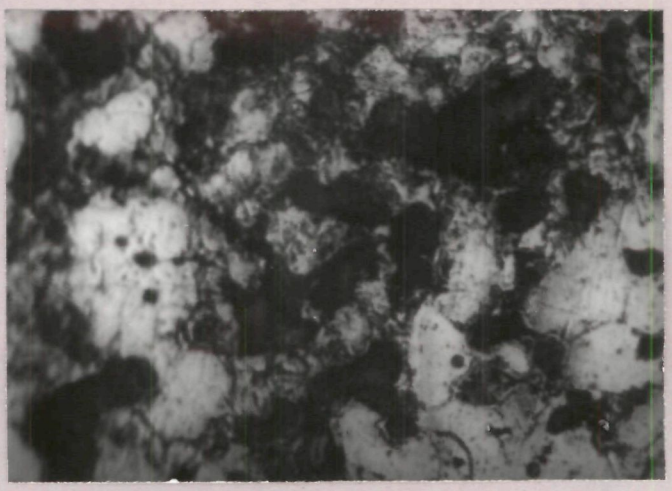

(c) PASC80 - 0·6C - 2Cu

Fig. 3·35

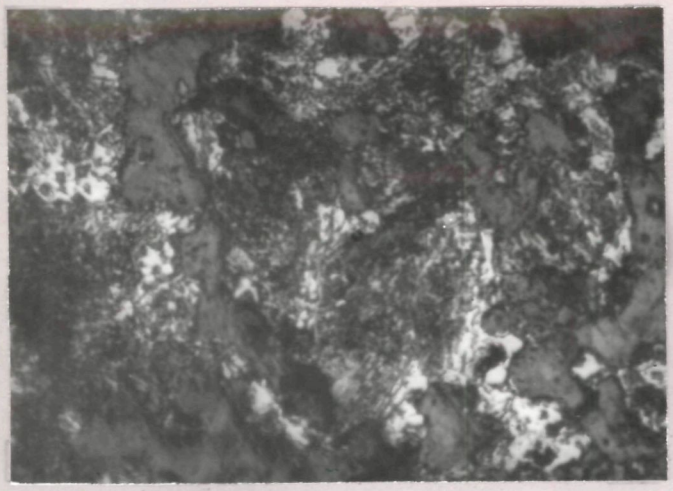

(d) PASC80 - 0·6C - 2Ni

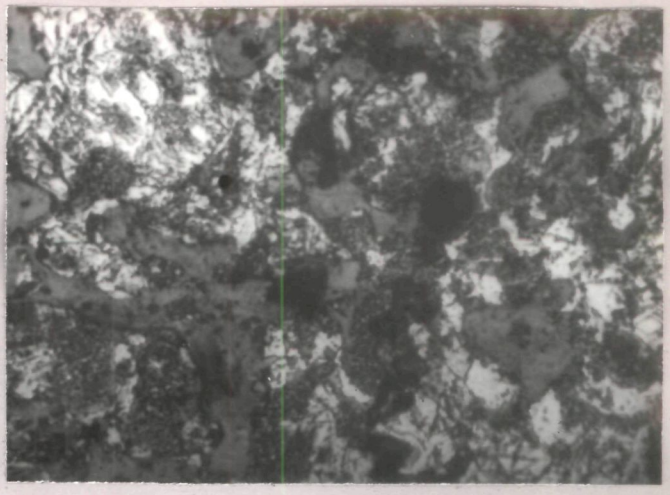

(e) PASC80 - 0·6C - 2Mo

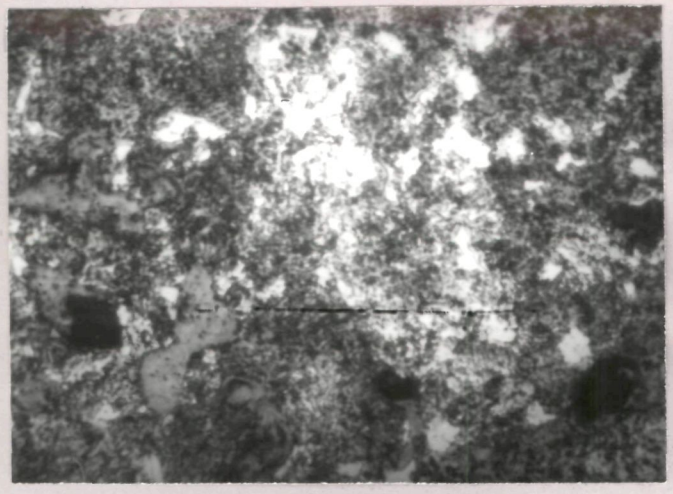

(f) PASC80 - 0·6C - 2MCM

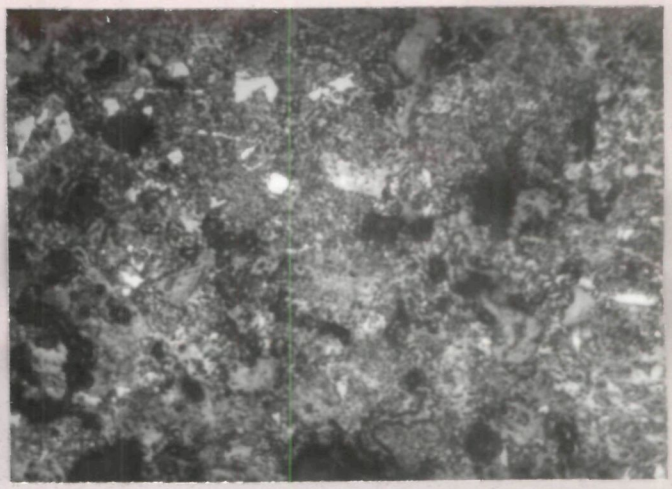

(g) PASC80 - 0·6C - 2MVM

Fig. 3·35

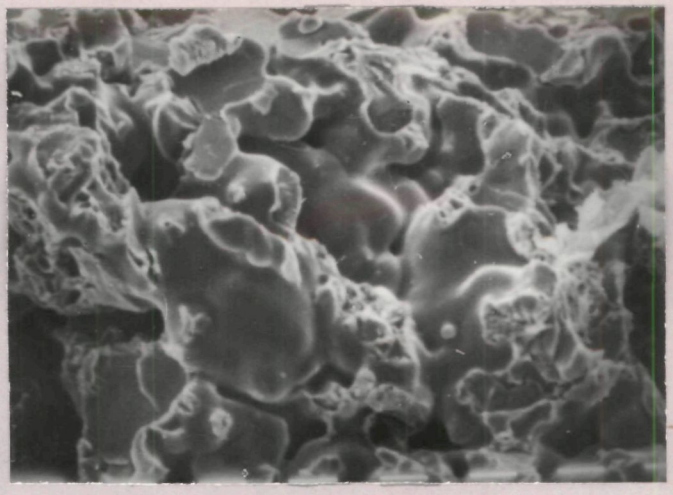

(a) PASC30-0·3C- 2Cu

800X

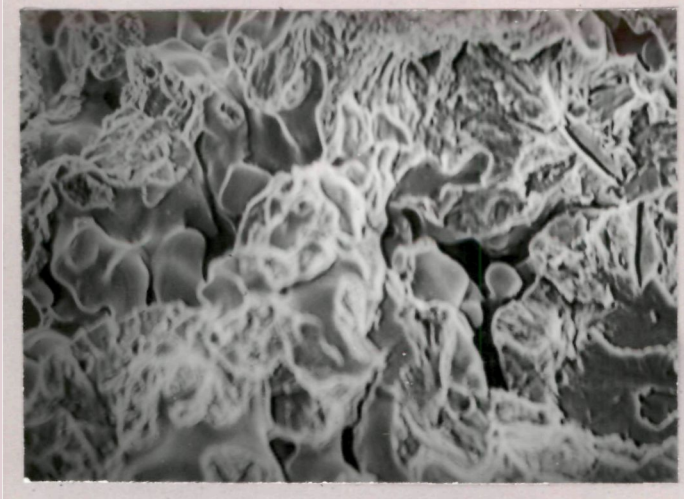

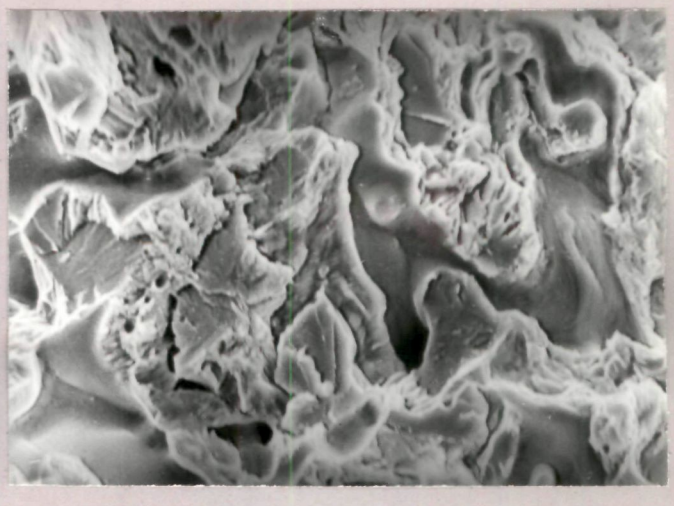

(b) 600X PASC30-0·6C-2Cu (b) 1200X

Fig. 3·36

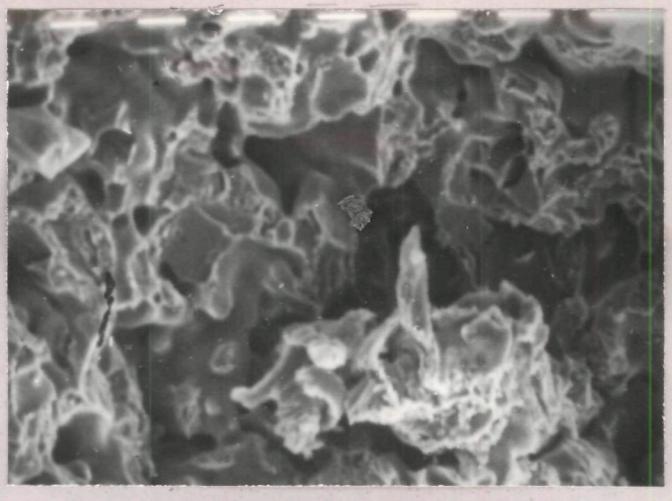

(a) PASC30-0·3C-2Ni

800X

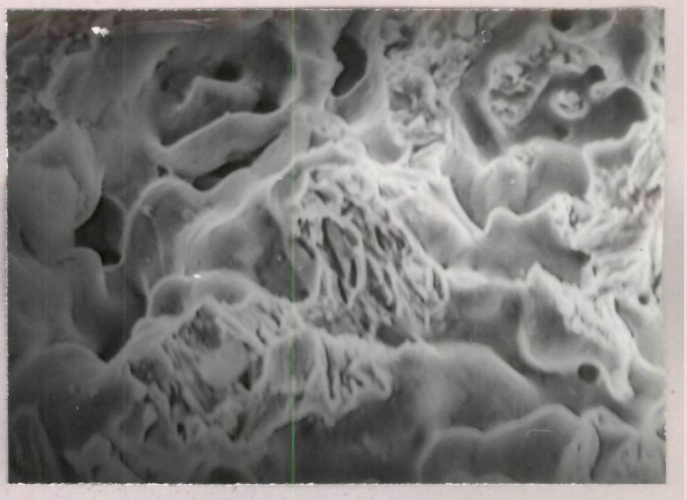

(b) 600X PASC30-0·6C-2Ni (b) 1200X

Fig. 3·37

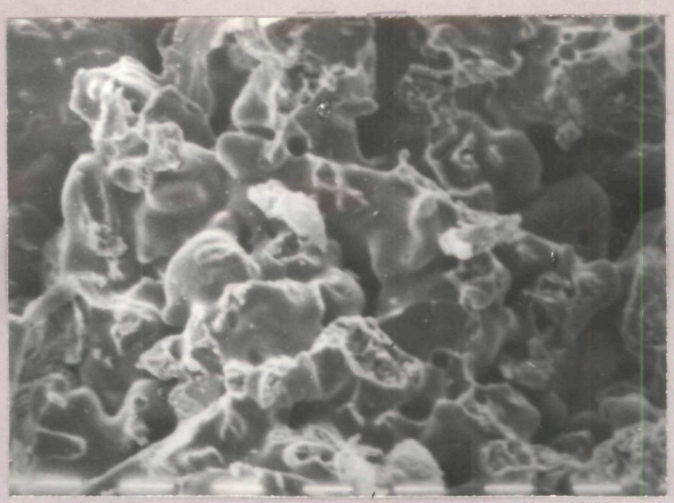

(a) PASC30 - 0·3C - 2Mo

800X

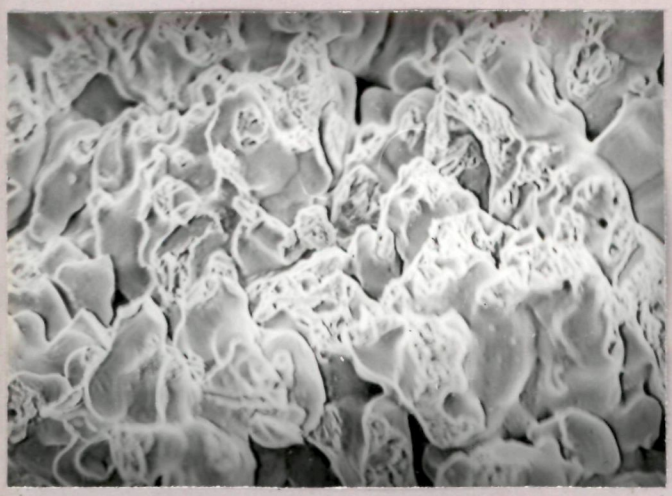

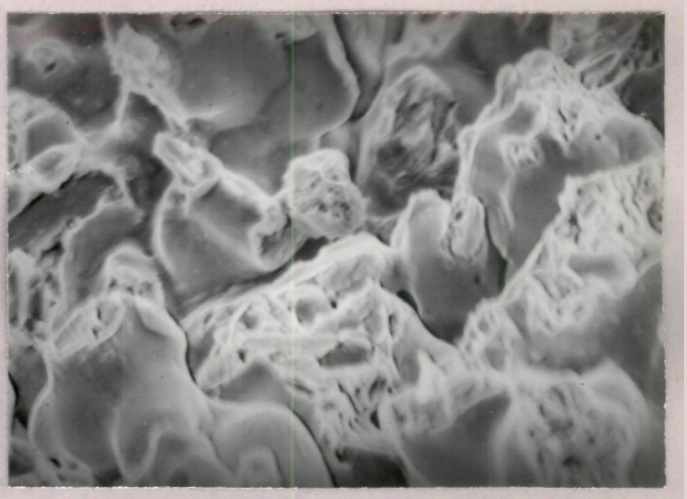

(b) 600X PASC30-0·6C-2Mo (b) 1200X

Fig. 3·38

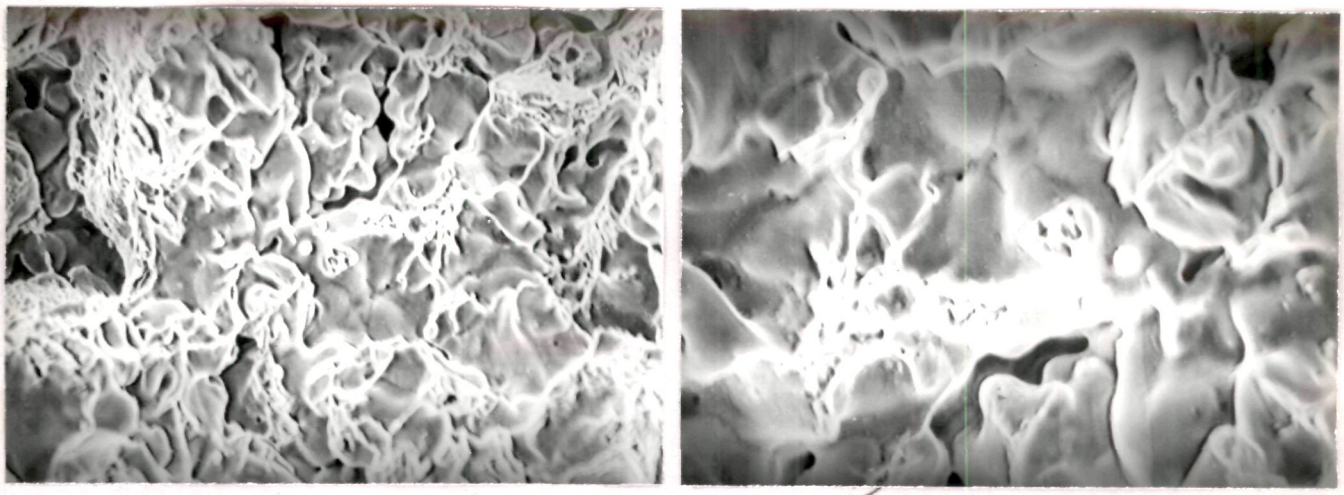

(a) 600X PASC30-0·3C-2MCM (a) 1200X

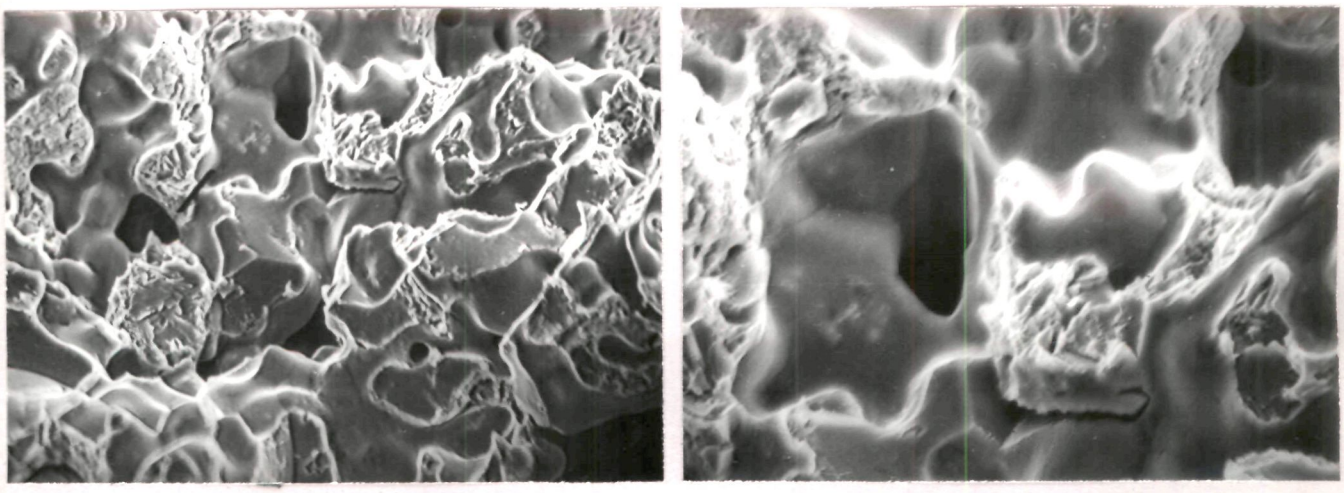

(b) 600X PASC30-0·6-2MCM (b) 1200X

Fig. 3·39

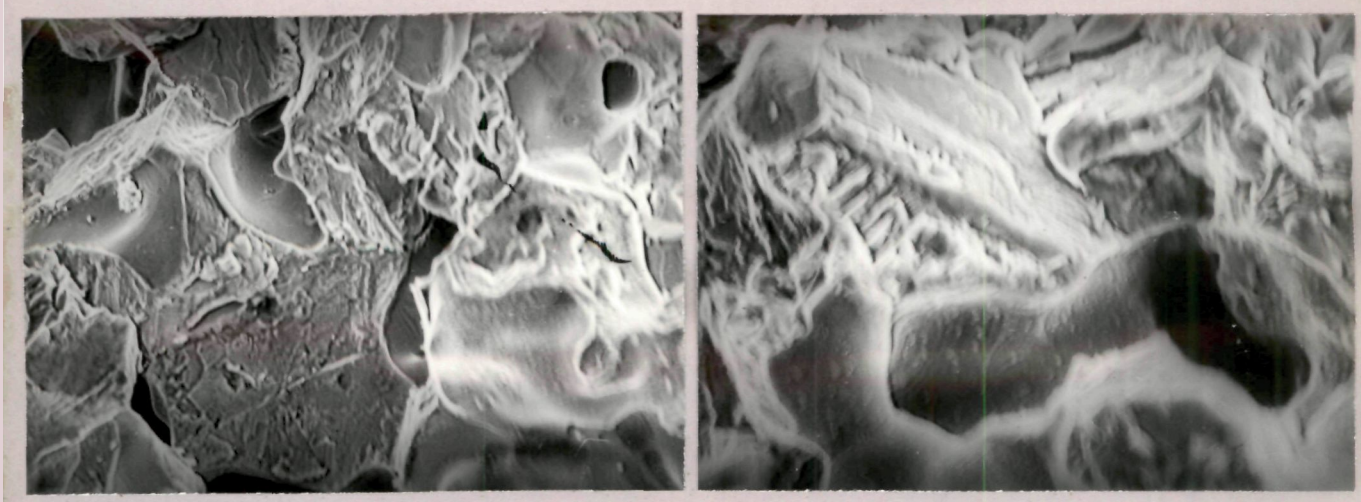

(c) 600X PASC80-0·6C-2MCM (c) 1200X

Fig. 3·39

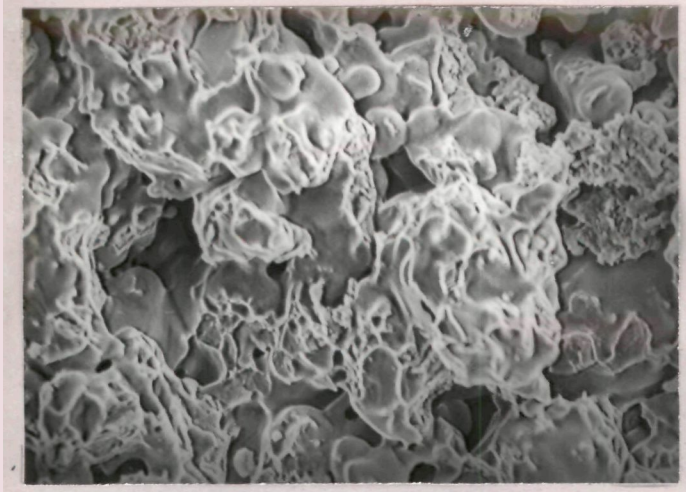

(a) 600X PASC30-0·3C-2MVM (a) 1200X

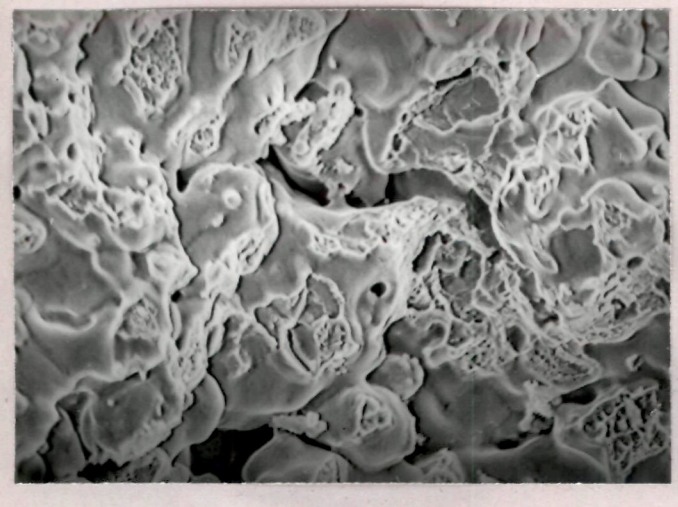

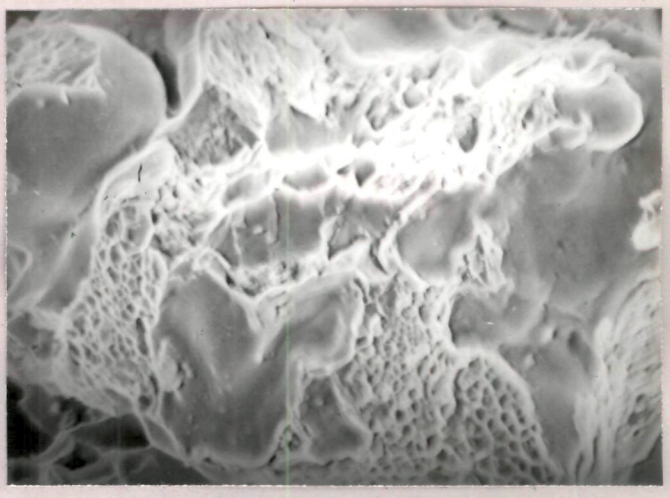

(b) 600X PASC30-0·6C-2MVM (b) 1200X

Fig. 3·40

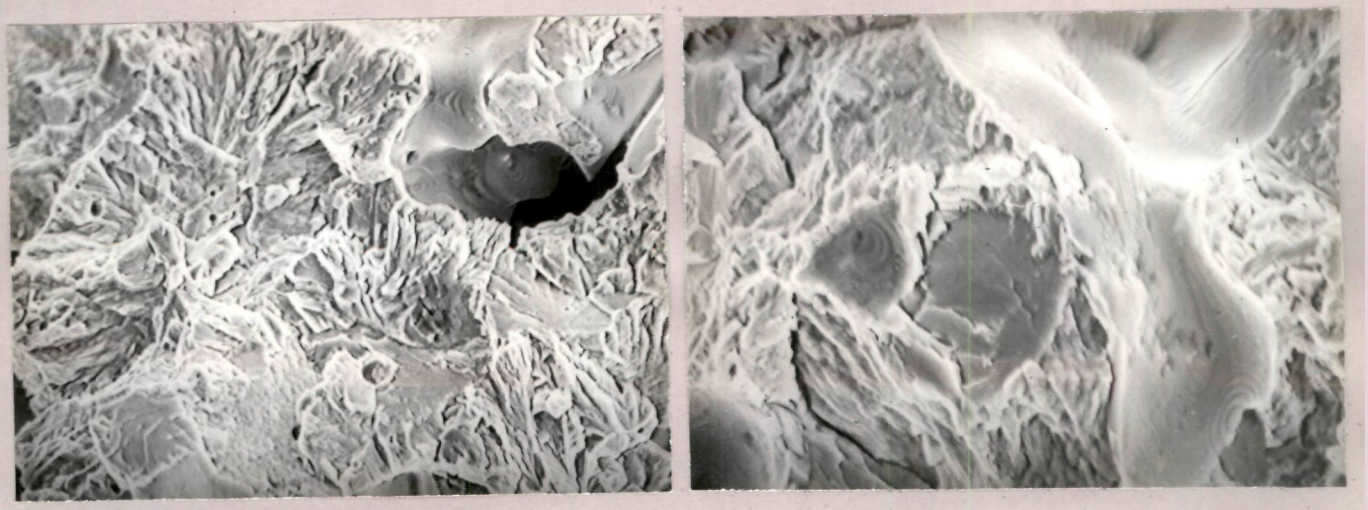

(c) 600 X PASC 80 - 0·6C - 2MVM (c) 1200 X

Fig. 3·40

Fig. 3.30 Sintered properties of PASC30-C- alloying element powder compacts sintered at 1393 K for 1.8 ks in dissociated ammonia. Compaction pressure 691 MPa.

Fig. 3.31 Sintered properties of PASC80-C- alloying element powder compacts sintered at 1393 K for 1.8 ks in dissociated ammonia. Compaction pressure 691 MPa.

Fig. 3.32 Tensile properties of PASC-C- alloying element powder compacts sintered at 1393 K for 1.8 ks in dissociated ammonia. Compaction pressure 691 MPa.

Fig. 3.33 Tensile properties of PASC80-C- alloying element powder compacts sintered at 1393 K for 1.8 ks in dissociated ammonia. Compaction pressure 691 MPa.

Fig. 3.34 Shrinkage ratio and volumetric shrinkage of PASC30/80-C- alloying element powder compacts sintered at 1393 K for 1.8 ks in dissociated ammonia. Compaction pressure 691 MPa.

Fig. 3.35 Microstructures of steels sintered at 1393 K for 1.8 ks in dissociated ammonia, compaction pressure 691 MPa Mag. 400X, Nital etched.

Fig. 3.36 Scanning Electron Fractographs of broken tensile test pieces, sintered at 1393 K for 1.8 ks in dissociated ammonia. Compaction pressure 691 MPa.

Fig. 3.37 Scanning Electron Fractographs of broken tensile test pieces, sintered at 1393 K for 1.8 ks in dissociated ammonia. Compaction pressure 691 MPa.

Fig. 3.38 Scanning Electron Fractographs of broken tensile test pieces, sintered at 1393 K for 1.8 ks in dissociated ammonia. Compaction pressure 691 MPa.

Fig. 3.39 Scanning Electron Fractographs of broken tensile test pieces, sintered at 1393 K for 1.8 ks in dissociated ammonia. Compaction pressure 691 MPa.

Fig. 3.40 Scanning Electron Fractographs of broken tensile test pieces sintered at 1393 K for 1.8 ks in dissociated ammonia. Compaction pressure 691 MPa.

Part III

3.3 STEAM TREATMENT OF PASC POWDER COMPACTS

3.3.1 Kinetic studies

Kinetic studies of steam treatment on sintered PNC powder compacts at 500°C has shown that below 30 minutes of treatment times, variation of weight gain with treatment times is linear (Figs. 3.1-3.5). Further, because of atomized iron powder, higher sintered densities have been obtained in PASC powder compacts (Figs. 3.41-3.65 and Table III.3.2), particularly in higher P-content of 0.8 %. Hence steam treatment times were varied from 45 to 120 minutes. In all the PASC powder compacts either 0.3 or 0.6 % combined C are present.

3.3.1.1 PASC-Cu-C compacts

There is a rapid increase in mass gain with treatment times from 45 to 60 minutes in case of almost all the compacts irrespective of Cu, P or C levels (Fig. 3.41). 0.3 % C and 1 % Cu in PASC30 sintered powder compacts increase the oxidation rate (Fig. 3.41a). However, this situation is not so evident at higher P-content of 0.8 % (Fig. 3.41b). When Cu-content is increased from 1 to 2 % keeping the C-content constant, weight gain invariably increases (Figs. 3.41a and b).

Table III.3.1 Green density levels of Fe-P compacts containing various alloying additions; compaction pressure : 691 MPa

Alloy system	Green density Mg/m^3	Alloy system	Green density Mg/m^3
PASC30	7.086	PASC80	7.090
PASC30-0.3C-1Cu	7.095	PASC80-0.3C-1Cu	7.092
PASC30-0.3C-2Cu	7.093	PASC80-0.3C-2Cu	7.094
PASC30-0.6C-1Cu	7.084	PASC80-0.6C-1Cu	7.085
PASC30-0.6C-2Cu	7.094	PASC80-0.6C-2Cu	7.087
PASC30-0.3C-1Ni	7.095	PASC30-0.3C-1Ni	7.088
PASC30-0.3C-2Ni	7.094	PASC30-0.3C-2Ni	7.096
PASC30-0.6C-1Ni	7.094	PASC30-0.6C-1Ni	7.088
PASC30-0.6C-2Ni	7.094	PASC30-0.6C-2Ni	7.086
PASC30-0.3C-1Mo	7.095	PASC80-0.3C-1Mo	7.093
PASC30-0.3C-2Mo	7.096	PASC80-0.3C-2Mo	7.093
PASC30-0.6C-1Mo	7.094	PASC80-0.6C-1Mo	7.095
PASC30-0.6C-2Mo	7.095	PASC80-0.6C-2Mo	7.093

Continued ....

Table III.3.1 continued

Alloy system	Green density Mg/m^3	Alloy system	Green density Mg/m^3
PASC30-0.3C-1MCM	7.093	PASC80-0.3C-1MCM	7.087
PASC30-0.3C-2MCM	7.093	PASC80-0.3C-2MCM	7.086
PASC30-0.6C-1MCM	7.090	PASC80-0.6C-1MCM	7.090
PASC30-0.6C-2MCM	7.094	PASC80-0.6C-2MCM	7.112
PASC30-0.3C-1MVM	7.089	PASC80-0.3C-1MVM	7.087
PASC30-0.3C-2MVM	7.095	PASC80-0.3C-2MVM	7.091
PASC30-0.6C-1MVM	7.096	PASC80-0.6C-1MVM	7.093
PASC30-0.6C-2MVM	7.087	PASC80-0.6C-2MVM	7.092

Table III.3.2 Per cent porosity and Hardness of compacts sintered at 1120°C for 30 minutes in dissociated ammonia; compaction pressure 691 MPa.

Alloy	Per cent porosity	Hardness HV10	Alloy	Per cent porosity	Hardness HV10
PASC30	9.143	147	PASC80	8.359	157
PASC30-0.3C-1Cu	10.826	168	PASC80-0.3C-1Cu	10.457	175
PASC30-0.3C-2Cu	12.061	178	PASC80-0.3C-2Cu	11.313	228
PASC30-0.6C-1Cu	13.026	185	PASC80-0.6C-1Cu	10.494	236
PASC30-0.6C-2Cu	10.952	220	PASC80-0.6C-2Cu	10.222	240
PASC30-0.3C-1Ni	9.087	180	PASC80-0.3C-1Ni	8.686	186
PASC30-0.3C-2Ni	8.896	182	PASC80-0.3C-2Ni	8.264	188
PASC30-0.6C-1Ni	10.600	200	PASC80-0.6C-1Ni	8.125	197
PASC30-0.6C-2Ni	8.608	201	PASC80-0.6C-2Ni	8.191	223
PASC30-0.3C-1Mo	8.932	167	PASC80-0.3C-1Mo	8.492	174
PASC30-0.3C-2Mo	9.032	178	PASC80-0.3C-2Mo	8.340	227
PASC30-0.6C-1Mo	8.721	184	PASC80-0.6C-1Mo	8.189	237
PASC30-0.6C-2Mo	8.823	221	PASC80-0.6C-2Mo	8.280	240

Continued ....

Table III.3.2 continued

Alloy	Per cent porosity	Hardness HV10	Alloy	Per cent porosity	Hardness HV10
PASC30-0.3C-1MCM	11.845	168	PASC80-0.3C-1MCM	11.493	175
PASC30-0.3C-2MCM	12.338	178	PASC80-0.3C-2MCM	12.272	228
PASC30-0.6C-1MCM	11.709	184	PASC80-0.6C-1MCM	11.792	237
PASC30-0.6C-2MCM	11.960	220	PASC80-0.6C-2MCM	11.903	240
PASC30-0.3C-1MVM	11.909	167	PASC80-0.3C-1MVM	11.493	175
PASC30-0.3C-2MVM	12.200	178	PASC80-0.3C-2MVM	11.654	228
PASC30-0.6C-1MVM	11.580	183	PASC80-0.6C-1MVM	11.289	238
PASC30-0.6C-2MVM	12.140	220	PASC80-0.6C-2MVM	11.361	240

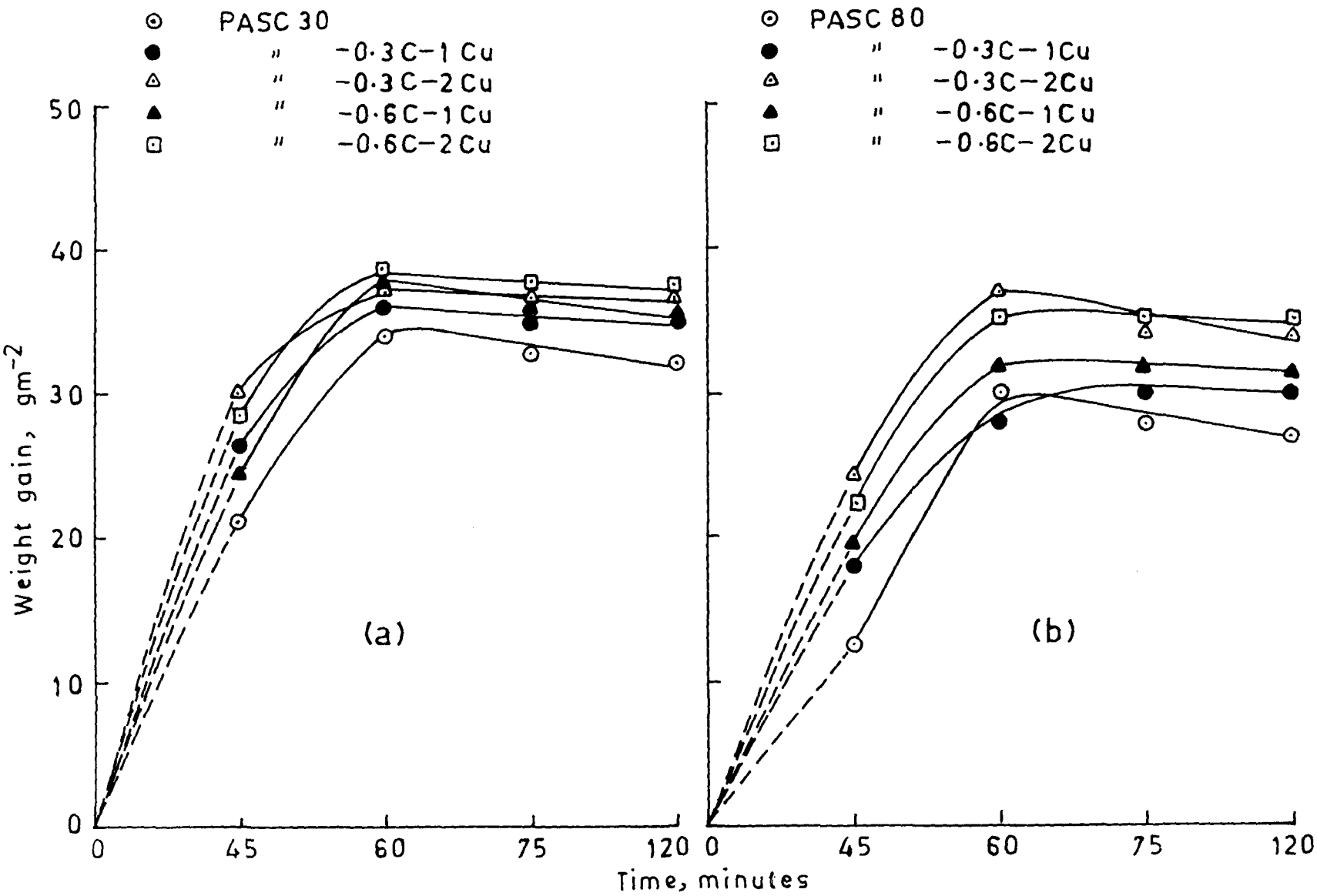

Fig. 3·41 Steam oxidation temperature 450°C

Such an effect of increase in oxidation rate is not noticed when C content is increased from 0.3 to 0.6 % at equivalent Cu levels. For example, in case of PASC80-1Cu compacts, increase of C content from 0.3 to 0.6 % increases oxidation rate (Fig. 3.41b) while in case of PASC80-2Cu compacts, such an increase of C content does not give any conclusive result. However, higher amount of P invariably decreases the amount of oxidation (Figs. 3.41 a and b).

When steam oxidation temperature is increased from 450 to 500°C there is hardly any change in variation of weight gain with steam treatment times with respect to Cu, C or P-contents. Increase in Cu content to 1 and 2 % increases the rate of oxidation (Fig. 3.42 a and b).

When steam oxidation time was further increased to 527°C, the weight gain level decreases and the curves become more clearly well-defined (Figs. 3.43 a and b). It can be clearly seen that 0.3 % C and 1 % Cu increase the oxidation which further increases when Cu content is increased to 2 % (Figs. 3.43 a and b). Similar situation is observed at higher C-contents of 0.6 % .

Increase in oxidation temperature to 550 and 600°C does not change the kinetic curve except that the magnitude of weight gain increases again with increasing steam oxida-

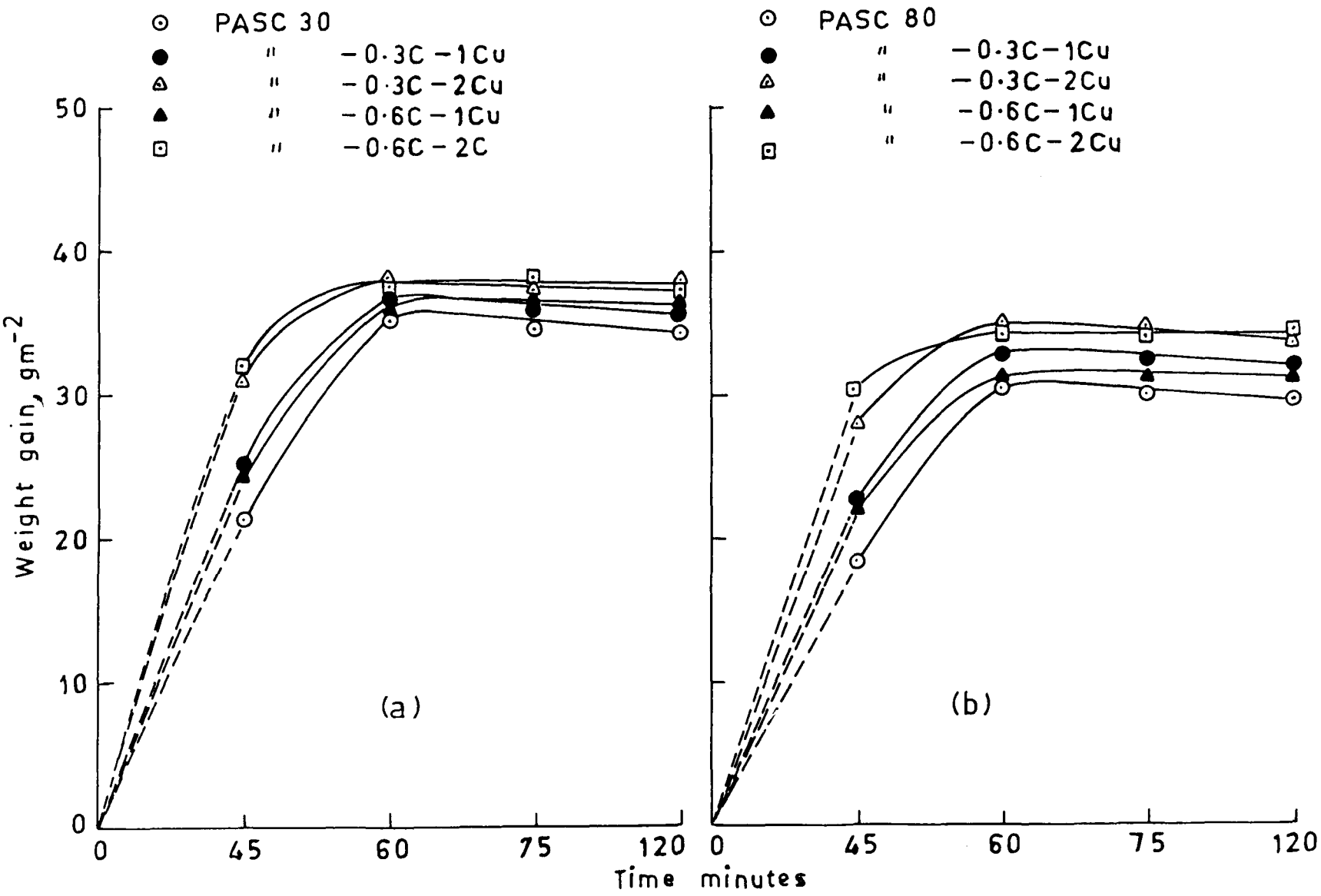

Fig. 3·42 Steam oxidation temperature 500°C

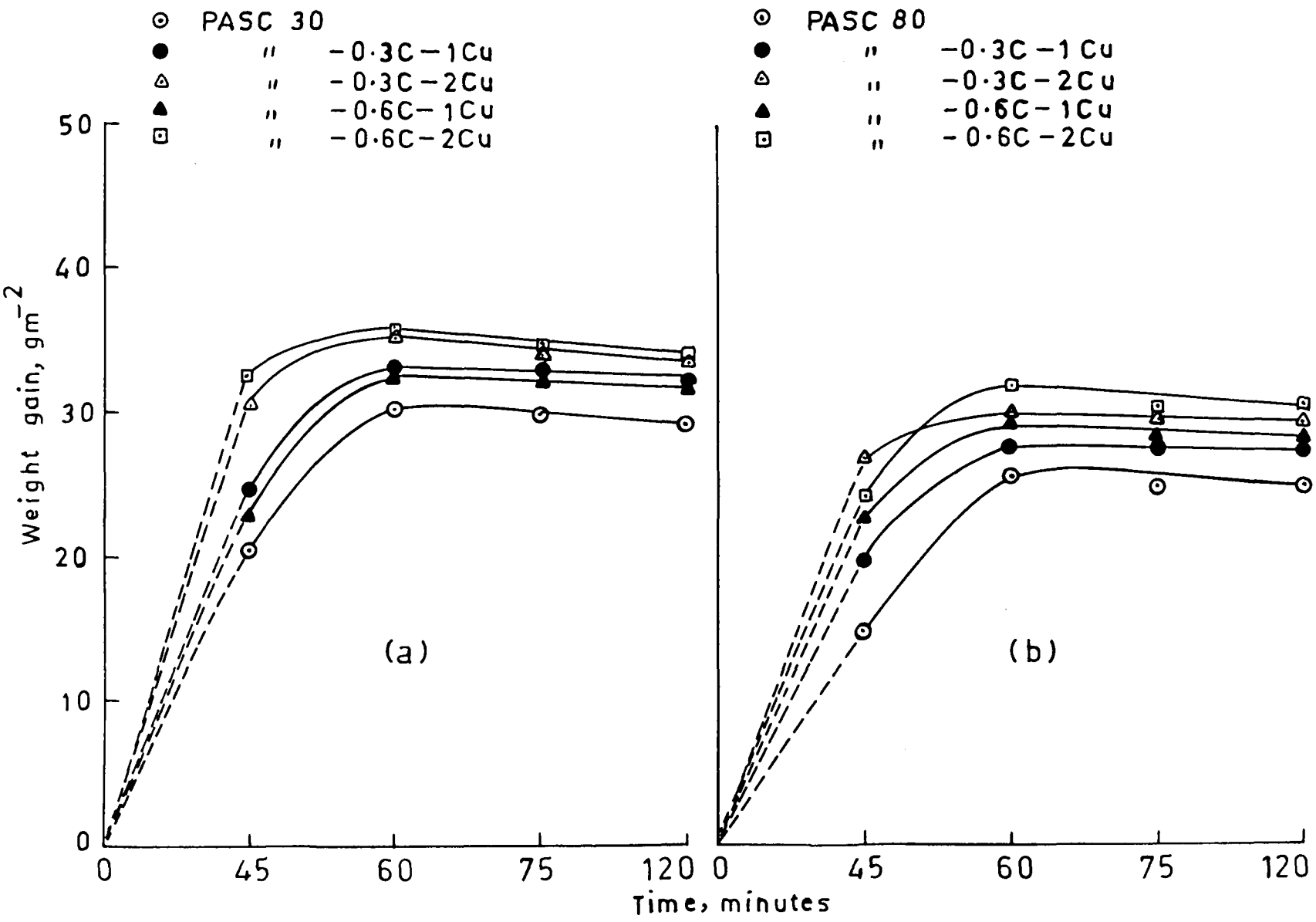

Fig. 3·43 Steam oxidation temperature 527°C

tion temperature after 527°C (Figs. 3.44 and 3.45 a and b). One important point to note is that at steam oxidation temperature of 600°C, in case of PASC80 sintered powder compacts increase in weight gain is large when 0.3 % C and 1 % Cu are added as compared to all other steam treatment temperatures (Figs. 3.41-3.45).

3.3.1.2 PASC-Ni-C compacts

At a treatment temperature of 450°C, with increase in oxidation time, weight gain increases and reaches a maximum at 60 minutes after which it remains constant upto 120 minutes of treatment times (Fig. 3.46). Such a constancy in weight gain after 60 minutes of treatment was not observed in case of Cu-containing compacts (Fig. 3.41). When 0.3 % C and 1 % Ni was added to PASC30 or PASC80 sintered powder compacts, there occurs an increase in weight gain at 45 minutes of treatment times while a decrease in weight gain at all other treatment times (Fig. 3.46 a and b). Keeping C and P levels constant, when Ni-content was increased from 1 to 2 % , there is invariably a decrease in weight gain at all treatment times. Keeping Ni and P concentrations constant, when C content was increased from 0.3 to 0.6 % weight gain increases at 1 % Ni level while decreases at 2 % Ni level (Figs. 3.46 a and b). Level of increase in weight in

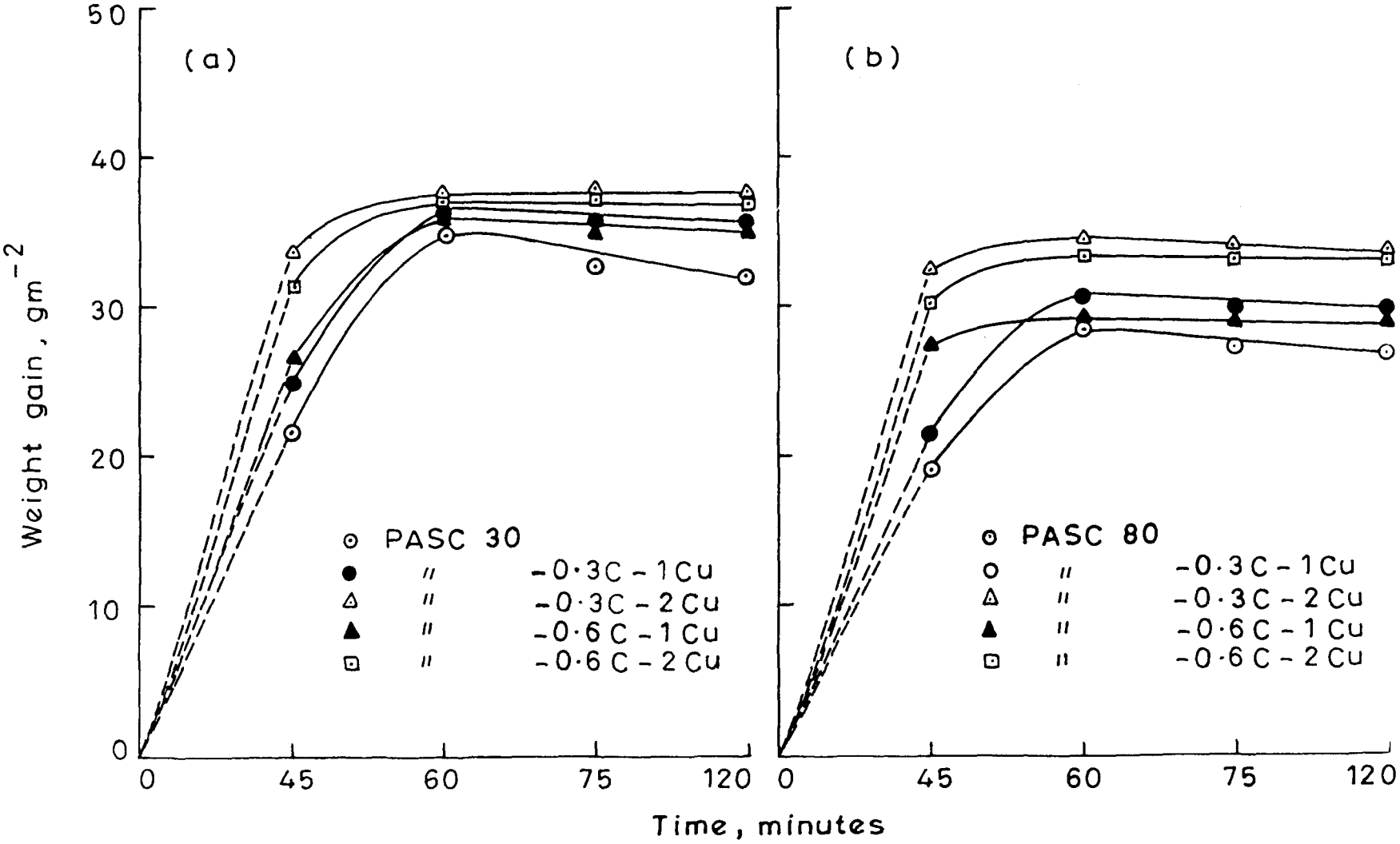

Fig. 3·44 Steam oxidation temperature 550°C

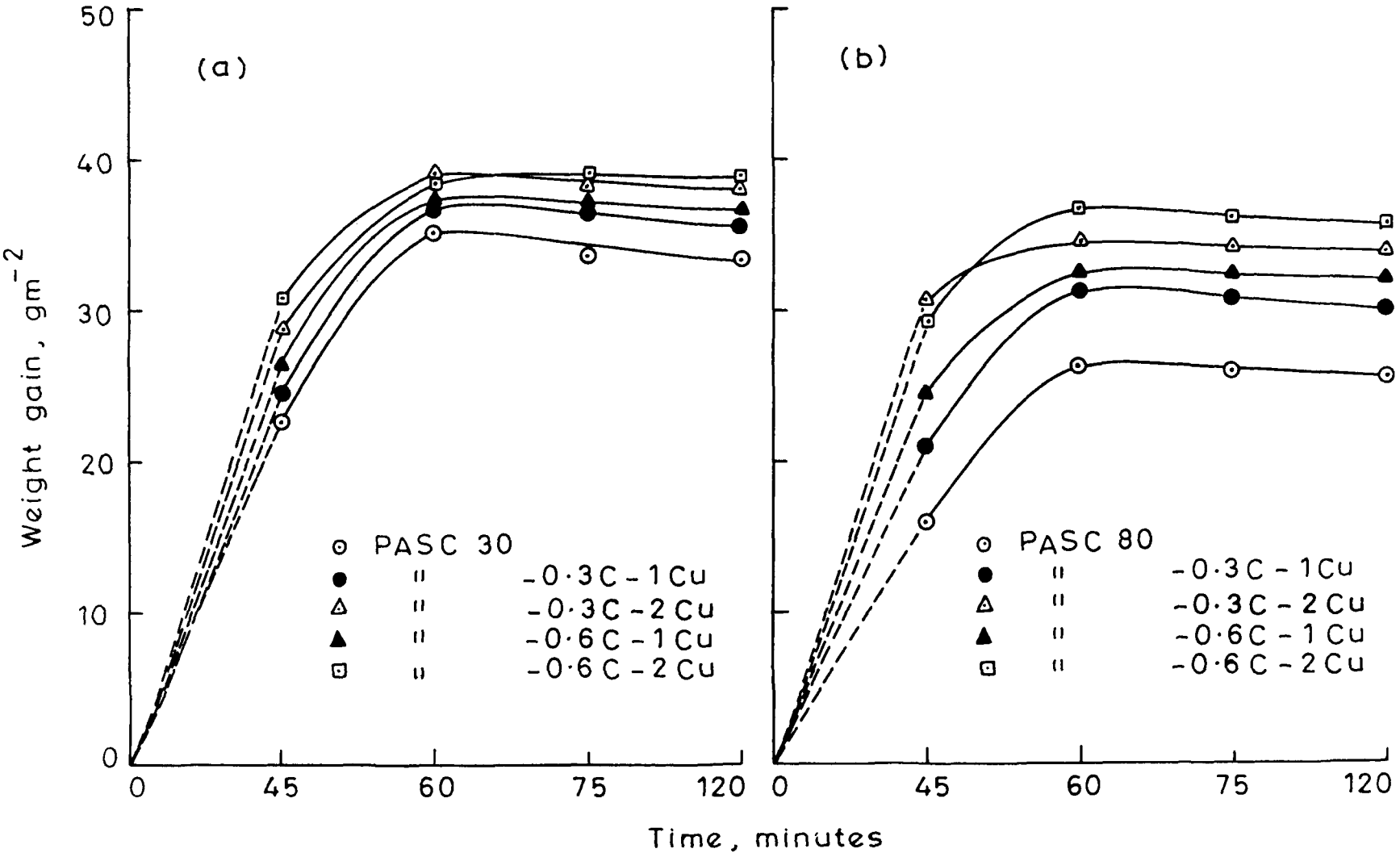

Fig. 3·45 Steam oxidation temperature 600°C

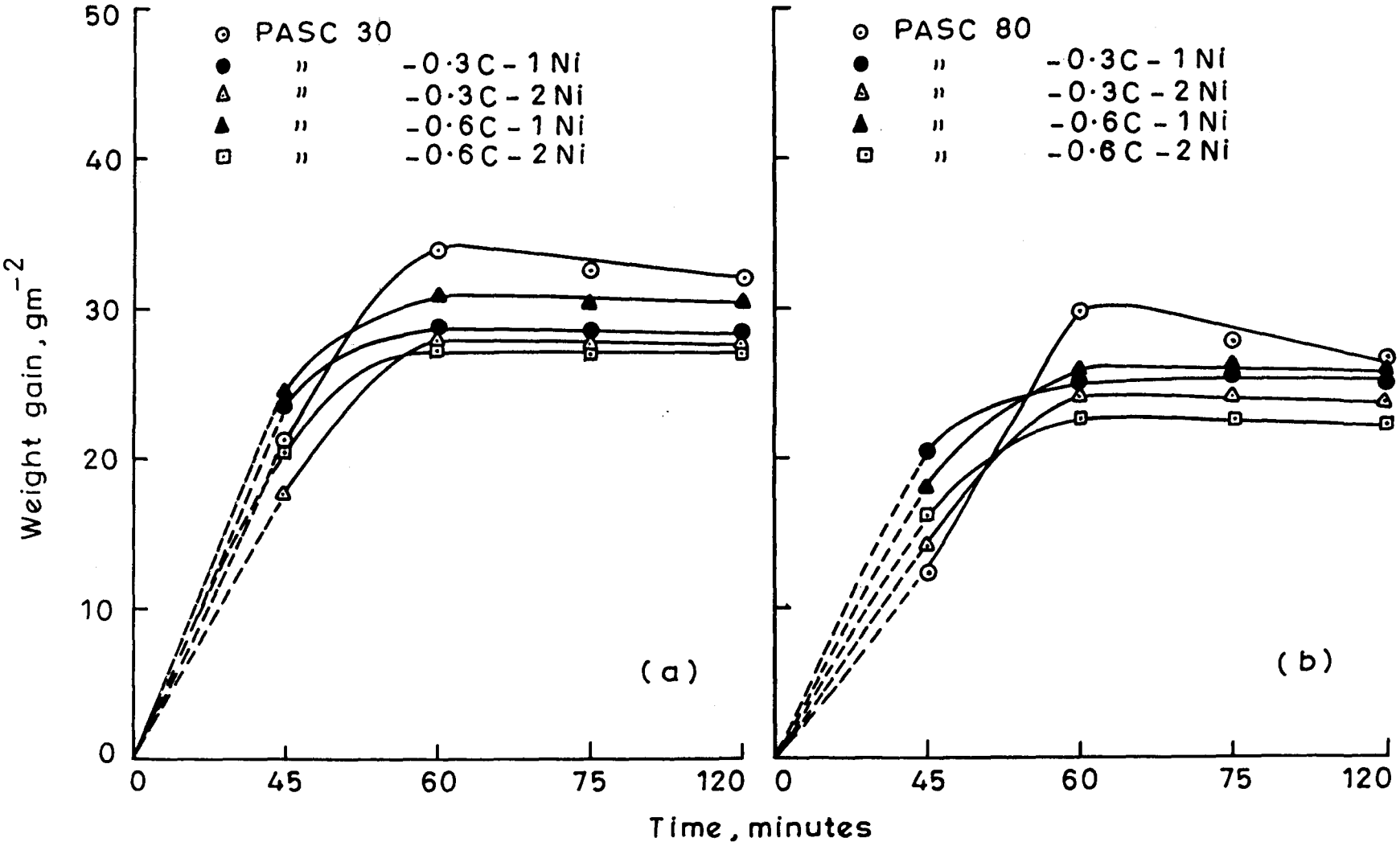

Fig. 3·46 Steam oxidation temperature 450°C

steam oxidized samples is less in case of Ni- containing compacts than that observed in case of Cu-containing samples (Fig. 3.41 and 3.46).

When steam oxidation temperature was increased to 500°C, there is no change in the trend of variation of weight gain with time except that increase in C content from 0.3 to 0.6 % increases weight gain at all P and Ni concentrations (Fig. 3.47 a and b).

When steam oxidation temperature was increased to 527°C, the curve is almost exactly similar to that of previous one (Figs. 3.47 and 3.48). When steam oxidation temperature was further increased to 550°C and 600°C, there is no change in the trend of weight gain variation with treatment time except that magnitude of weight gain increases again after 527°C (Fig. 3.49 and 3.50). However, constancy of weight gain after steam oxidation for 45 to 120 minutes is maintained at all treatment temperatures. Further, effect of alloying elements on oxidation is more marked at higher treatment temperatures of more than 527°C.

3.3.1.3 PASC-Mo-C compacts

At steam oxidation temperature of 450°C, in case of PASC30 sintered powder compact, weight gain increases with

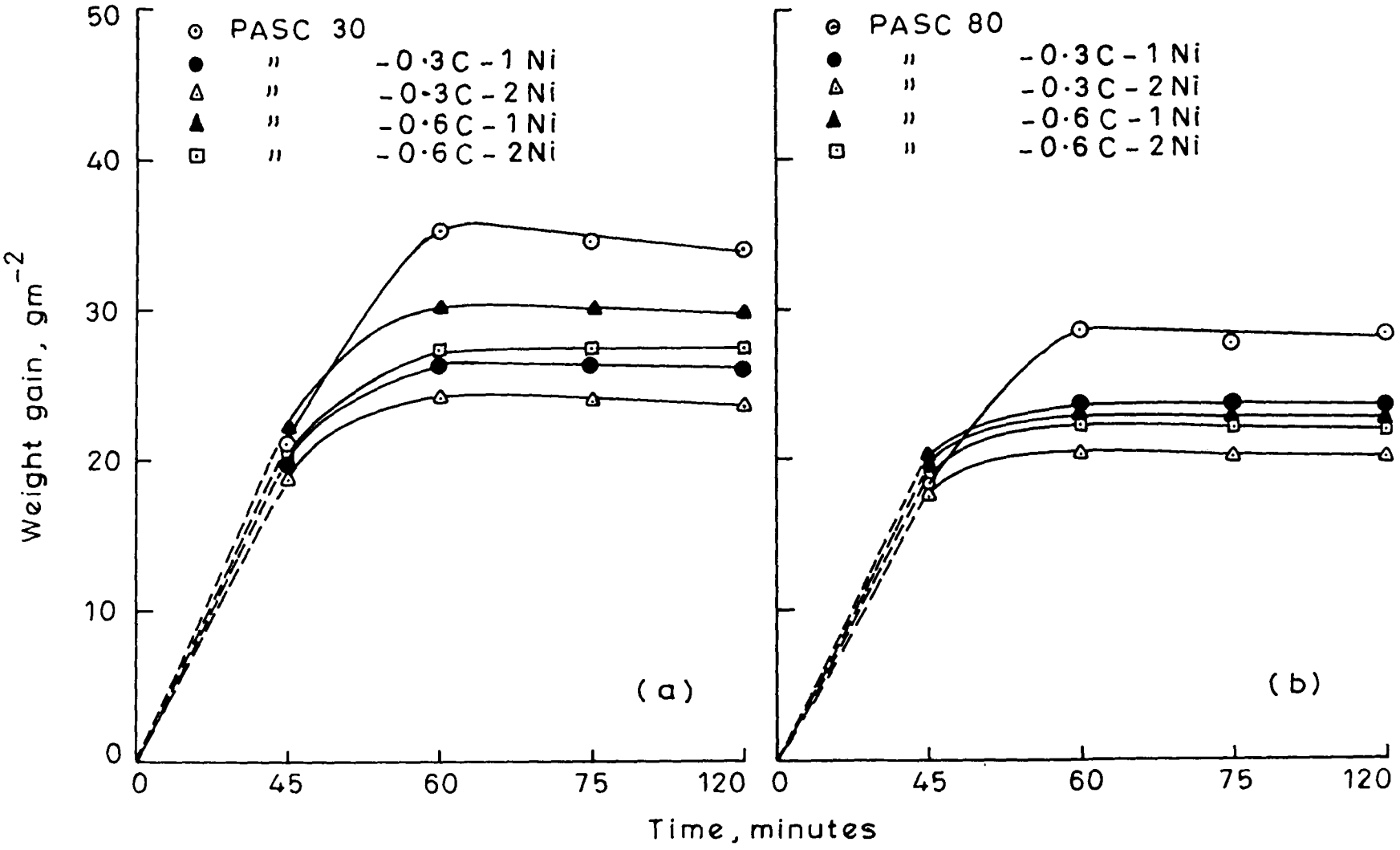

Fig. 3·47 Steam oxidation temperature 500°C

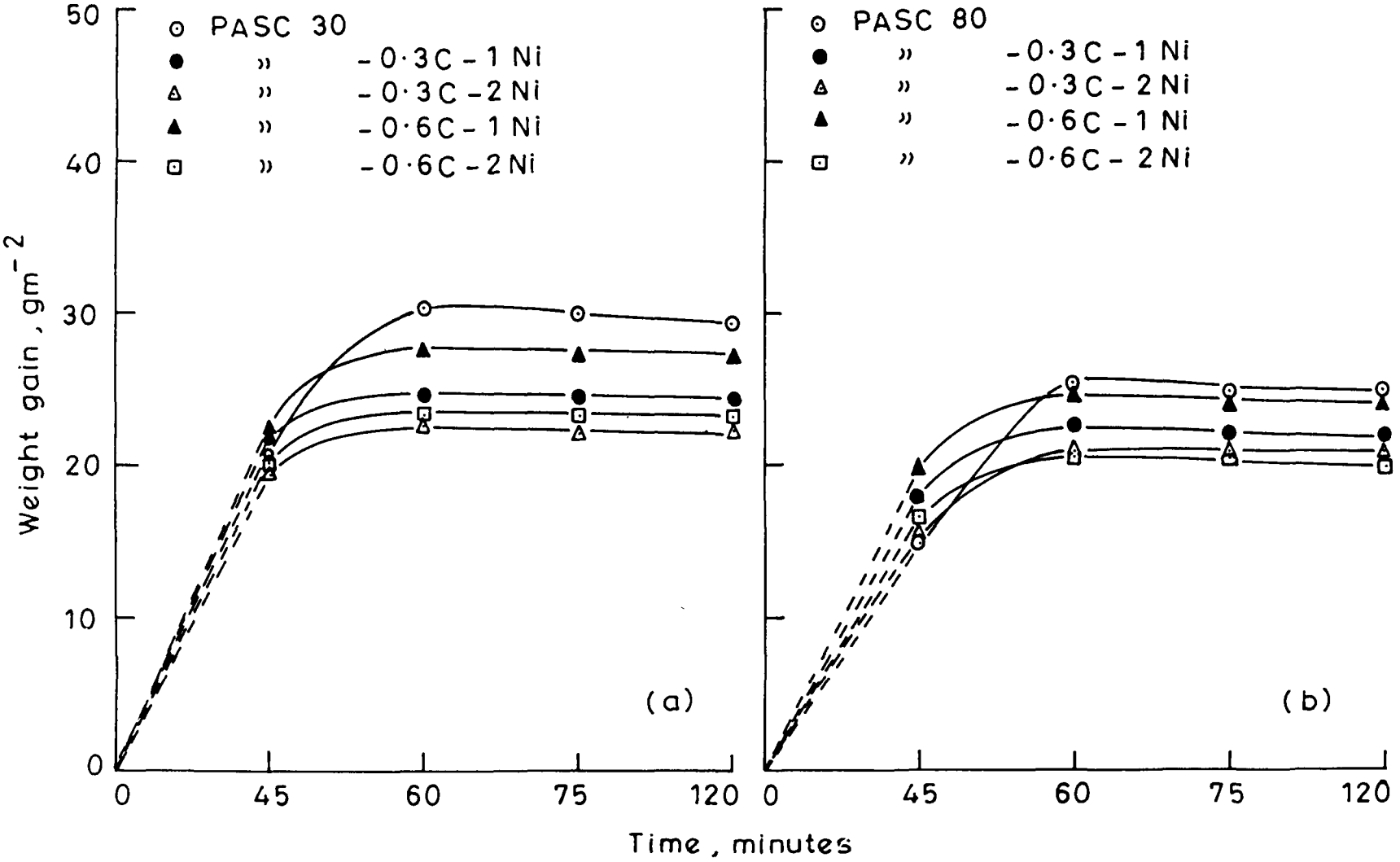

Fig. 3·48 Steam oxidation temperature 527 °C

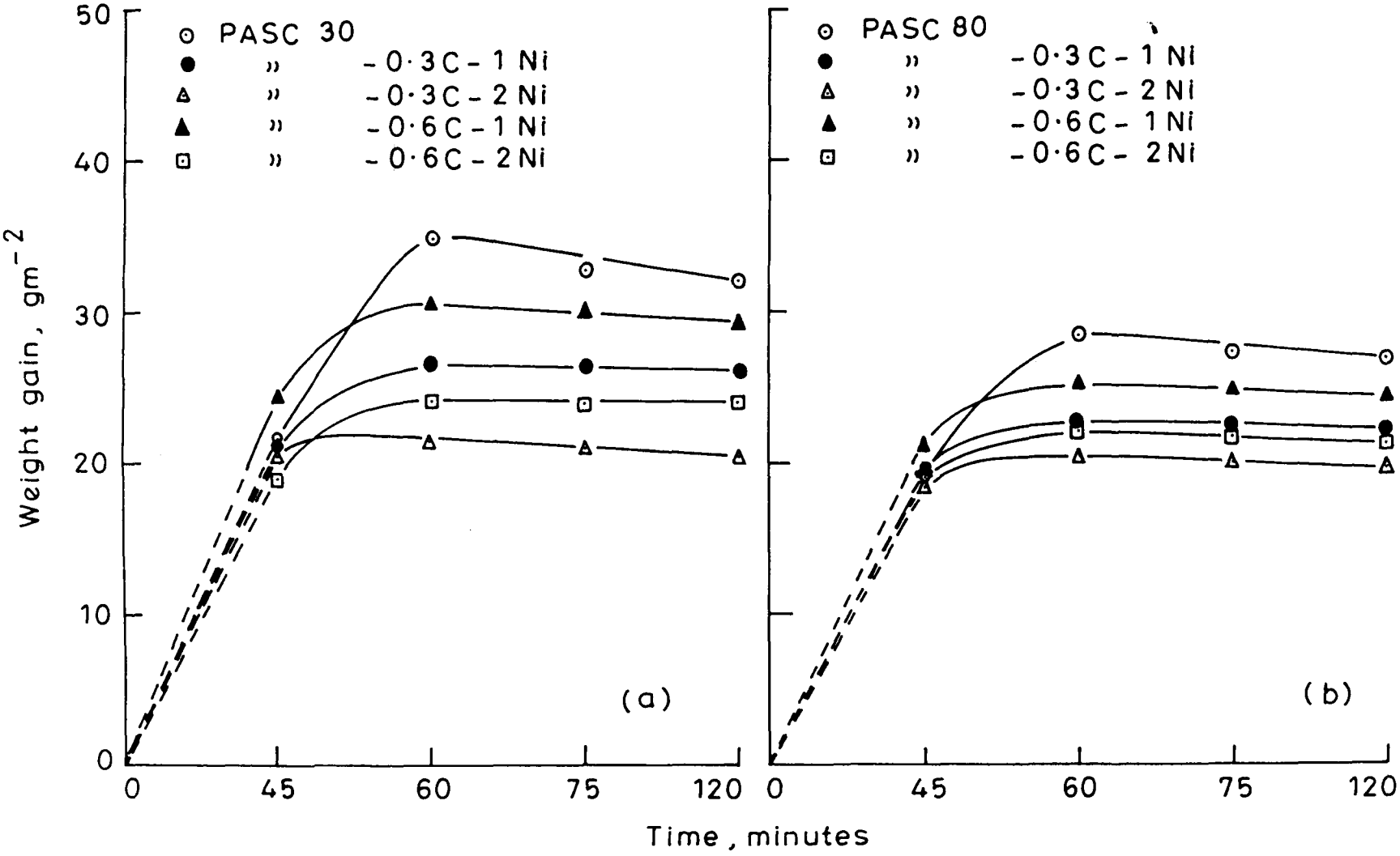

Fig. 3·49 Steam oxidation temperature 550°C

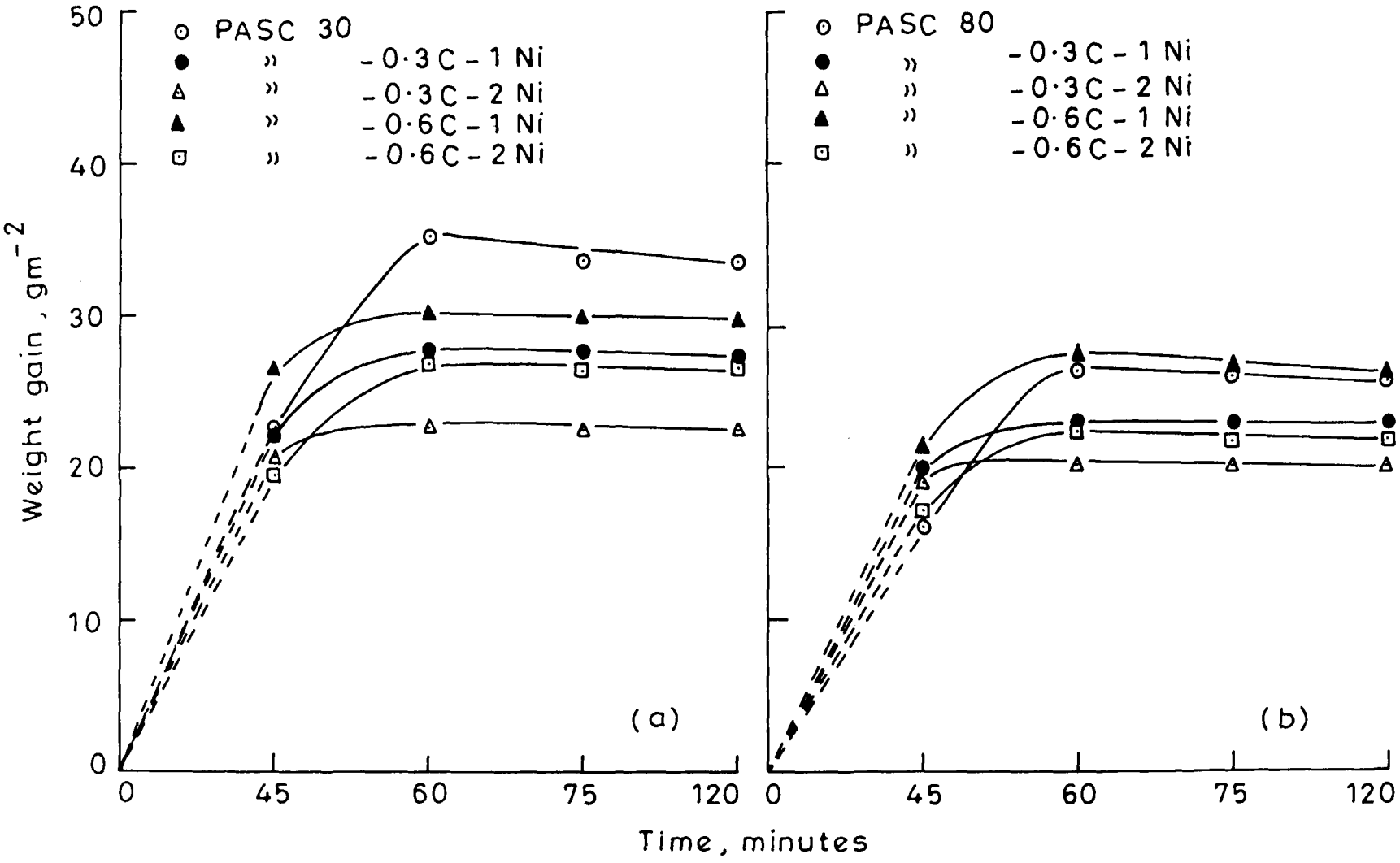

Fig. 3·50 Steam oxidation temperature 600°C

increase in treatment time upto 60 minutes after which there appears to be slight fall (Fig. 3.51). When 0.3 % C and 1 % Mo are added, there occurs a significant decrease in gain of weight. At 0.3 % C, when Mo content was increased from 1 to 2 % , there is a further significant decrease in weight gain (Fig. 3.51). When C content was increased from 0.3 to 0.6 % , there is a marginal increase in weight gain at either Mo content or phosphorus levels (Fig. 3.51 a and b). When phosphorus content was increased from 0.3 to 0.8 %, there is invariably a reduction in weight gain at equivalent C and Mo contents. After 60 minutes of steam oxidation, there appears to be no effect of treatment period on weight gain in all compositions of Mo-containing compacts However, from 45 to 60 minutes of treatment period, the rate of oxidation decreases and becomes constant at or below 60 minutes of treatment period.

When steam oxidation temperature was increased to 500°C, variation of weight gain with steam treatment time with respect to Mo, or P contents remains unchanged (Fig. 3.52). However, effect of increase of C content from 0.3 to 0.6 % is reversed and is noticed to decrease the weight gain. Except in case of plain PASC powder compacts, magnitude of weight decreases when steam oxidation temperature was increased from 450 to 500°C. (Figs. 3.51 and 3.52).

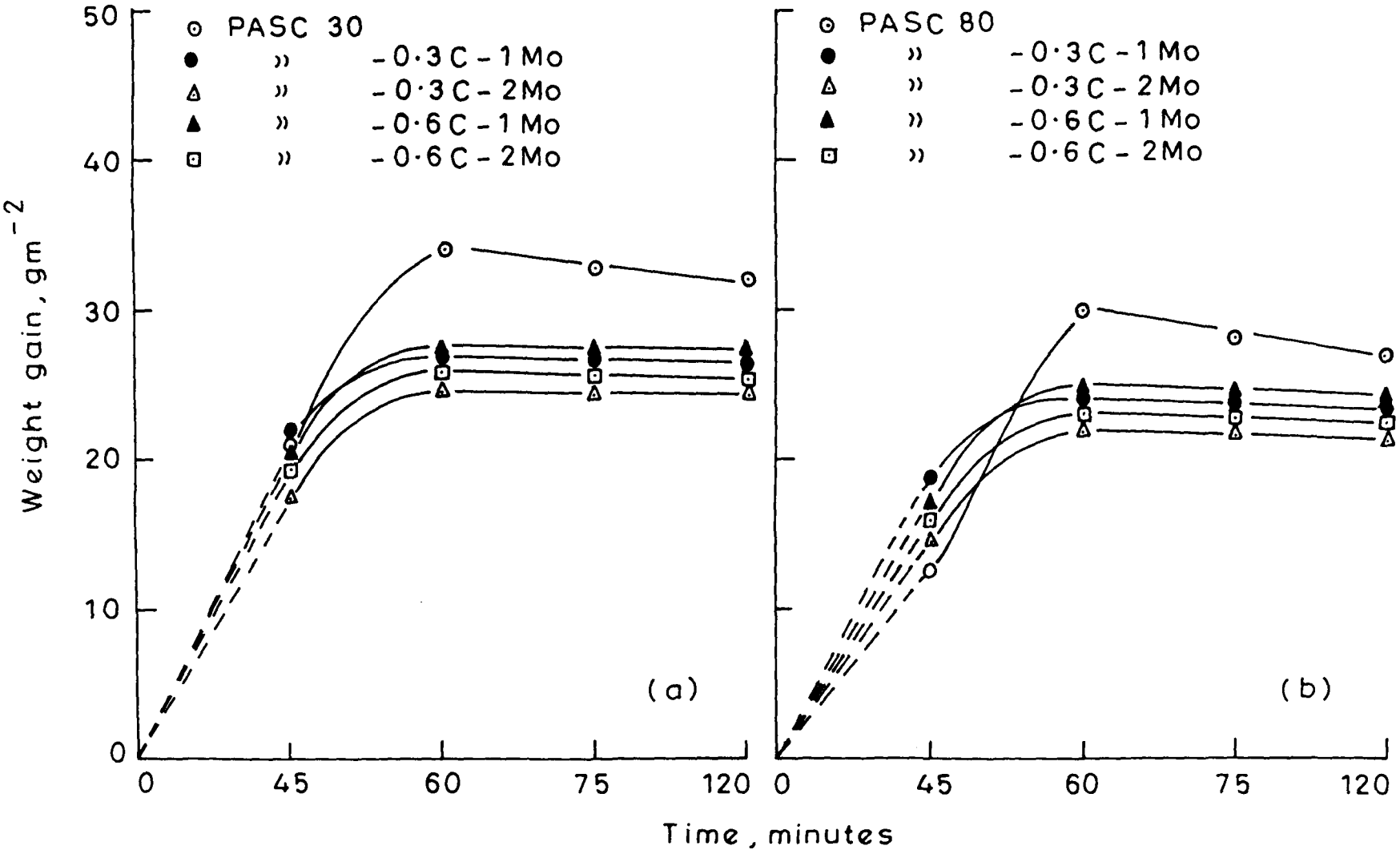

Fig. 3·51 Steam oxidation temperature 450°C

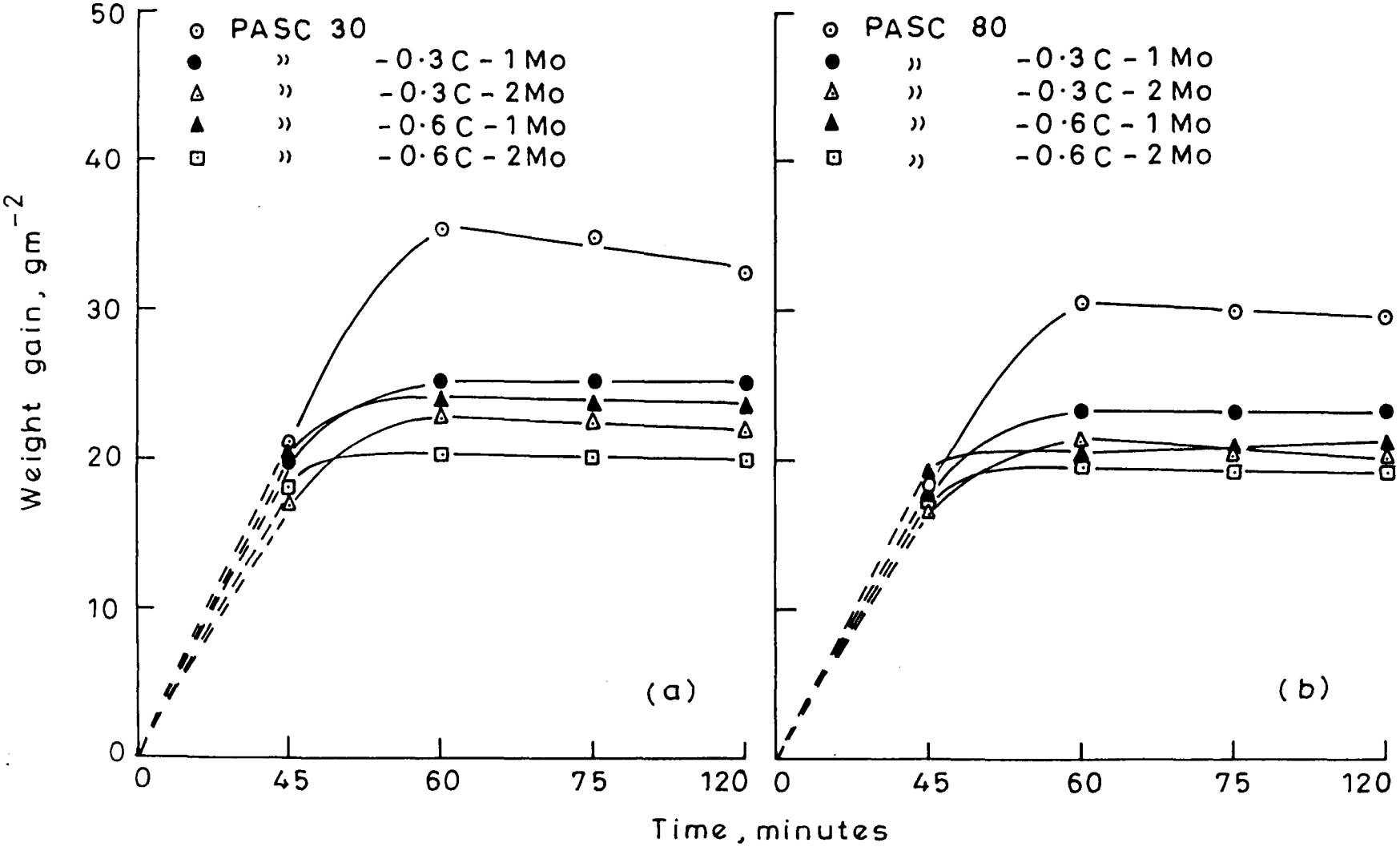

Fig. 3·52 Steam oxidation temperature 500°C

There is an indication that maximum in weight gain reaches at lower period.

When steam oxidation temperature was further increased to 527°C, the effect of 0.3 % C and 1 % Mo addition on magnitude of weight gain is decreased as compared to that observed at lower treatment temperature, at either P level (Fig. 3.53). The effect of increasing Mo, C or P contents on weight gain is similar to that observed in case of steam treatment carried out at 450°C.

When the steam oxidation temperature was increased further to 550 and 600°C (Figs. 3.54 and 3.55), effect of Mo, C or P on variation of weight gain with steam oxidation time remains qualitatively unchanged. However effect of adding 0.3 % C and 1 % Mo in decreasing the magnitude of weight gain increases with increase in steam oxidation temperature particularly at lower P-level of 0.3 %, Also, the difference in weight gain at 45 and 60 minutes of treatment period goes on decreasing with increase in steam treatment temperature (Figs. 3.51-3.55). However, constancy of weight after 60 minutes of treatment period is maintained in all compositions and at all temperature.

3.3.1.4 PASC-MCM-C compacts

At steam oxidation temperature of 450°C, when 0.3 %

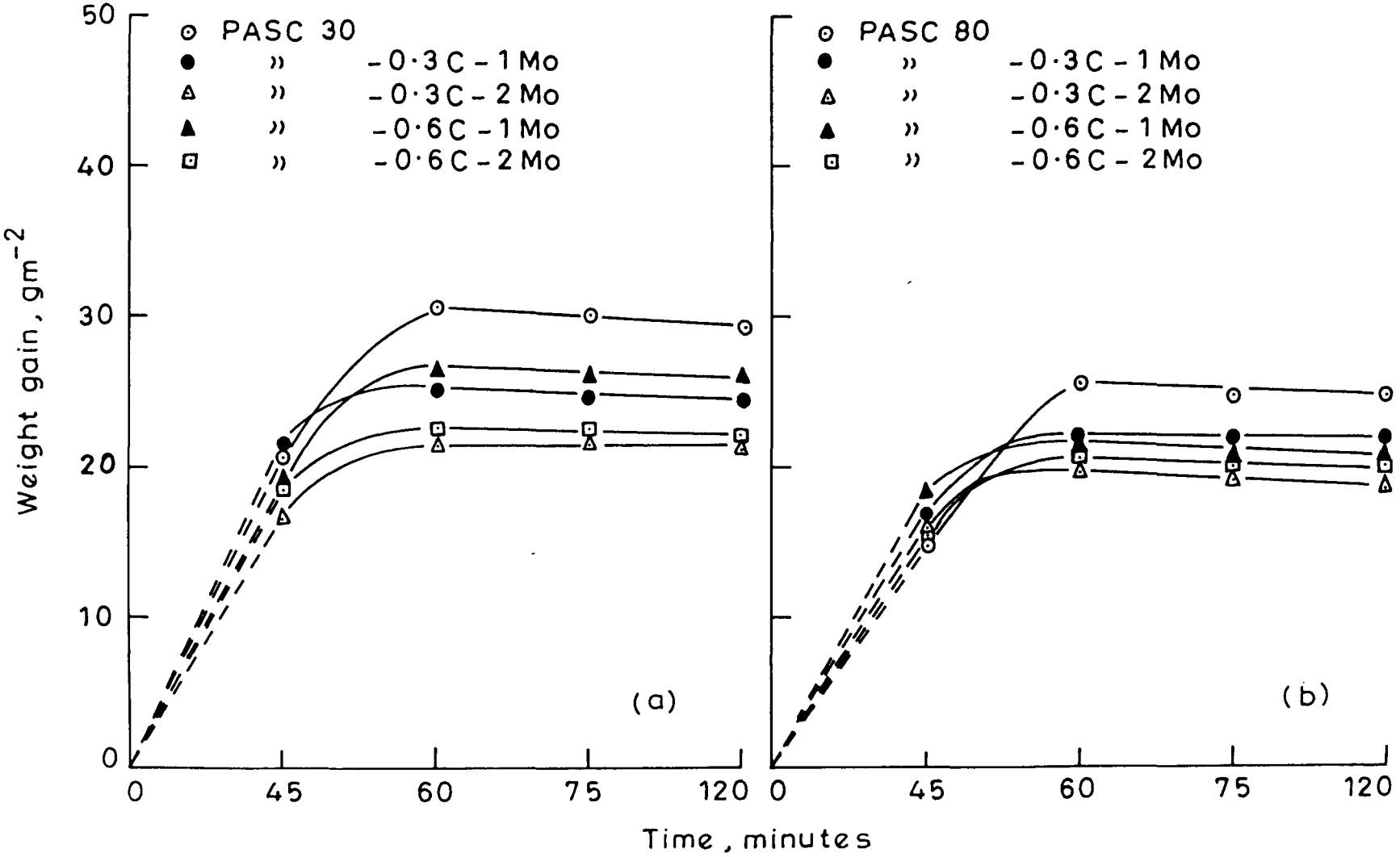

Fig. 3·53 Steam oxidation temperature 527°C

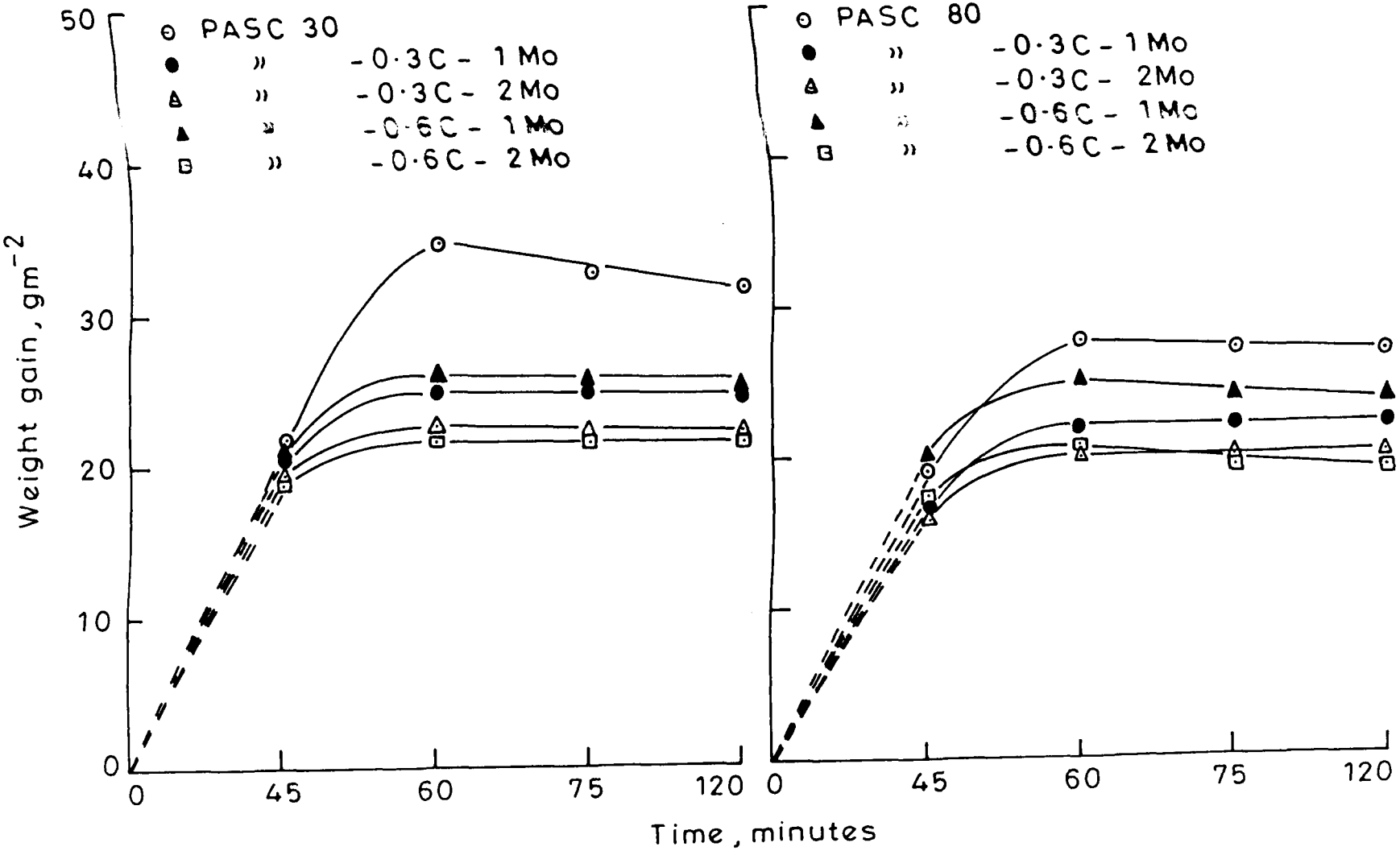

Fig. 3·54 Steam oxidation temperature 550°C

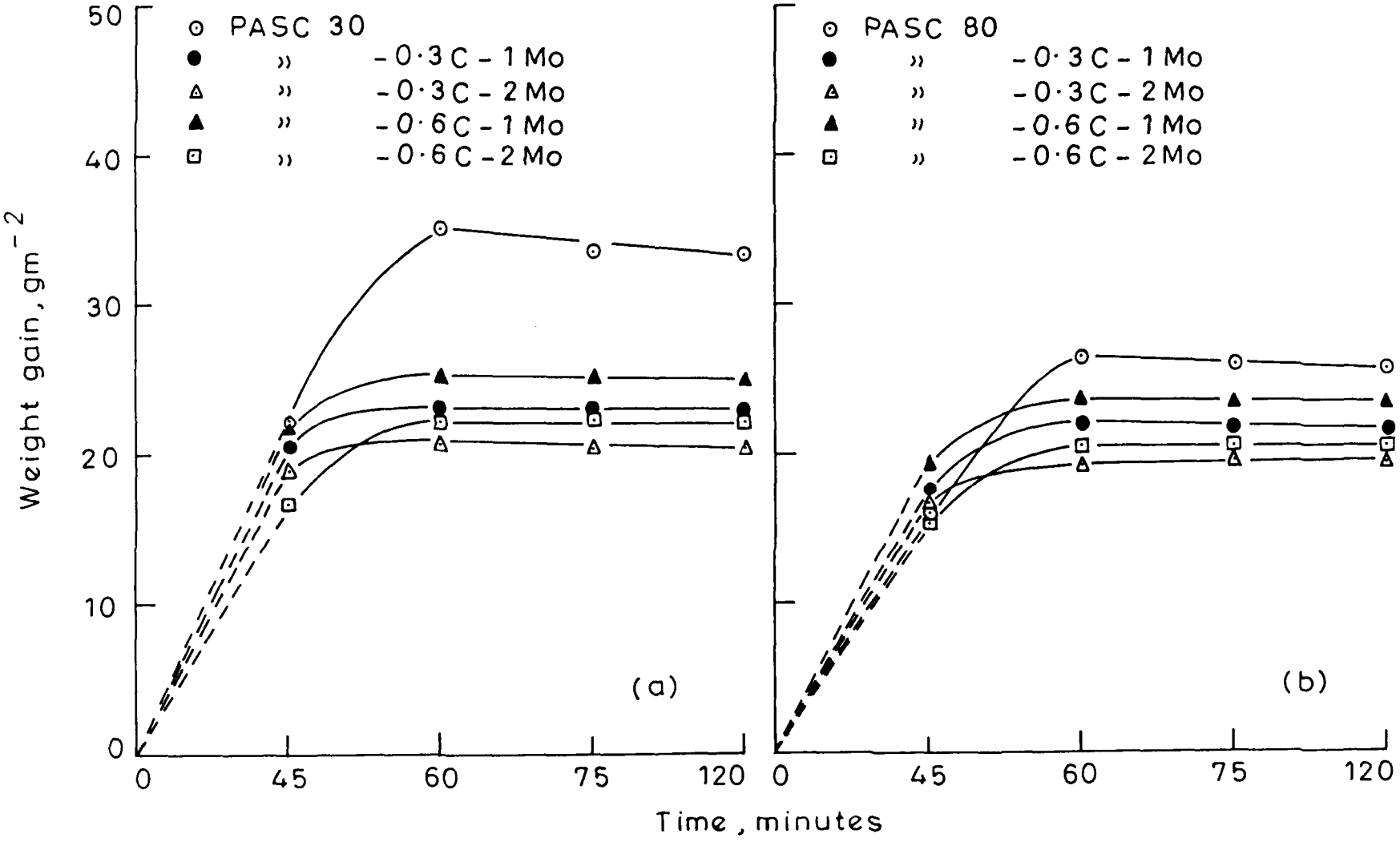

Fig. 3·55 Steam oxidation temperature 600°C

C and 1 % MCM are added to PASC30 powder compact, there occurs a significant increase in weight gain at all treatment times and that the magnitude of weight gain remains constant (Fig. 3.56). When MCM content is further increased to 2 % keeping C level at 0.3 % , weight gain further increases (Fig. 3.56 a and b). When C content is increased keeping MCM and P levels constant, there is either no change or very slight increase in weight gain. When P content is increased from 0.3 to 0.8 %, there is invariably a decrease in weight gain in all compositions and at all treatment times. However, rate of oxidation in the initial period of oxidation is marginally higher than Cu-containing compacts and significantly higher than Ni and Mo-containing compacts. However, constancy in weight is achieved at 60 minutes of steam treatment period (Fig. 3.56).

When the steam oxidation temperature is increased from 450 to 500°C, variation of weight gain with steam treatment time as a function of composition remains unchanged (Fig. 3.57). With further increase of steam oxidation temperature to 527°C, the pattern of curve remains the same but magnitude of weight gain decreases. However, the effect of higher C, MCM or P in increasing or decreasing the extent of oxidation becomes more evident and uniformily defined (Fig. 3.58).

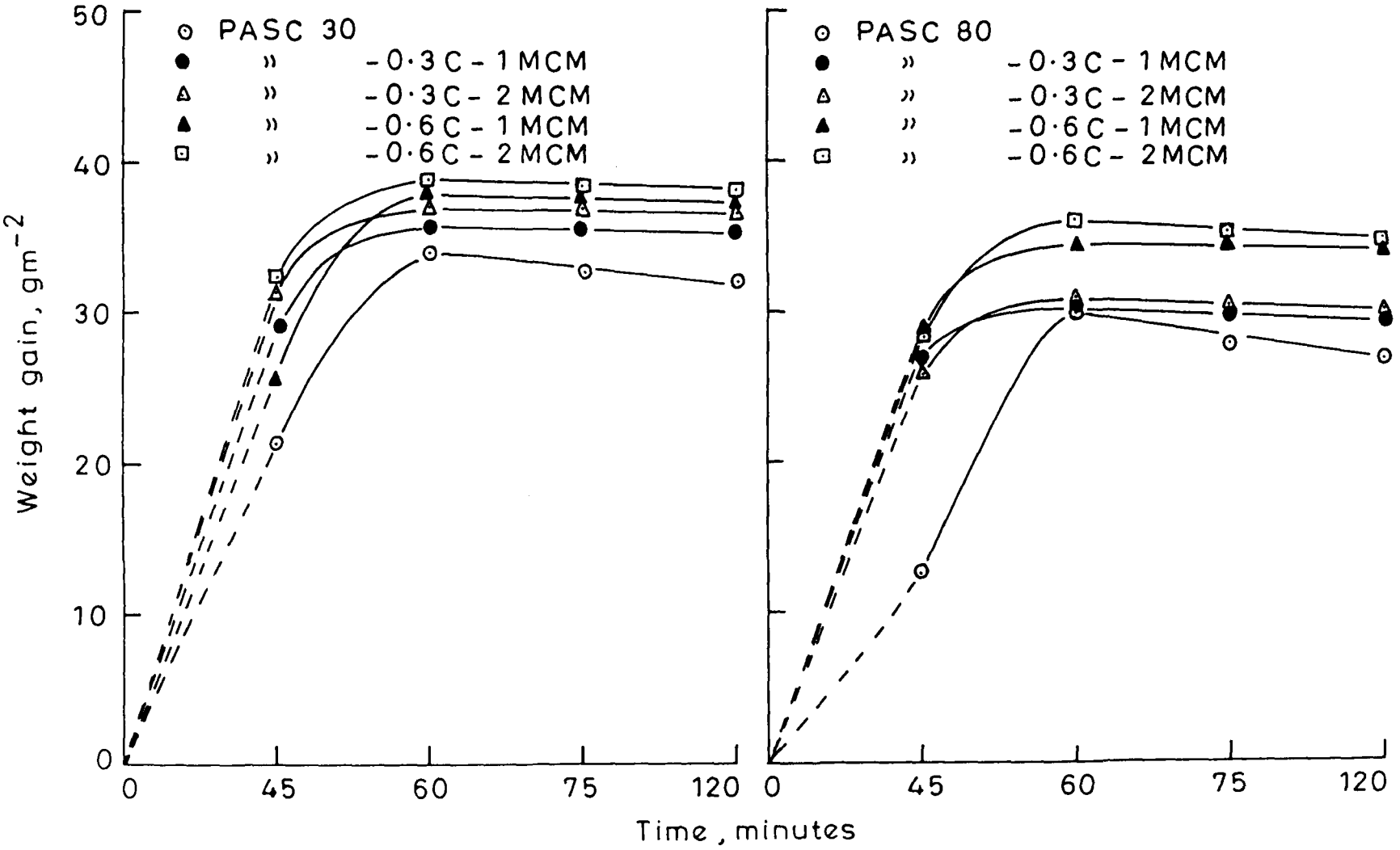

Fig. 3·56 Steam oxidation temperature 450°C

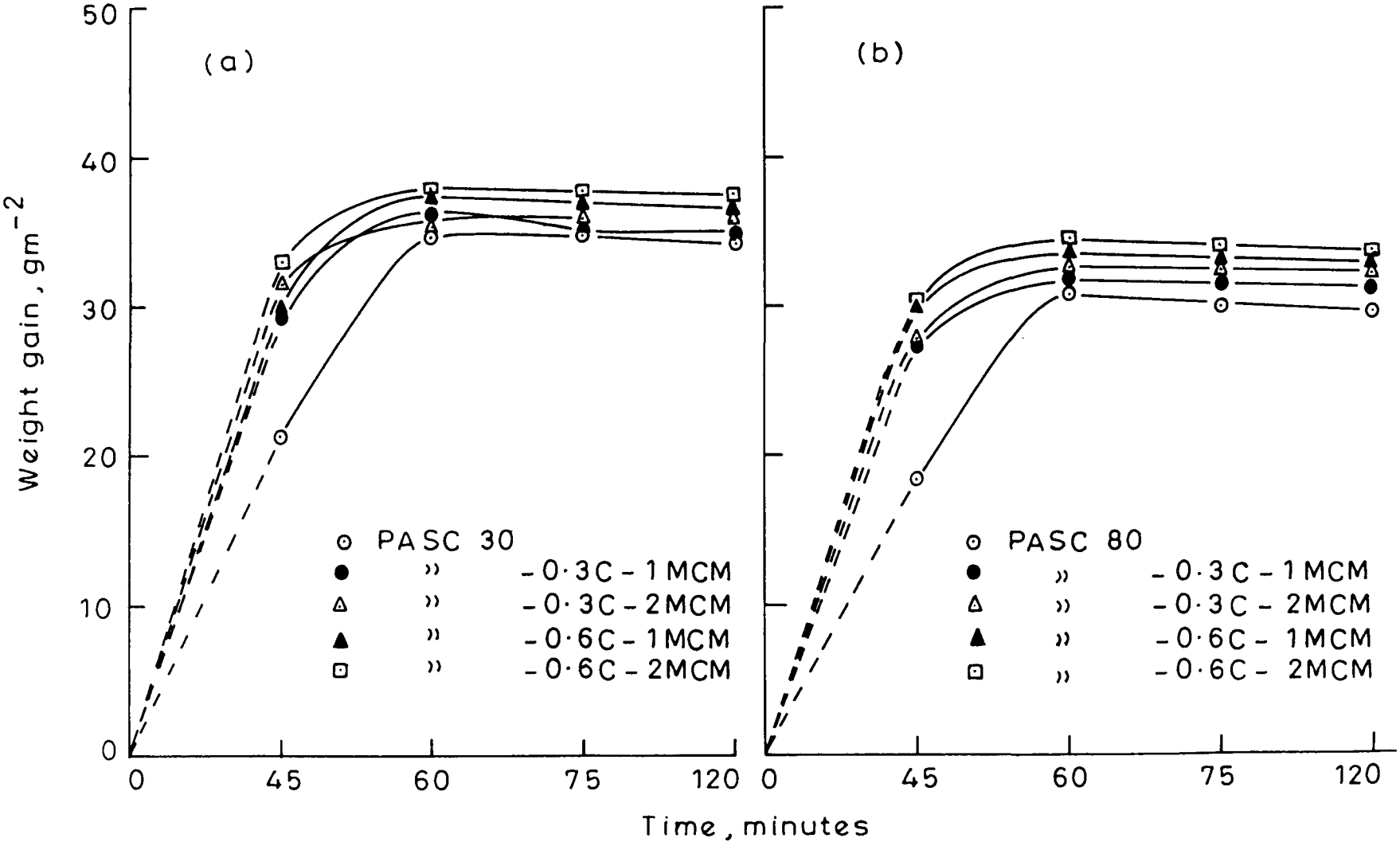

Fig. 3·57 Steam oxidation temperature 500°C

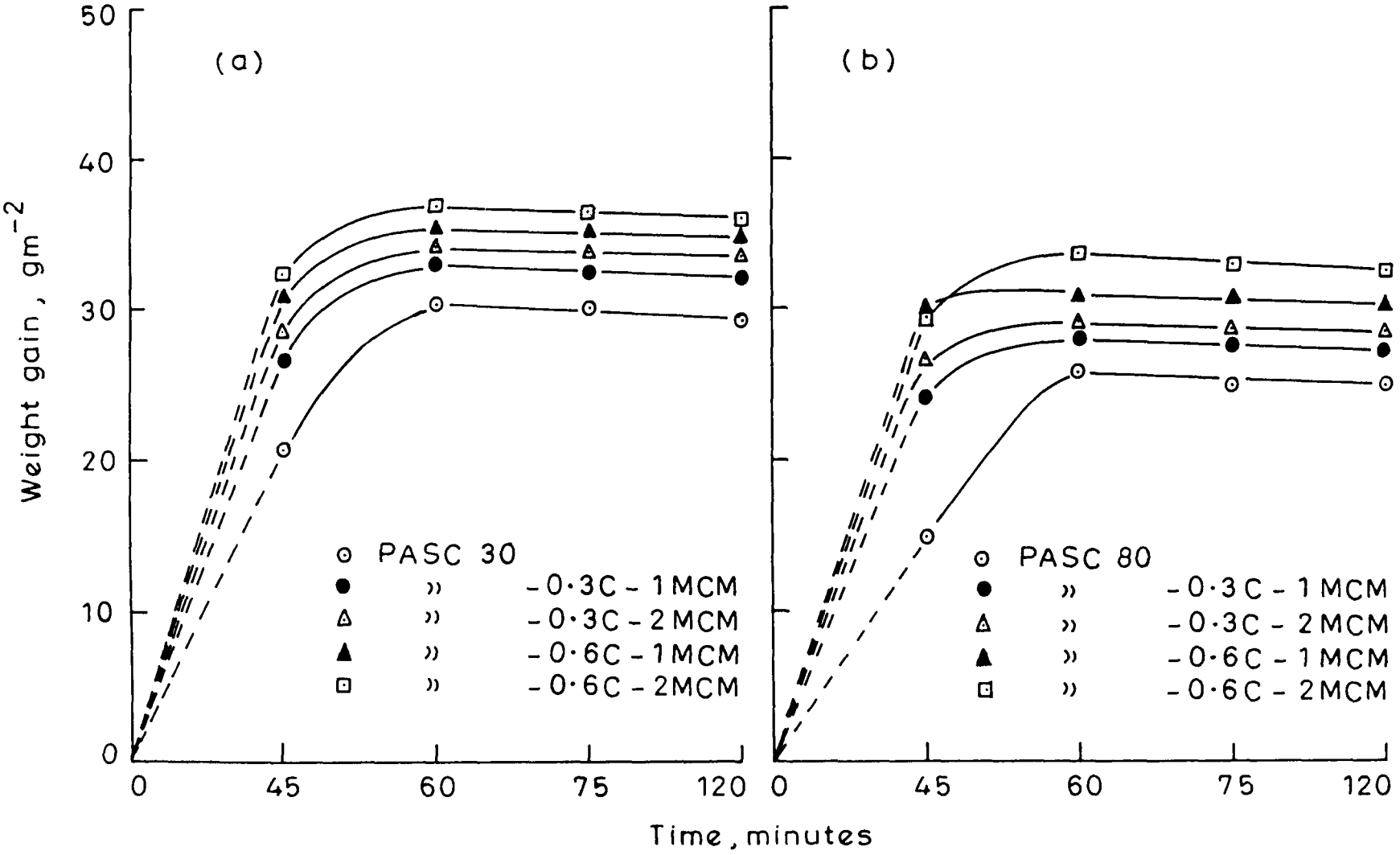

Fig. 3·58 Steam oxidation temperature 527°C

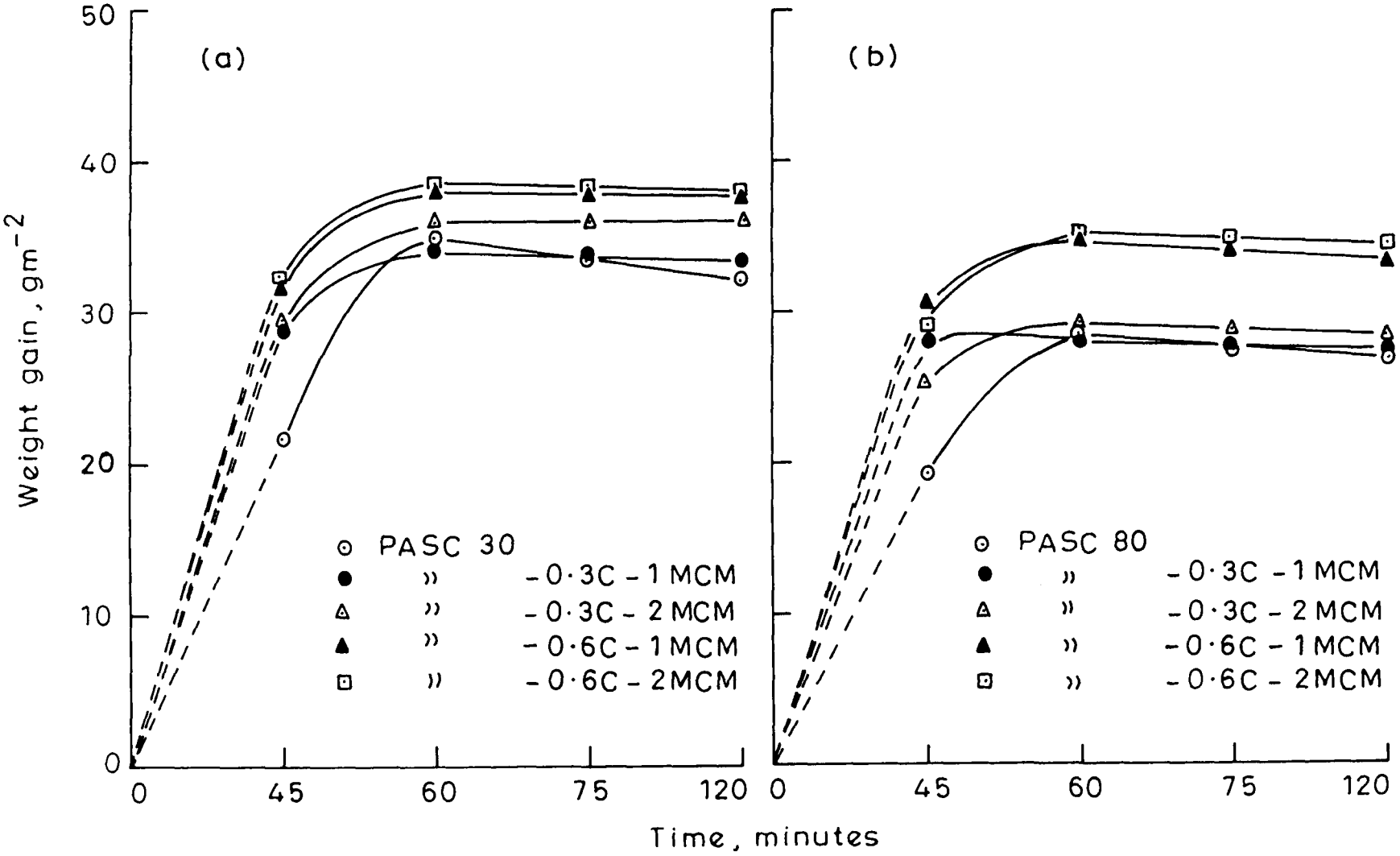

Fig. 3·59 Steam oxidation temperature 550°C

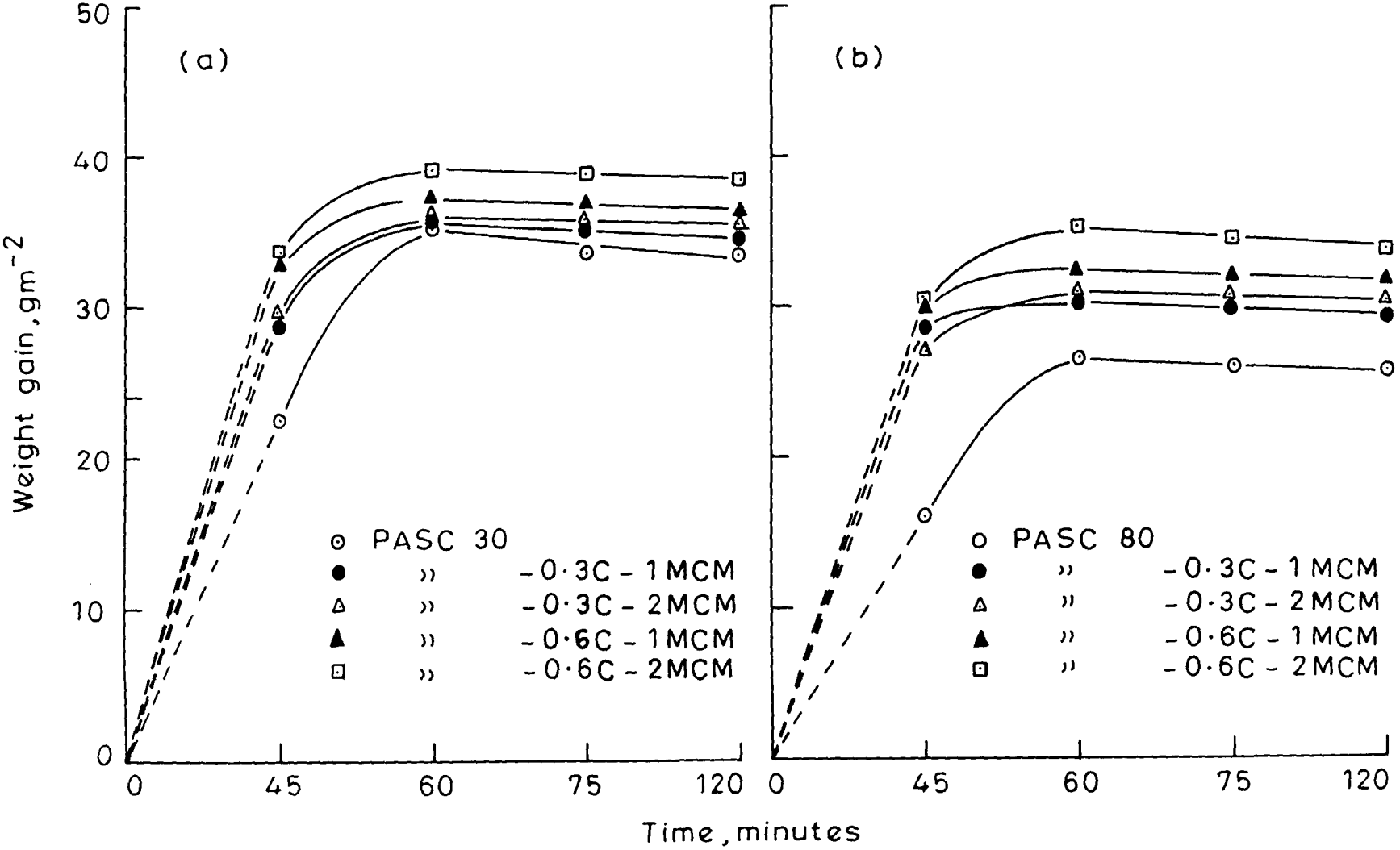

Fig. 3·60 Steam oxidation temperature 600°C

It is observed that with increase of steam oxidation temperature (Figs. 3.57-3.60), maximum in weight gain is arrived at shorter and shorter period of steam treatment successively.

3.3.1.5 PASC-MVM-C compacts

At a treatment temperature of 450°C, the effect of adding 0.3 % C and 1 % MVM in increasing weight gain of sintered powder compacts from PASC30 and PASC80 are almost exactly similar to that observed in case of MCM- containing compacts (Figs. 3.56 and 3.61). The effect of increasing MVM and C contents are also similar.

With increase in steam oxidation temperature to 500°C and onwards (Figs. 3.62-3.65), magnitude of weight gain decreases upto 527°C (Figs. 3.61-3.63) and then increases again (Figs. 3.64 and 3.65). However, maximum in weight gain is reached at ever decreasing treatment time with increasing steam oxidation temperature. Maximum in weight gain seems to have occurred at 45 to 50 minutes of treatment times.

3.3.2 Hardness of steam treated samples

3.3.2.1 PASC-Cu-C compacts

With increase in steam oxidation time hardness

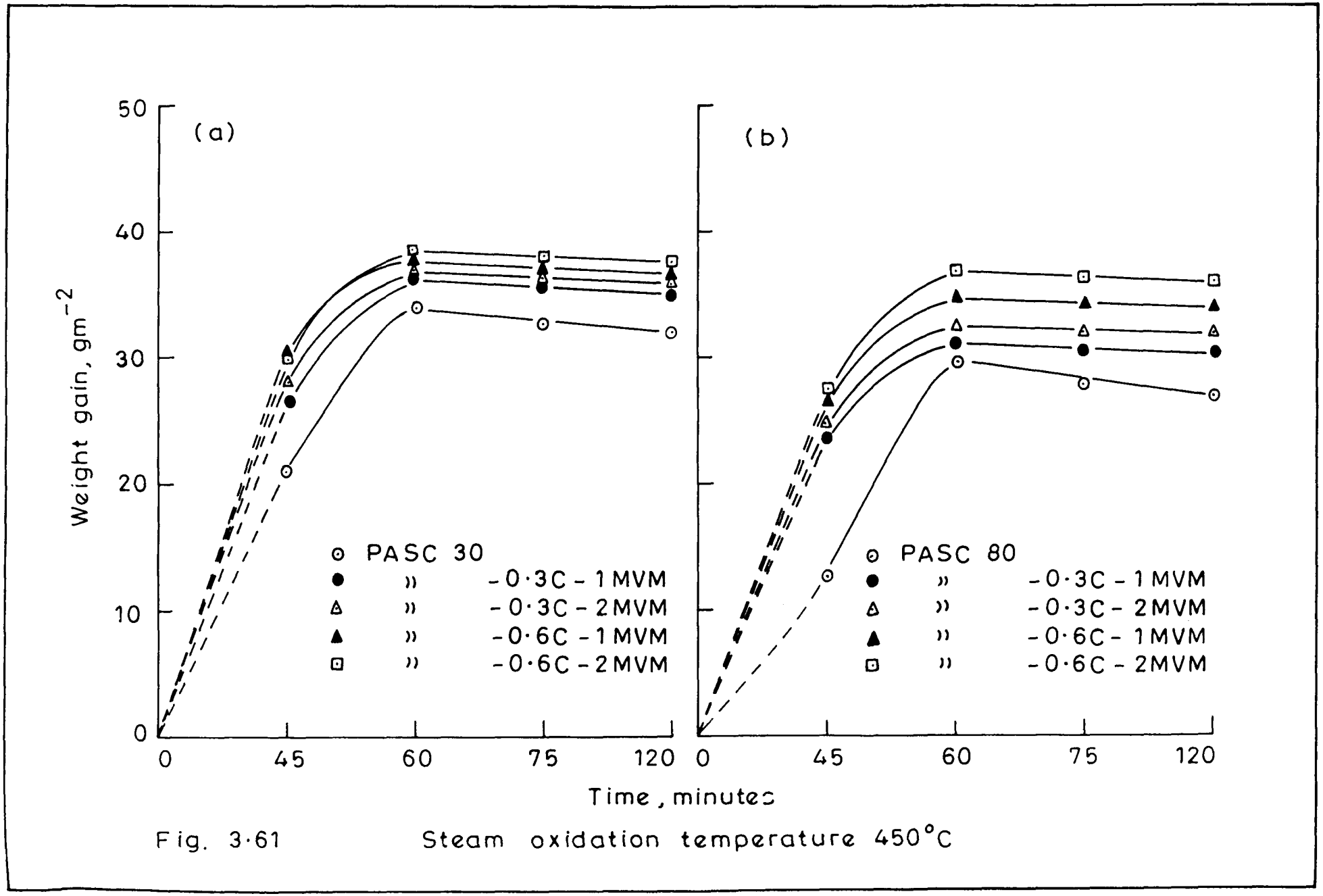

Fig. 3·61 Steam oxidation temperature 450°C

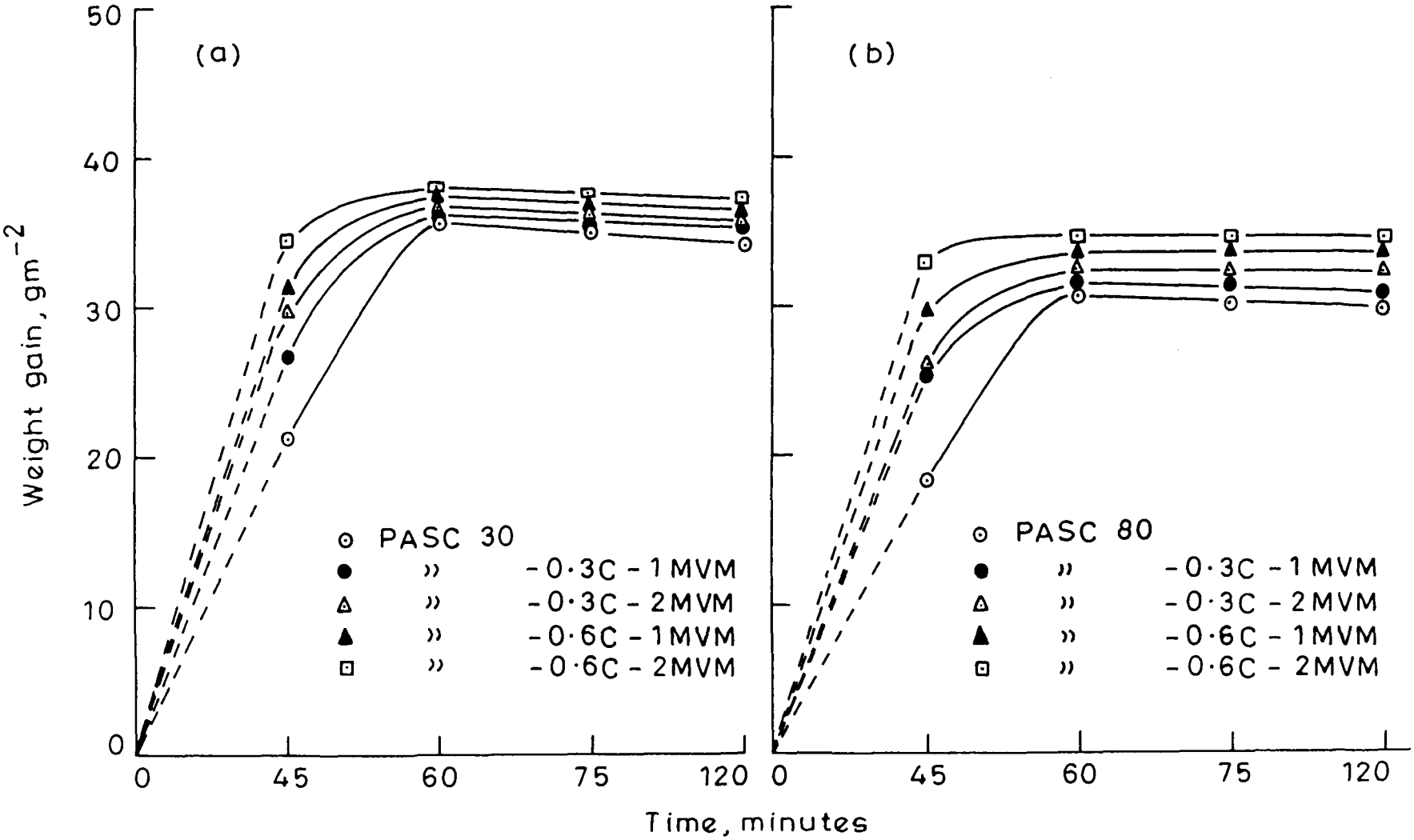

Fig. 3·62 Steam oxidation temperature 500°C

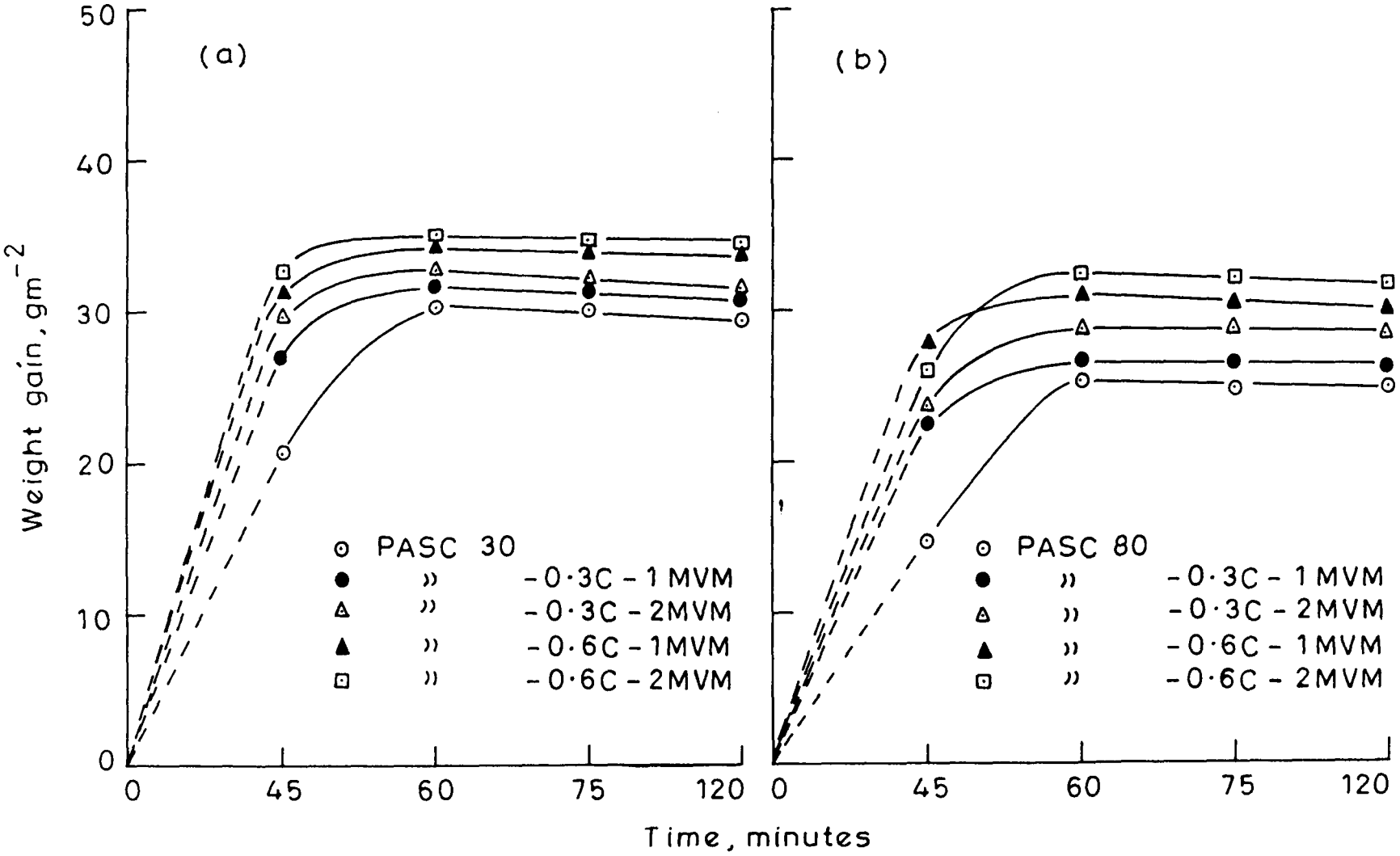

Fig. 3·63 Steam oxidation temperature 527°C

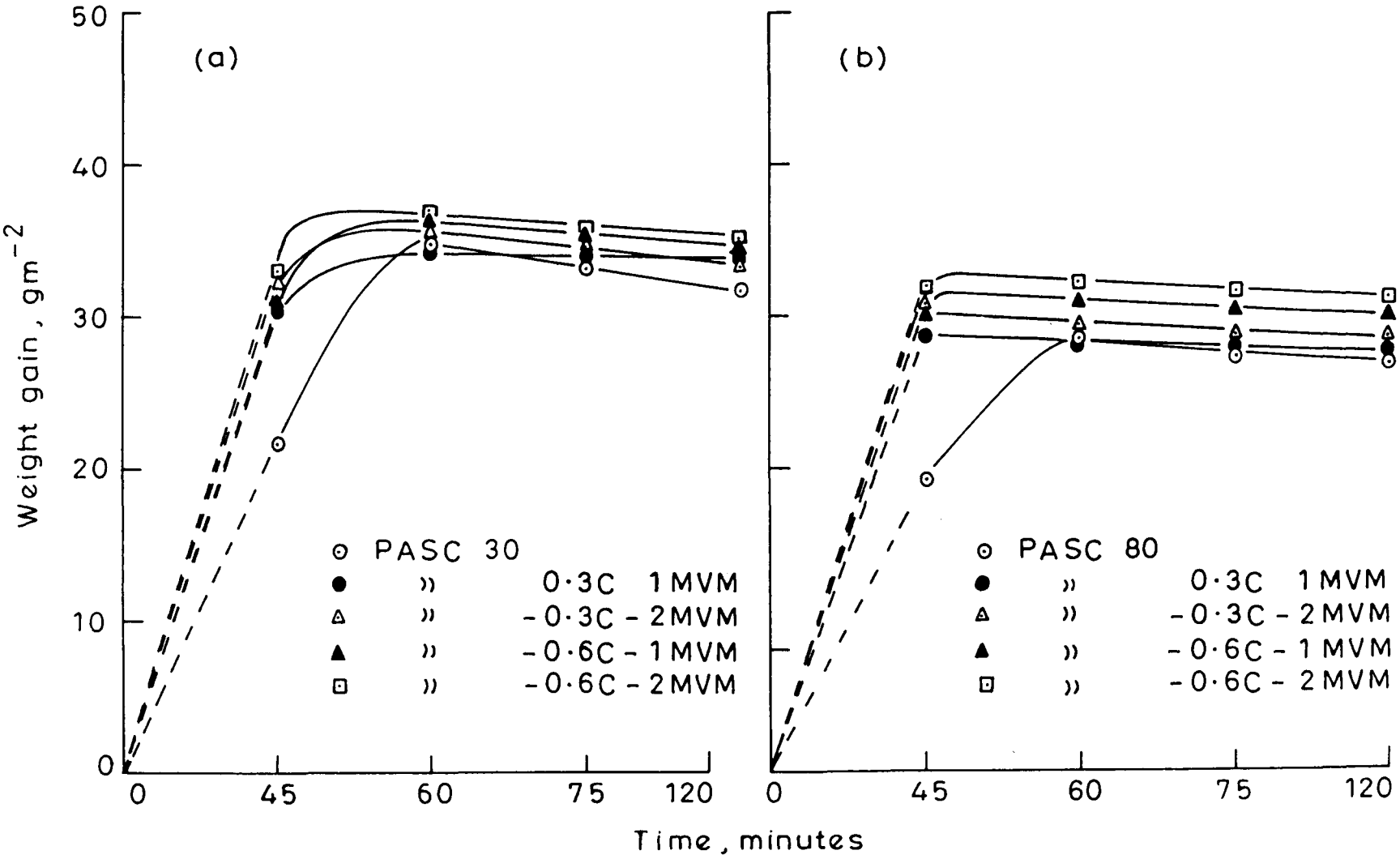

Fig. 3·64 Steam oxidation temperature 550°C

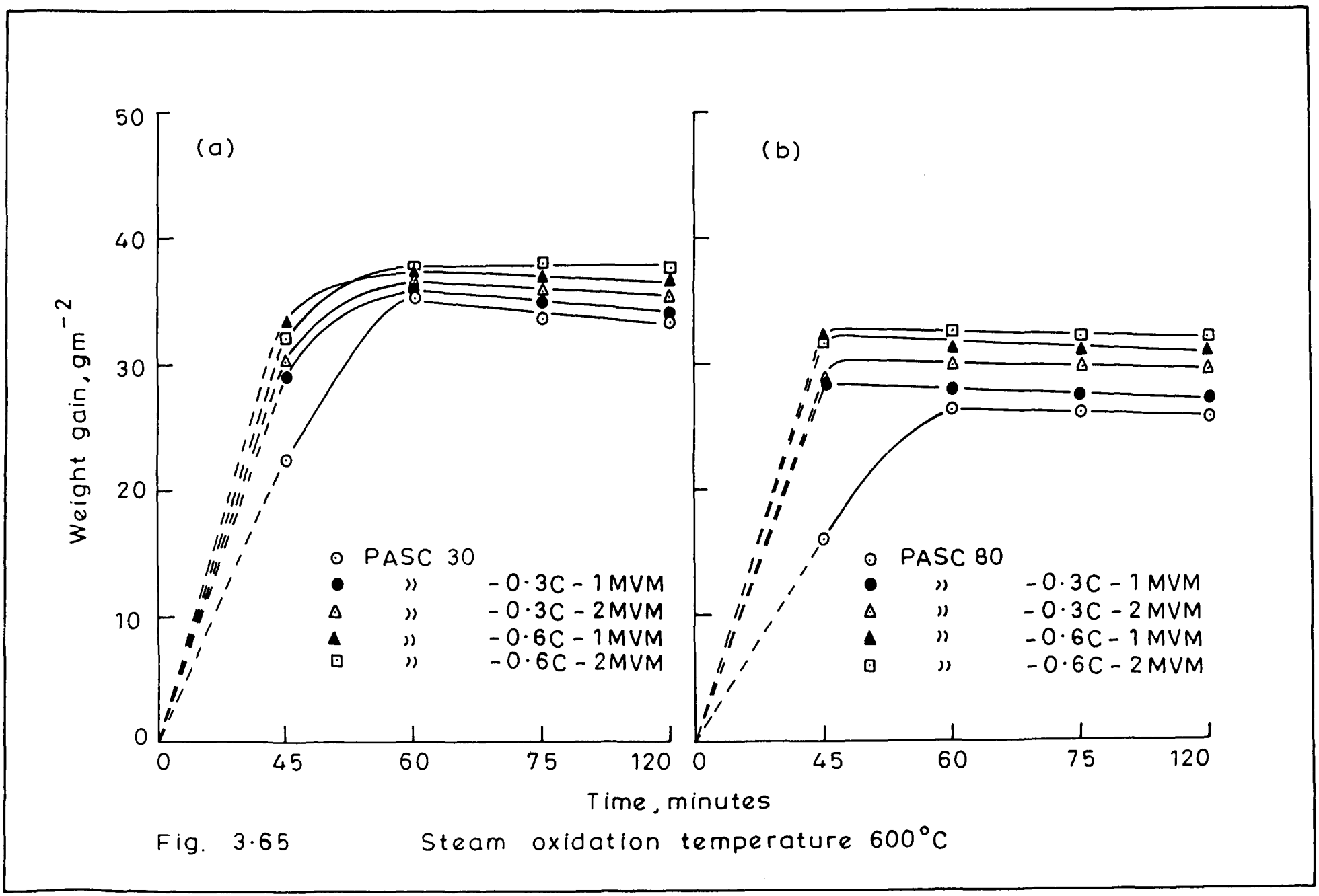

Fig. 3·65 Steam oxidation temperature 600°C

increases (Fig. 3.66a) in case of PASC30 sintered powder compacts treated at 450°C. When 0.3 % C and 1 % Cu are added to PASC30 powder compacts, there is no change in variation of hardness with steam treatment times. The benefit of sintered hardness by 0.3 % C and 1 % Cu is carried over in steam treated case. When Cu- content is increased to 1 % keeping C at the same level of 0.3 % , there is a significant improvement in steam treated hardness and that hardness goes on increasing with increase in treatment times upto 60 minutes after which it remains constant (Fig. 3.66a). When C content is increased from 0.3 to 0.6 % at 1 % Cu- level, there is a small improvement in hardness due to steam treatment. At higher C content of 0.6 %, when Cu- content is increased from 1 to 2 % , hardness increases with steam oxidation time but effect of steam treatment is marginal and much less than that in case of 0.3 % C- containing PASC30 powder compact. When P-content is increased from 0.3 to 0.8 % , there does not appear to be any benefit of steam treatment on hardness and variation of hardness with time of steam oxidation as a function of alloying elements remains unchanged except that significant benefit of increasing Cu content over steam treated hardness is evident at 0.6 % C level (Fig. 3.66 b).

When steam oxidation temperature was increased from

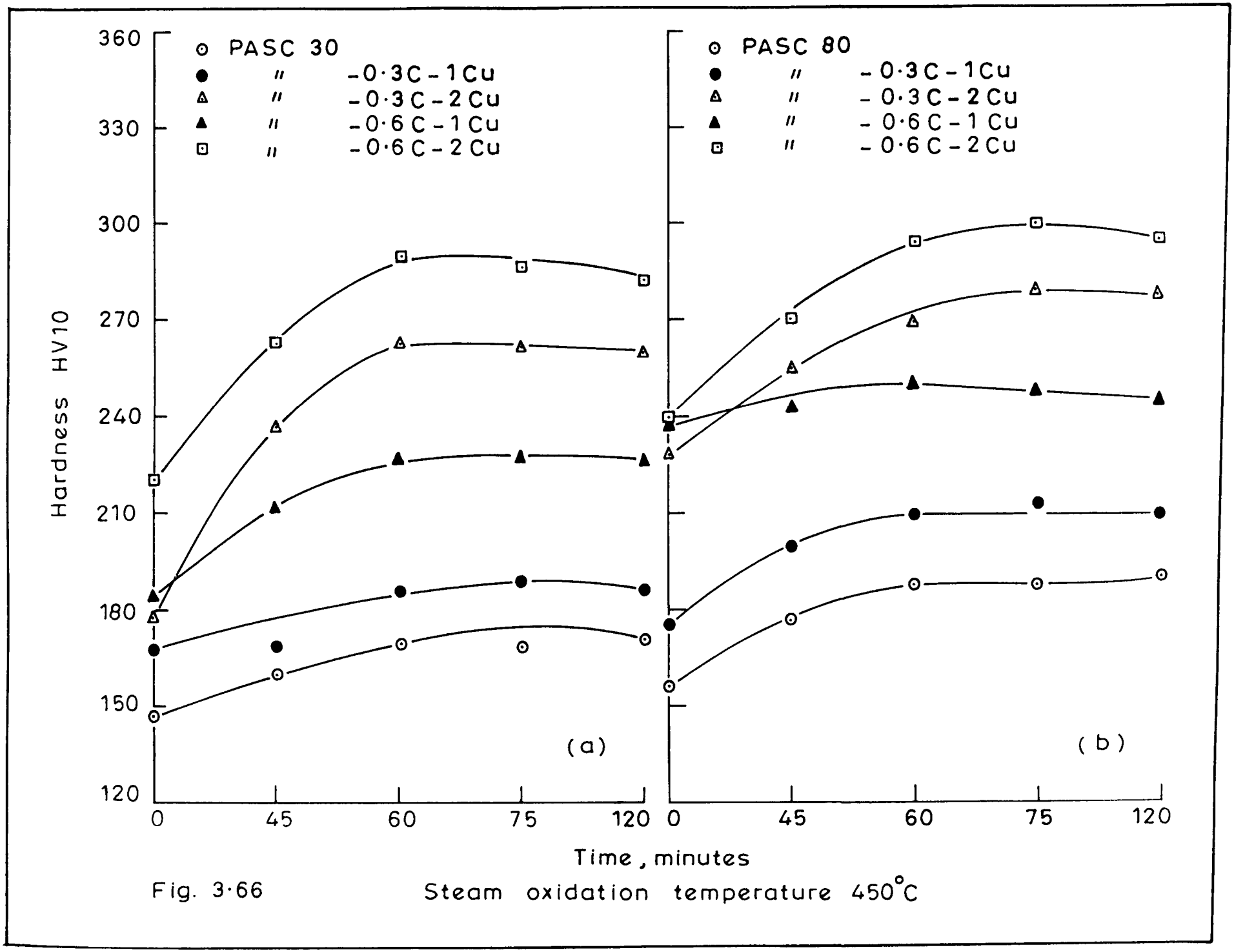

Fig. 3·66 Steam oxidation temperature 450°C

450 to 500°C, there occurs an increase in hardness with steam treatment times upto over 45 minutes in PASC30 as well as PASC80 sintered powder compacts (Fig. 3.67). 0.3 % C and 1 % Cu addition do not give any hardness benefit due to steam treatment (Figs. 3.67 a and b). When copper content is increased from 1 to 2 % keeping C-level same, there occurs significant improvement in hardness with increase in steam oxidation period upto certain time. However, when C content is increased from 0.3 to 0.6 % keeping Cu-level constant, there is hardly any improvement in hardness of steam treated samples due to increase in C-contents only (Fig. 3.67). However, steam treatment upto 45 minutes, brings about significant improvement in hardness over as sintered hardness of each alloy composition. Magnitude of increase in steam treated hardness is more in case of higher Cu-containing compacts as compared to that in case of higher C-containing compacts (Fig. 3.67).

When steam oxidation temperature was increased to 527°C (Fig. 3.68), variation of hardness with steam treatment period in respect of increasing Cu, C or P-content remains unchanged. However, magnitude of increase in hardness due to steam oxidation marginally increases in all the compositions as compared to that treated at 500°C (Figs. 3.67 and 3.68).

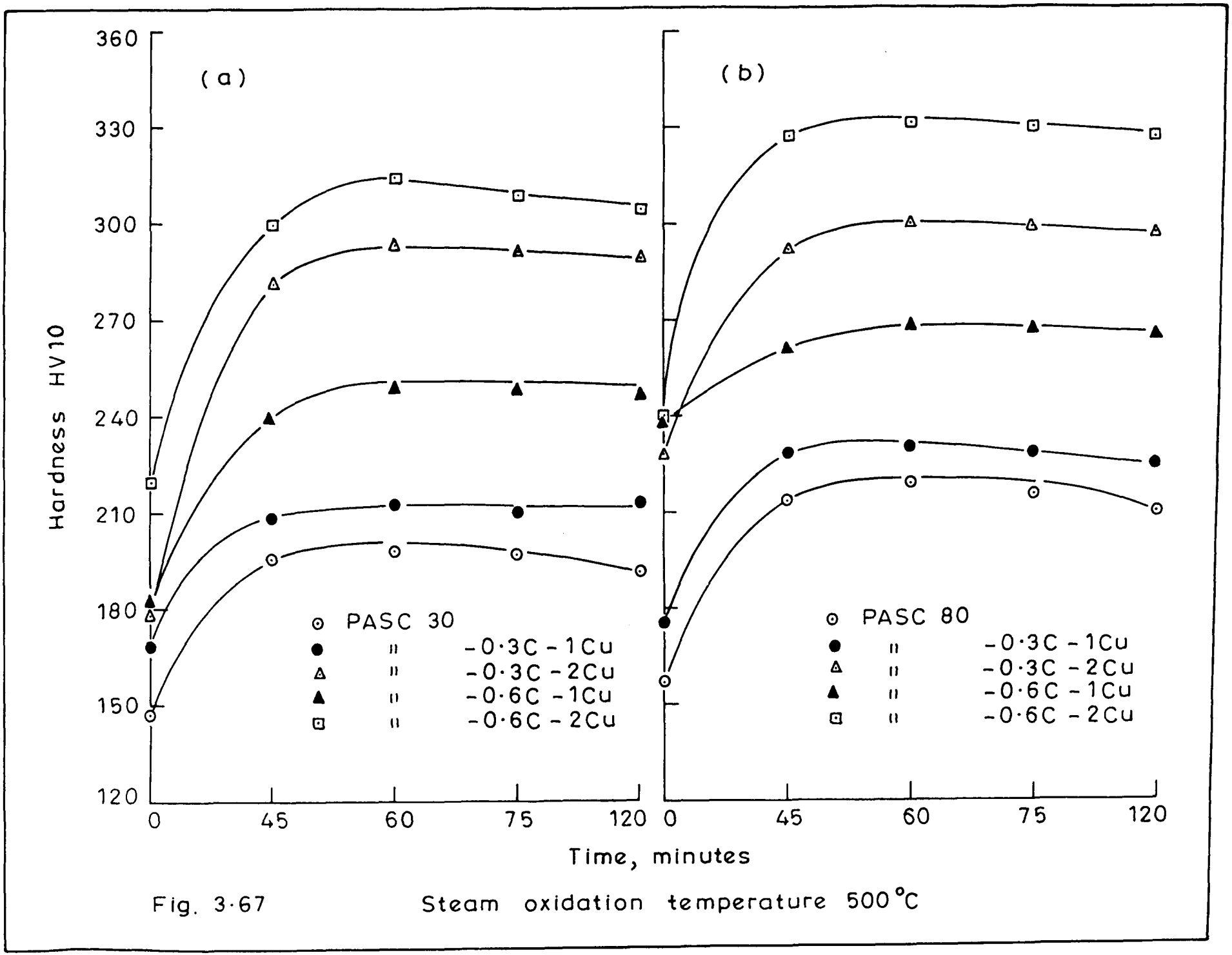

Fig. 3·67 Steam oxidation temperature 500 °C

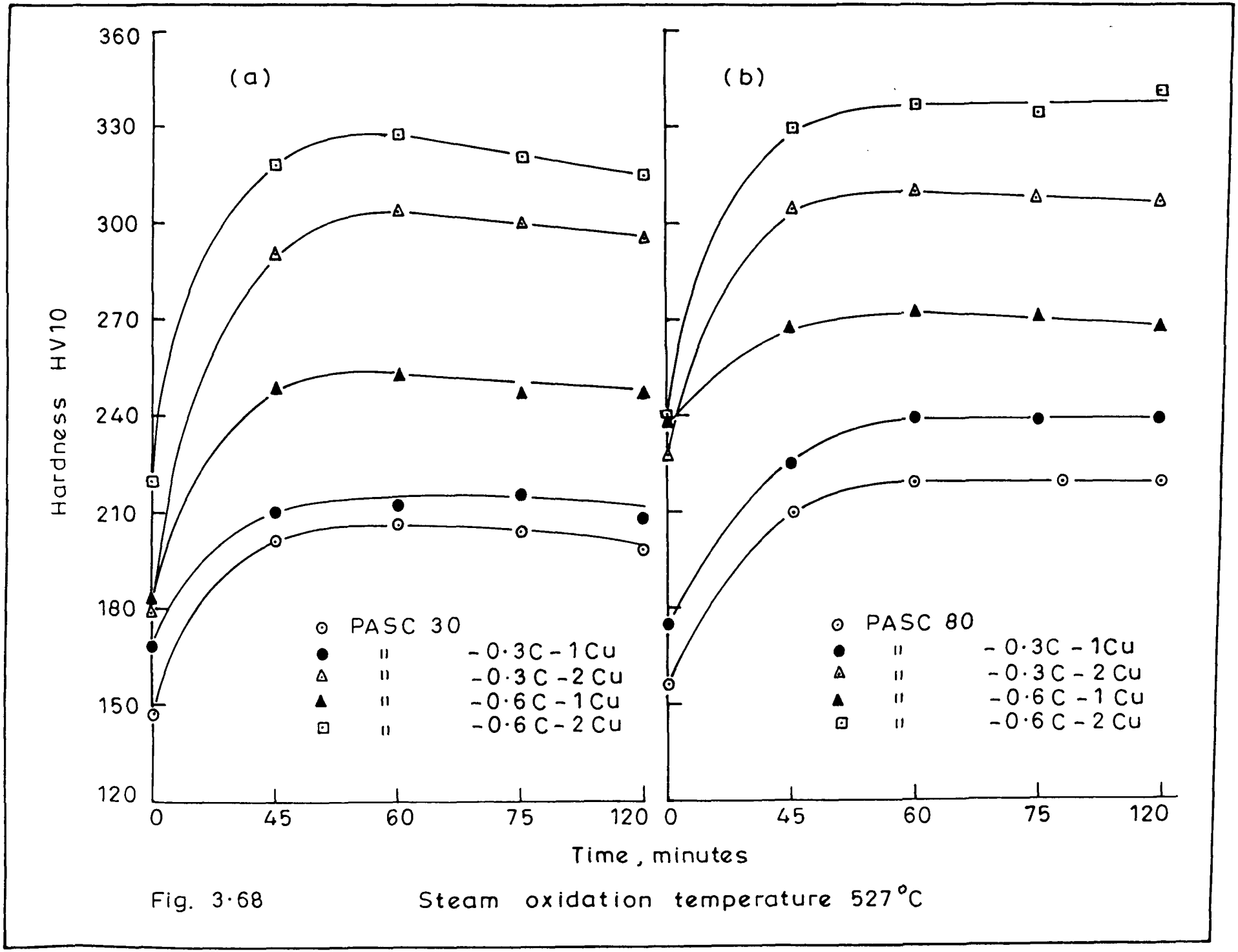

Fig. 3·68 Steam oxidation temperature 527°C

When steam treatment temperature was further increased to 550°C (Fig. 3.69) nature of plot remains qualitatively same. However, improvement in hardness due to steam treatment is less and maximum in hardness is achieved at 60 minutes of treatment times which is more evident in case of PASC80 sintered powder compacts (Fig. 3.69 a and b).

When steam oxidation temperature was further increased to 600°C (Fig. 3.70), there is no change in the variation of hardness with steam oxidation period. Improvement in hardness of PASC30 powder compact due to steam treatment is carried over in other alloy compositions except that increase in Cu- content from 1 to 2 % significantly increases steam treated hardness. In general, saturation in hardness after steam treatment is arrived earlier in higher Cu- containing compacts and to a lesser extent in higher P- containing compacts.

3.3.2.2 PASC-Ni-C compacts

At steam oxidation temperature of 450°C, in case of PASC30 sintered powder compacts, addition of 0.3 % C and 1 % Cu does not produce effect of alloying elements on steam treated hardness (Fig. 3.71). When Ni- content was

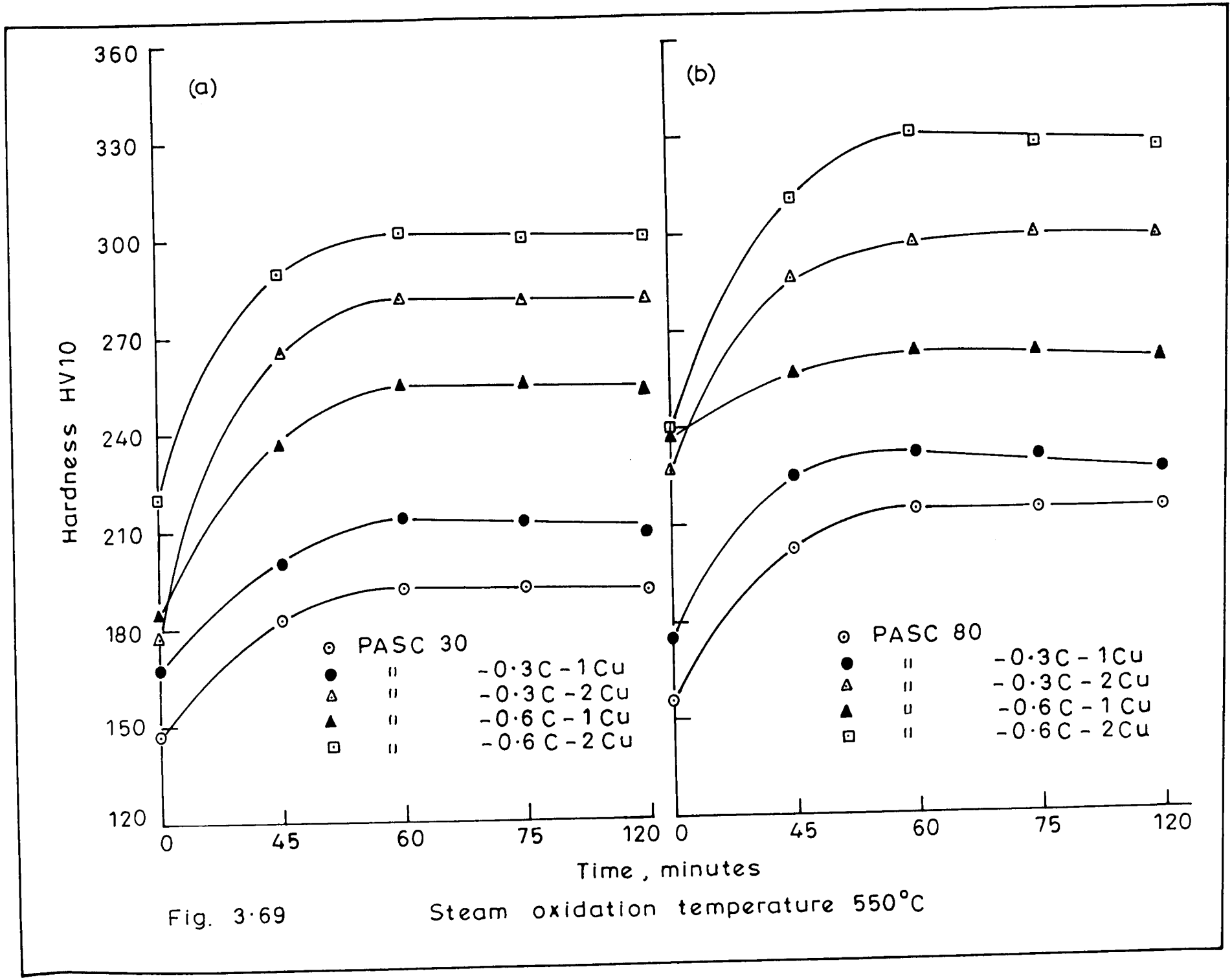

Fig. 3·69 Steam oxidation temperature 550°C

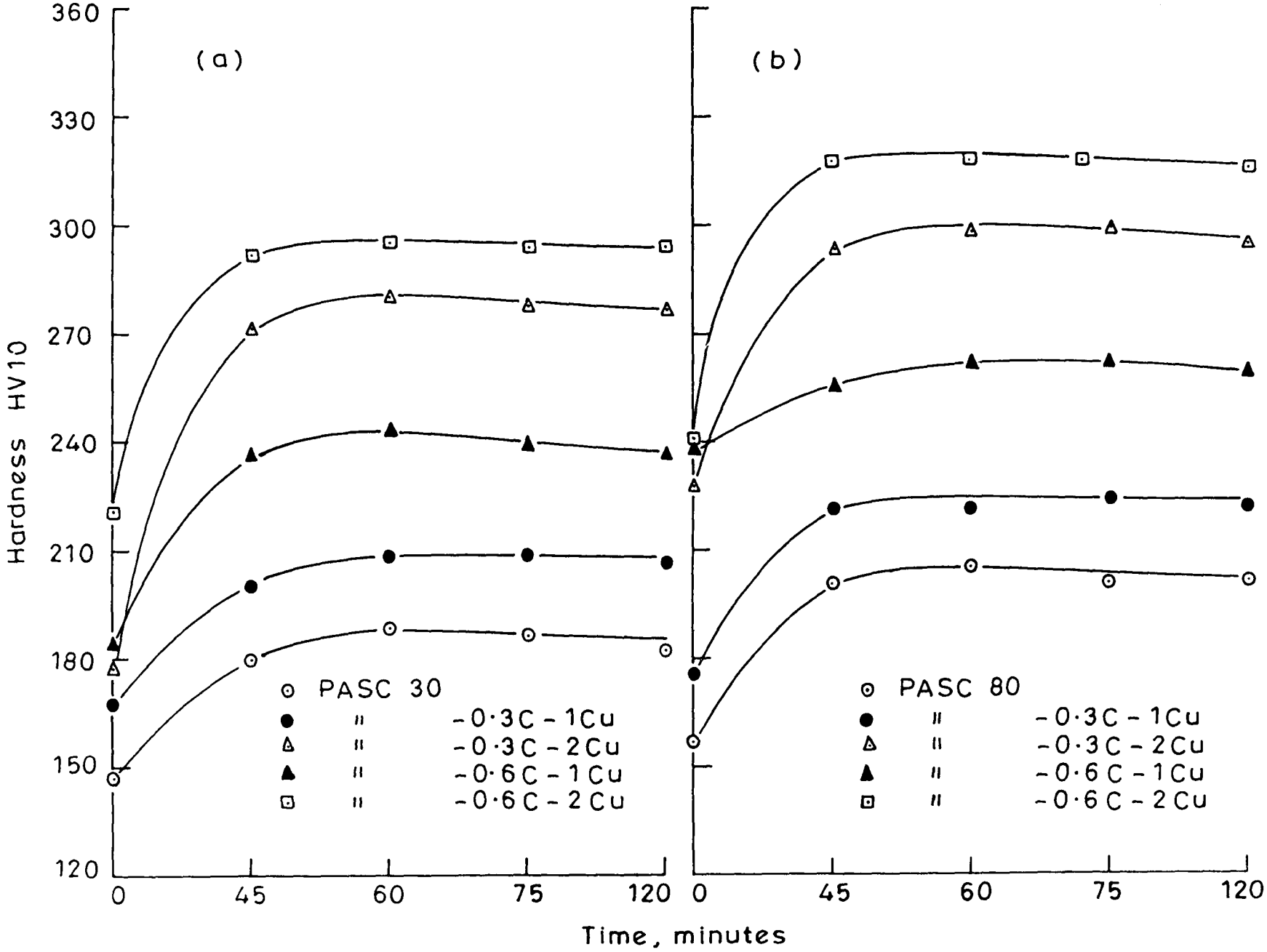

Fig. 3·70 Steam oxidation temperature 600°C

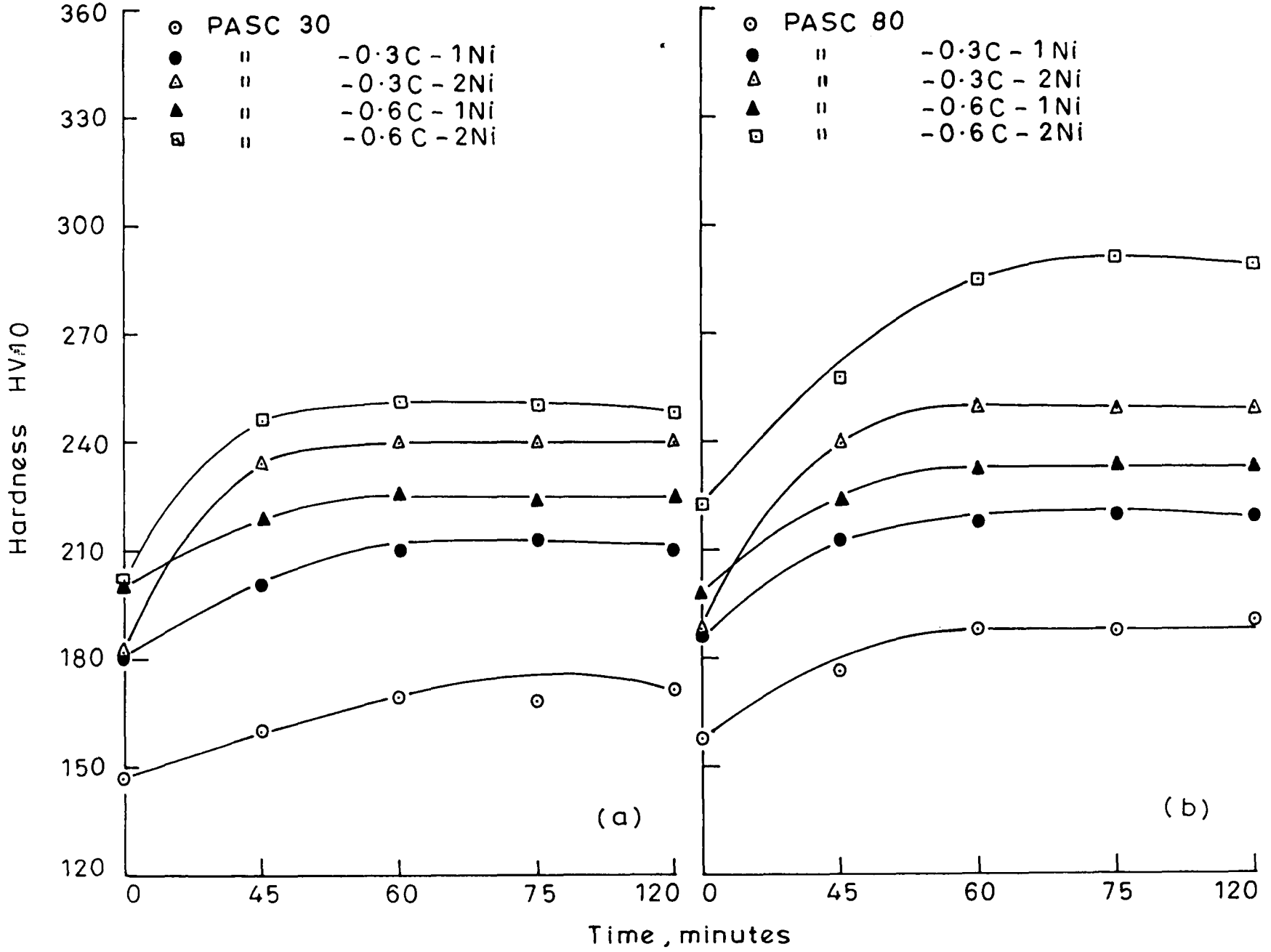

Fig. 3·71 Steam oxidation temperature 450°C

increased from 1 to 2 % keeping C- level constant there is increase in hardness with increase in steam oxidation period. Such an effect is not observed when C- content is increased from 0.3 to 0.6 % keeping Ni- level constant. Increase in P- content from 0.3 to 0.8 % does not affect hardness after steam treatment at 450°C (Fig. 3.71 a and b). Saturation in hardness is observed at or above 60 minutes of treatment period.

When steam oxidation temperature was increased to 500°C (Fig. 3.72), there occurs a significant increase in hardness after steam treatment upto 60 minutes of oxidation period after which hardness is levelled off in compacts based on PASC30 as well as PASC80 powders. Level of increase in hardness after steam treatment increases as compared to that observed in case of 450°C steam treatment (Fig. 3.71 and 3.72).

When steam treatment temperature was further increased to 527°C, effect of 0.3 % C and 1 % Ni on steam treated hardness is significant in case of PASC30 as well as PASC80 sintered powder compacts (Fig. 3.73). However, there is significant effect of higher amount of alloying elements on steam treated hardness over that of as sintered compacts, particularly in case of compacts containing higher amount

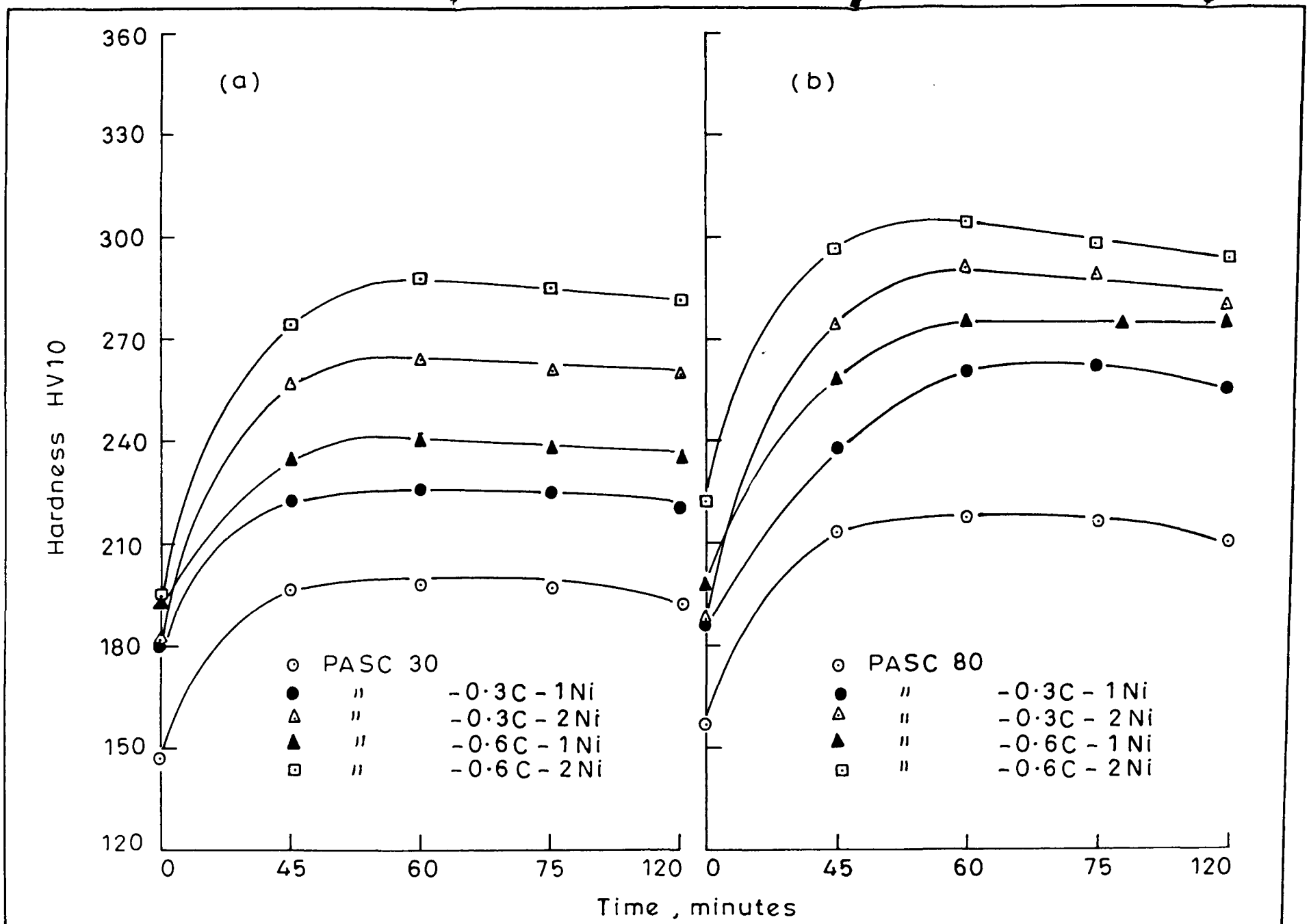

Fig. 3·72 Steam oxidation temperature 500°C

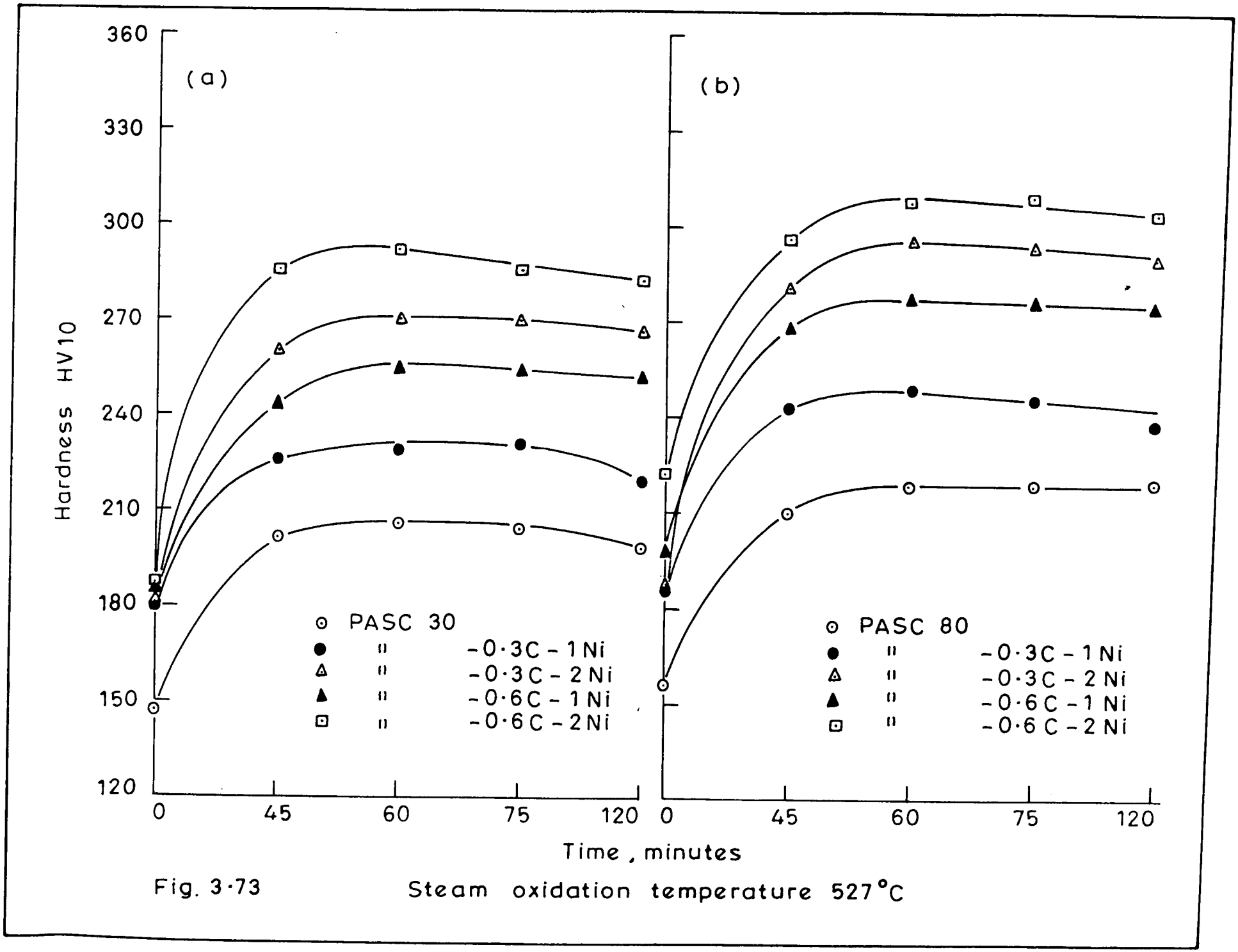

Fig. 3·73 Steam oxidation temperature 527°C

of Ni. In case of Ni- containing compacts, effect of higher amount of phosphorus on hardness due to steam treatment alone is insignificant.

When steam treatment temperature was further increased to 550 and 600°C (Figs. 3.74 and 3.75), variation of hardness with steam treatment time remains unchanged. Rather, there is a slight reduction in bulk hardness of steam treated samples as compared to that observed in case of 527°C treatment (Fig. 3.73). Saturation in hardness of steam treated samples is achieved at times of 60 minutes or lower and at higher temperatures, saturation is achieved earlier (Fig. 3.73-3.75).

3.3.2.3 PASC-Mo-C compacts

At a temperature of 450°C, when 0.3 % C and 1 % Mo are added to PASC30 powder compacts there is significant increase in hardness with steam treatment time (Fig. 3.76a). When P-content is increased from 0.3 to 0.8 % hardness benefit brought about by 0.3 % C and 1 % Mo in case of steam treated samples is much higher (Fig. 3.76b). At 1 % Mo level, when C content is increased from 0.3 to 0.6 %, there is only marginal increase in hardness of steam treated samples. This effect of increase of C- content on hardness of steam treated sample remains unchanged even at higher

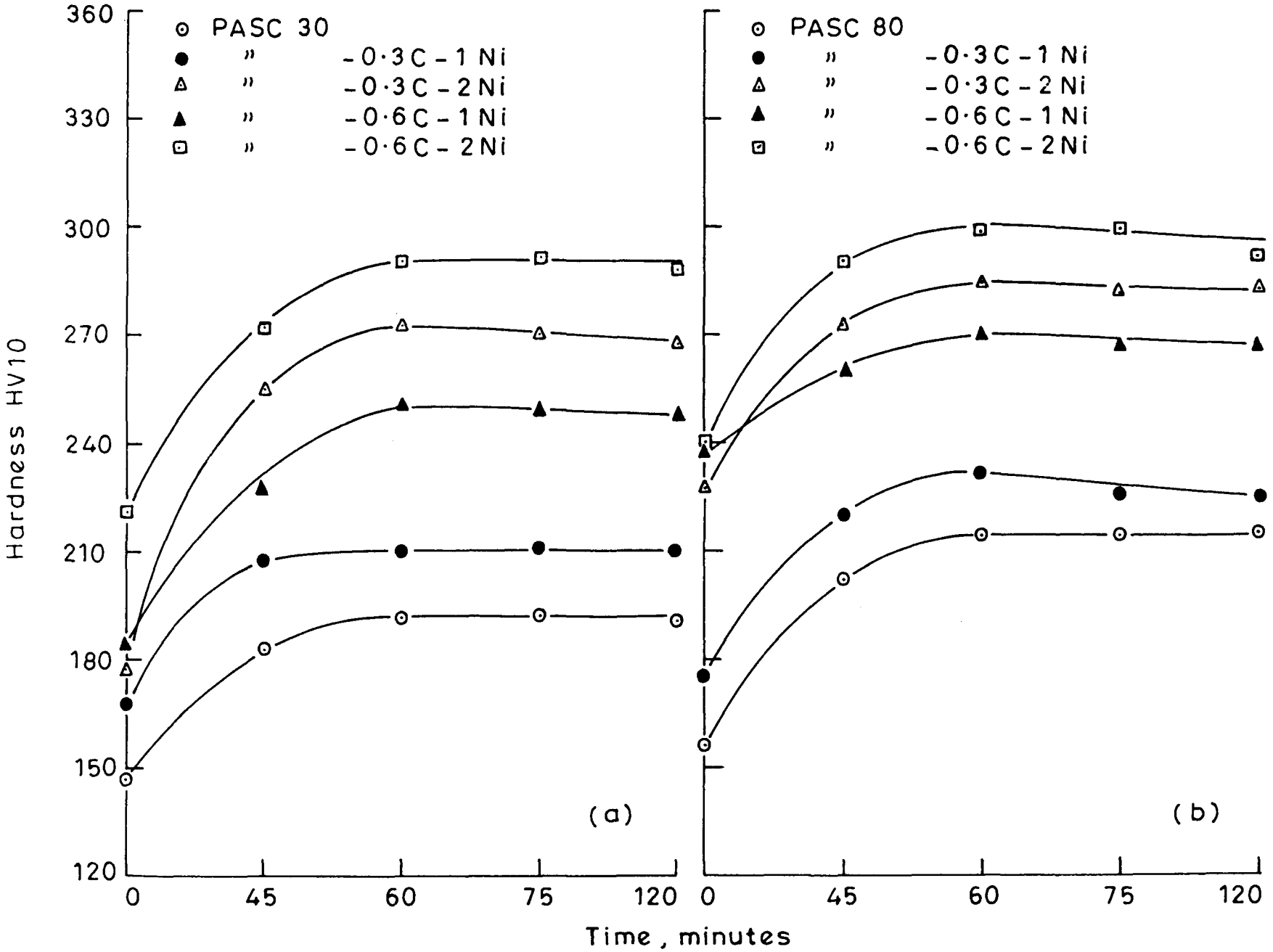

Fig. 3·74 Steam oxidation temperature 550°C

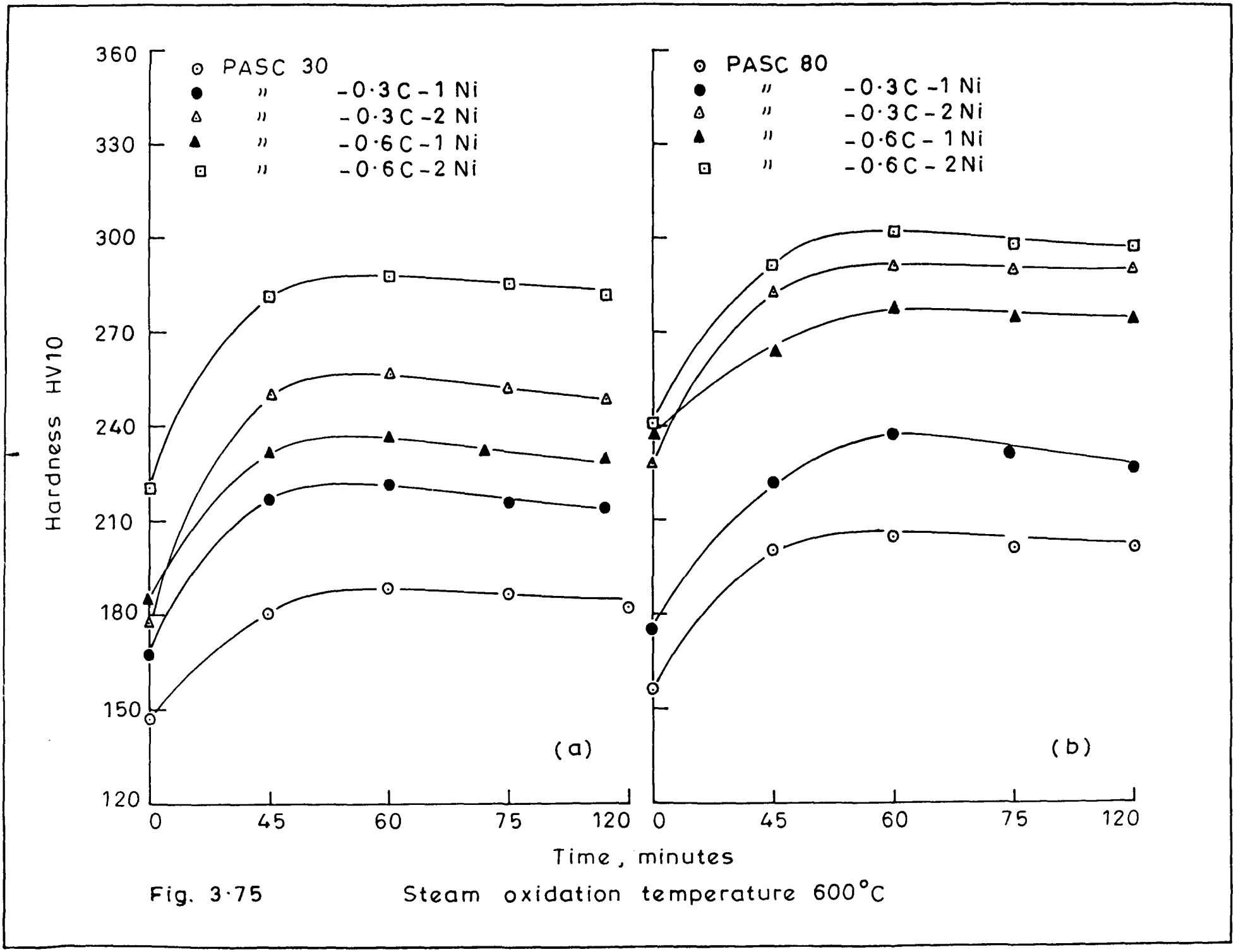

Fig. 3·75 Steam oxidation temperature 600°C

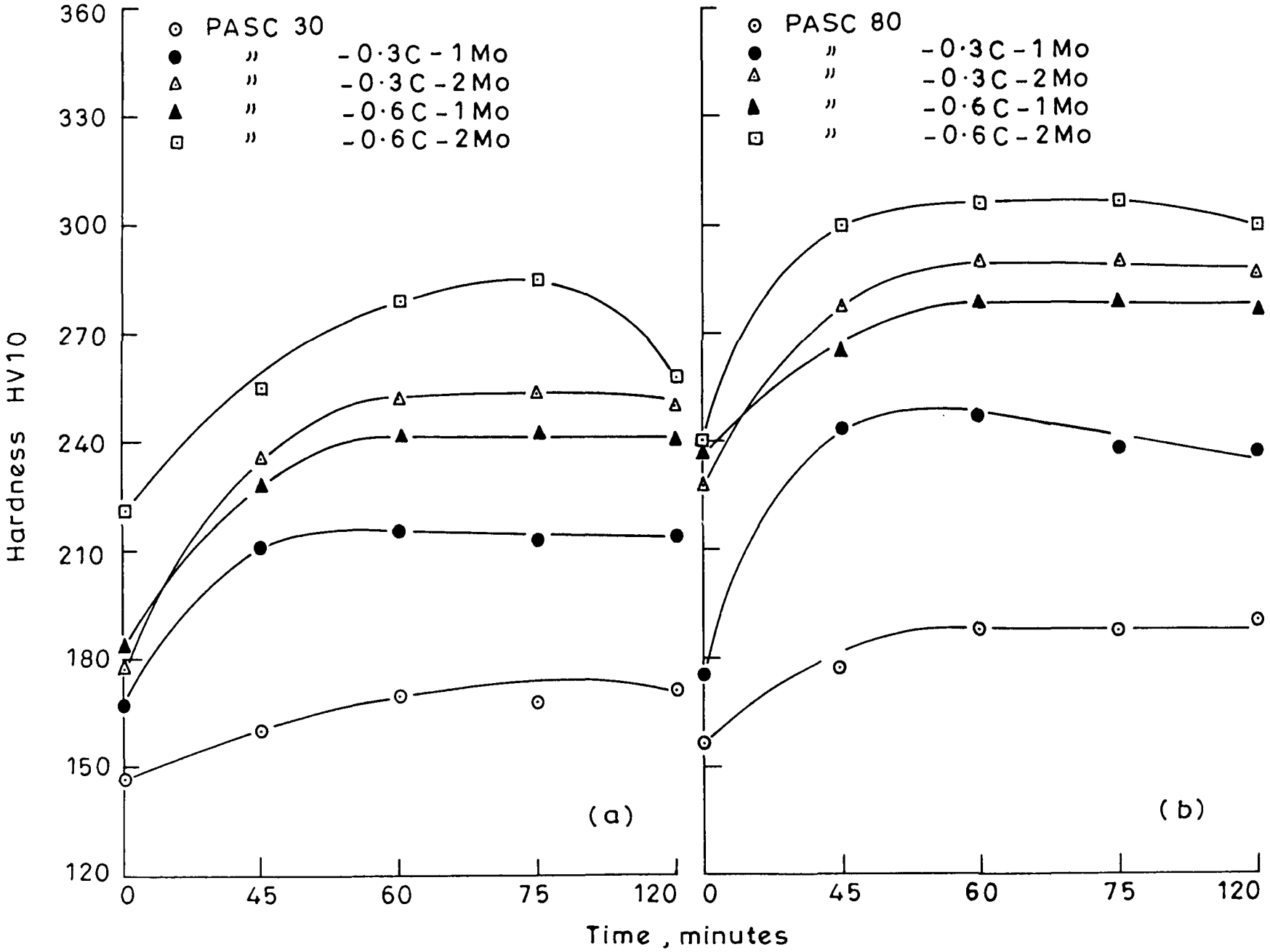

Fig. 3·76 Steam oxidation temperature 450°C

Mo- level of 2 %. Similar situation prevails when Mo-content is increased from 1 to 2 % at equivalent C or P-level (Fig. 3.76 a and b). Saturation in hardness is achieved at 60 minutes of treatment times or higher. When steam oxidation temperature was increased to 500°C, variation of hardness with steam treatment time in respect of effect of C, P or Mo remains qualitatively unchanged (Fig. 3.77). However, there occurs a significant increase in hardness of steam treated samples over that of as sintered compacts in case of all compositions of compacts. Effect of increase of Mo from 1 to 2 % in increasing hardness of steam treated samples is considerable (Fig. 3.77) while there is marginal effect of increase of P on hardness improvement of steam treated samples. The time required to reach maximum hardness during steam treatment is also shortened to less than 60 minutes and in some cases is reduced to 45 minutes (Fig. 3.77) at higher Mo and P contents.

When temperature of steam treatment is further increased to 527°C, there is no qualitative change in variation of hardness with time (Fig. 3.78) but increase in hardness due to steam treatment is higher as compared to those observed in case of lower temperature steam treatment (Figs. 3.76-3.78). In many compositions, an increase in hardness of 40 to 60 % over that of as sintered samples is

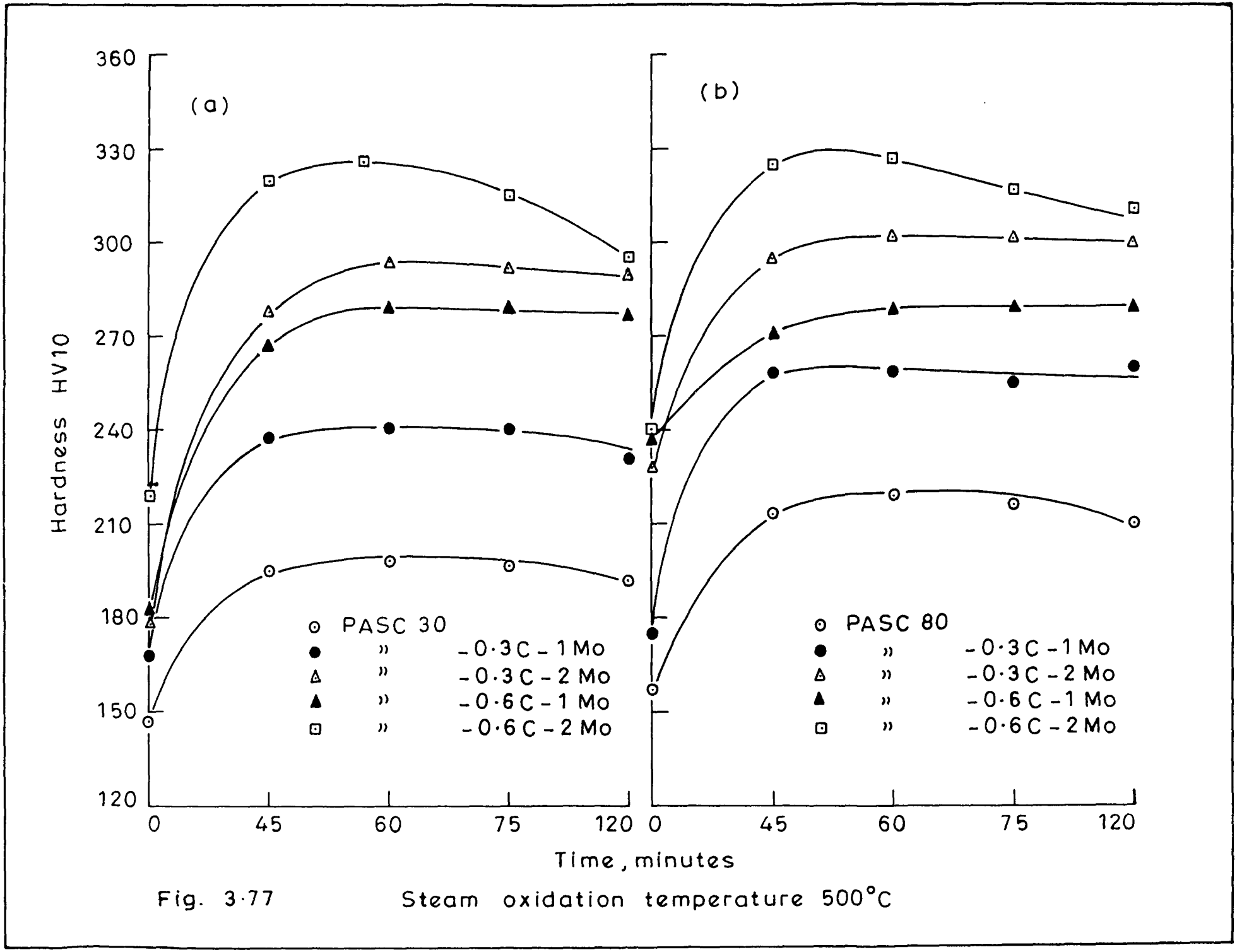

Fig. 3·77 Steam oxidation temperature 500°C

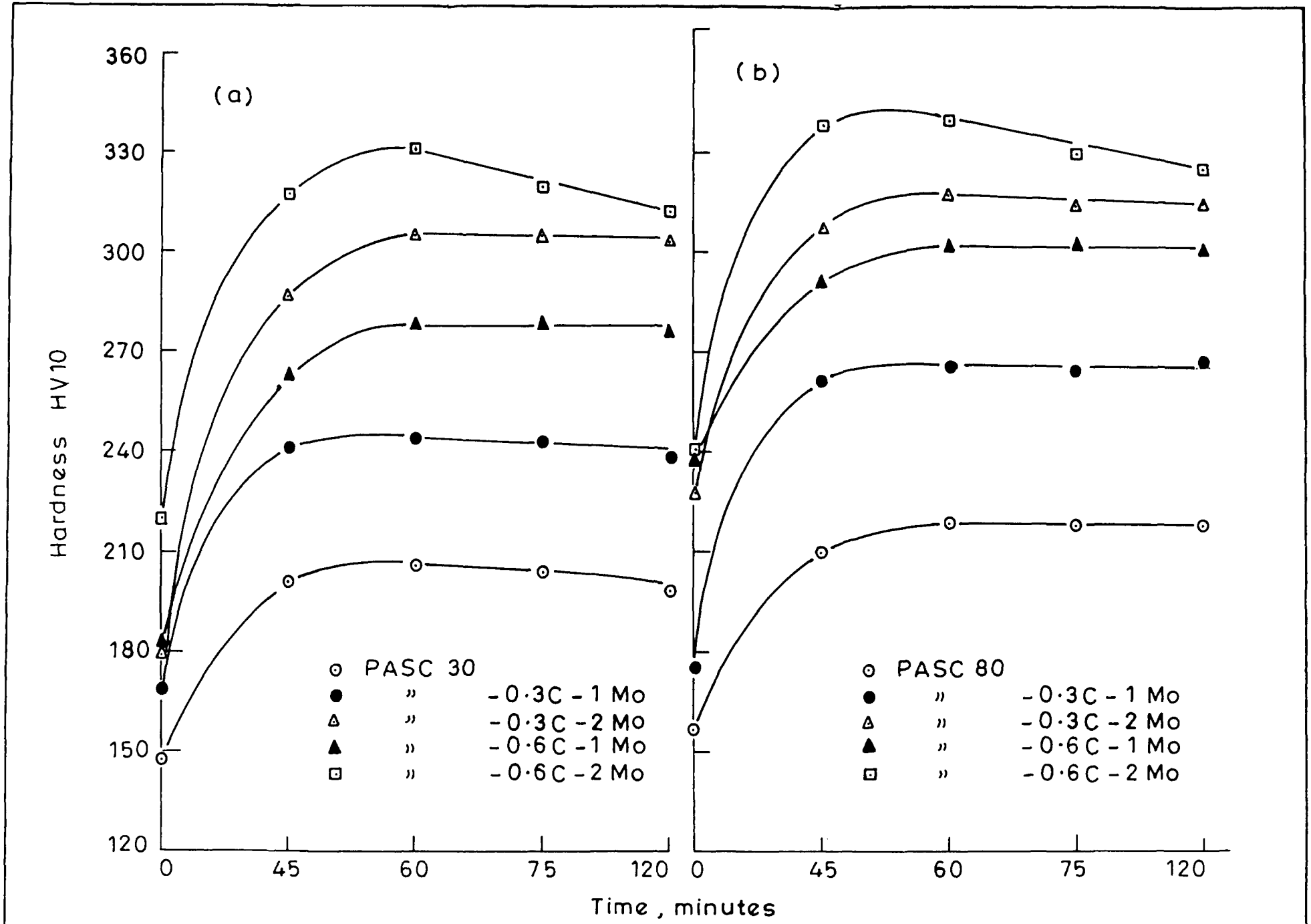

Fig. 3·78 Steam oxidation temperature 527°C

achieved after steam treatment for 45 to 60 minutes. One important point to note is that even increase of C- content from 0.3 to 0.6 % marginally increase hardness of steam treated samples. However, effect of increase of Mo- content from 1 to 2 % in enhancing the hardness of steam treated samples is much more considerable.

When steam treatment temperature is further increased to 550 and 600°C there occurs a slight decrease in hardness after steam treatment (Figs. 3.79 and 3.80) but nature of the curve remains qualitatively same. The time required to achieve saturation value of hardness is also unaffected by increase in steam oxidation temperature above 527°C. Effect of increase of C from 0.3 to 0.6 % does not deteriorate hardness after steam treatment in any composition of PASC-Mo-C compacts at any treatment temperature and for any period of steam treatment (Figs. 3.76-3.80).

3.3.2.4 PASC-MCM-C compacts

As already stated in first chapter MCM contains Mn, Cr, Mo.

In case of PASC30 sintered powder compacts, when 0.3 % C and 1 % MCM are added, there occurs a significant increase in hardness with steam treatment period which

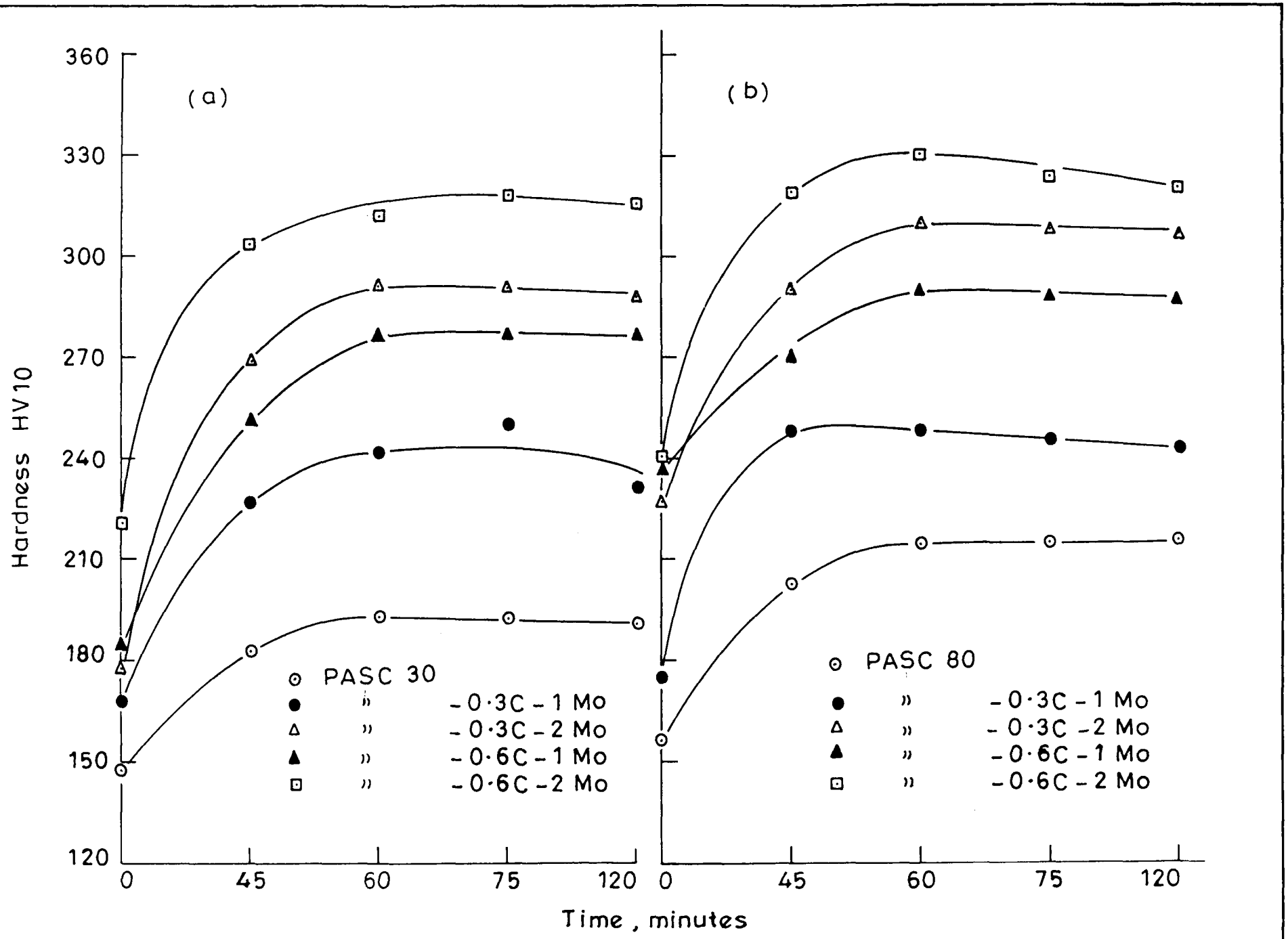

Fig. 3·79 Steam oxidation temperature 550°C

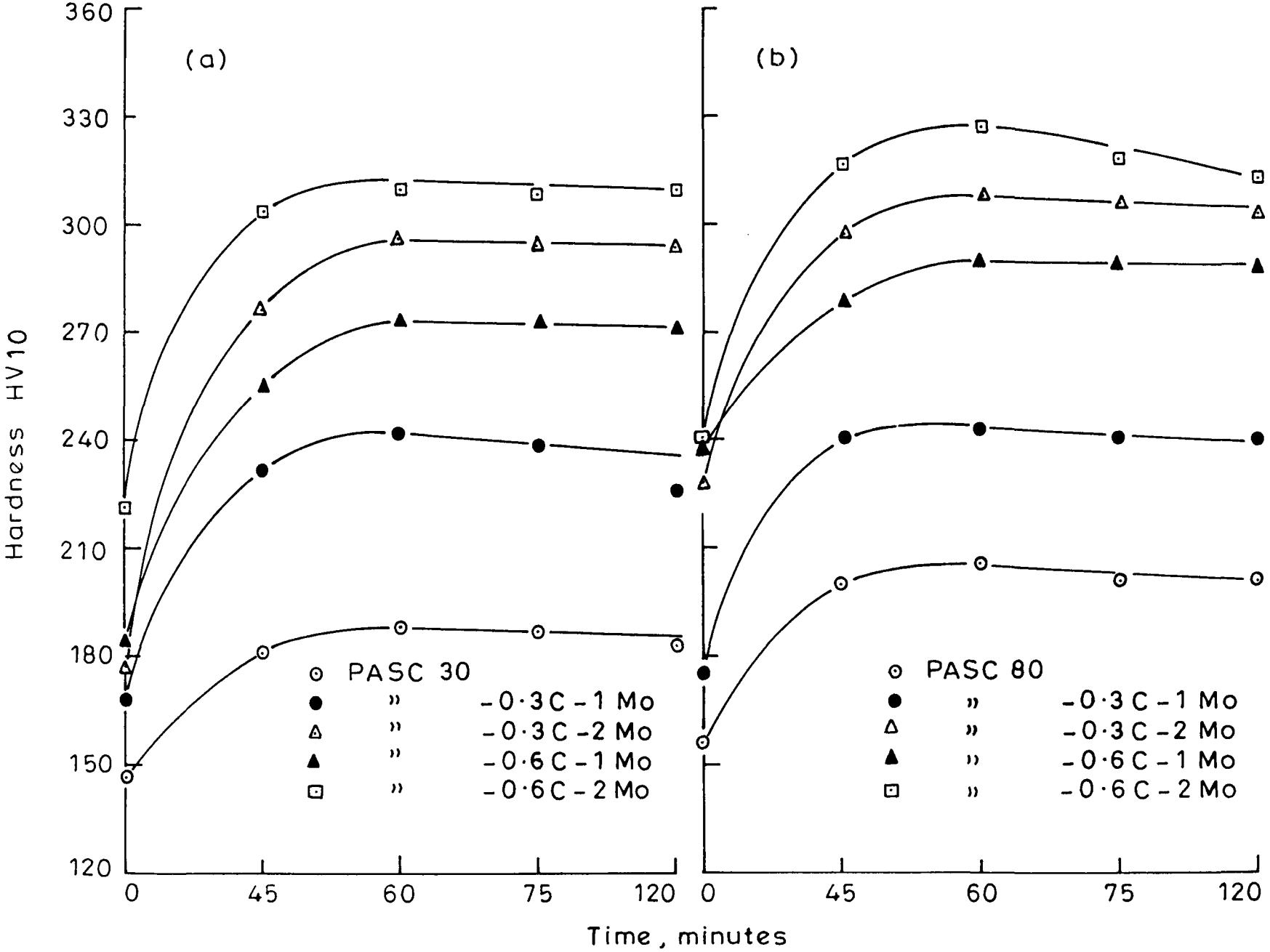

Fig. 3·80 Steam oxidation temperature 600°C

goes on increasing upto at least 60 minutes of treatment at 450°C. When C contents are increased from 0.3 to 0.6 % keeping MCM at 1 % level, there occurs a significant increase in hardness (Fig. 3.81) contrary to the behaviour observed in case of other alloy systems described earlier. However, when MCM content is increased from 1 to 2 % keeping C at 0.3 % level, hardness is still higher. Similar behaviour of increase in hardness after steam treatment due to the effect of C or MCM is observed at higher C or MCM levels. Saturation in hardness is achieved at 60 minutes of steam treatment time in case of PASC30 based sintered powder compacts while at 75 minutes of treatment time in case of PASC80 based powder compacts (Fig. 3.81 a and b). Further, hardness improvement in case of PASC80 based powder compacts after steam treatment is generally lower.

When steam oxidation temperature is increased to 500°C, the variation of hardness with steam treatment time as a function of C, P or MCM remains same except that PASC80 based powder compact gives higher steam treated hardness as compared to PASC30 based powder compacts as observed in earlier systems, although contribution to total steam treated hardness is also due to improvement in sintered hardness because of presence of higher amount

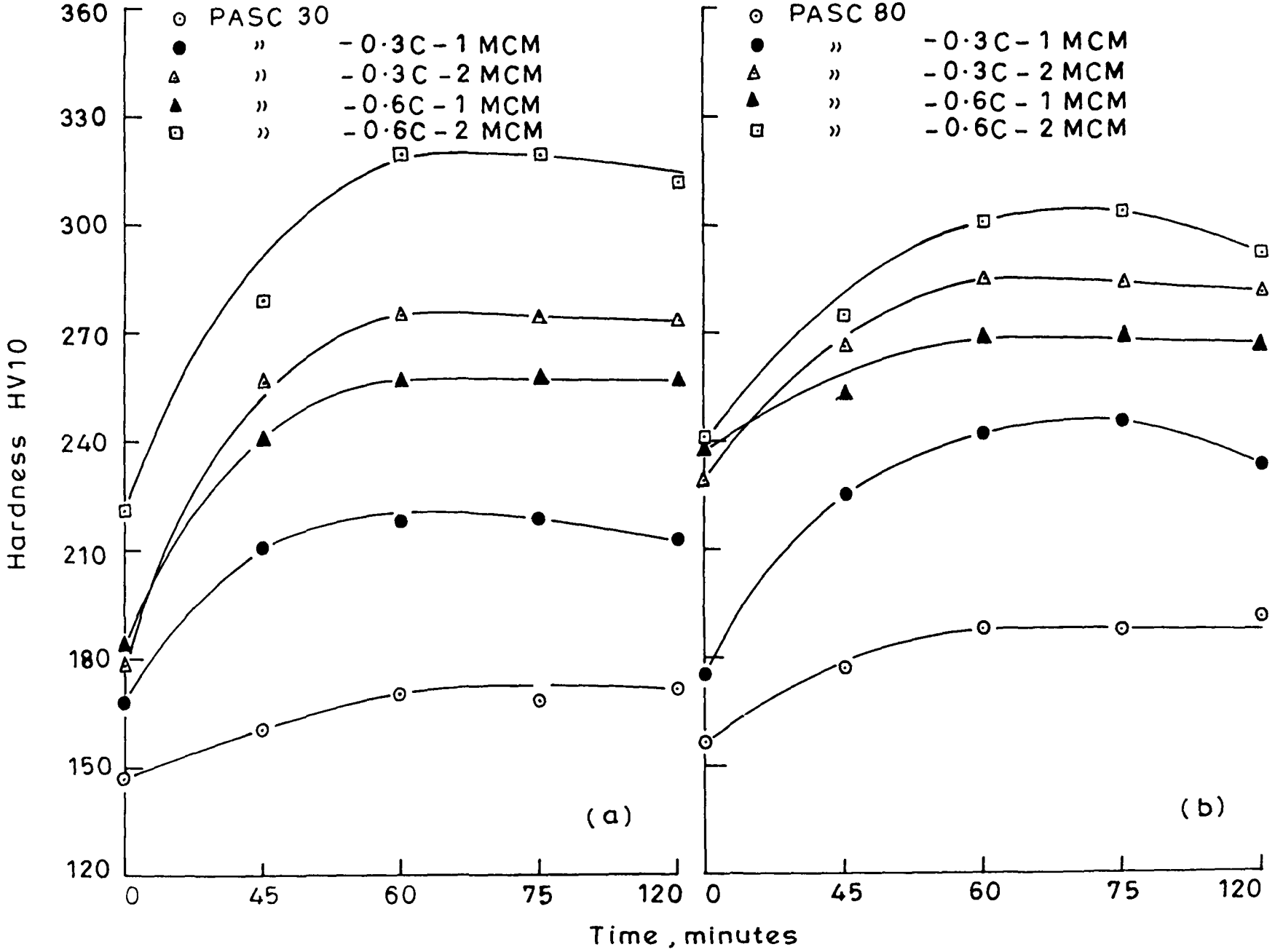

Fig. 3·81 Steam oxidation temperature 450°C

of P (Fig. 3.82 a and b). Time of steam treatment required for getting the maximum in hardness values is shortened to 60 minutes in case of PASC80 based powder compacts (Fig. 3.81 b and 3.82 b).

When steam oxidation temperature was increased to 527°C, variation of hardness with steam treatment time in respect of effect of alloying elements remains unchanged (Fig. 3.83), but time required for reaching saturation value of hardness is further shortened to less than 60 minutes and occasionally 45 minutes, particularly at higher level of 0.6 % C and 2 % MCM in both PASC30 and PASC80 based powder compacts. However, the magnitude of increase in steam treated hardness of higher MCM and carbon containing compacts are particularly high, of the order of 80 % in case of samples treated at both 500 and 527°C (Figs. 3.82 and 3.83).

When steam oxidation temperature is further increased to 550 and 600°C (Figs. 3.84 and 3.85), increase of hardness with steam treatment time remains unchanged. However, increase in hardness after steam treatment decreases and time required for attaining saturation in hardness value is also increased to about 60 minutes (Figs. 3.84 to 3.85).

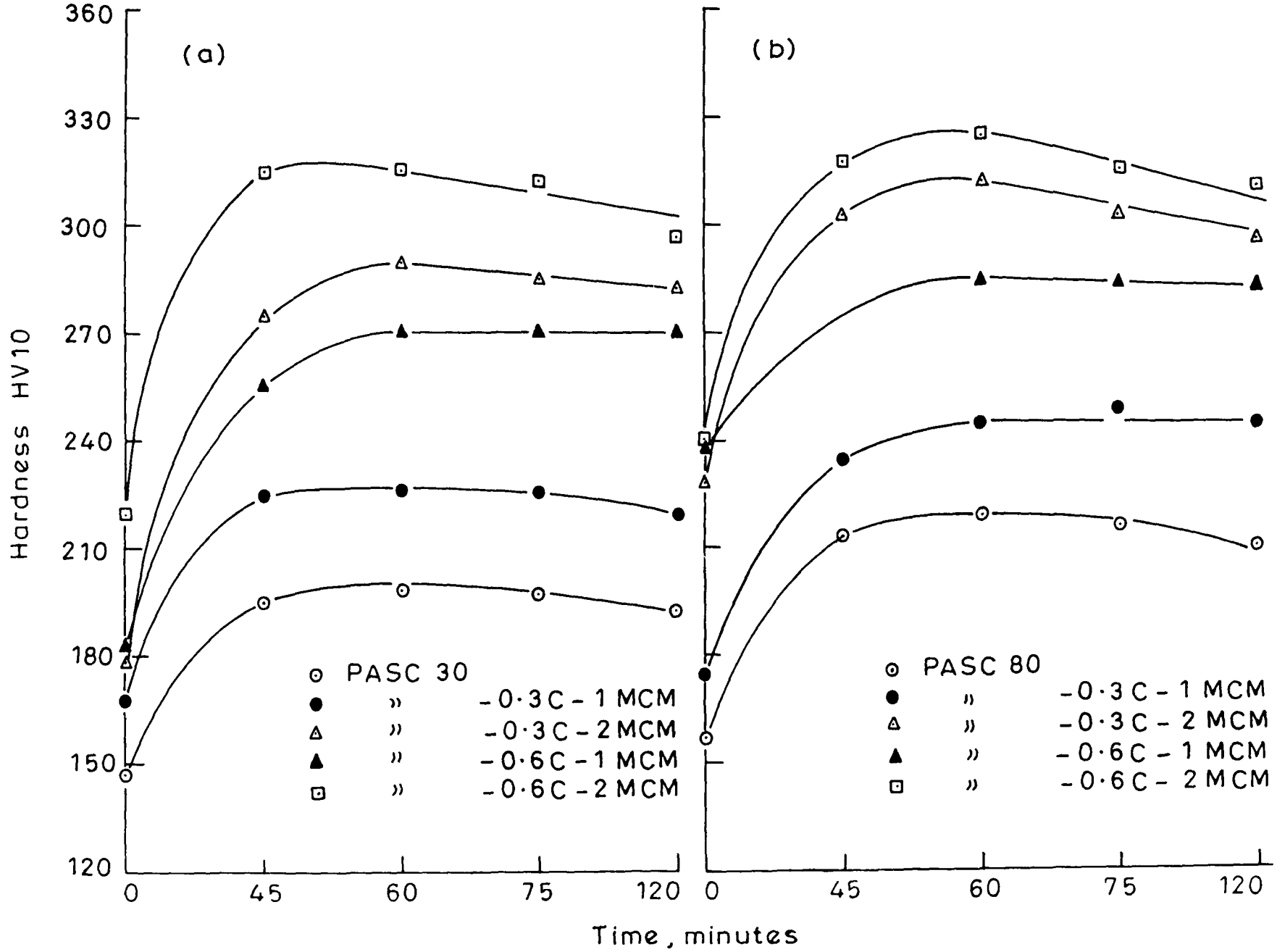

Fig. 3·82 Steam oxidation temperature 500°C

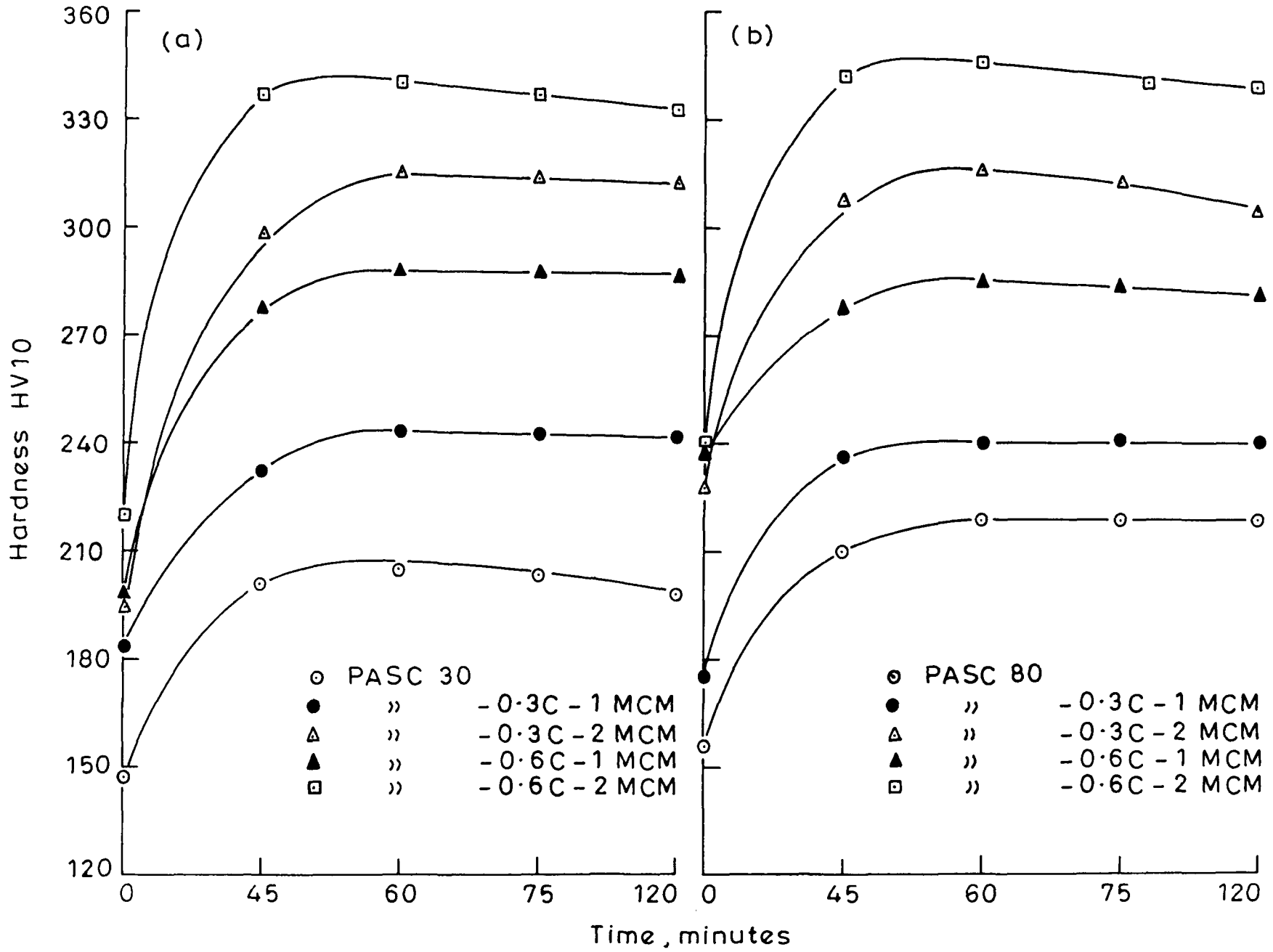

Fig. 3·83 Steam oxidation temperature 527°C

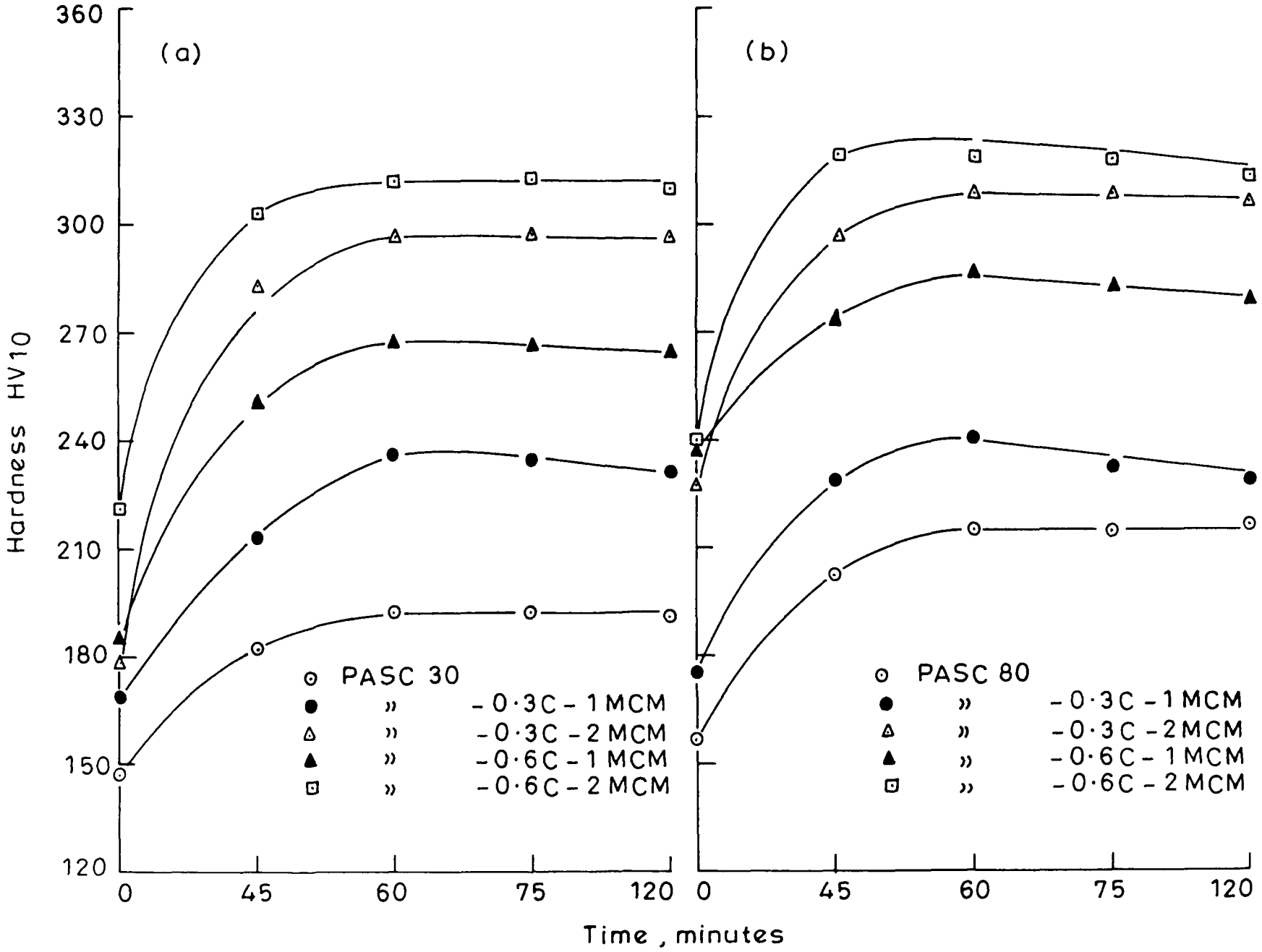

Fig. 3·84 Steam oxidation temperature 550°C

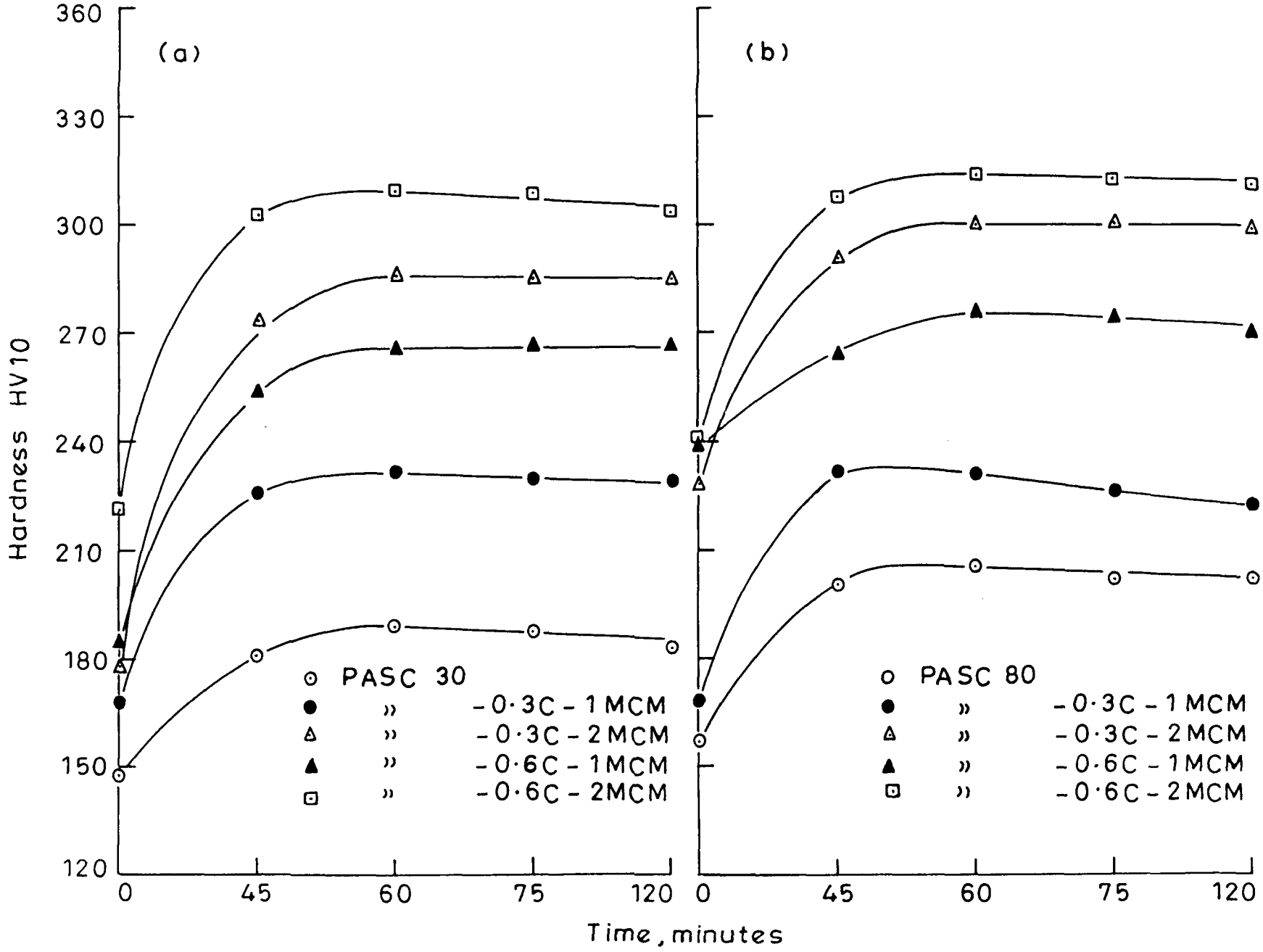

Fig. 3·85 Steam oxidation temperature 600°C

3.3.2.5 PASC-MVM-C compacts

In case of PASC30 or PASC80 sintered powder compacts, steam treated at 450°C, there occurs, in general, an increase in hardness with increase in treatment time upto at least 60 minutes after which it remains constant at all compositions of C or MVM (Fig. 3.86a). Effect of adding 0.3 % C and 1 % MVM on steam treated hardness of PASC80 sintered powder compact is higher than that of PASC30 powder compact (Fig. 3.86 a and b). When C content is increased from 0.3 to 0.6 % keeping MVM level constant, there is no improvement in hardness after steam treatment due only to C at either P or MVM levels (Fig. 3.86), and improvement in sintered hardness due to increase in C-content is carried over in steam treated case. However, in general, increase of MVM content from 1 to 2 % marginally increases hardness of steam treated samples. Higher P-content gives higher hardness benefit after steam treatment in case of MVM-containing compacts. However, hardness level achieved in case of MVM- containing compacts is much lower than in case of MCM containing compacts (Fig. 3.81 and 3.86).

When steam oxidation temperature was increased from 450 to 500°C, variation of hardness with steam treatment time in respect of C, P or MVM contents remains

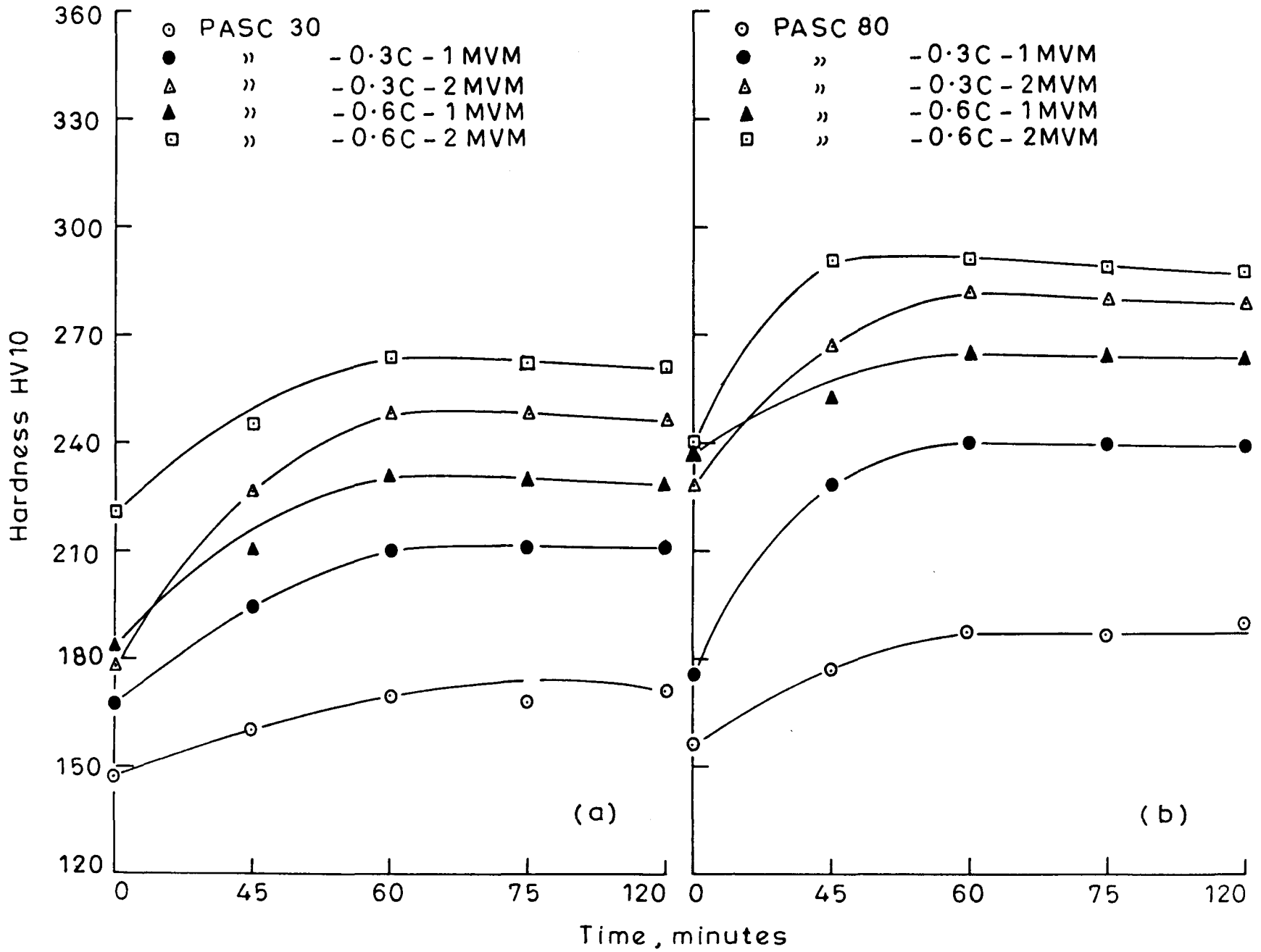

Fig. 3·86 Steam oxidation temperature 450°C

unchanged (Fig. 3.87). However, the difference in magnitude of hardness benefit between MCM- and MVM- containing steam treated samples is narrowed down and is lower (Figs. 3.82 and 3.87) as compared to that observed in case of 450°C steam treatment (Figs. 3.81 and 3.86).

When steam oxidation temperature was further increased to 527°C, nature of curve remains qualitatively unchanged (Fig. 3.88). However, saturation in hardness values is achieved at steam oxidation period of at or lower than 60 minutes. Further, the difference in hardness values between MCM- and MVM- containing steam treated samples is further narrowed down (Fig. 3.83 and 3.88). Also, effect of increasing C or MVM contents keeping the other elements constant on improvement in hardness of steam treated samples becomes obvious.

There is almost no change in variation of hardness with steam treatment period when steam oxidation temperature is further increased to 550 and 600°C (Figs. 3.89 and 3.90).

3.3.3 Structural studies

Microstructural examinations of steam treated samples were carried out in two parts. Optical metallography of all compositions in each of the five alloy systems steam

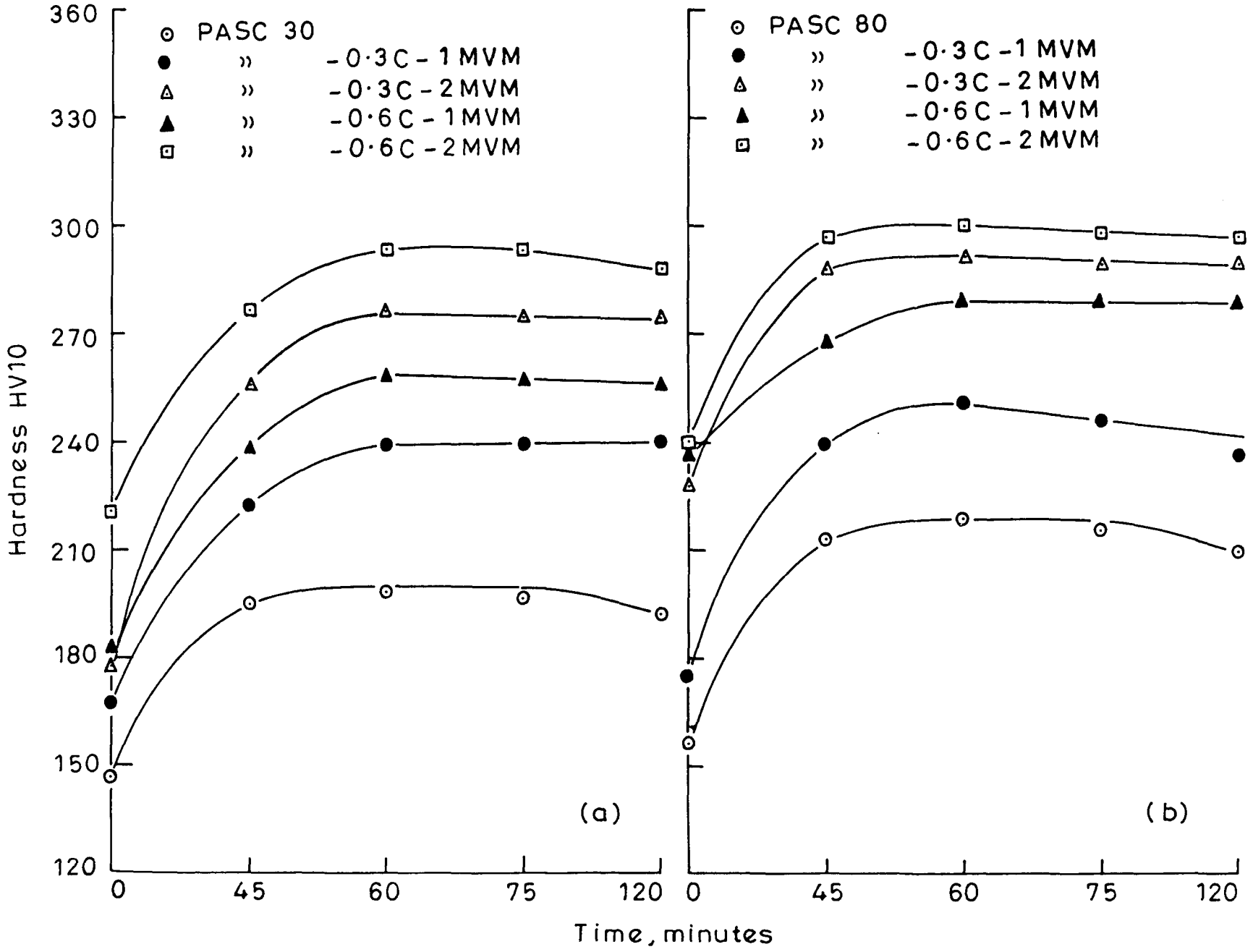

Fig. 3·87 Steam oxidation temperature 500°C

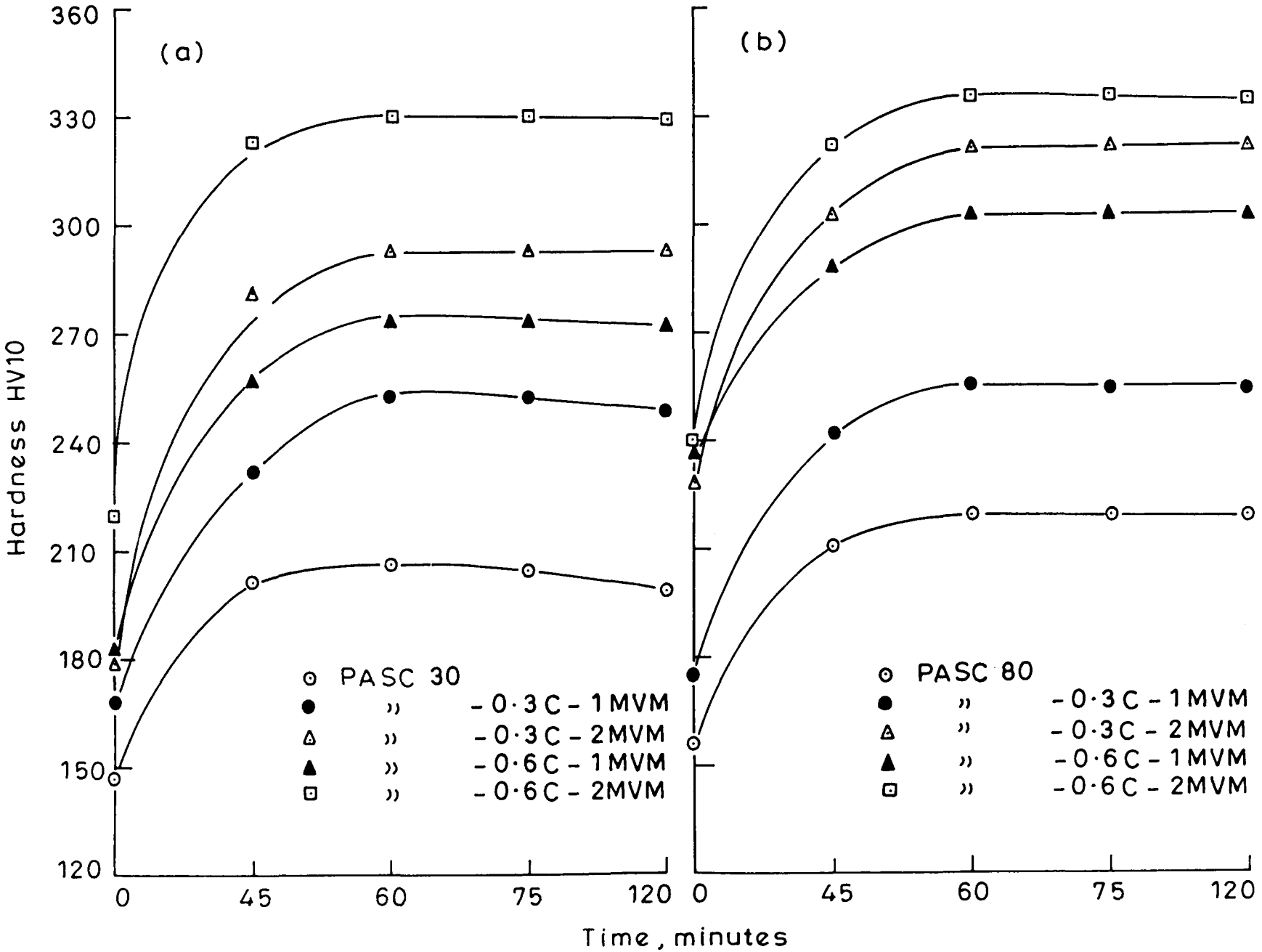

Fig. 3·88 Steam oxidation temperature 527°C

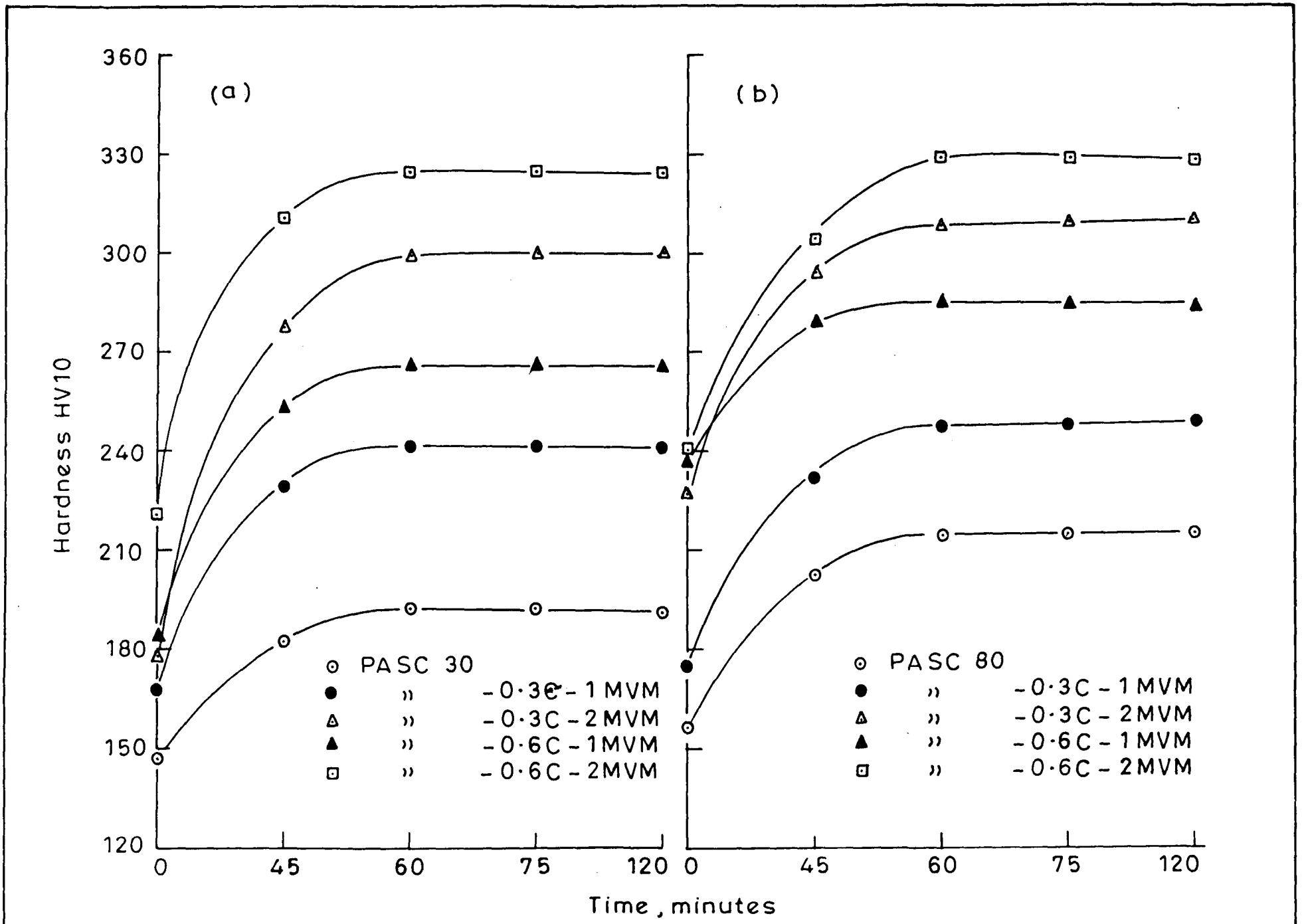

Fig. 3·89 Steam oxidation temperature 550°C

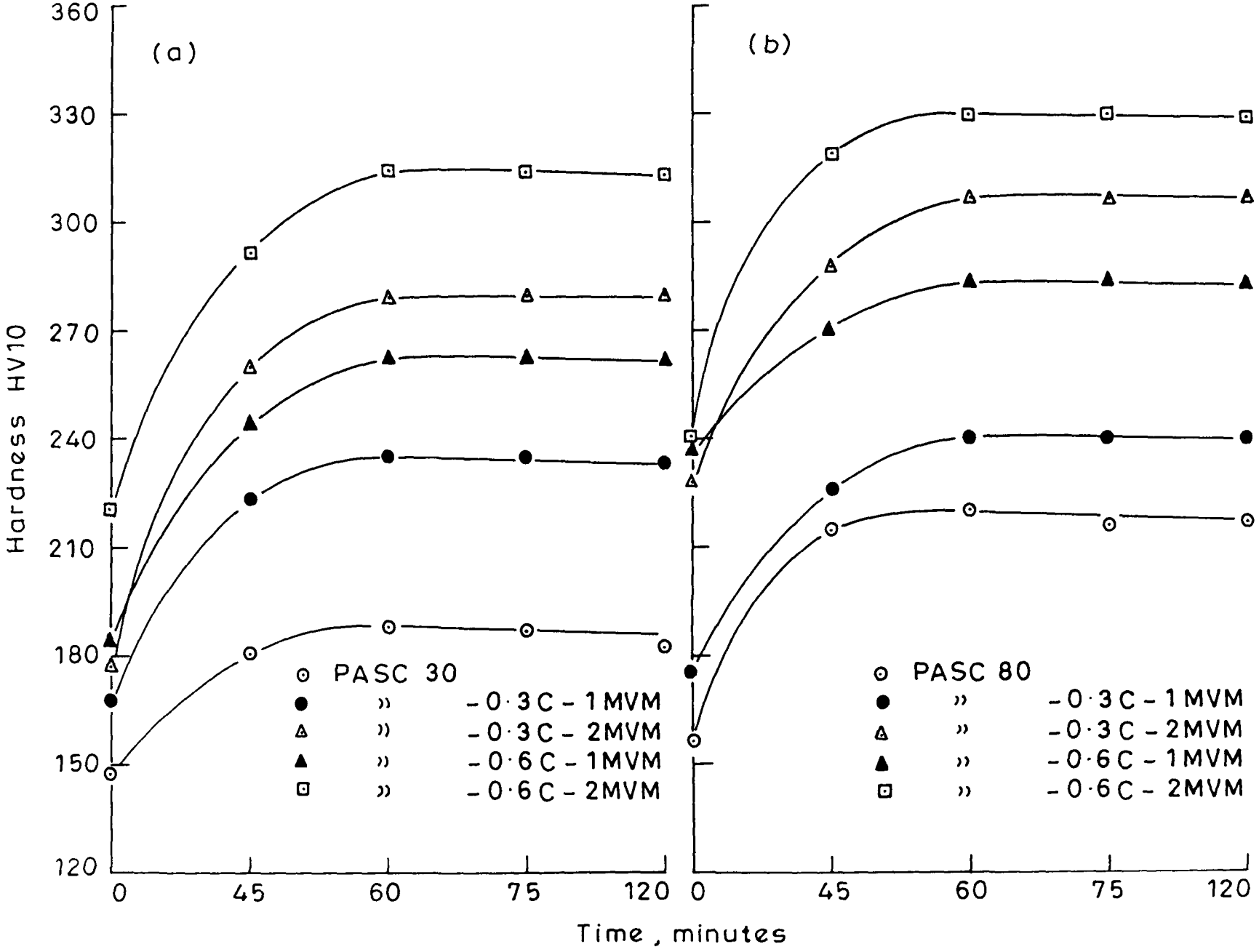

Fig. 3·90 Steam oxidation temperature 600°C

treated at 450 (the minimum temperature of oxidation), 527 (the near optimum ascertained by preliminary studies and results of hardness and weight gain) and 600°C (the highest temperature used) for 45 and 120 minutes were carried out. However, in many situations, no new qualitative or even quantitative informations are obtained and hence only selected few have been reported in this chapter. Among the selected few also, since variation in composition is often low and time and temperature of oxidation used are within the application range, the influence of such factors on change of microstructure is not noticable. However, some of the reported microstructures are for completeness. All the microstructures reported are at transition zone i.e., at oxide and matrix layer. In many cases oxide layers produced were very thin or non-uniform at lower temperature or longer period of oxidation, effort has been made to preserve them. While in other situations, oxide layers were occasionally brittle and cracked during grinding and polishing and so sometimes gives microstructure which is not in confirmity with weight gain and hardness data.

Scanning electron microscopy of one composition in each alloy system at both the levels of C, steam treated at 527°C for 120 minutes have been carried out. The

purpose of this study was to show oxide layer, distinction between pores and second phase particles and to differentiate between type, nature and shape of phases in pearlite or transformation products in sintered and steam treated samples.

3.3.3.1 PASC-Cu-C compacts

3.3.3.1.1 Optical metallography

In case of PASC30 sintered compacts, although pores are not spheroidal in shape, they are isolated (Fig. 3.91a). Only surface seems to have oxidized at a steam oxidation temperature of 450°C for 45 minutes. When 0.3 % C and 1 % Cu are added to sintered PASC30 powder compacts, there is increase in thickness of oxide layer and some oxidation seems to have occurred in the open channels and interconnected pore network (Fig. 3.91b). When C content is increased from 0.3 to 0.6 % microstructural study does not show any change in oxide layer but the matrix shows significant increase in proportion of pearlite in sintered compact (Fig. 3.91c). Steam oxidation does not seem to have changed the nature or morphology of phases. When P-content was increased from 0.3 to 0.8 % oxidation rate invariably decreases (Fig. 3.92). However, higher amount of P is found to increase the grain size. Matrix of PASC80

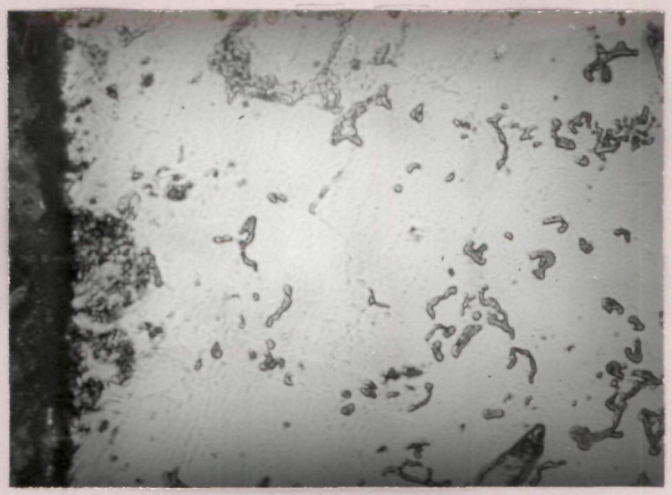

(a) PASC30

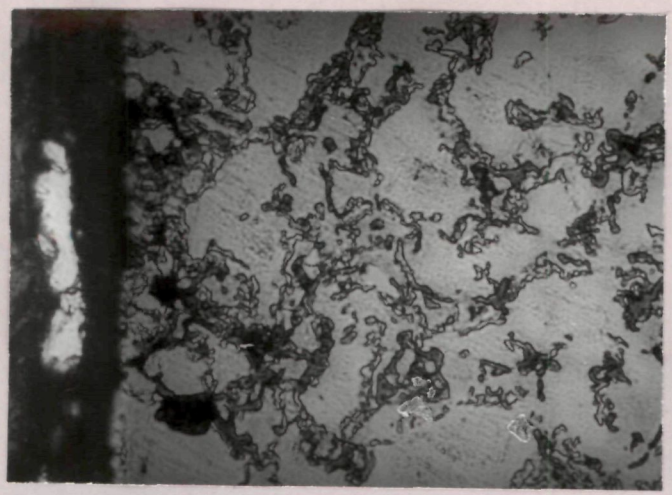

(b) PASC30 - 0·3C - 1Cu

(c) PASC30 - 0·6C - 1Cu

Fig. 3·91

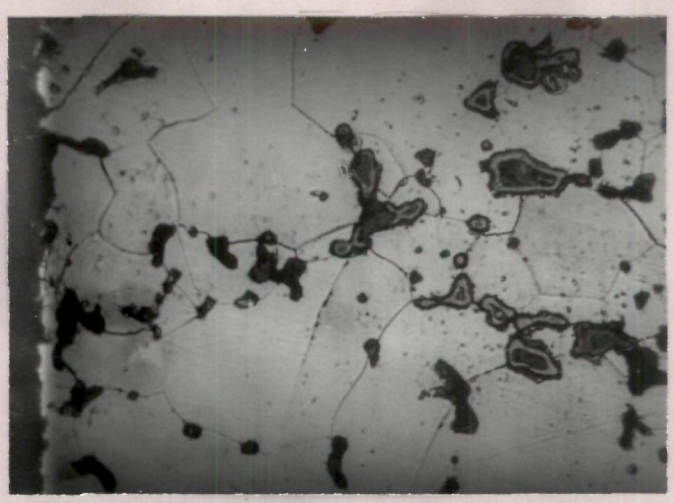

(a) PASC80

(b) PASC80 - 0·3C - 1Cu

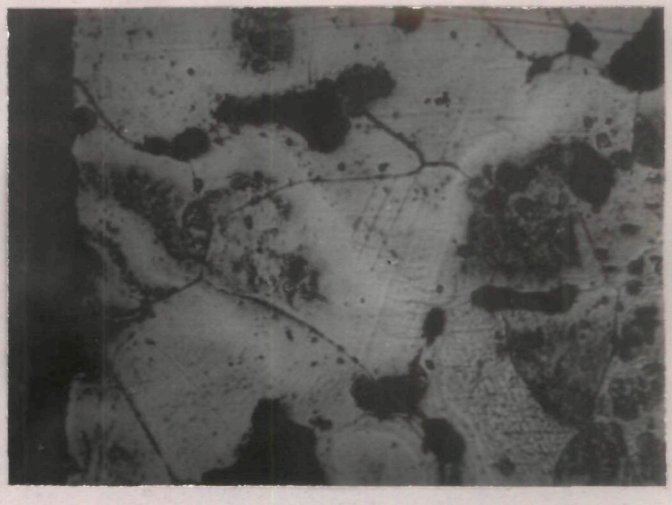

(c) PASC80 - 0·3C - 2Cu

Fig. 3·92

sintered and steam oxidized compact is single phase ferritic with pores along the grain boundaries which have occasionally oxidized if exposed to steam (Fig. 3.92 a). 0.6 % C addition does not significantly change the phase and the grain size and it appears that this amount of C is retained in the ferritic phase (Fig. 3.92 b). Higher amount of Cu simply brings about non-homogeneity in structure. (Fig. 3.92 c).

When steam oxidation temperature was increased from 450 to 527°C, there is no qualitative change in the structure of the matrix but oxide layers developed seem to be more uniform and well defined structurally (Fig. 3.93 a, b and c). When steam oxidation period was increased from 45 to 120 minutes at 527°C, deeper penetration of steam and interdiffusion of oxygen and metal seems to have occurred; oxide layers produced are also irregular and hazy (Fig. 3.94 a and b). Keeping the steam oxidation temperature constant, when P-content was increased from 0.3 to 0.8 %, larger grains with well defined grain boundaries are obtained which are characteristic of the effect of P on sintering (Fig. 3.95 a). However, when 0.6 % C and 1 % Cu are introduced into PASC80 powder premixes and compacts sintered and steam oxidized, pearlitic phase in the matrix is fine and there appears to be

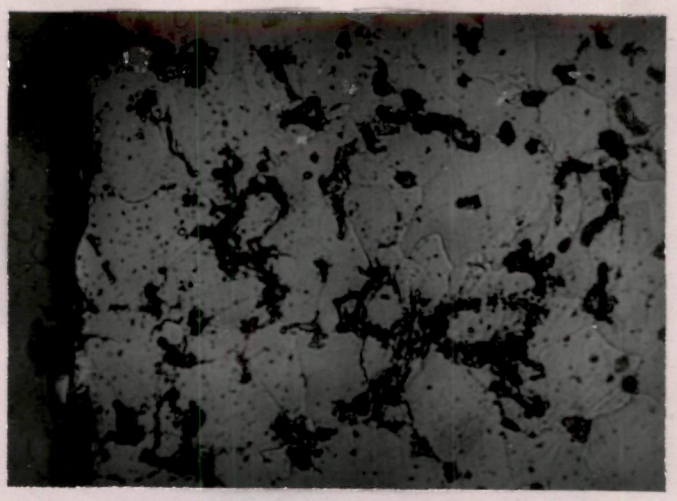

(a) PASC30

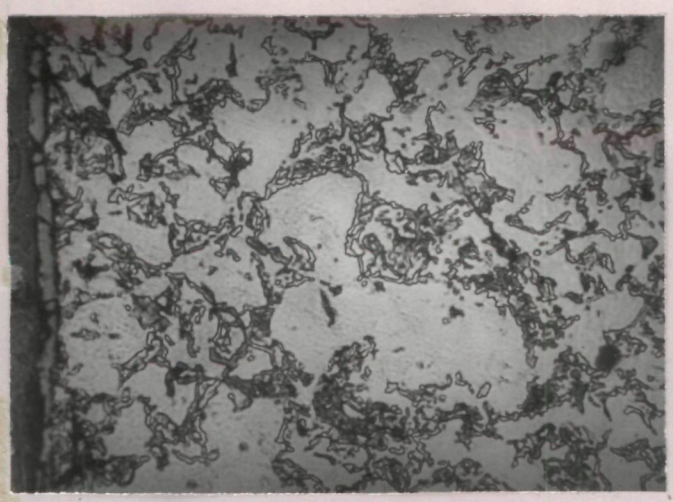

(b) PASC30 - 0·3C - 2Cu

(c) PASC30 - 0·6C - 1Cu

Fig. 3·93

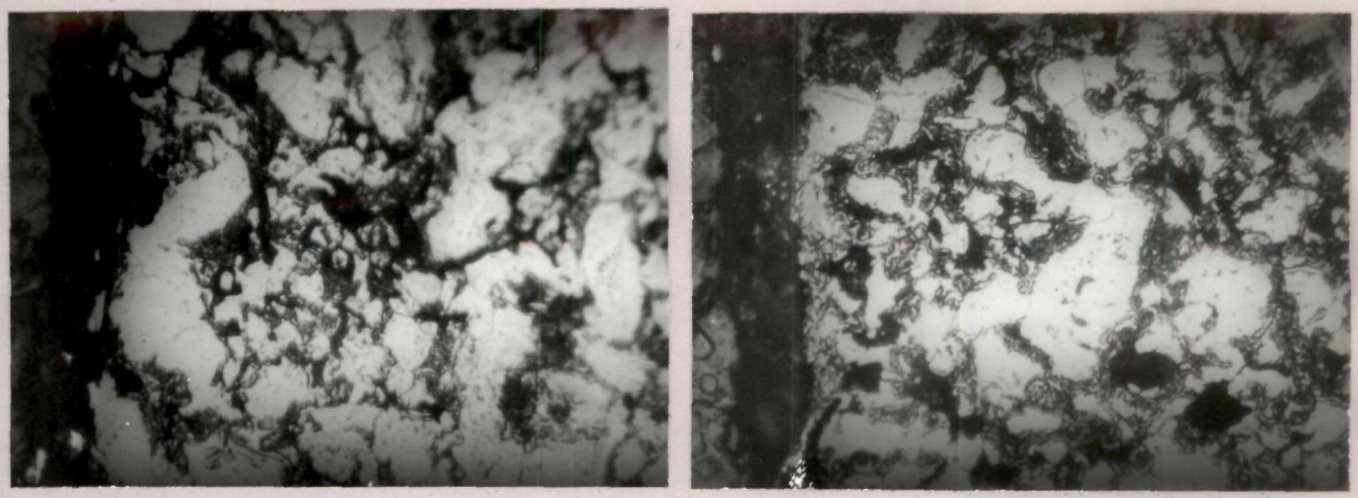

(a) PASC30 (b) PASC30 - 0·3C - 2Cu

Fig. 3·94

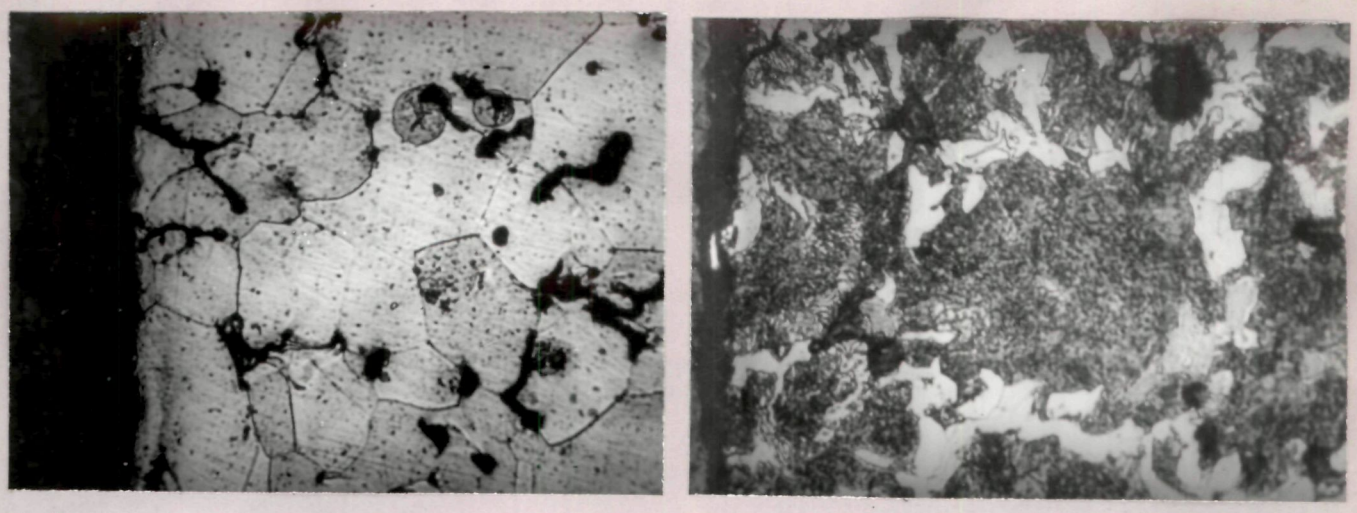

(a) PASC80 (b) PASC80 - 0·6C - 1Cu

Fig. 3·95

dispersion of some other phase as well (Fig. 3.95 b) which is surprizingly less evident at higher steam oxidation temperatures (Fig. 3.96 a and b).

3.3.3.1.2 Scanning electron microscopy

Scanning electron microscopy study of PASC30-0.3C-2Cu sintered and steam treated compact at 527°C for 120 minutes shows interdiffusion of C and oxygen (Fig. 3.97 a) which show two oxide particles within the matrix. There are indications of some oxygen mobility along the grain boundary also. Increase of P-content from 0.3 to 0.8 % keeping C and Cu contents constant confirms the results of optical microscopy (Fig. 3.92) that 0.3 % C is taken into solid solution with phosphorus ferrite (Fig. 3.98). When C content is increased to 0.6 % in case of PASC30-2Cu compact, proportion of pearlite increases and at majority of places very regular, well oriented and lamellar pearlite is obtained (Fig. 3.99). Higher amount of P is again responsible for retention of C in single phase solid solution state (Fig. 3.100).

3.3.3.2 PASC-Ni-C compacts

3.3.3.2.1 Optical metallography

At a steam oxidation temperature of 450°C treated

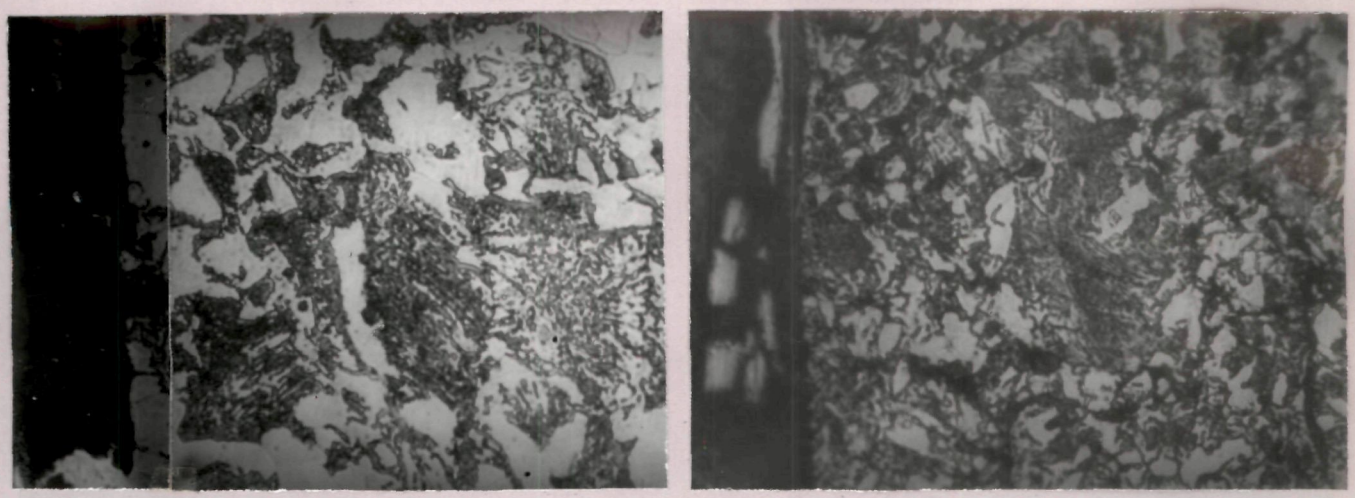

(a) PASC30 - 0·3C - 2Cu (b) PASC30 - 0·6C - 1Cu

Fig. 3·96

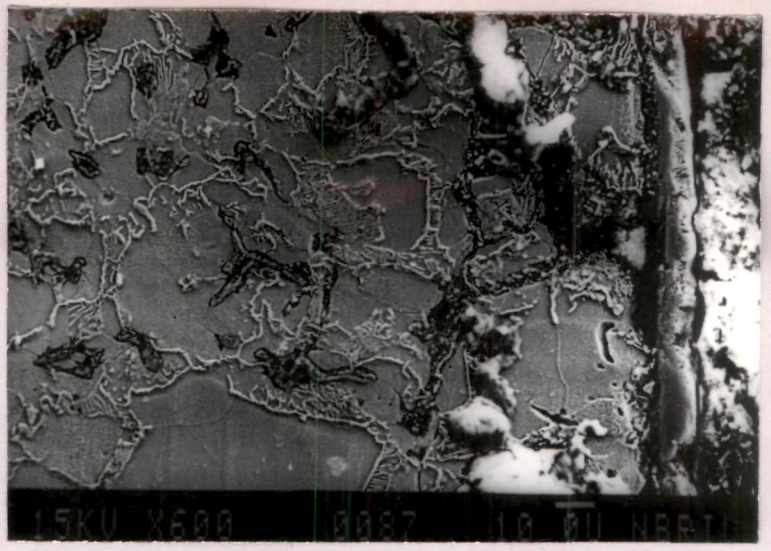

(a)

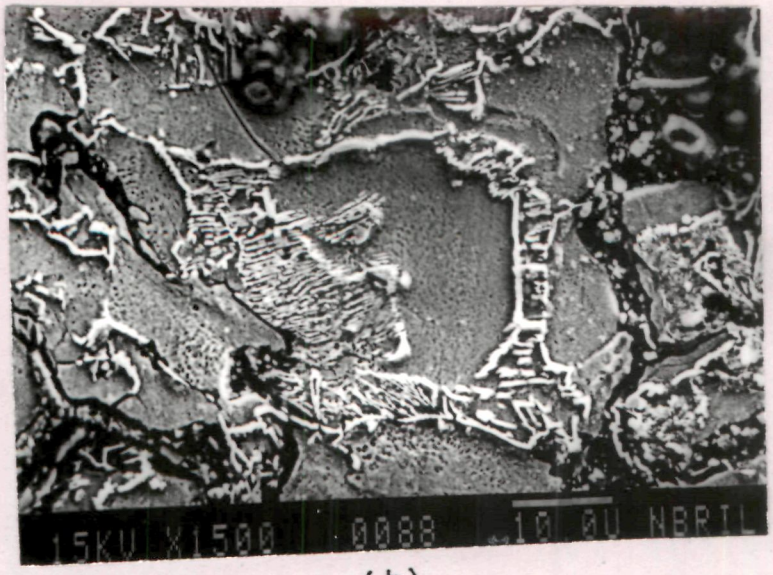

(b)

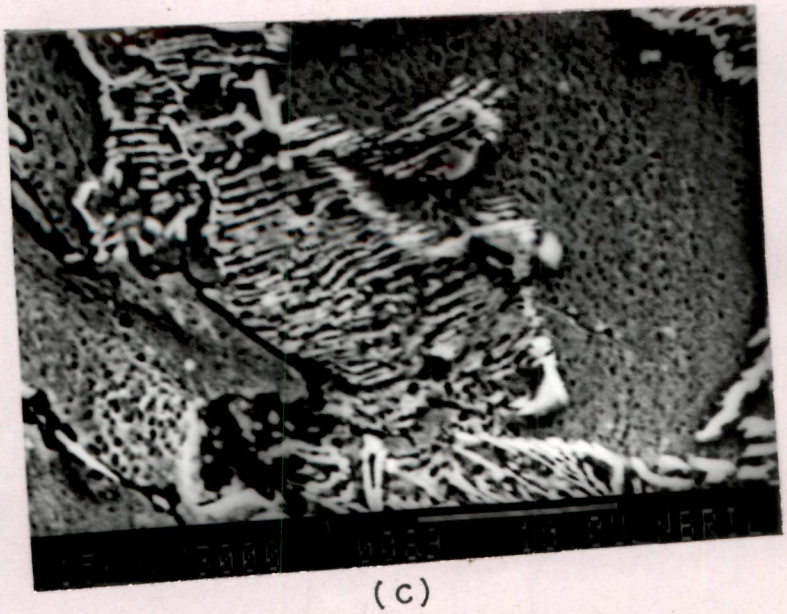

(c)

PASC30 - 0·3C - 2Cu

Fig. 3·97

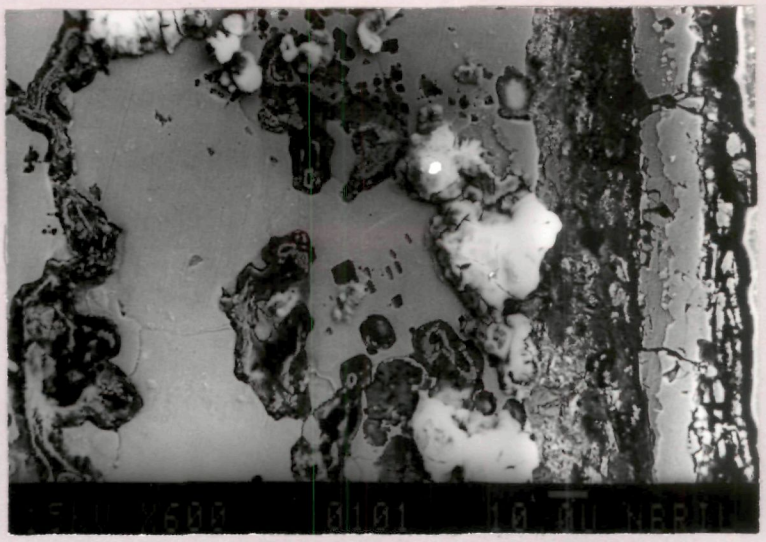

(a)

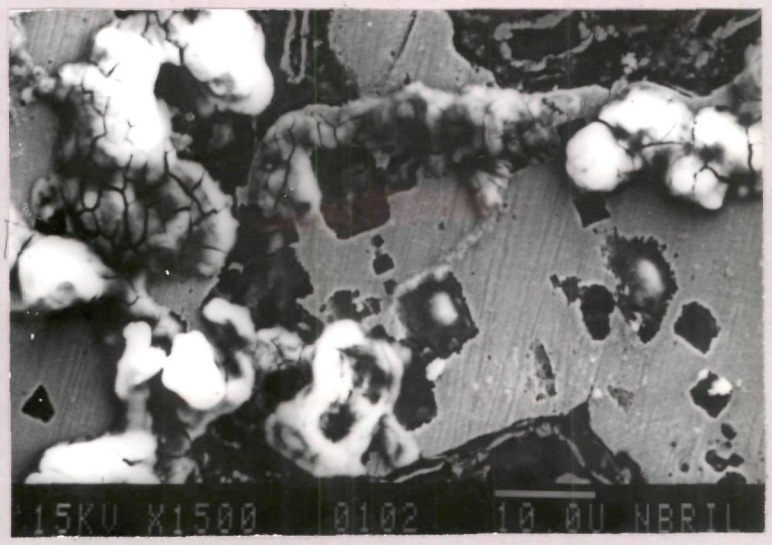

(b)

PASC80 - 0·3C - 2Cu

Fig. 3·98

(a)

(b)

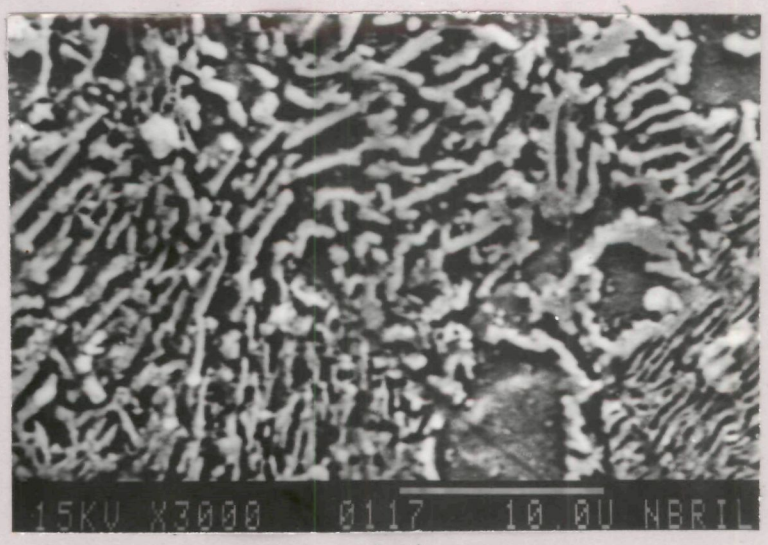

(c)

PASC30 - 0·6C-2Cu

Fig. 3·99

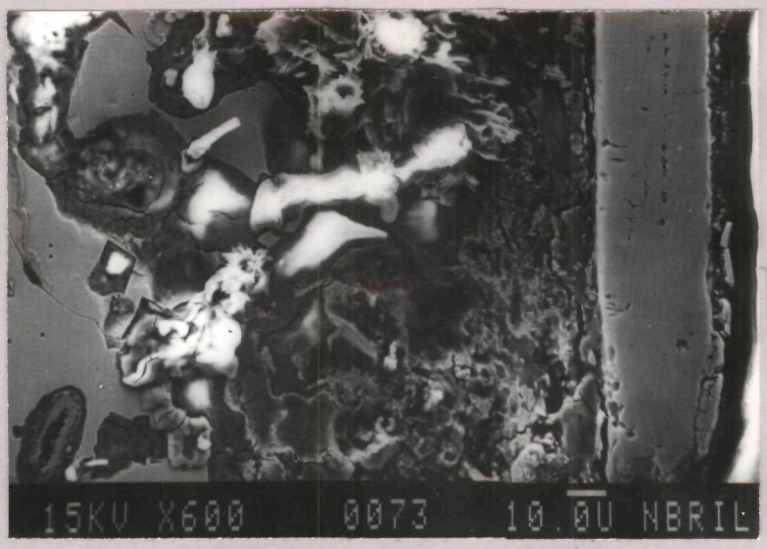

(a)

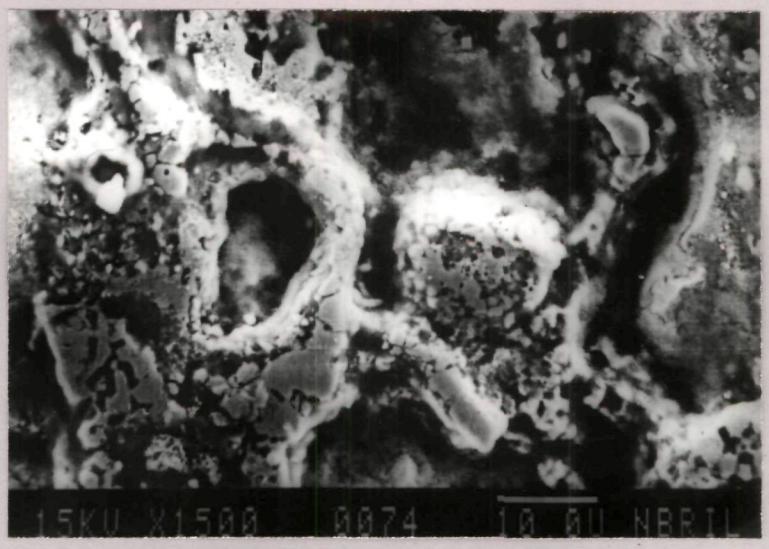

(b)

PASC80 - 0·6C - 2Cu

Fig. 3·100

for 45 minutes, reasonably defined oxide layers is obtained in case of PASC30-0.3C-Ni compact (Fig. 3.101 a). Effect of steam oxidation on matrix structure is insignificant. Higher C content increases the proportion of fine pearlitic phase. (Fig. 3.101 b). When P-content is increased from 0.3 to 0.8 % at equivalent C and Ni- contents, C is taken into solution and proportion of ferrite increases in the matrix (Figs. 3.102) with associated pore rounding. When steam oxidation period was increased to 120 minutes, extent of oxidation increases, grain polygonizes, diffusion of oxygen is more extensive and decomposition of some other phases are indicated (Fig. 3.103). When steam oxidation temperature was increased from 450 to 527°C maintaining both C and Ni- contents constant, there is no change in the matrix structure (Fig. 3.104), and uniformity of the oxide layer but thickness of scale increases and oxide layer appears to be more compact and dense (Figs. 3.101 and 3.104). Increase in P-content from 0.3 to 0.8 % at the same level of other alloying elements present in sintered steel and at the same condition of steam treatment, simply spheroidizes the pores in the matrix and decreases the proportion of pearlite there by decreasing the oxide thickness marginally (Fig. 3.105). Increase in time of oxidation from 45 to 120 minutes at 527°C of treatment

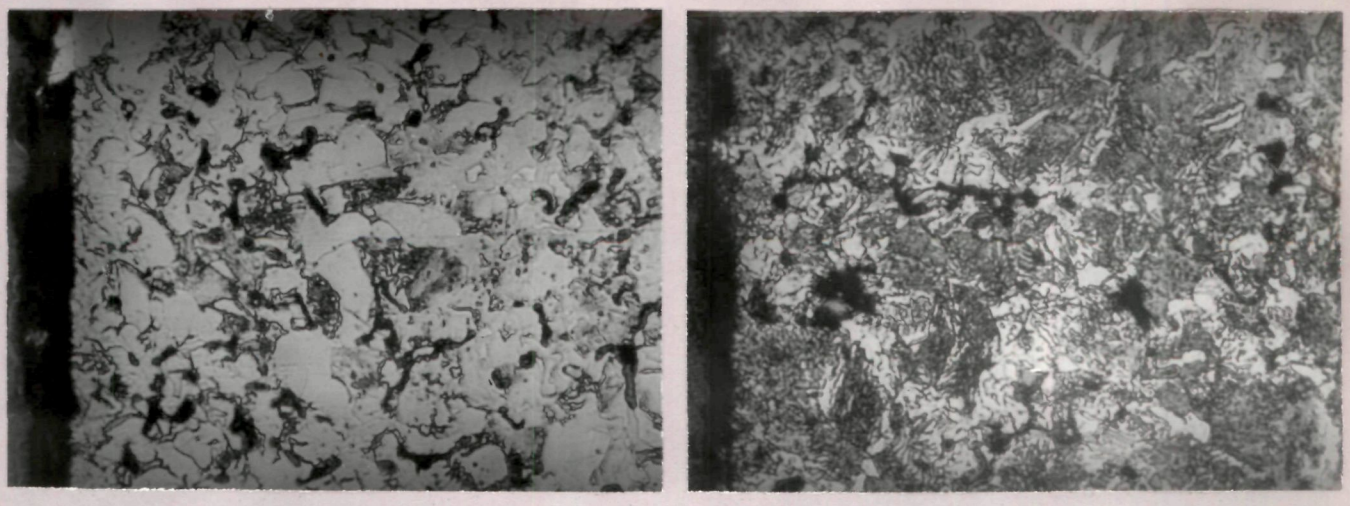

(a) PASC30 - 0·3C - 1Ni (b) PASC30 - 0·6C - 1Ni

Fig. 3·101

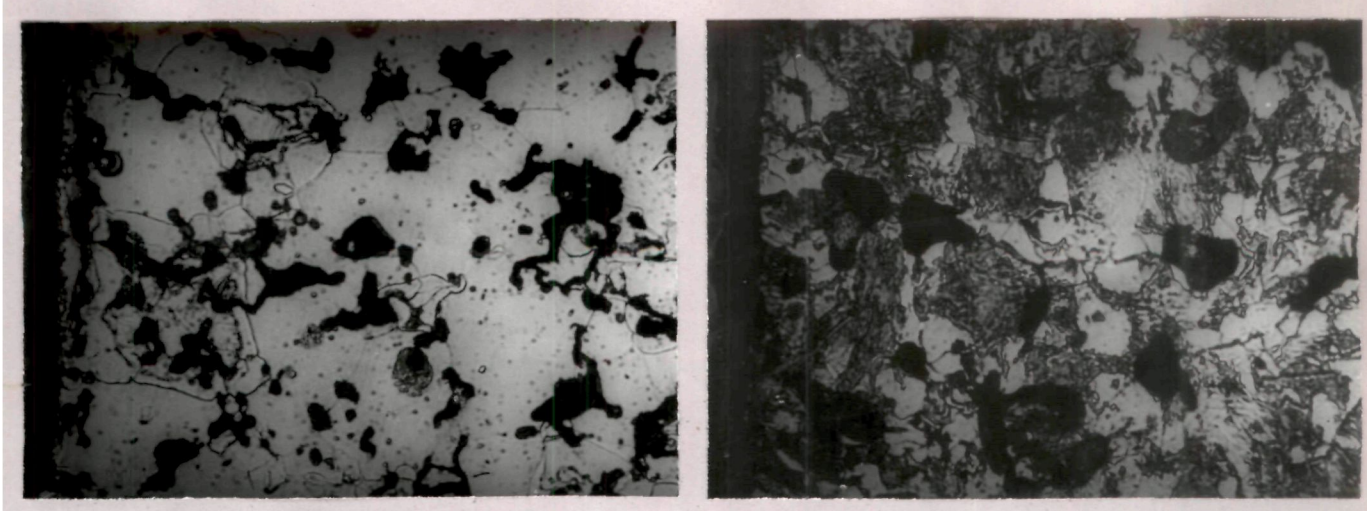

(a) PASC80 - 0·3C - 1Ni (b) PASC80 - 0·6C - 1Ni

Fig. 3·102

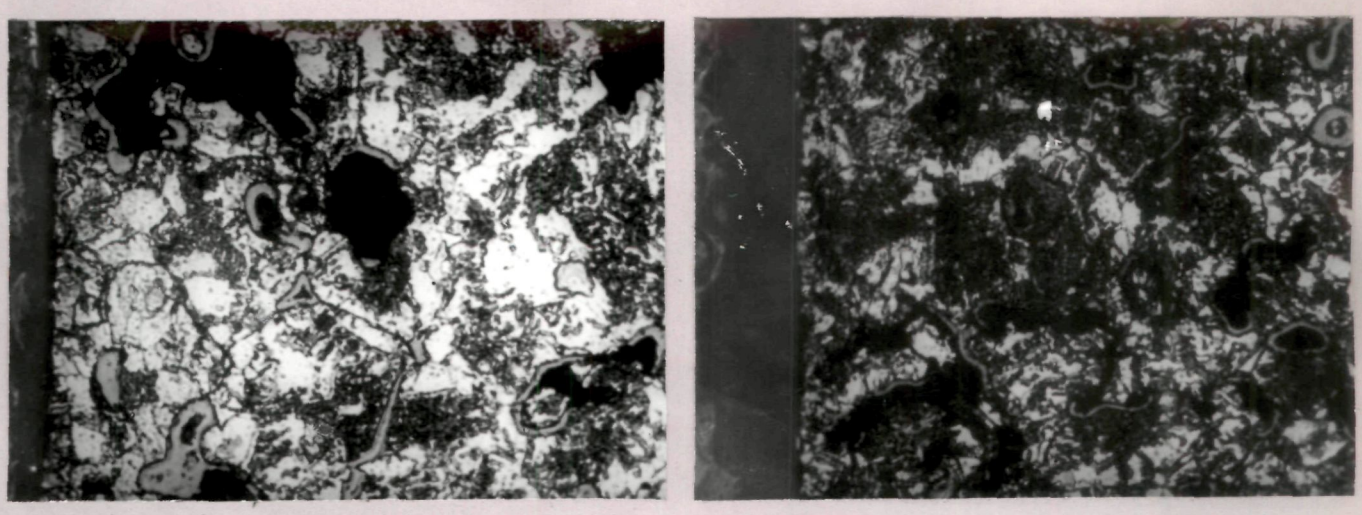

(a) PASC80 - 0·6C - 1Ni (b) PASC80 - 0·6C - 2Ni

Fig. 3·103

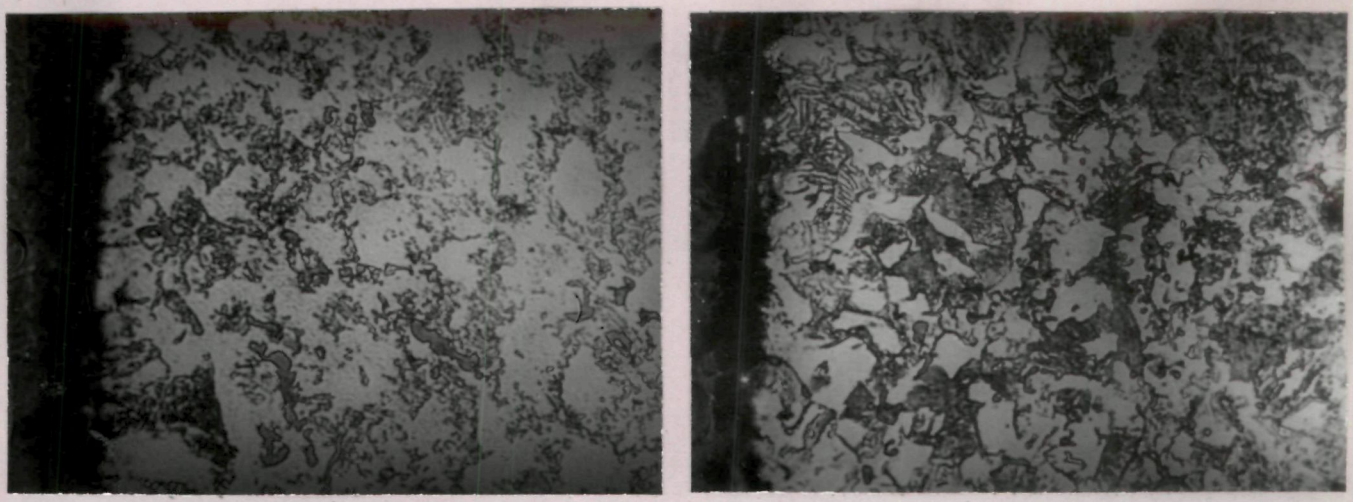

(a) PASC30 – 0·3C – 1Ni (b) PASC30 – 0·6C – 2Ni

Fig. 3·104

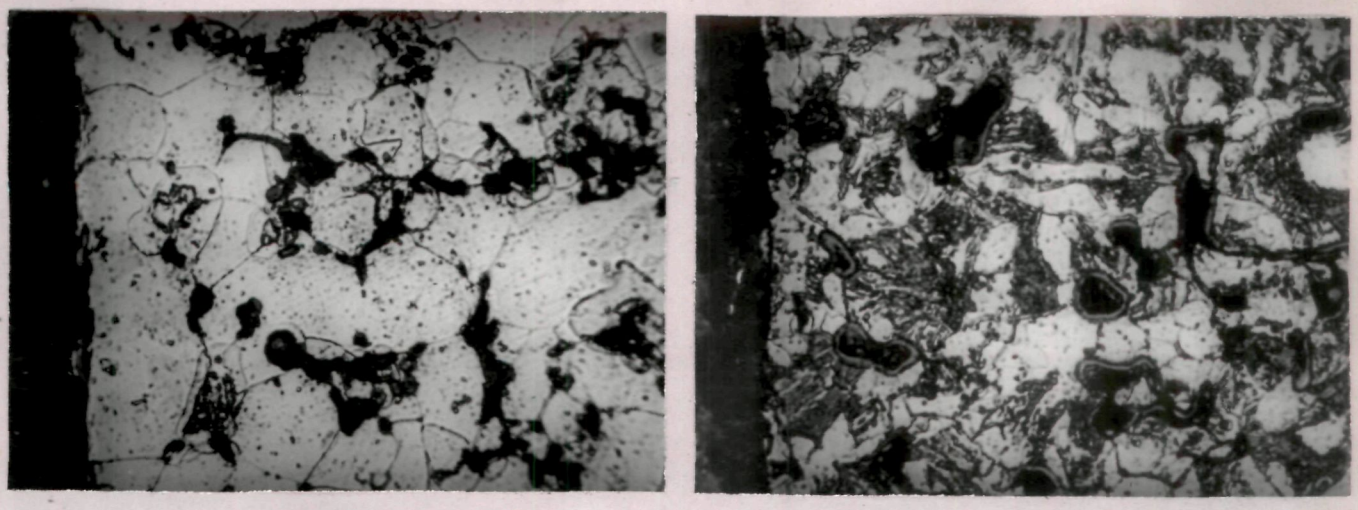

(a) PASC80 - 0·3C - 1Ni (b) PASC80 - 0·6C - 1Ni

Fig. 3·105

layer becomes slightly non-uniform and hazy. Proportion of pearlite also decreases in the vicinity of transition zone and there appears to have occurred some shift in oxide layer and a change in the constituent of oxide. Increase in temperature further to 600°C decreases the proportion of pearlite in the matrix near the oxide layer (Fig. 3.107). Higher amount of phosphorus decreases the proportion of pearlite which is again increased by Ni and C contents (Fig. 3.108). When steam oxidation time was increased to 120 minutes at the same temperature and composition, oxidation is increased both at the surface and in the interior and non-uniformity in definition and composition of oxide layers are apparent (Fig. 3.109 a and b).

3.3.3.2.2 Scanning electron microscopy

Scanning electron picture of PASC30-0.3C-2Ni sintered compact steam treated at 527°C for 120 minutes shows non-uniform and thick oxide layer (Fig. 3.110). Oxidation seems to have occurred within the matrix and is more intense as compared to identical Cu-containing oxidized compacts (Fig. 3.97). The proportion of pearlite in the matrix is slightly more in case of Ni- containing compacts while just near the oxide layer is more in case of Cu- containing compacts. The

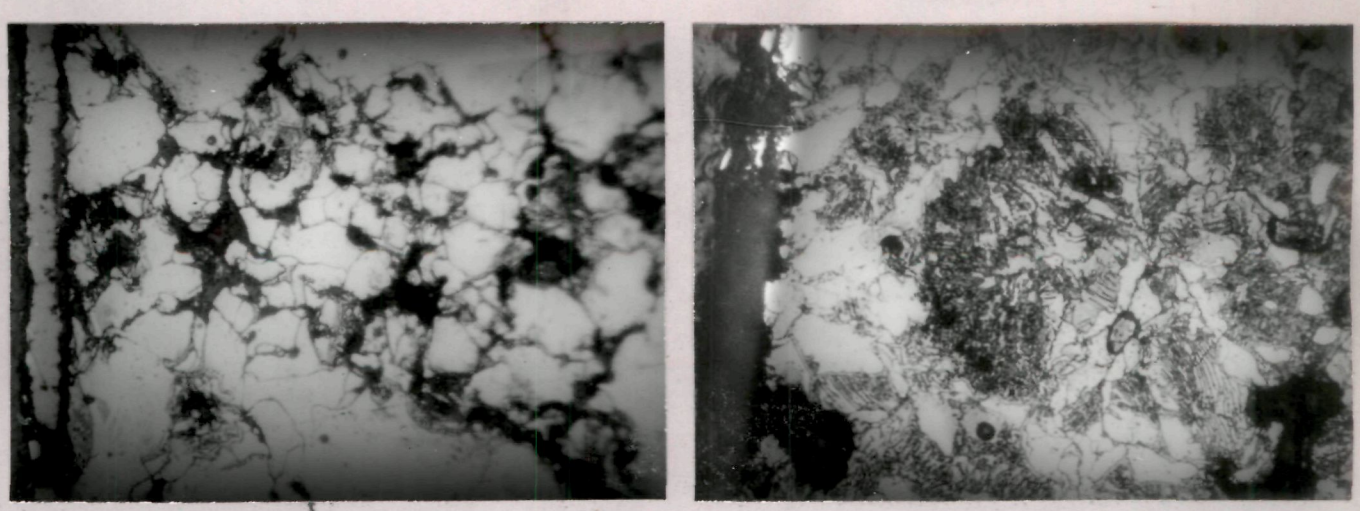

(a) PASC80 - 0·3C - 1Ni (b) PASC80 - 0·6C - 2Ni

Fig. 3·106

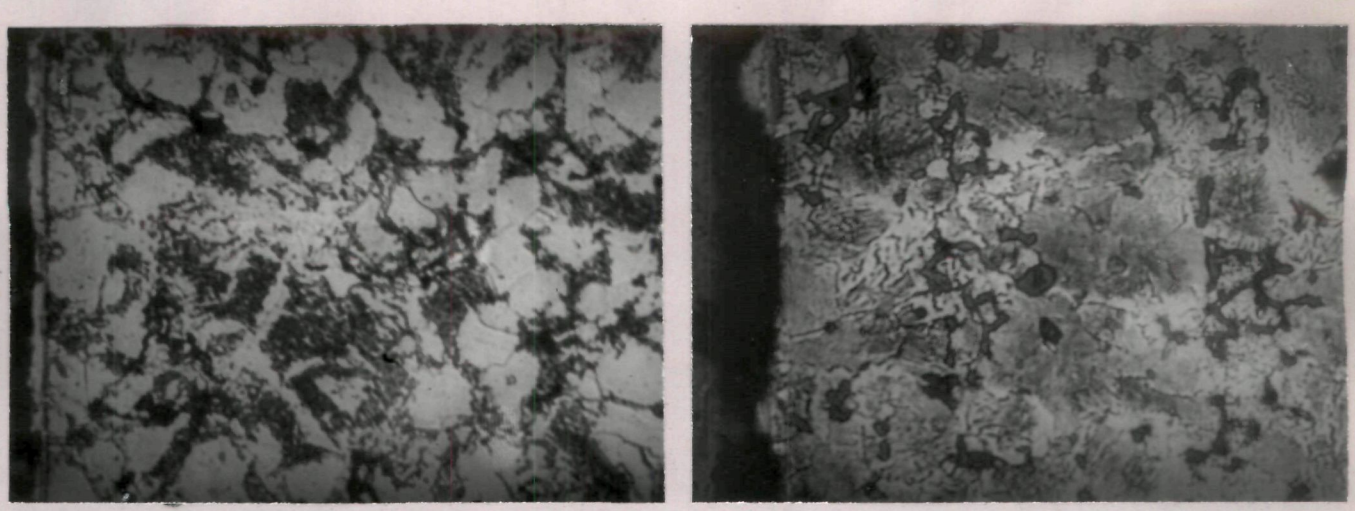

(a) PASC30 - 0·3C - 1Ni (b) PASC30 - 0·6C - 2Ni

Fig. 3·107

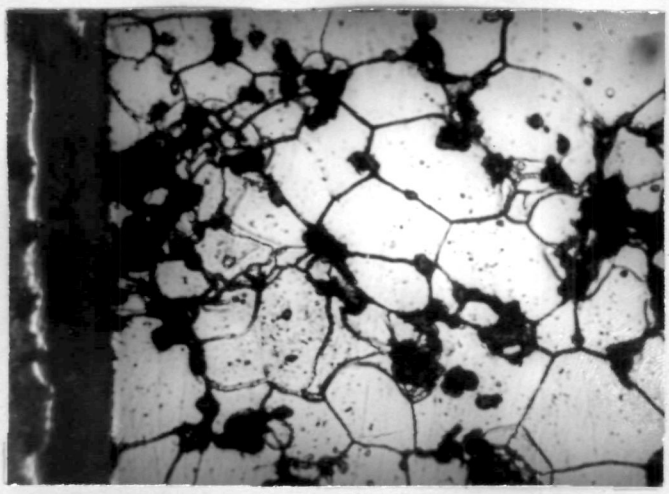

(a) PASC 80 - 0·3C - 1 Ni

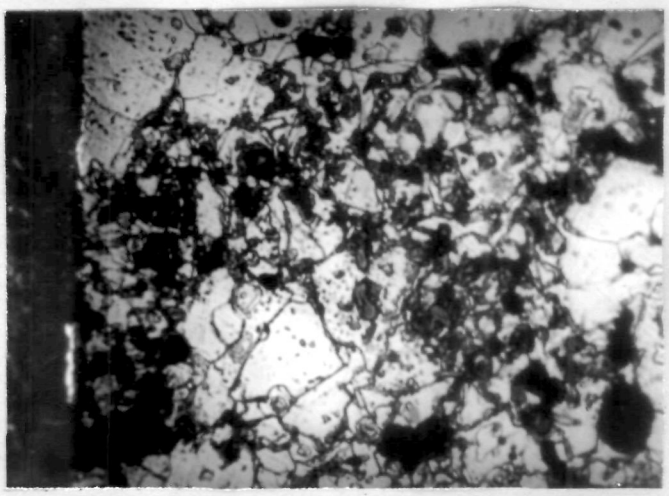

(b) PASC 80 - 0·3C - 2 Ni

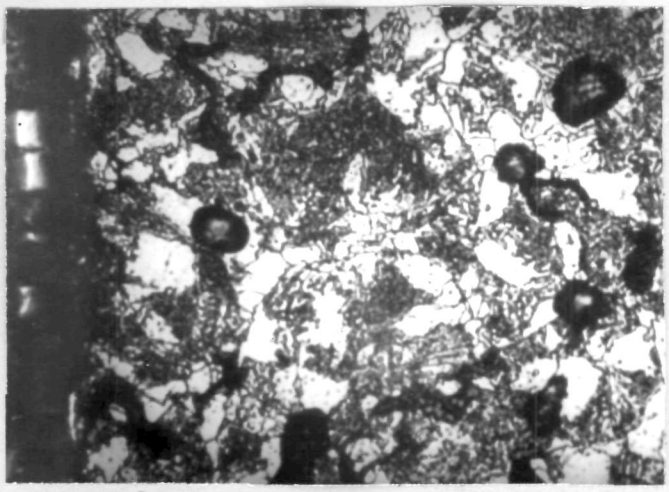

(c) PASC 80 - 0·6C - 1 Ni

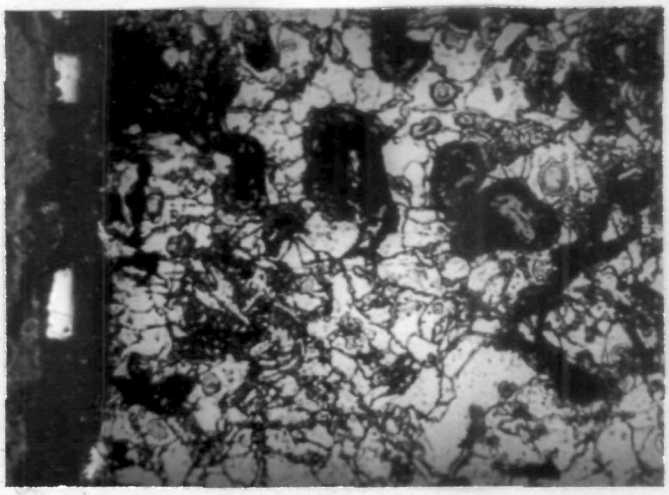

(d) PASC 80 - 0·6C - 2 Ni

Fig. 3·108

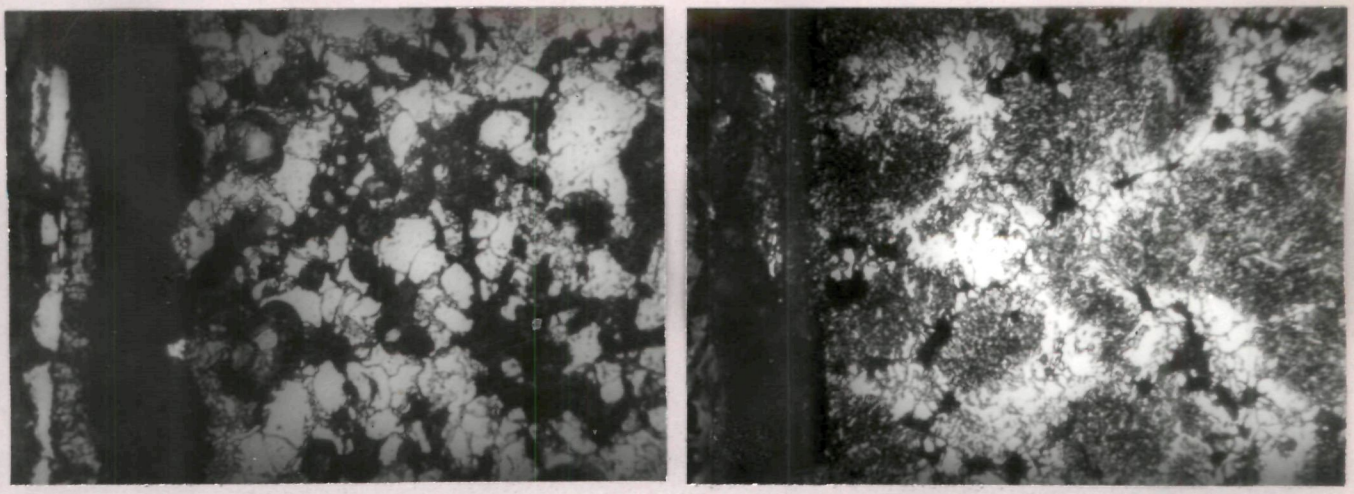

(a) PASC30 - 0·3C - 1Ni (b) PASC30 - 0·6C - 2Ni

Fig. 3·109

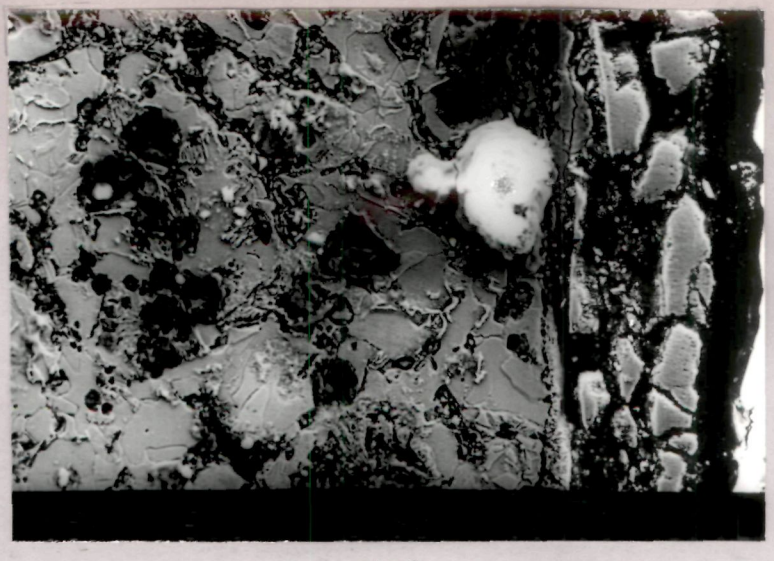

(a)

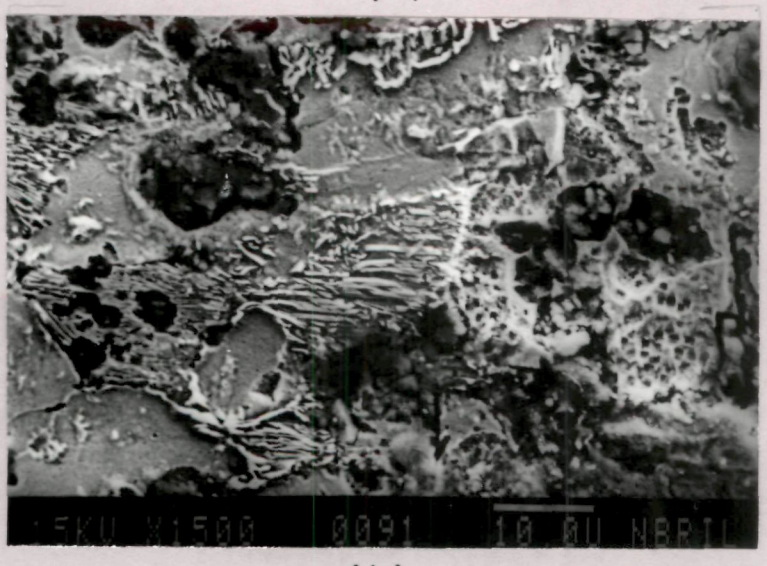

(b)

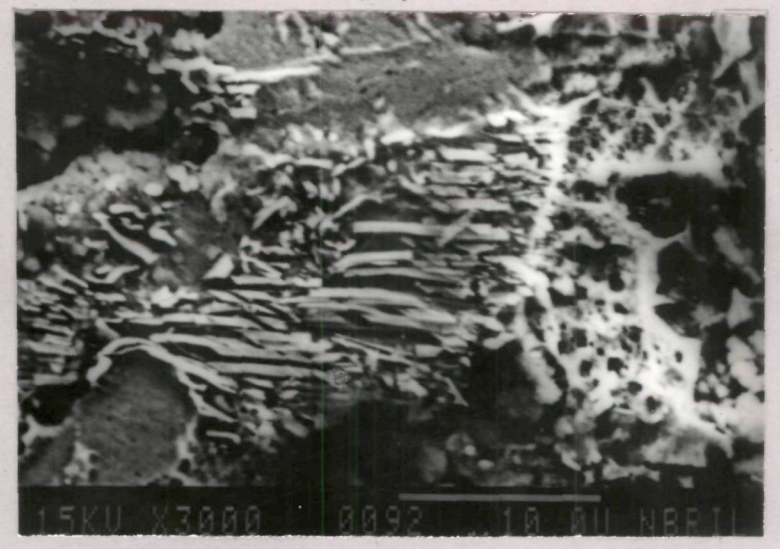

(c)

PASC30 - 0·3C - 2Ni

Fig. 3·110

pearlitic structure in Ni- containing compact appears to be textured while in case of similar Cu- containing compact is randomly oriented (Figs. 3.97 and 3.110). Increase in P-content to 0.8 % reduces the proportion of pearlite (Fig. 3.111) in the matrix and decreases the thickness of oxide layer. In case of PASC80-0.3C-2Ni sintered compact and steam treated at 527°C even upto 120 minutes of steam oxidation gives a well defined and uniform oxide layer. However, oxidation seems to have occurred within and on the periphery of the pores (Fig. 3.111 a,b and c). Proportion of pearlite is also more in case of higher P, Ni-containing compacts as compared to identical Cu-containing compacts (Figs. 3.98 and 3.111).

The picture of PASC30-0.6C-2Ni sintered compact steam treated for 120 minutes at 527°C shows thick oxide layer (Fig. 3.112), thicker than in case of Cu-containing compact having identical chemistry and steam treatment conditions undergone (Fig. 3.99). The microstructure in the matrix is almost fully pearlitic with uniform lamellae of carbide and ferrite oriented in definite direction. Higher amount of phosphorus decreases the pearlitic constituent and decreases the thickness of oxide layer (Fig.3.113).

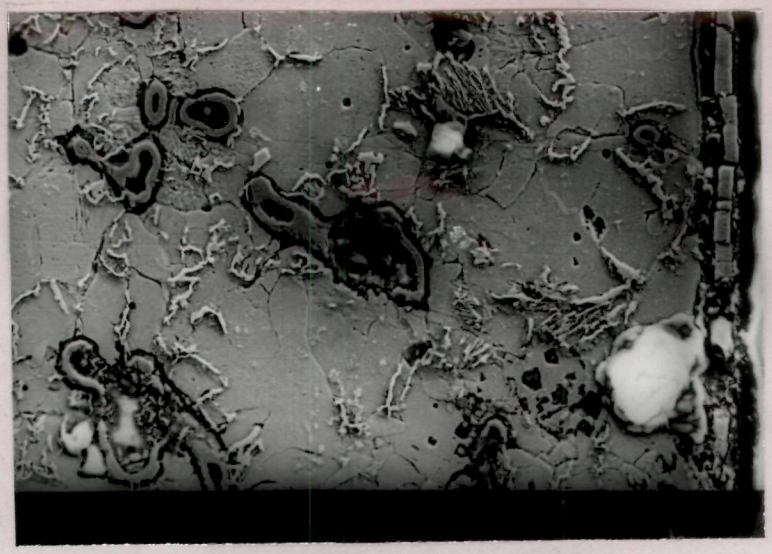

(a)

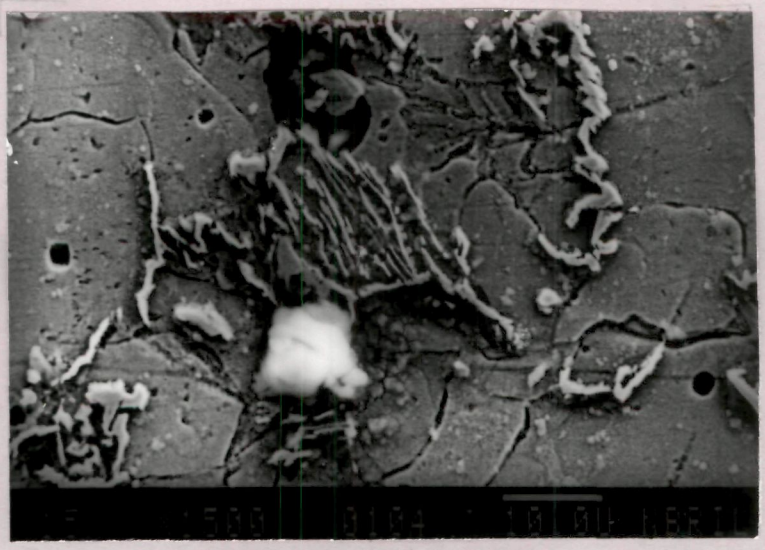

(b)

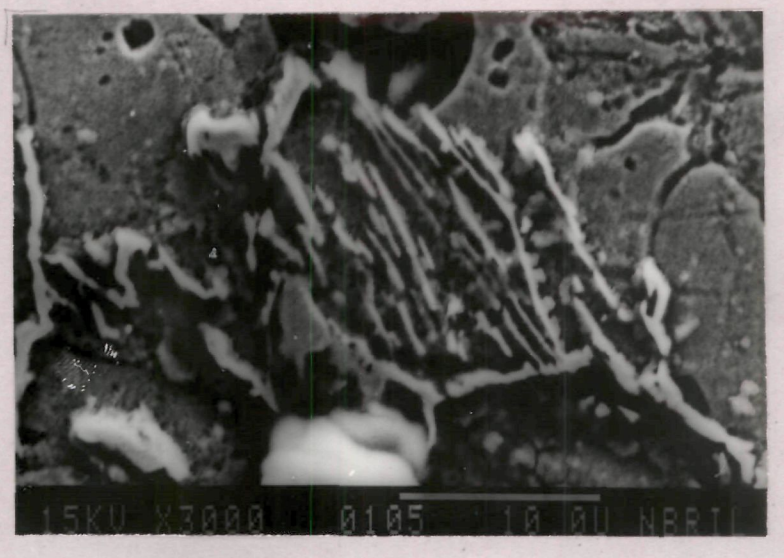

(c)

PASC80 - 0·3C - 2Ni

Fig. 3·111

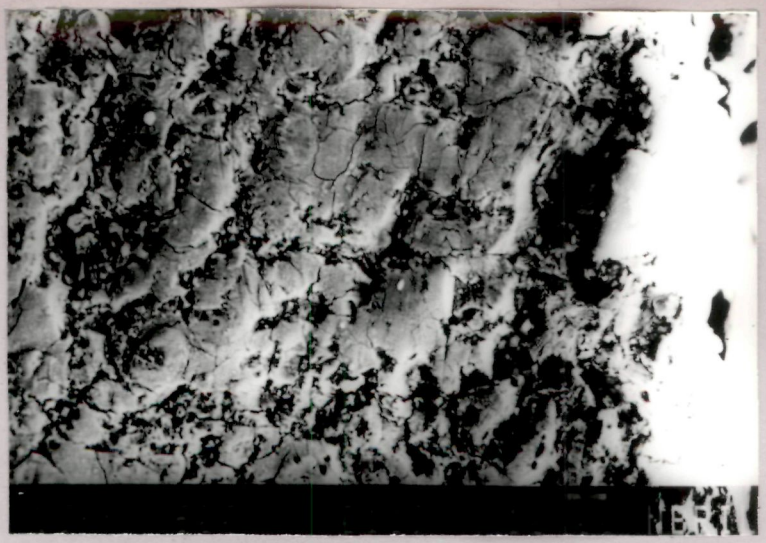

(a)

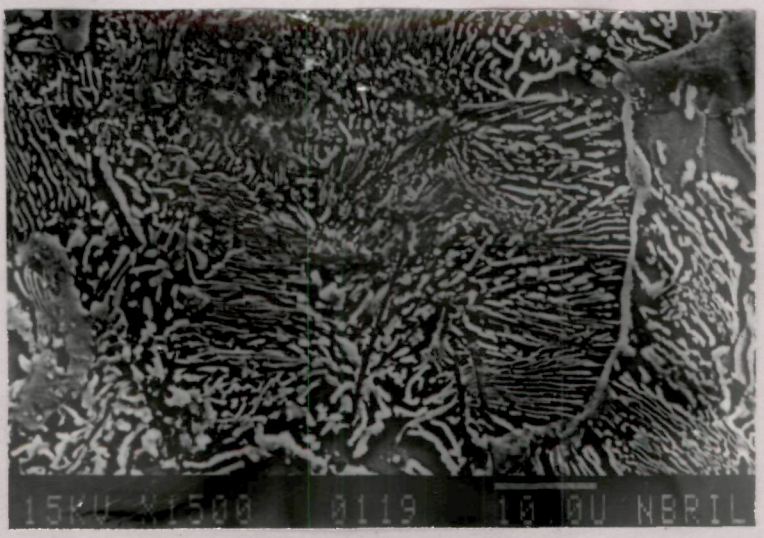

(b)

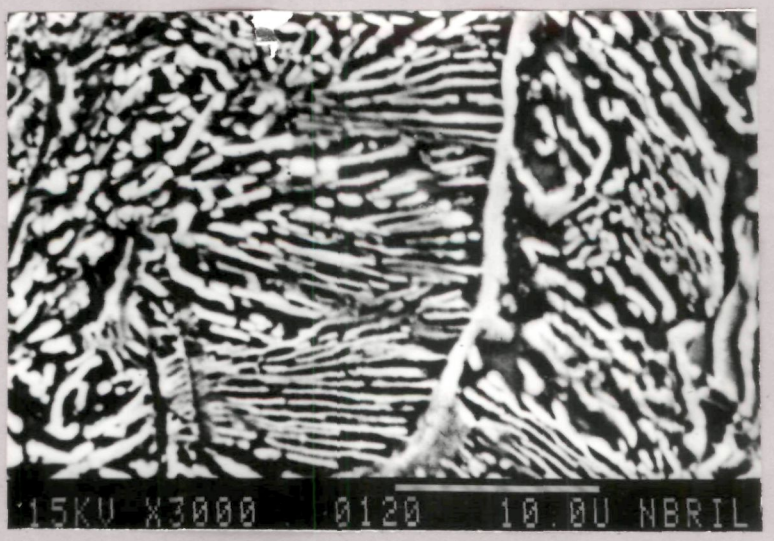

(c)

PASC 30 - 0·6C - 2Ni

Fig. 3·112

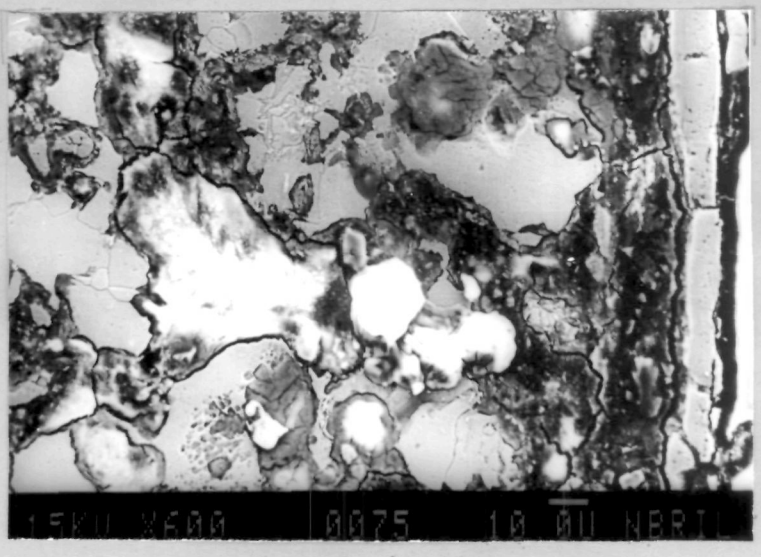

(a)

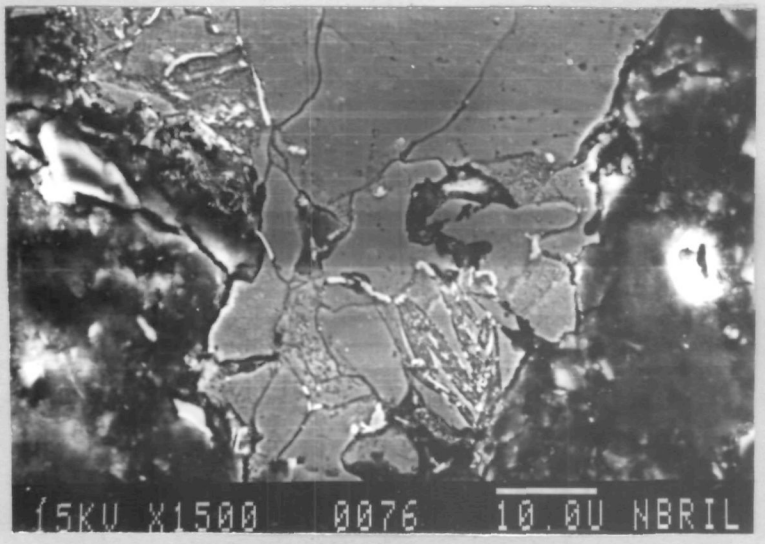

(b)

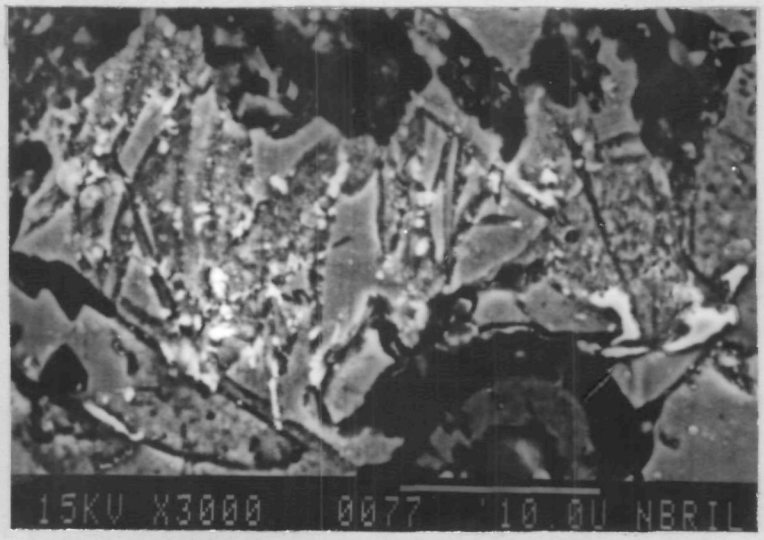

(c)

PASC80 - 0·6C - 2Ni

Fig. 3·113

3.3.3.3 PASC-Mo-C compacts

3.3.3.3.1 Optical metallography

At steam oxidation temperature of 450°C for 45 minutes of treatment time, thin but uniform oxide layer is obtained in case of PASC30-0.3C-2Mo compact (Fig. 3.114). Increase of C content to 0.6 % does not change the microstructure of oxide layer. With an increase in P-content from 0.3 to 0.8 % there is no change in qualitative nature of oxidation but matrix grains are large and more uniform (Fig. 3.115). Increase in oxidation period gives intensive oxidation both at the surface and in the interior (Fig. 3.116).

Increase in steam oxidation temperature to 527°C shows relatively uniform oxide layer with non-uniform microstructure, just below the surface (Fig. 3.117). There are indications of oxidation around the pores and second phases and non-uniformity in size of grains of different phases. When phosphorus content was increased from 0.3 to 0.8 % (Fig. 3.118), proportion of second phases increase but uniformity and definition of layers improves. Increase in oxidation period to 120 minutes enhances the oxidation rate and gives ring of oxide/second phases around pores and some of the matrix grains (Fig.

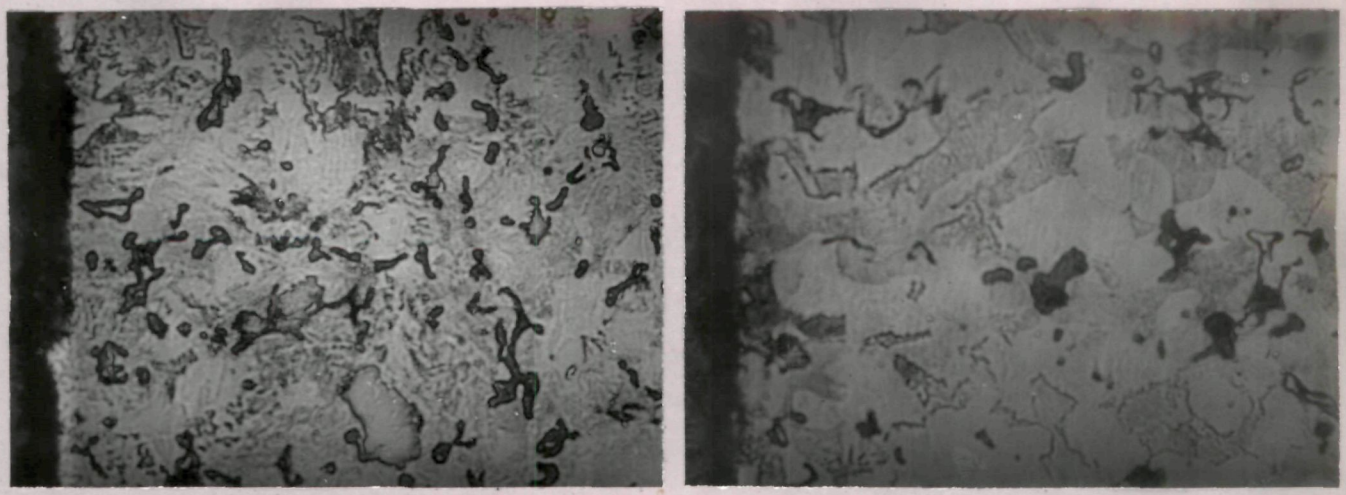

(a) PASC30 - 0·3C - 2Mo (b) PASC30 - 0·6C - 1Mo

Fig. 3·114

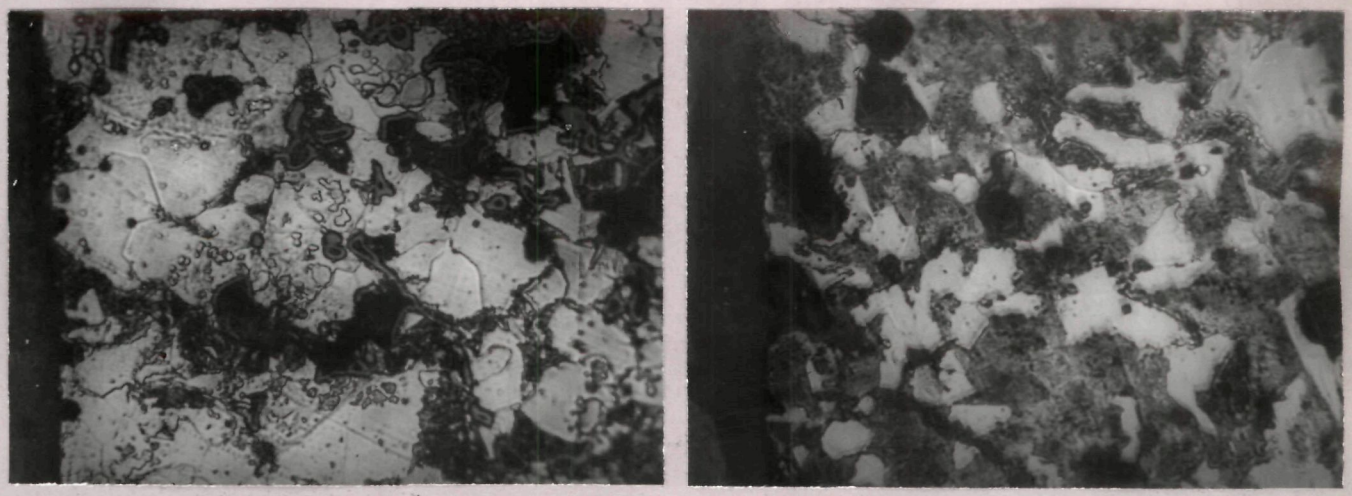

(a) PASC80 - 0·3C - 2Mo (b) PASC80 - 0·6C - 1Mo

Fig. 3·115

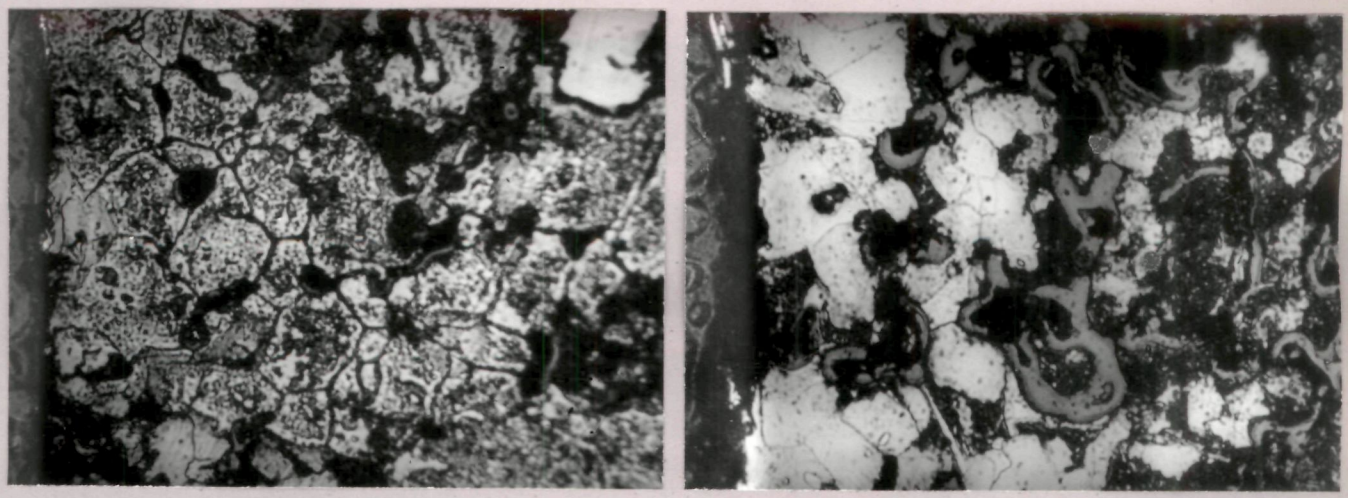

(a) PASC80 - 0·3C - 2Mo (b) PASC80 - 0·6C - 1Mo

Fig. 3·116

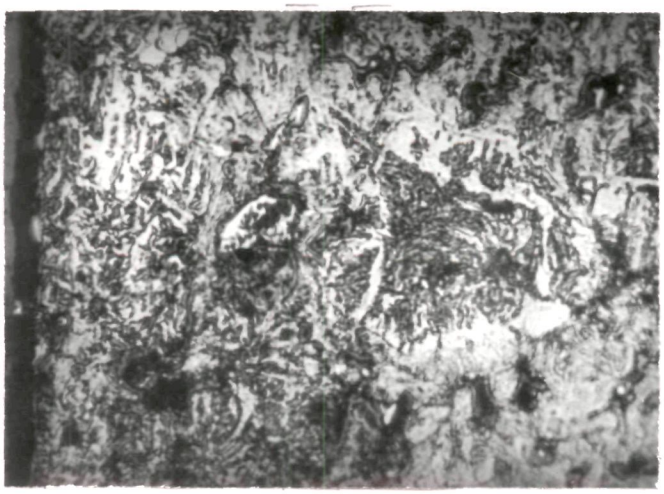

(a) PASC30 - 0·3C - 2Mo

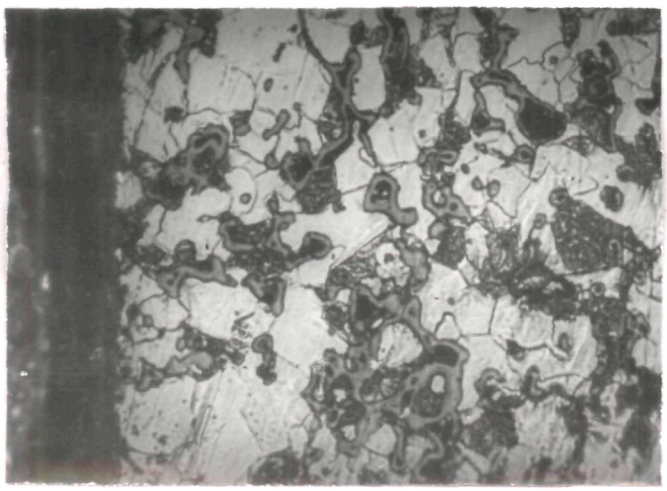

(b) PASC30 - 0·6C - 1Mo

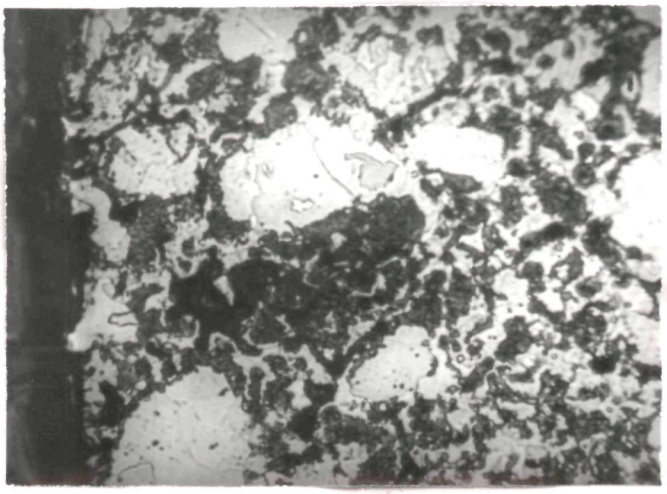

(c) PASC30 - 0·6C - 2Mo

Fig. 3·117

(a) PASC80 - 0·3C - 2Mo

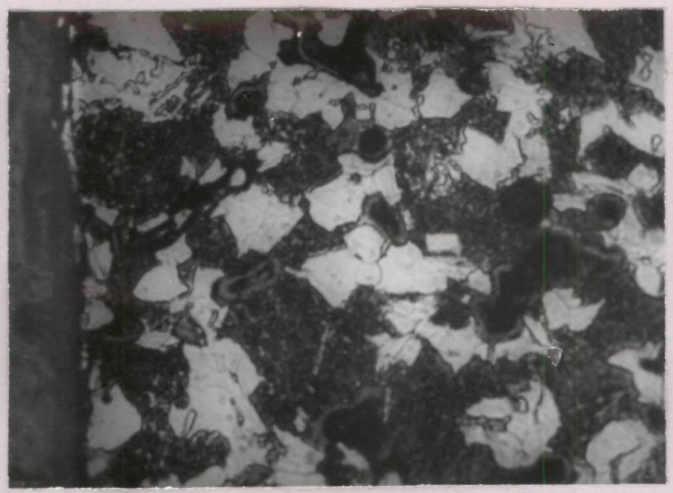

(b) PASC80 - 0·6C - 1Mo

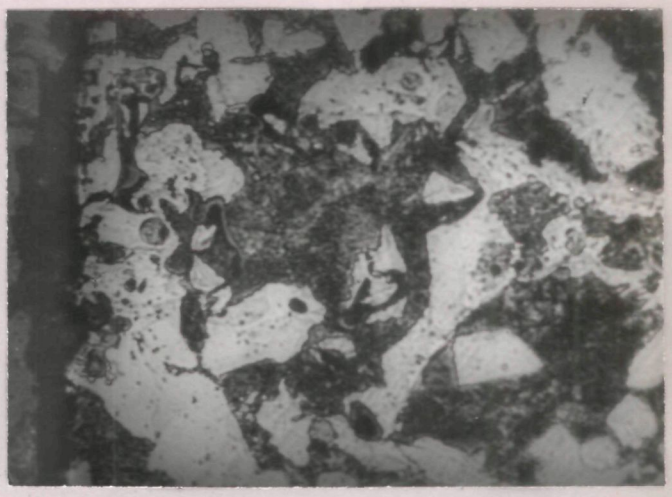

(c) PASC80 - 0·6C - 2Mo

Fig. 3·118

PASC80 - 0·6C - 2Mo

Fig. 3·119

3.119). When steam oxidation temperature was increased, matrix grains becomes uniform, oxidation increases but the layer of oxide appears to have shifted and reduced (Fig. 3.120). Increase of oxidation period to 120 minutes at 600°C increases the oxidation rate significantly, reduces the proportion of pearlitic and carbidic phase and causes oxidation around and within the pores/second phase particles (Fig. 3.121). Increase in P-content from 0.3 to 0.8 % improves the oxide layer in respect of definition and increases the size of the grains (Fig. 3.122).

3.3.3.3.2 Scanning electron microscopy

Scanning electron picture shows (Fig. 3.123 a) that Mo-containing compact in general gives sharp and well defined grains. Steam oxidation at 527°C for 120 minutes gives non-uniform oxide layer. Matrix consists of different phases (Fig. 3.123 b), a pearlitic type phase, a carbidic phase and some grains appear to have some precipitate particles (Fig. 3.123 b and c). Increase in P-content to 0.8 % decreases the thickness of oxide layer and proportion of phases other than ferrite matrix (Fig. 3.124). All the multiphase structural constituents appear to be oriented in characteristic direction (Fig. 3.124 b and c). Evidence of large number of big size pore appears

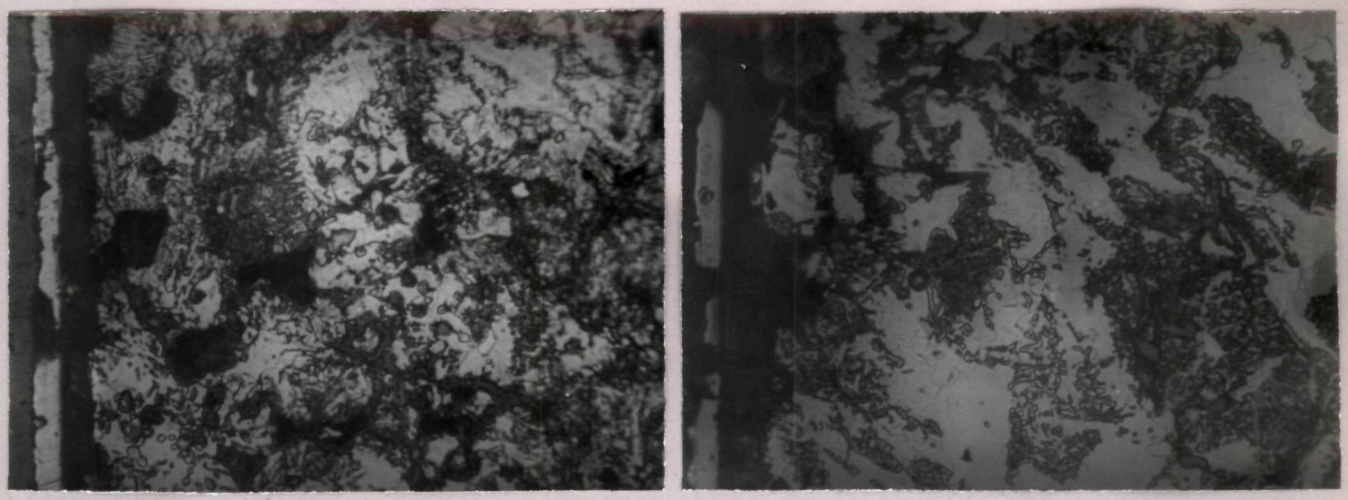

(a) PASC30 - 0·3C - 2Mo (b) PASC30 - 0·6C - 1Mo

Fig. 3·120

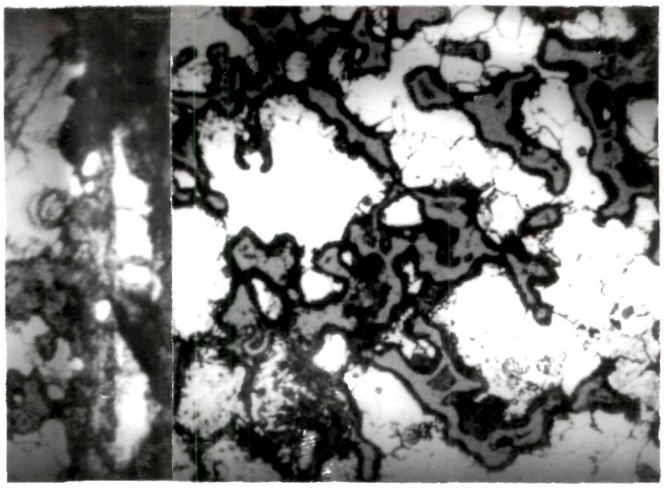

PASC 30 - 0·6C - 1Mo

Fig. 3·121

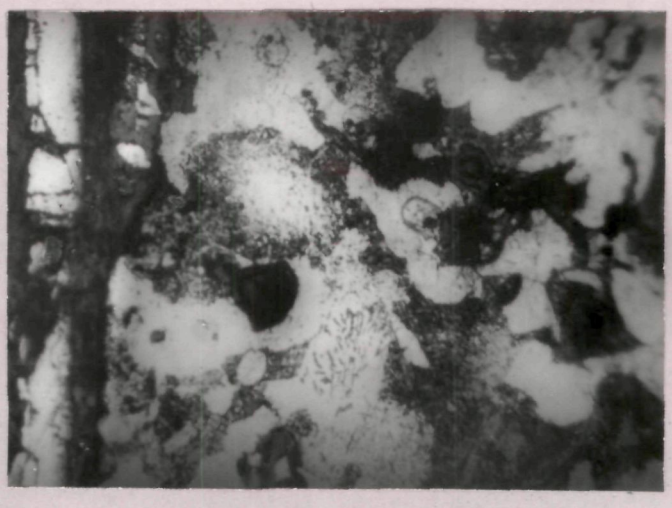

PASC 80 - 0·6C - 1Mo

Fig. 3·122

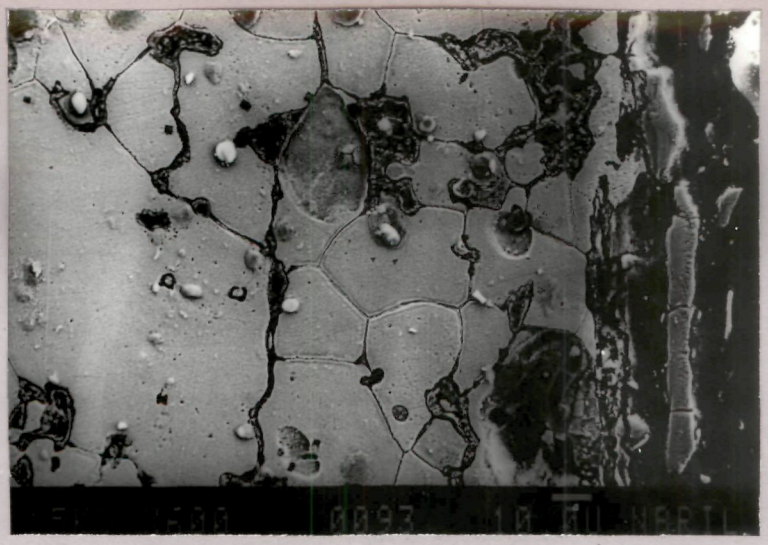

(a)

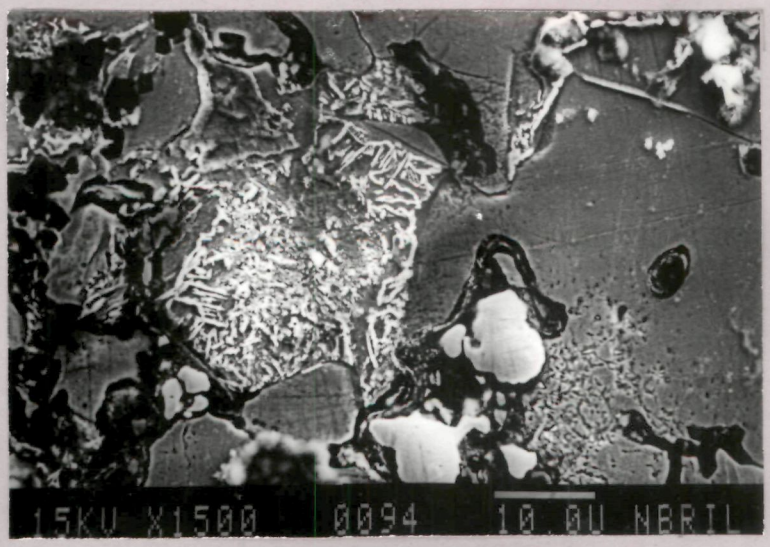

(b)

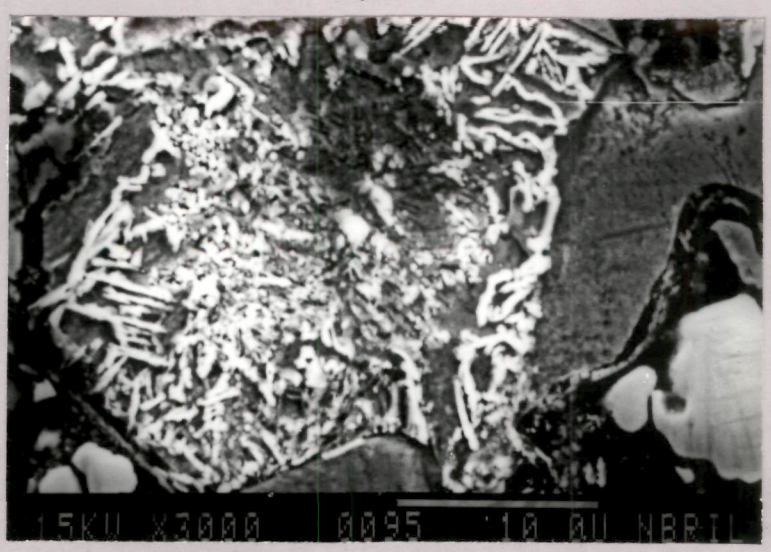

(c)

PASC30 - 0·3C - 2Mo

Fig. 3·123

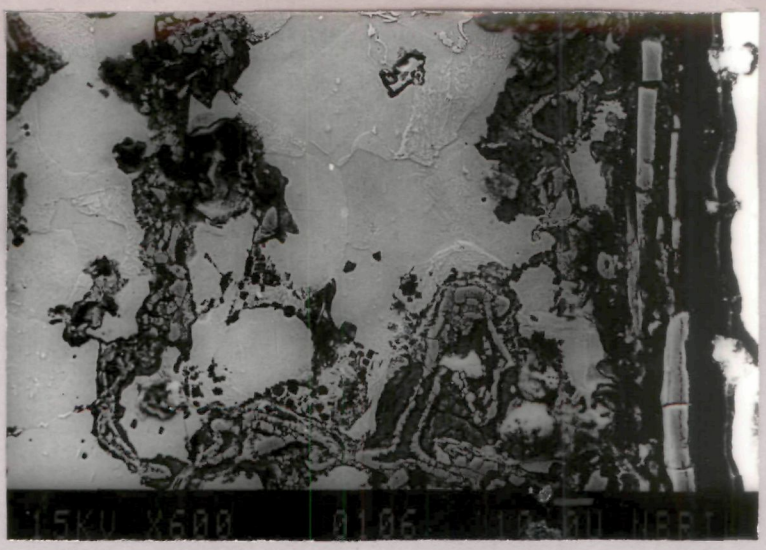

(a)

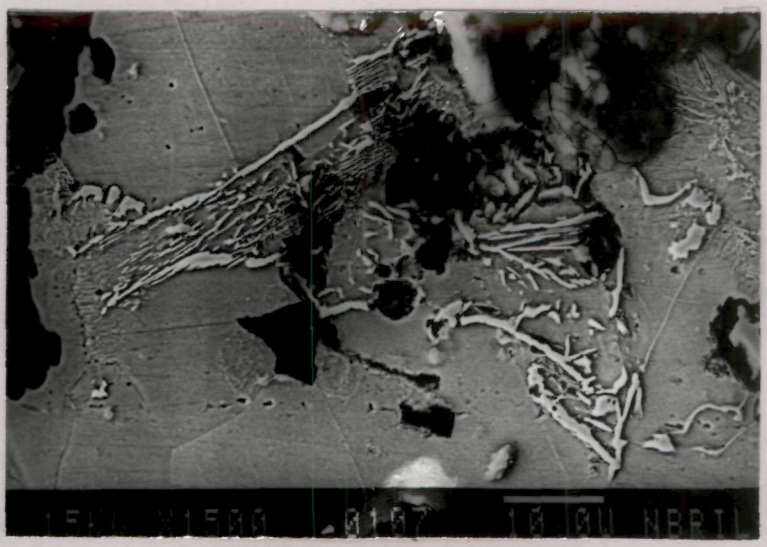

(b)

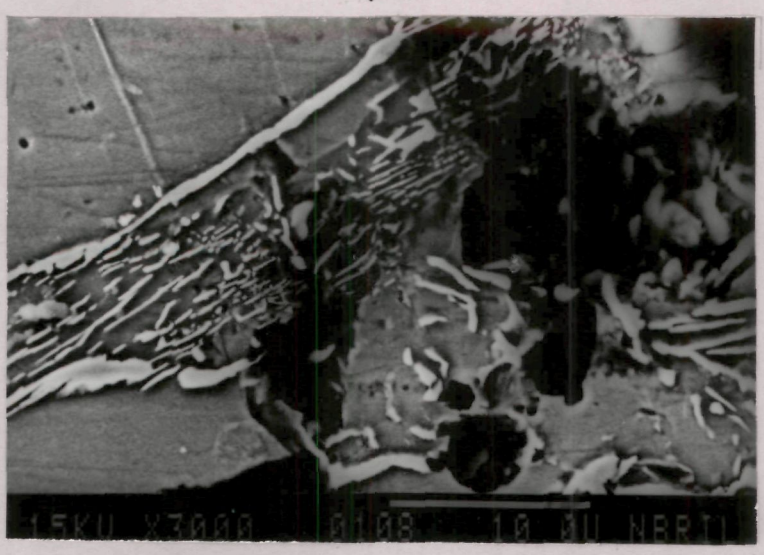

(c)

PASC80 - 0·3C - 2Mo

Fig. 3·124

to be due to cracking and removal of some hard phase during grinding and polishing.

Increase in C content to 0.6 % increase the proportion of double phase constituent (Fig. 3.125). Some of these double phase constituent seems to be pearlitic while other whose length is too short and are accicular in nature appear to be bainitic, martensitic or some mixed carbides. When phosphorus was increased to 0.8 % there is a small reduction in double phase constituent (pearlite) but the amount of second and fine phase increases (Fig. 3.126).

3.3.3.4 PASC-MCM-C compacts

3.3.3.4.1 Optical metallography

In case of PASC30-0.3C-1MCM sintered compact, oxidation is considerable at a treatment temperature of 450°C for 45 minutes. Oxidation occurs also within interior of the sample (Fig. 3.127a) through interconnected channel. Increase of C content to 0.6 % increases the proportion of double phase constituent (Fig. 3.127b). Increase of steam oxidation period from 45 to 120 minutes increases the extent of oxidation in the body of the sample (Fig. 3.128). Increase in phosphorus content from 0.3 to

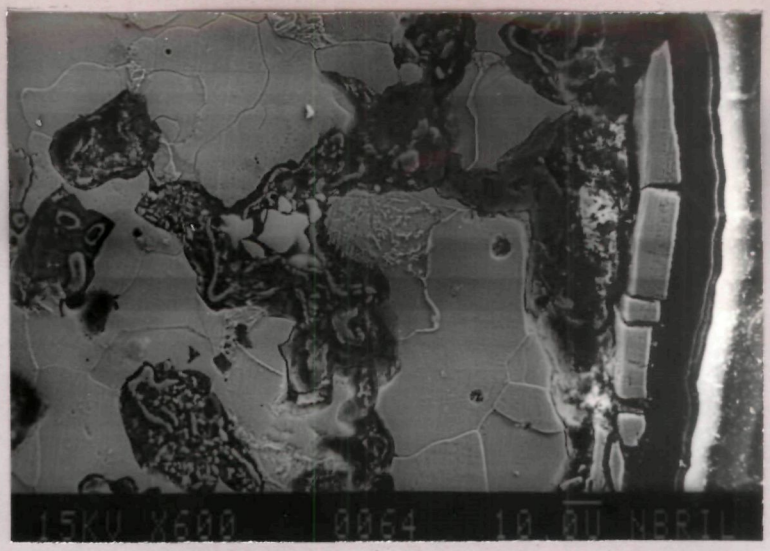

(a)

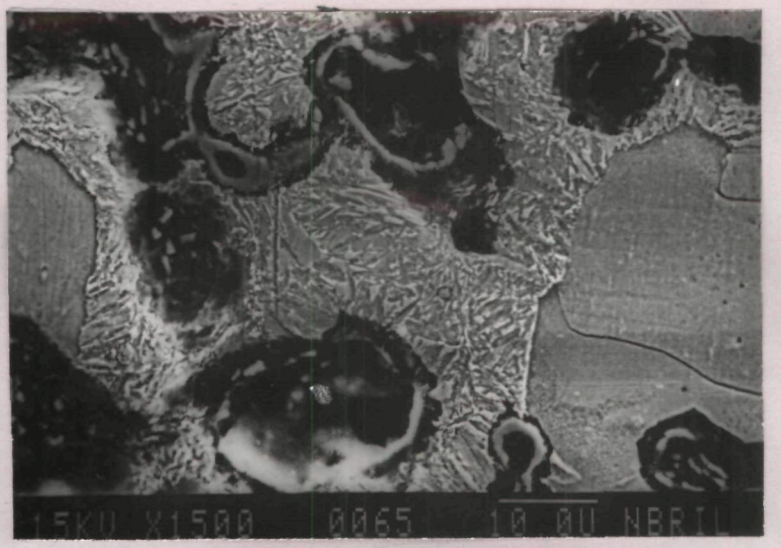

(b)

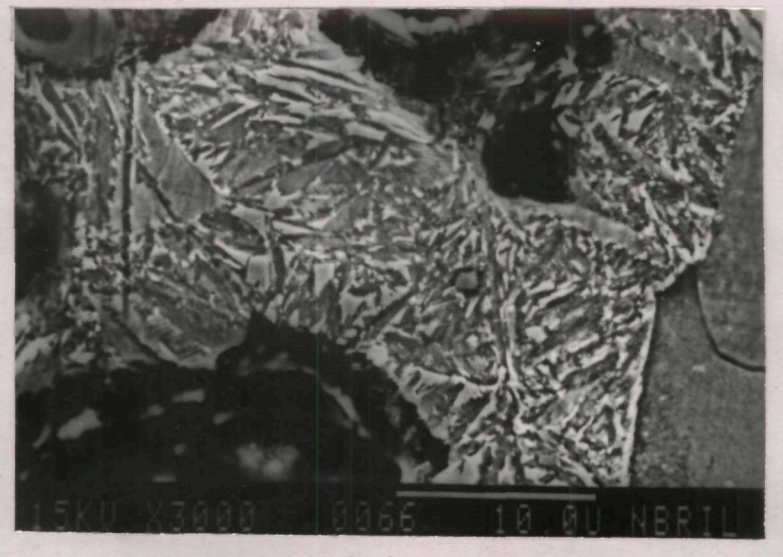

(c)

PASC 30 – 0·6C – 2 Mo

Fig. 3·125

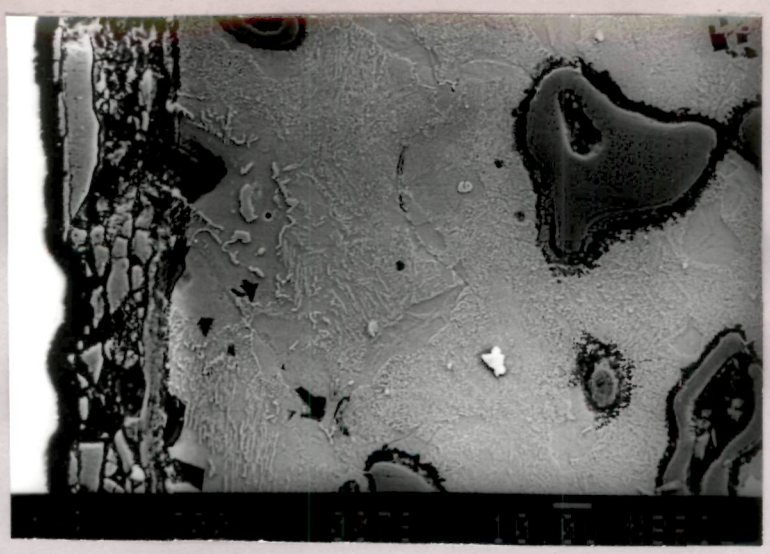

(a)

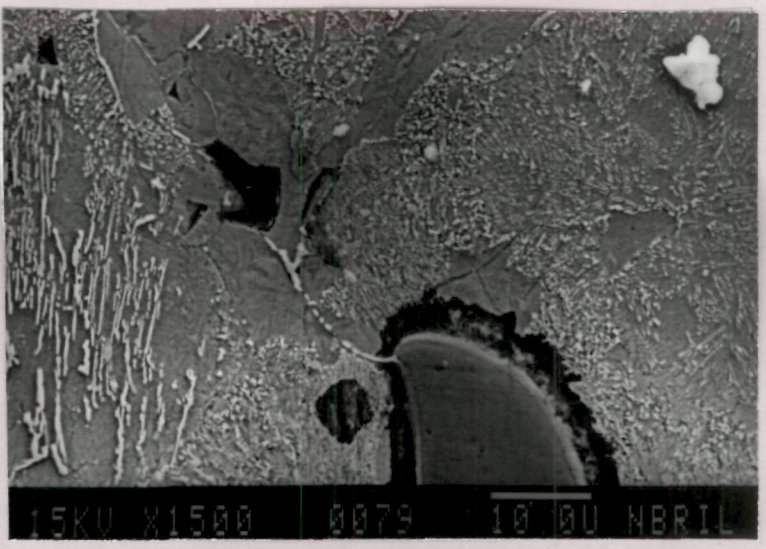

(b)

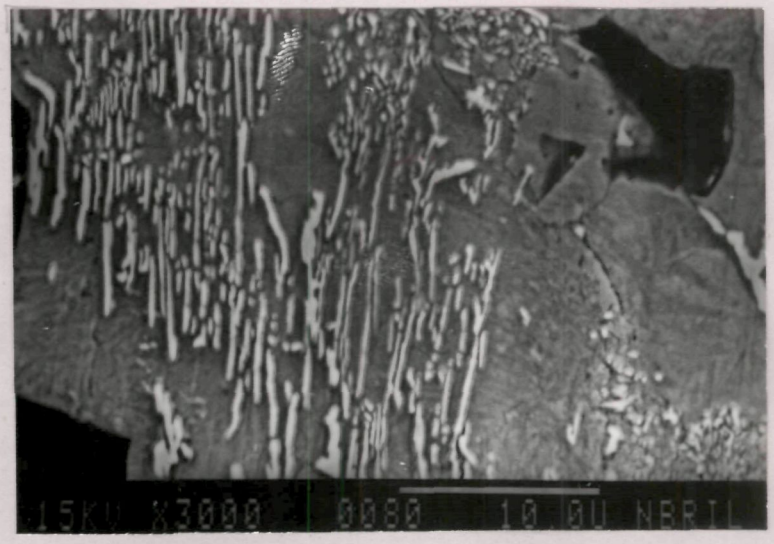

(c)

PASC80 - 0·6C - 2Mo

Fig. 3·126

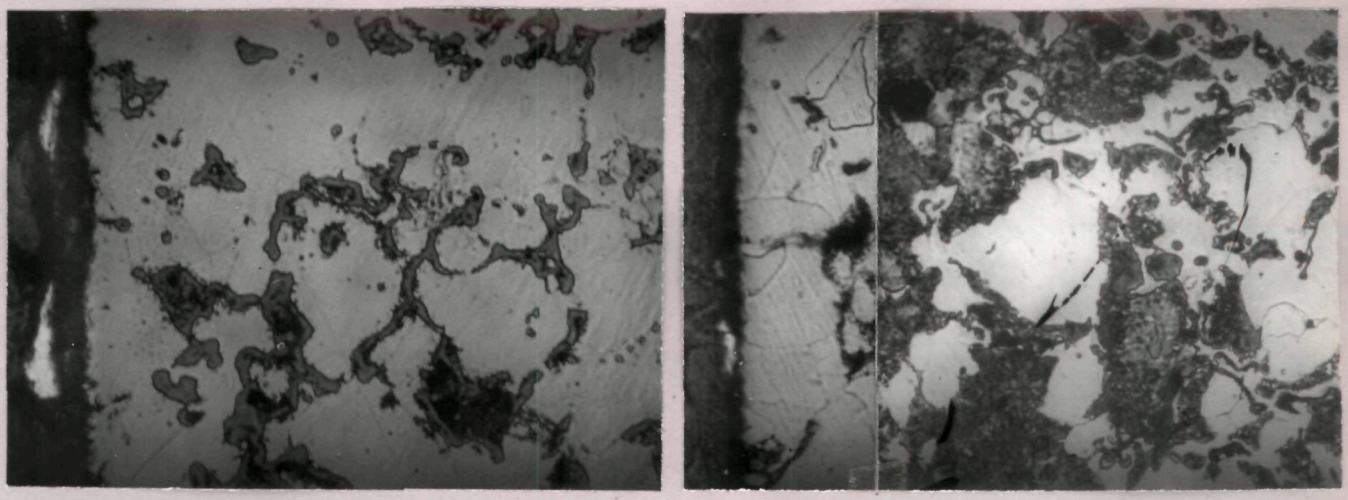

(a) PASC30 - 0·3C - 1MCM (b) PASC30 - 0·6C - 1MCM

Fig. 3·127

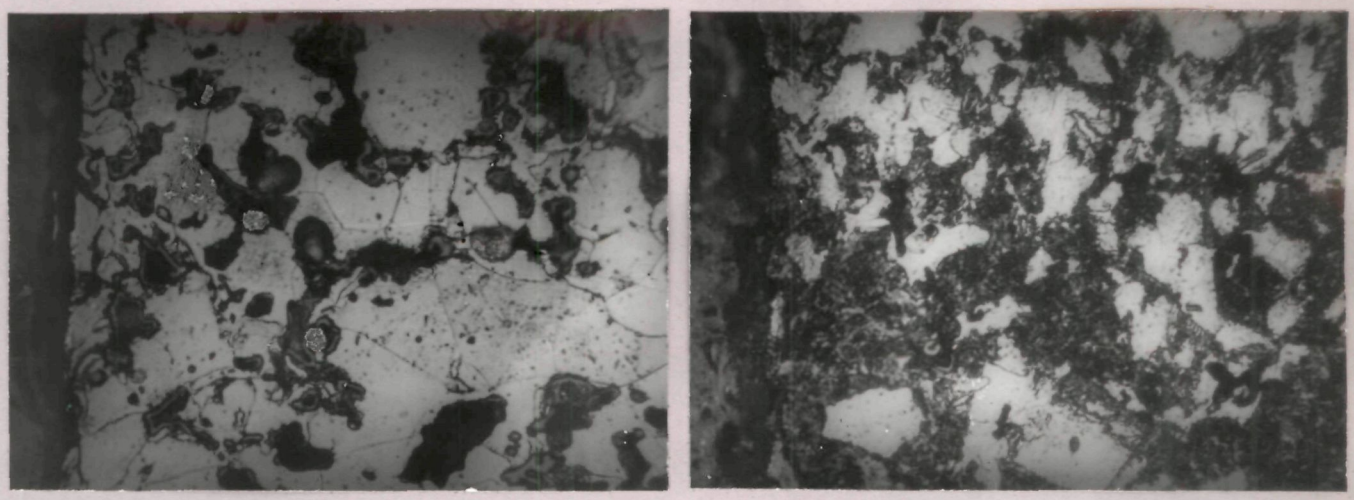

(a) PASC30 - 0·3C - 1MCM (b) PASC30 - 0·6C - 1MCM

Fig. 3·128

to 0.8 % decreases the oxidation (Fig. 3.129). However, some big pores are observed in case of samples containing 0.6 % C and 2 % MCM (Fig. 3.129 d). Increase in oxidation period to 120 minutes makes oxide layers non-uniform (Fig. 3.130). Presence of mixed phases in the matrix of the steam treated samples are evident in case of higher MCM-containing samples (Figs. 3.130 b and d). Increase in temperature of steam treatment from 450 to 527°C gives relatively uniform structure both in the matrix and the scale (Fig. 3.131). However, evidence of non-uniform and mixed type structure is more in this case (Fig. 3.131 b). Increase in phosphorus content from 0.3 to 0.8 % decreases the thickness of oxide layer (Fig. 132). Longer steam treatment period gives thicker oxide layer and makes the microstructure of the matrix non-uniform with big pores at localized regions (Fig. 3.133). Increase in oxidation temperature to 600°C appears to have increased the number of phases (Fig. 3.134), particularly in higher MCM-containing compacts (Fig. 3.135). However, at lower C, MCM and P content, structure is relatively uniform (Fig. 3.136). Comparision of microstructure for different composition shows that higher MCM increases the proportion of pearlitic or double phase constituent (Fig. 3.137 a and b). Increase in C content naturally increases the pearlitic constituent (Fig. 3.137 b and c).

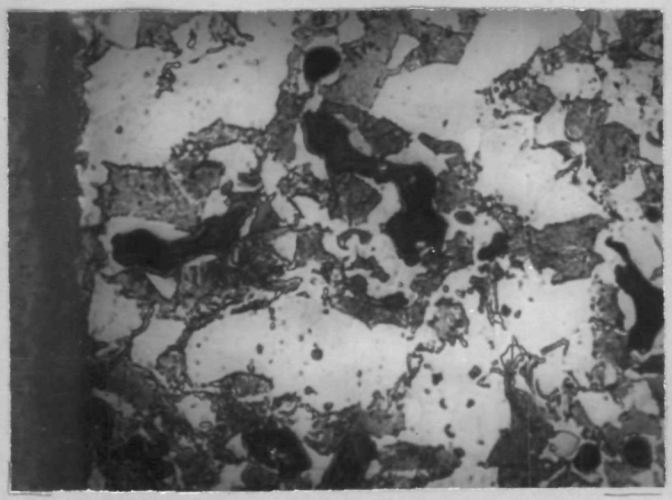

(a) PASC80 - 0·3C - 1MCM

(b) PASC80 - 0·3C - 2MCM

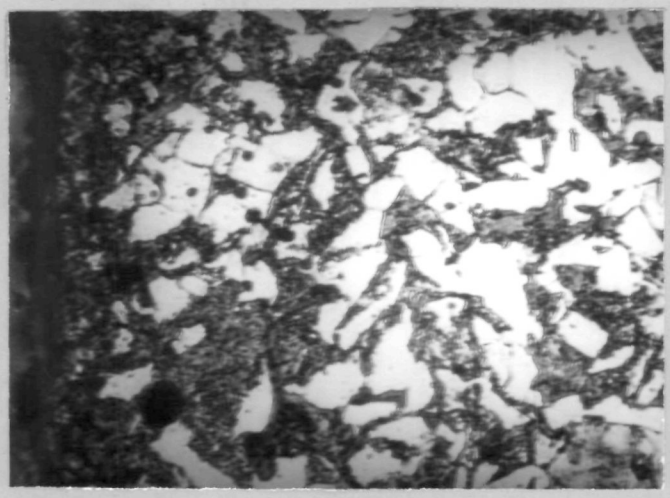

(c) PASC80 - 0·6C - 1MCM

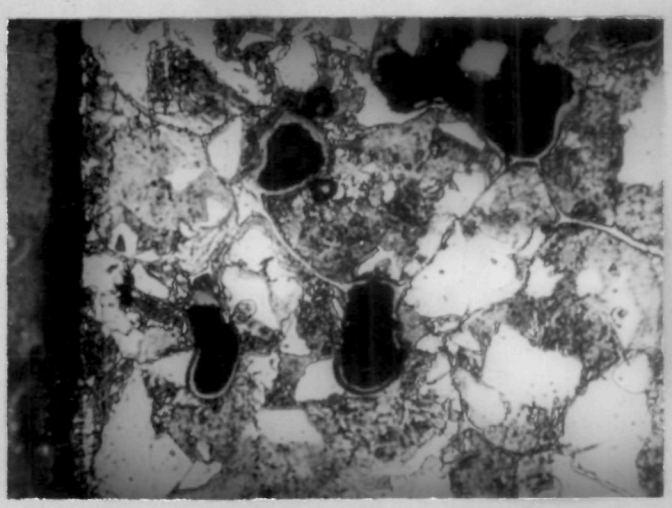

(d) PASC80 - 0·6C - 2MCM

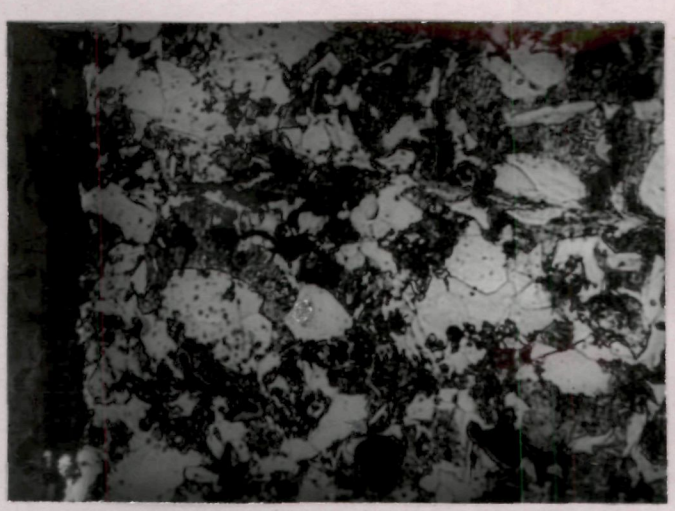

(a) PASC80 - 0·3C - 1MCM

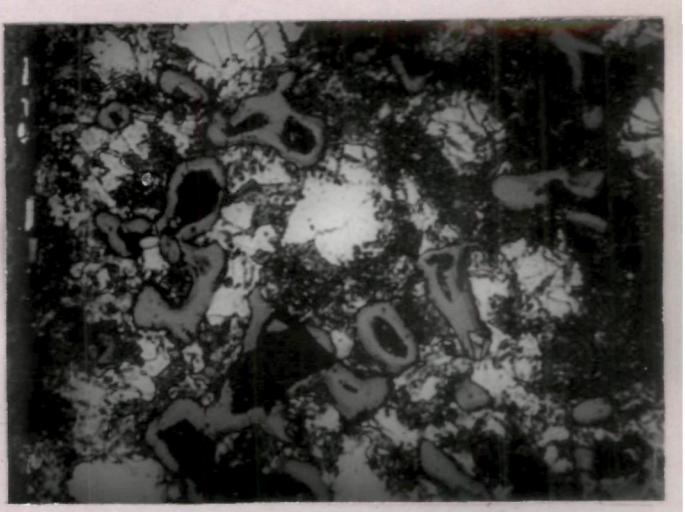

(b) PASC80 - 0·3C - 2MCM

(c) PASC80 - 0·6C - 1MCM

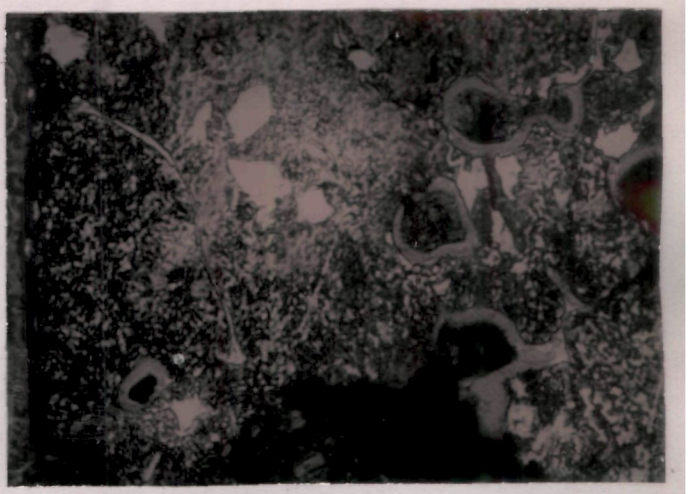

(d) PASC80 - 0·6C - 2MCM

Fig. 3·130

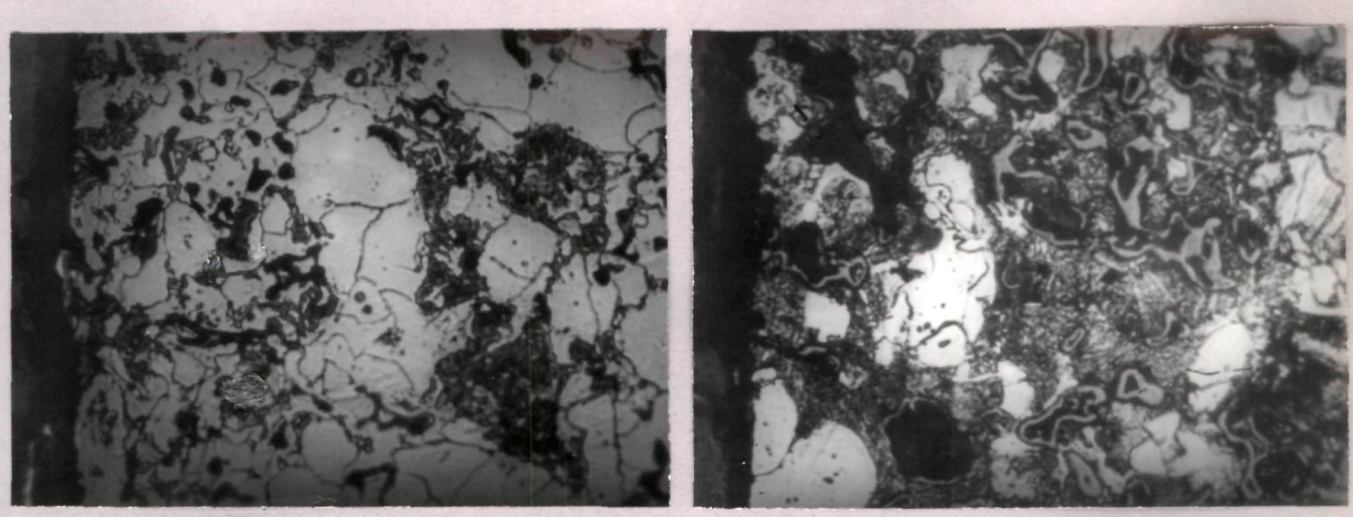

(a) PASC30 - 0·3C - 2MCM (b) PASC30 - 0·6C - 2MCM

Fig. 3·131

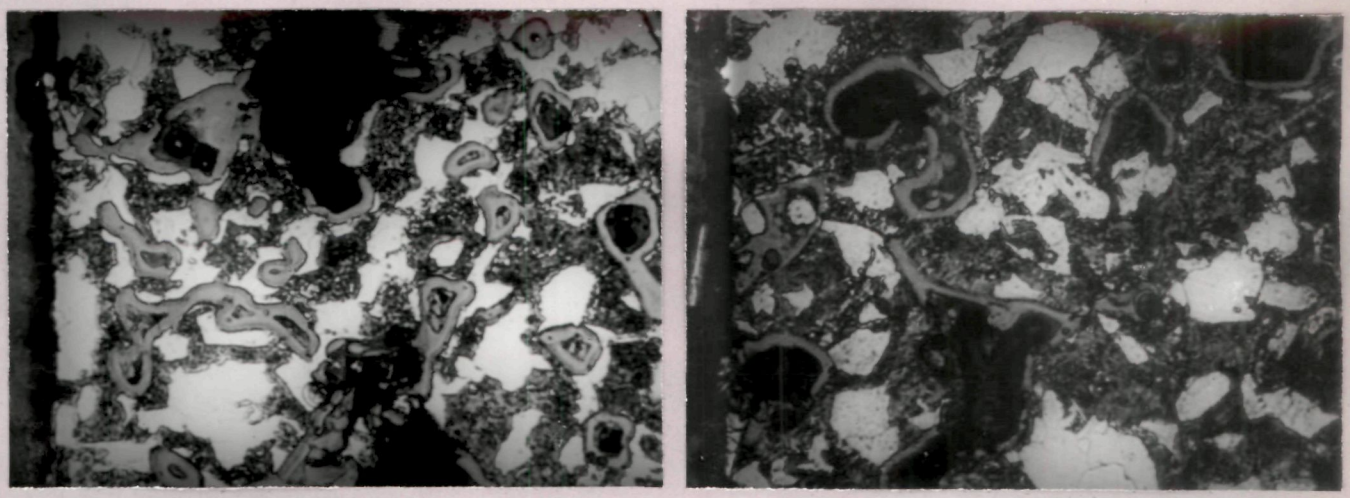

(a) PASC80 - 0·3C - 2MCM (b) PASC80 - 0·6C - 2MCM

Fig. 3·132

PASC80 - 0·6C - 1MCM

Fig. 3·133

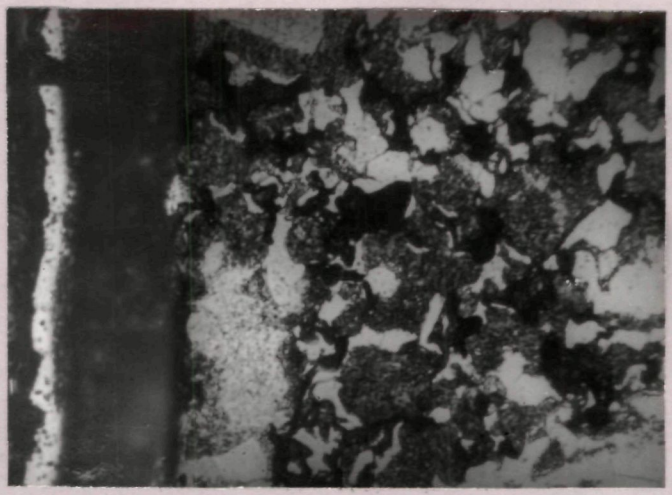

PASC 30 - 0·6C - 1MCM

Fig. 3·134

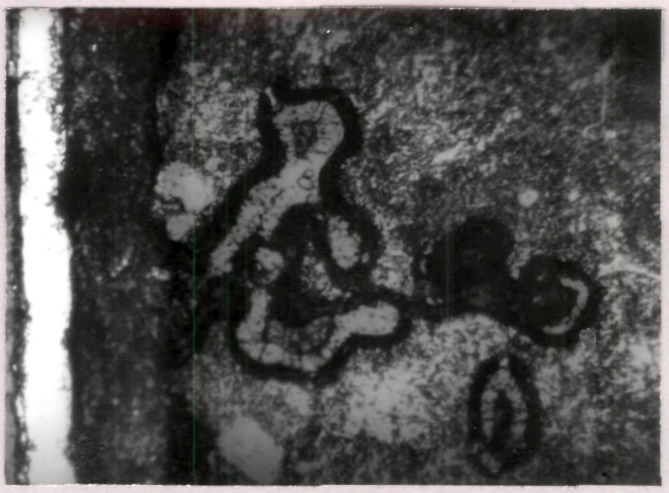

PASC80 - 0·6C - 2MCM

Fig. 3·135

PASC30 - 0·3C - 1MCM

Fig. 3·136

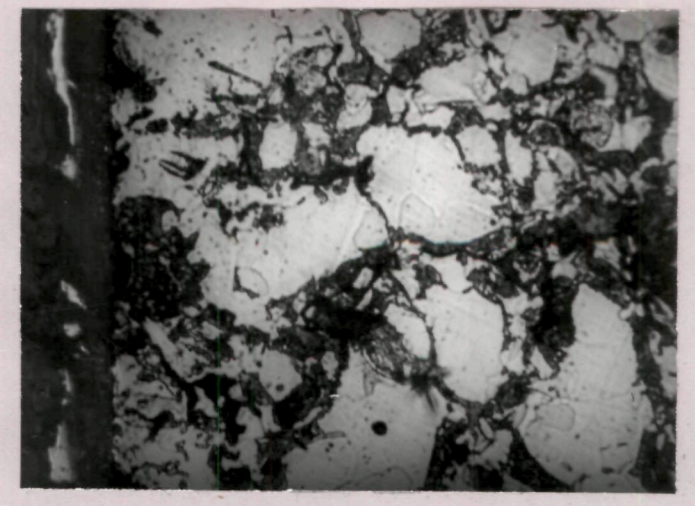

(a) PASC80 - 0·3C - 1MCM

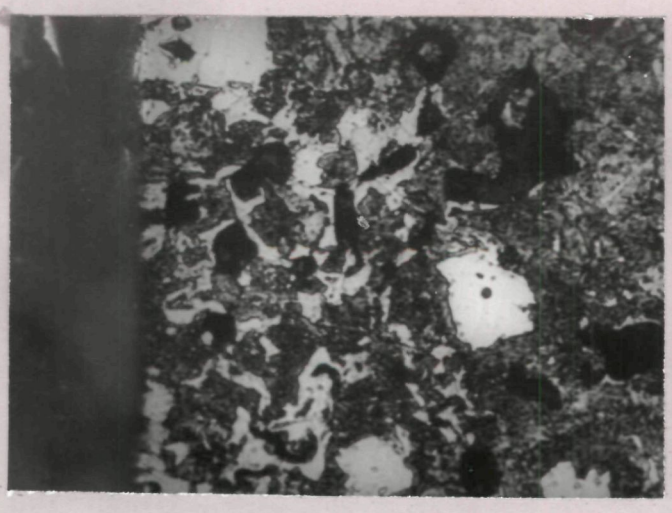

(b) PASC80 - 0·3C - 2MCM

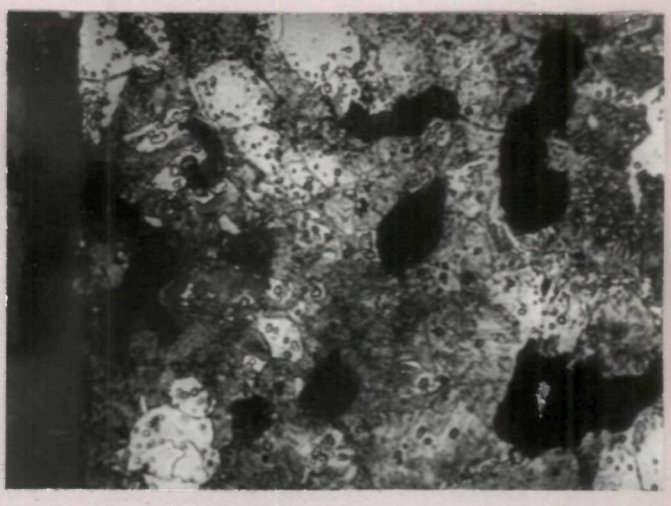

(c) PASC80 - 0·6C - 2MCM

Fig. 3·137

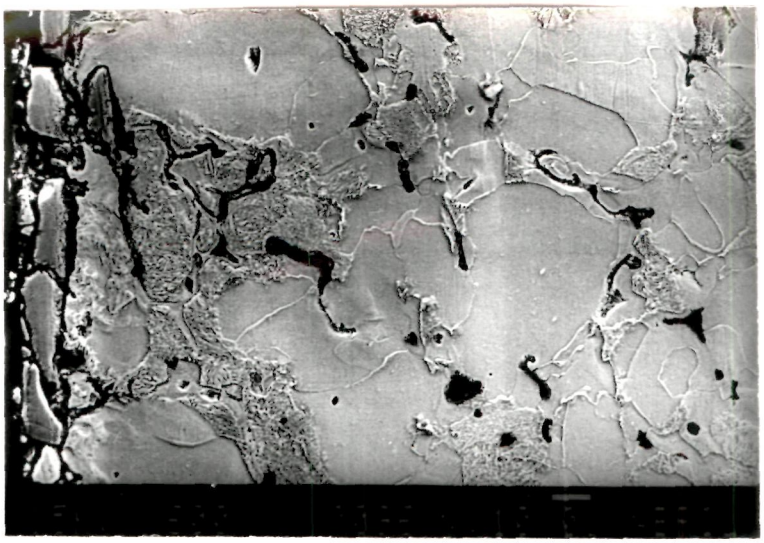

(a)

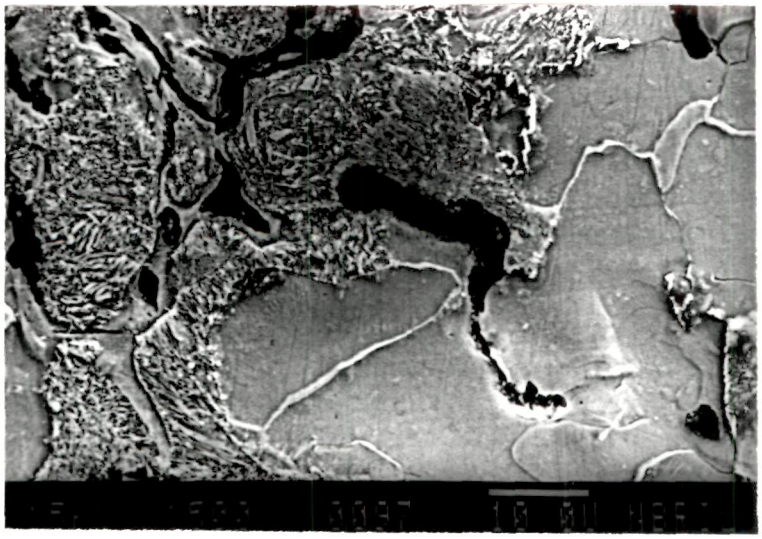

(b)

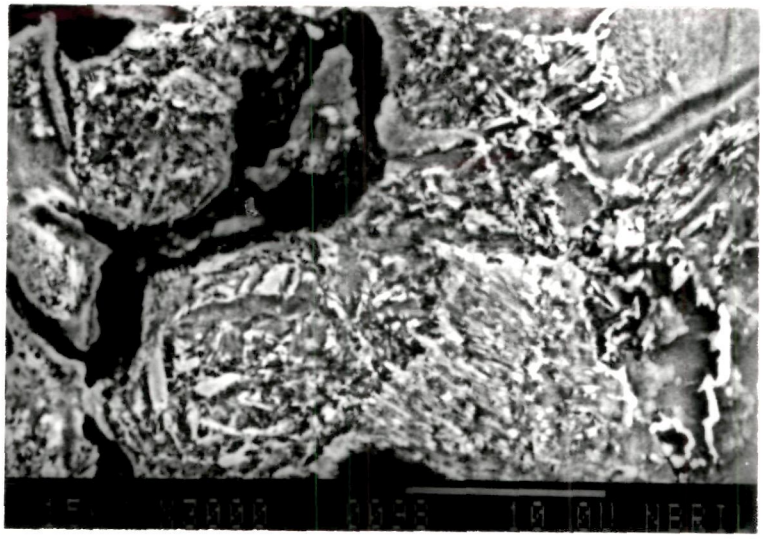

(c)

PASC30 - 0·3C - 2MCM

Fig. 3·138

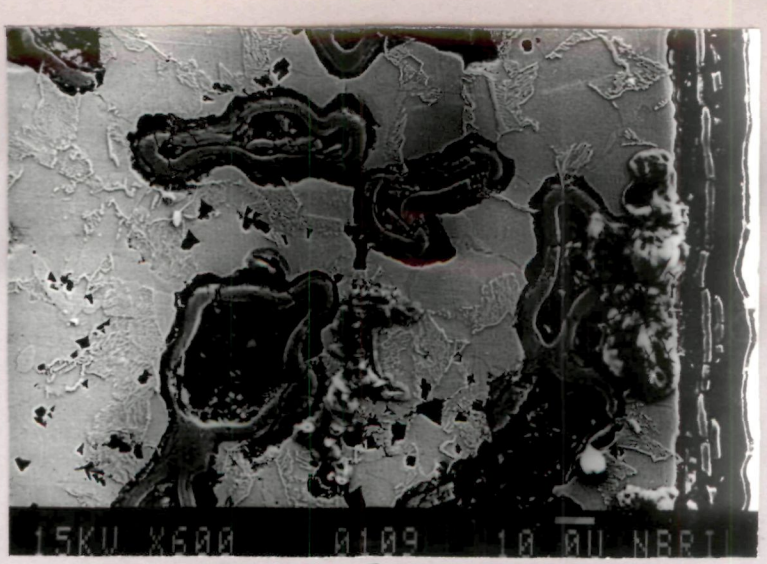

a

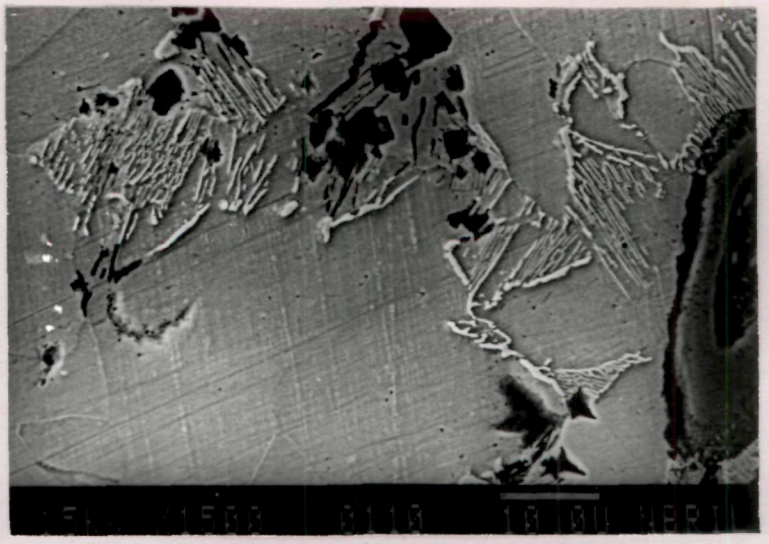

b

(c)

PA SC80 - 0·3C - 2MCM

Fig. 3·139

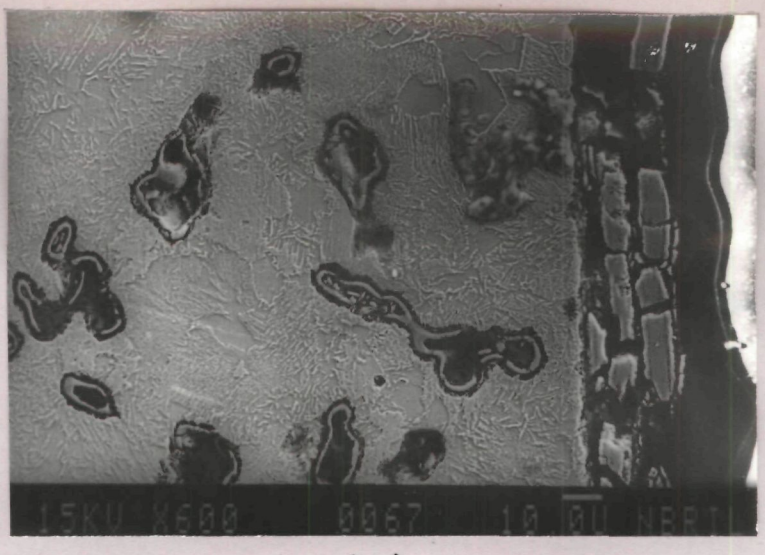

(a)

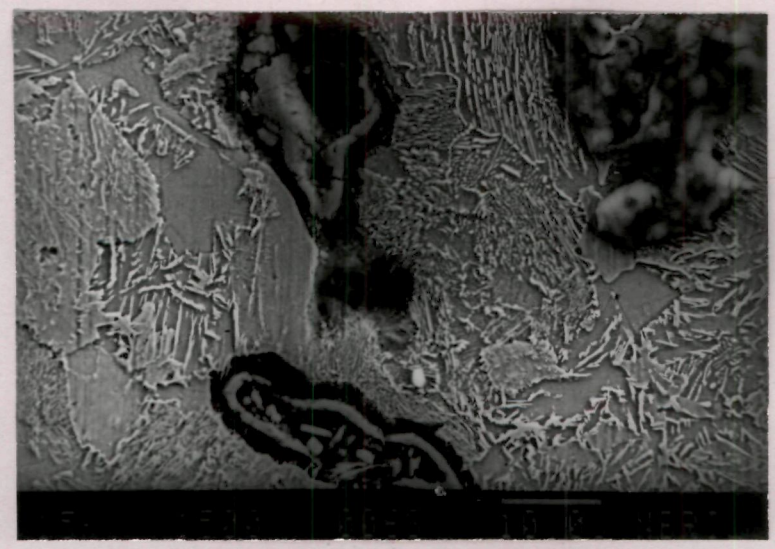

(b)

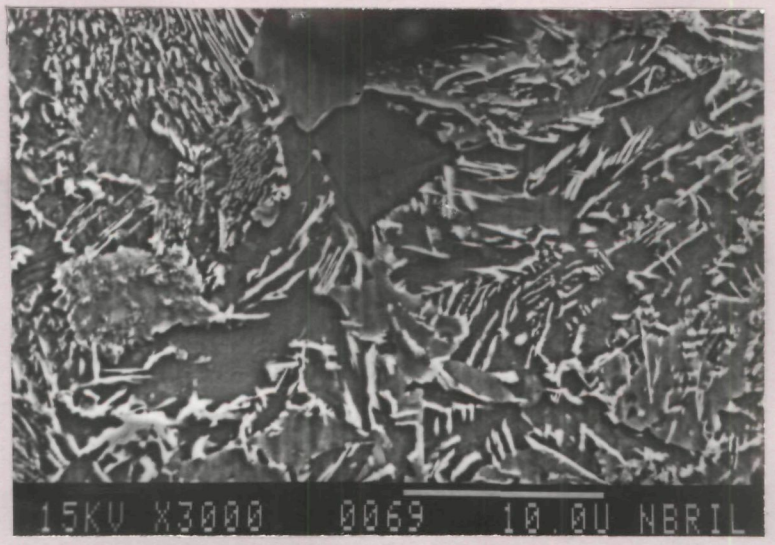

(c)

PASC 30 - 0·6C - 2MCM

Fig. 3·140

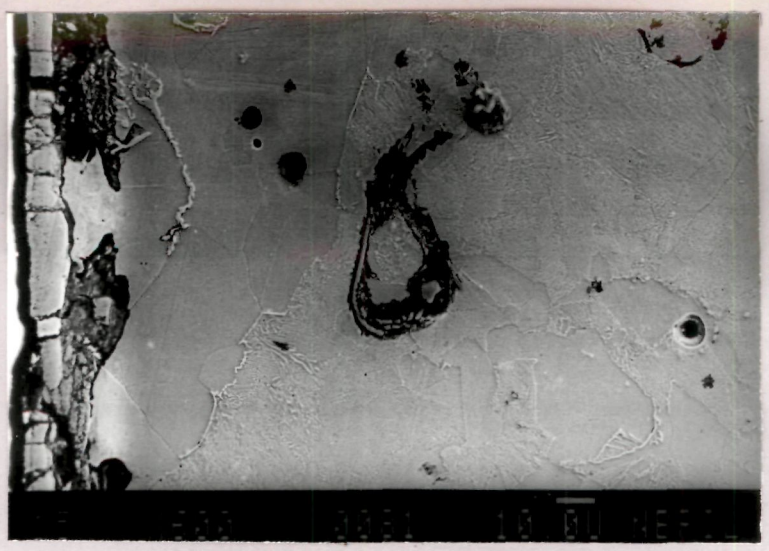

(a)

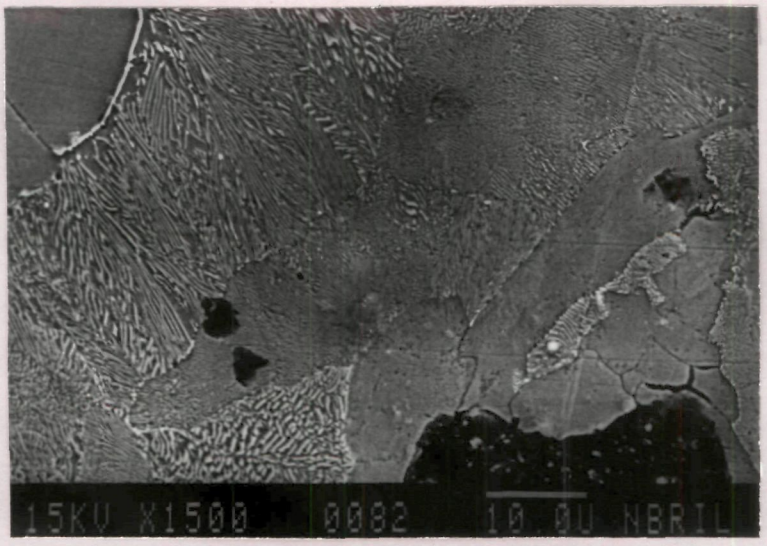

(b)

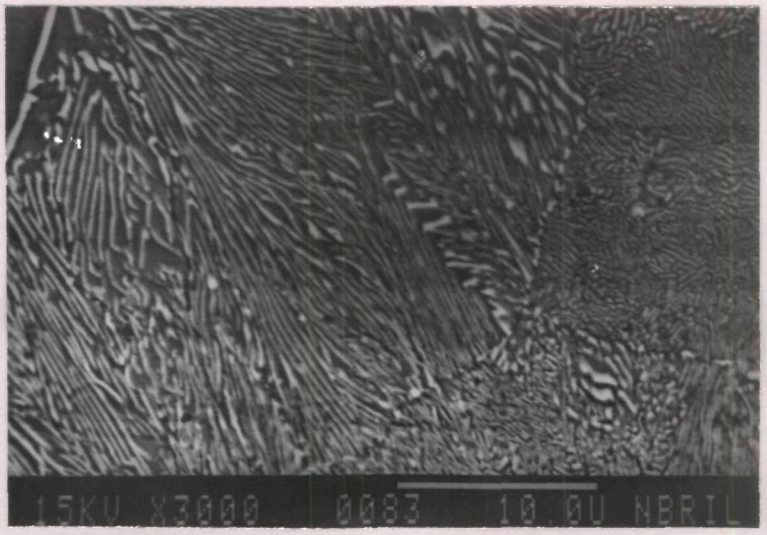

(c)

PASC80 - 0·6C - 2MCM

Fig. 3·141

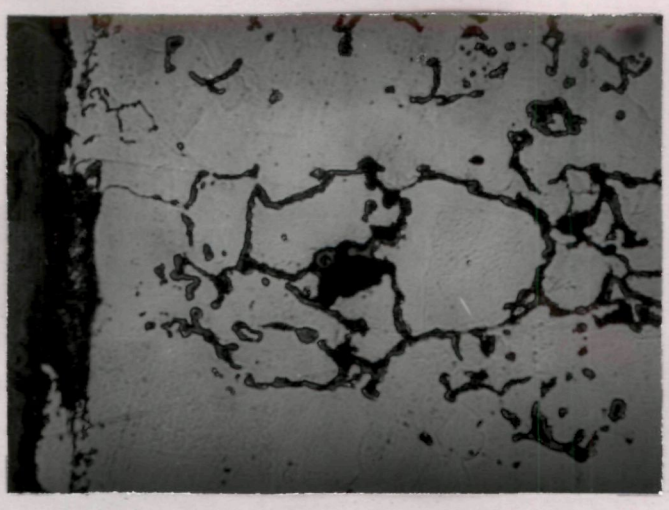

(a) PASC 30 - 0·3C - 1MVM

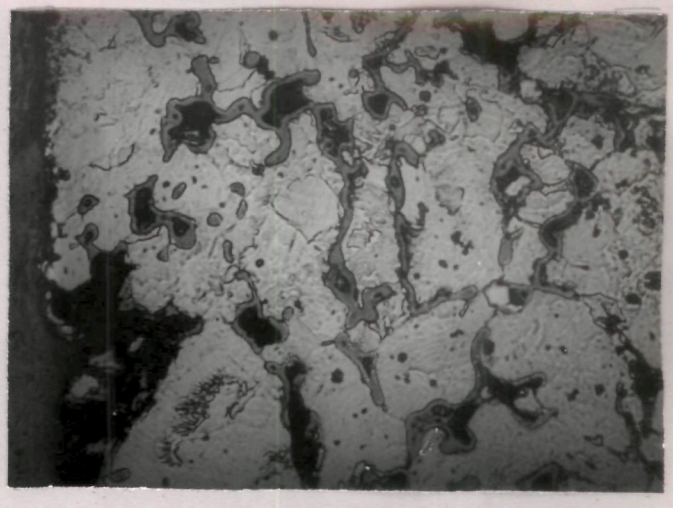

(b) PASC 30 - 0·6C - 1MVM

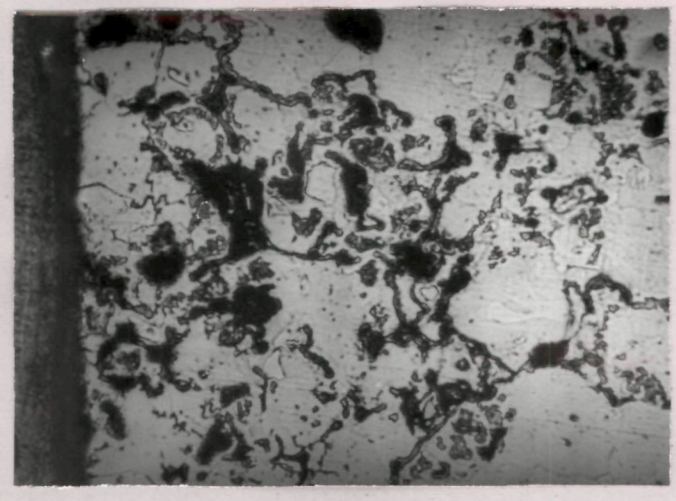

(c)

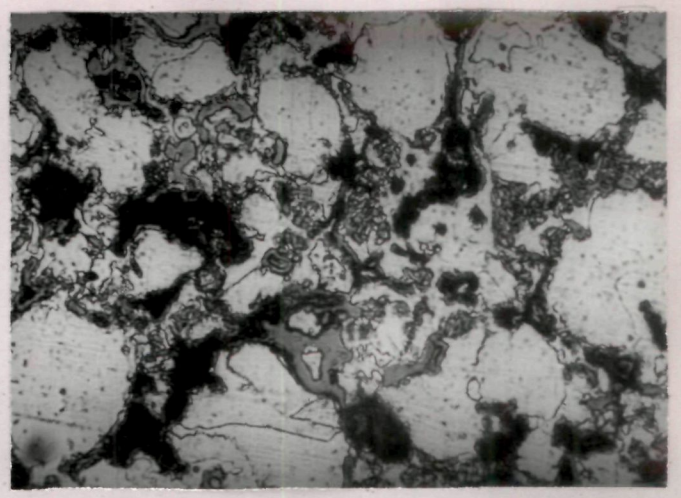

PASC 30 - 0·6C - 2MVM (d)

Fig. 3·142

results into increased oxidation (Fig. 3.143). Increase in P-content gives less oxidation (Fig. 3.144 a and b) and proportion of second-phase constituent increases with increase in C-content (Fig. 3.144 c and d). Increase in oxidation temperature to 527°C gives better microstructure but does not significantly improve definition and uniformity of oxide layers (Fig. 3.145). In general, microstructure of MVM-containing compacts are similar to that observed in case of MCM-containing compacts (Figs. 3.127-3.141 and 3.142-3.154). Increase in oxidation temperature to 600°C brings about heterogeneity in the structure of the matrix as well as oxide layer (Fig. 3.148). The thickness of oxide layer and extent of oxidation increases with increase in steam treatment period (Fig. 3.149). Higher amount of phosphorus decreases the extent of oxidation in the matrix (Fig. 3.150).

3.3.3.5.2 Scanning electron microscopy

Scanning electron picture of PASC30-0.3C-2MVM compact steam treated at 527°C for 120 minutes shows big pores in the matrix as well as just near the oxide boundary in the form of uniform layer (Fig. 3.151 and 3.153). This layer of pore decreases slightly with increase in P-content (Fig. 3.152 and 3.154). Higher amount of C increases the proportion of pearlitic phase (Fig. 3.153 and 3.154).

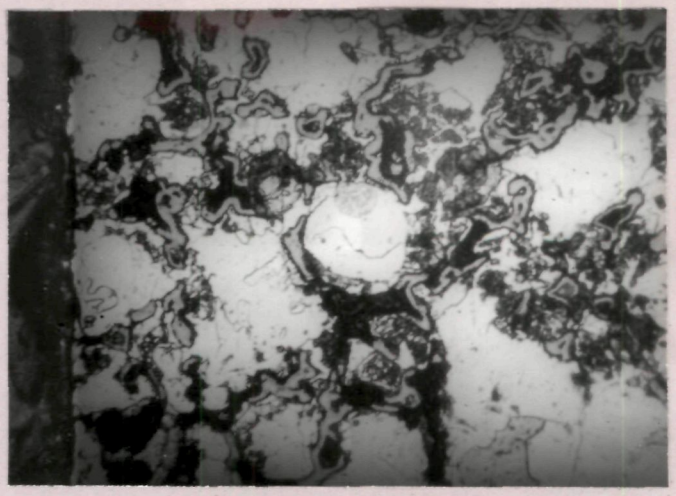

PASC30 - 0·6C - 1MVM

Fig. 3·143

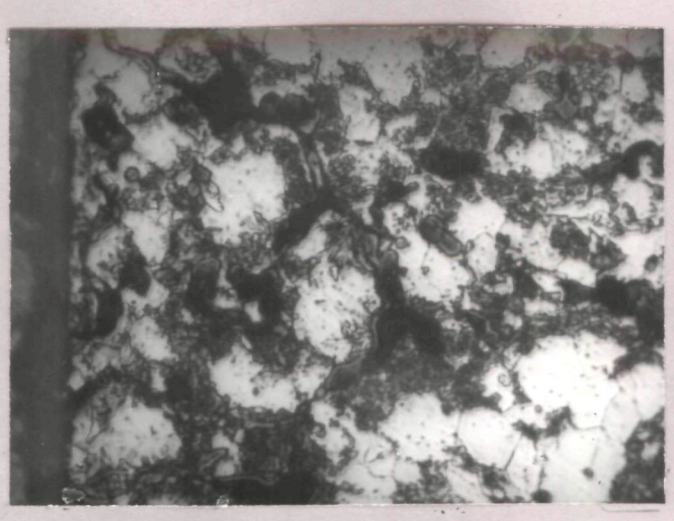

(a) PASC80 - 0·3C - 1MVM

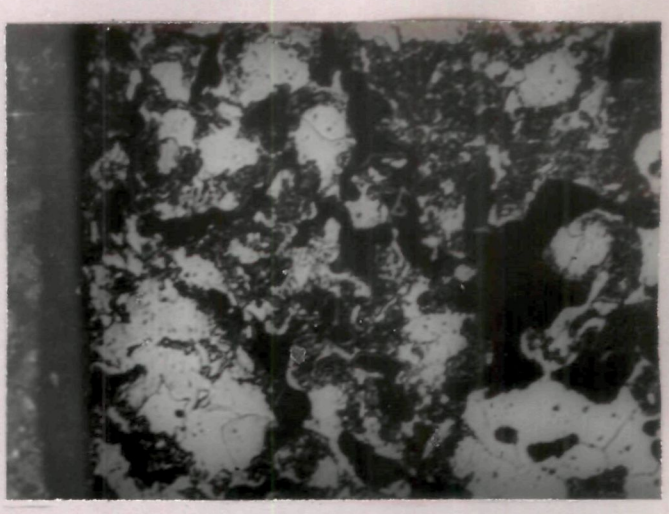

(b) PASC80 - 0·3C - 2MVM

(c) PASC80 - 0·6C - 1MVM

(d) PASC80 - 0·6C - 2MVM

Fig. 3·144

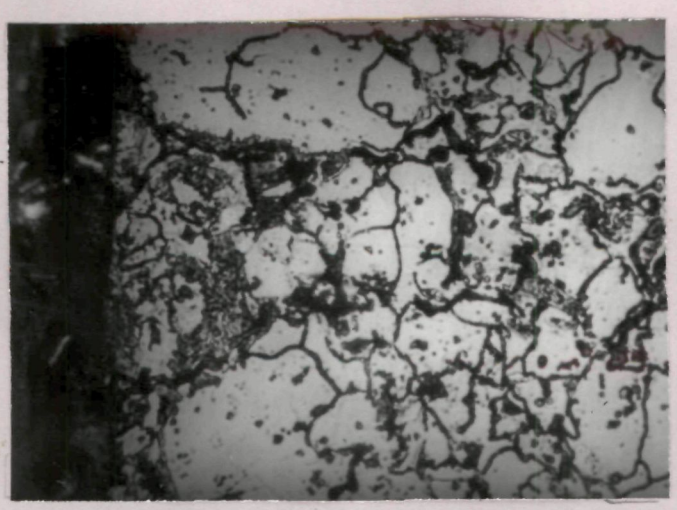

(a) PASC30 - 0·3C - 1MVM

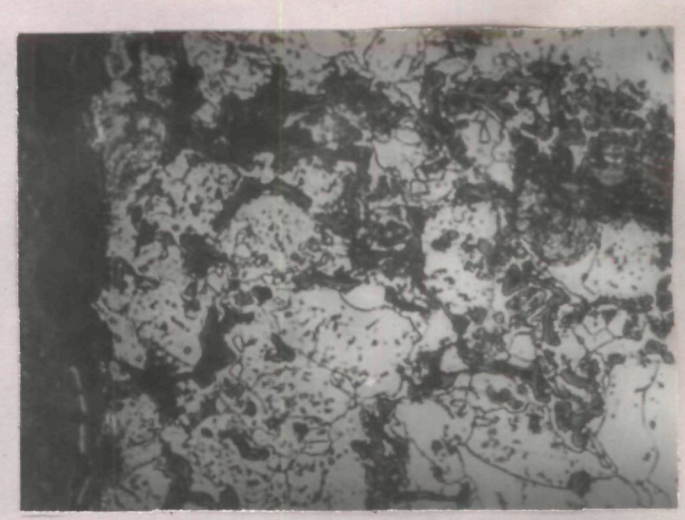

(b) PASC30 - 0·3C - 2MVM

(c) PASC30 - 0·6C - 1MVM

(d) PASC30 - 0·6C - 2MVM

Fig. 3·145

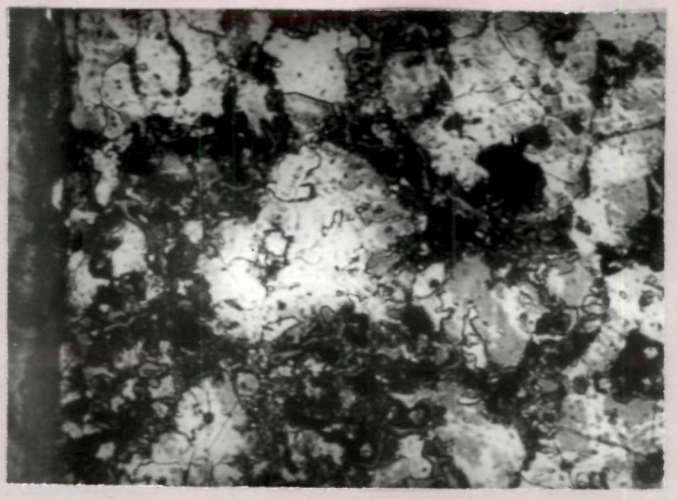

PASC80 - 0·3C - 2MVM

Fig. 3·146

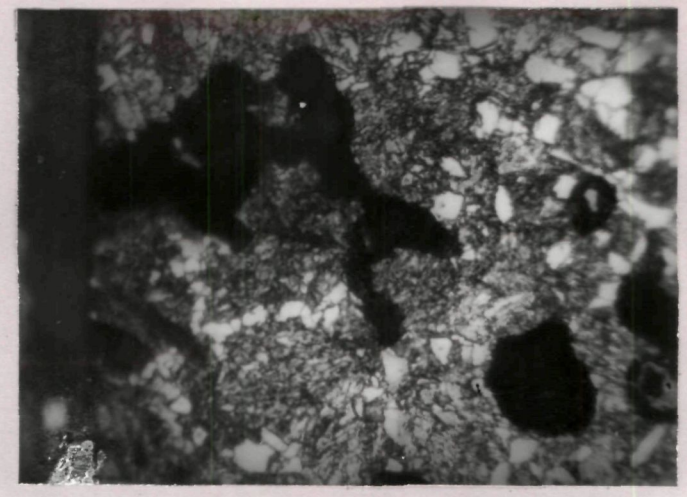

PASC80 - 0·6C - 2MVM

Fig. 3·147

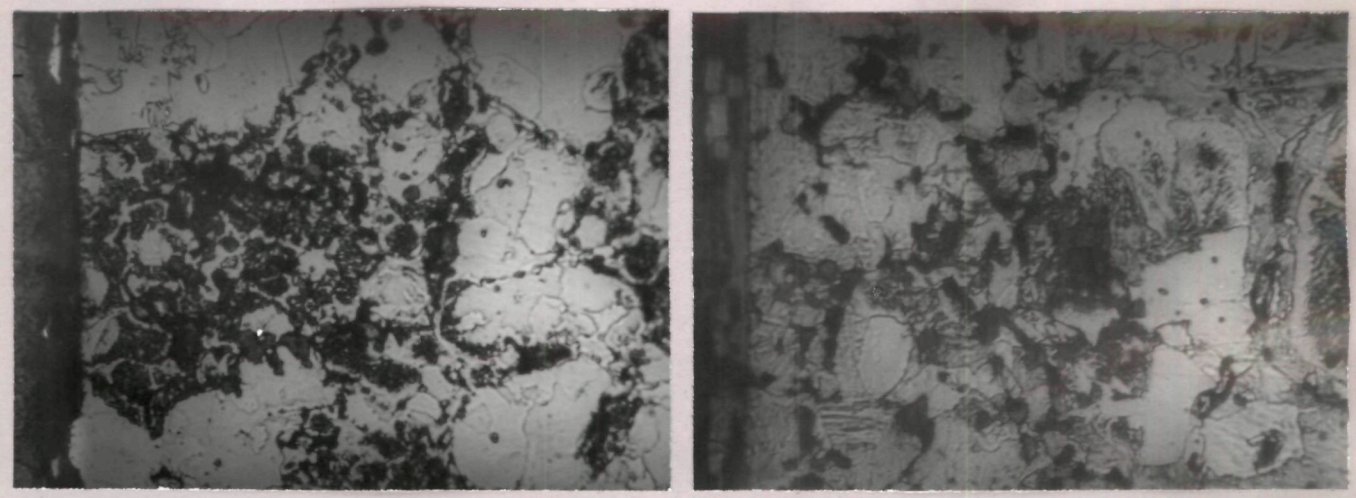

(a) PASC30 - 0·3C - 1MVM (b) PASC30 - 0·6C - 2MVM

Fig. 3·148

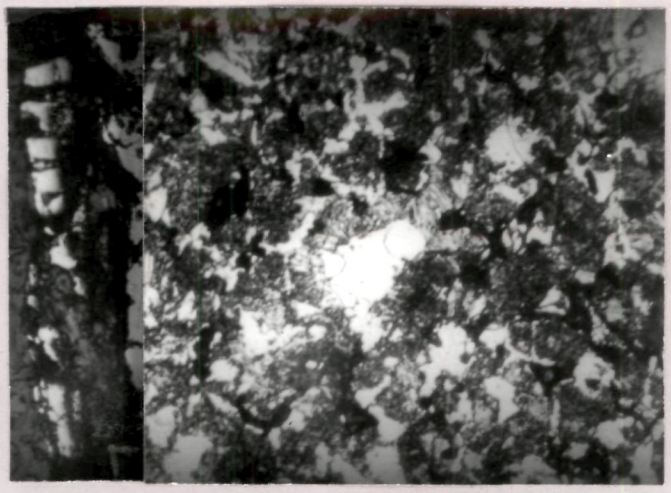

PASC30 - 0·6C - 2MVM

Fig. 3·149

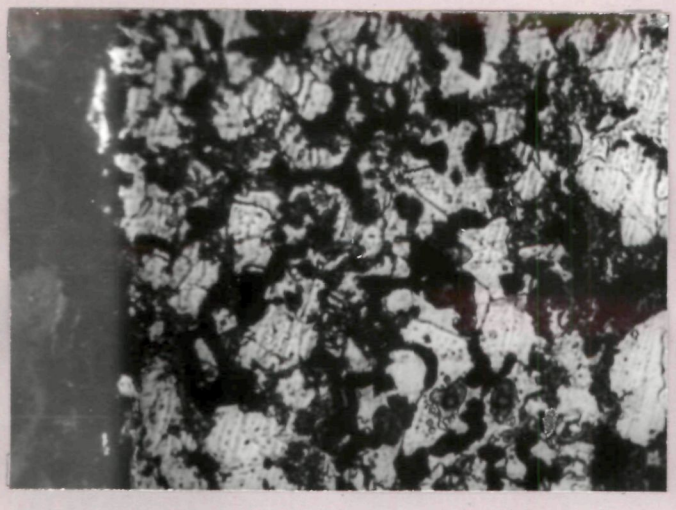

(a) PASC80 - 0·3C - 1MVM

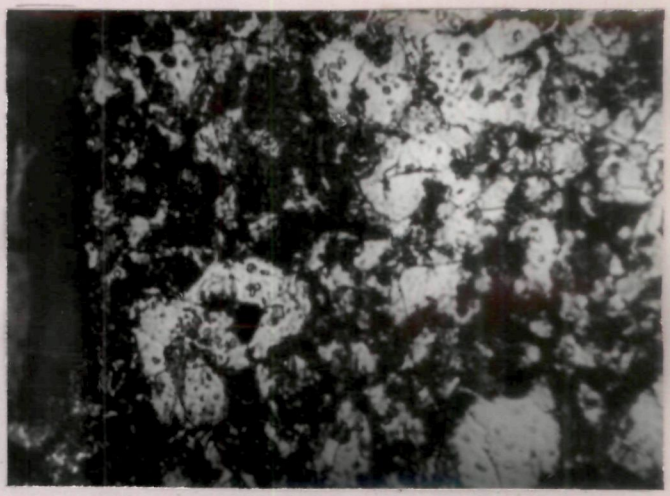

(b) PASC80 - 0·3C - 2MVM

(c) PASC80 - 0·6C - 1MVM

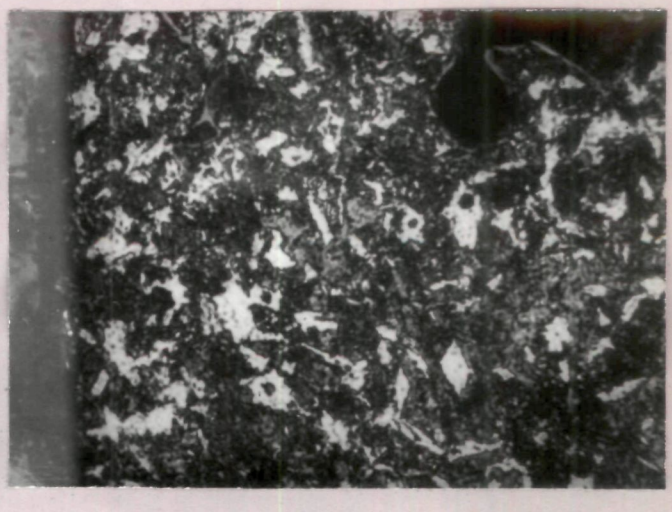

(d) PASC80 - 0·6C - 2MVM

Fig. 3·150

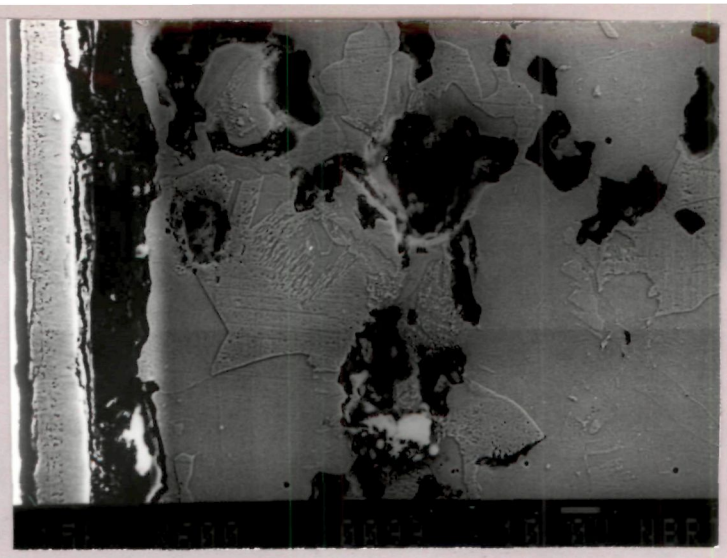

(a)

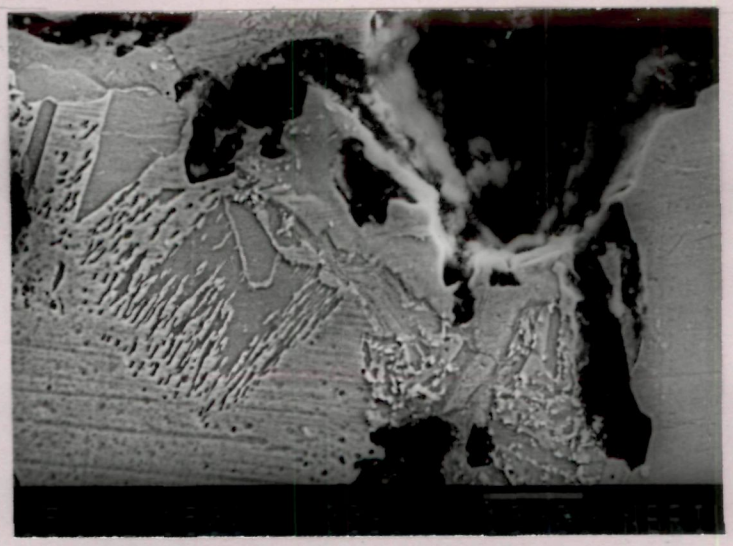

(b)

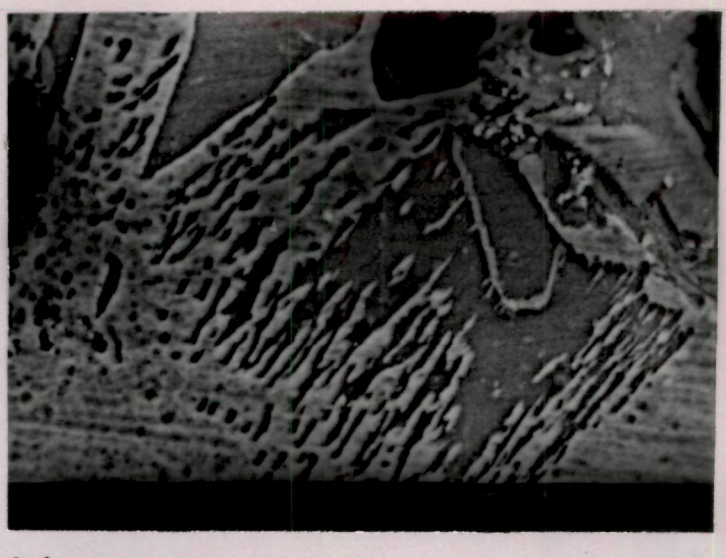

(c) PASC30 - 0·3C - 2MVM

Fig. 3·151

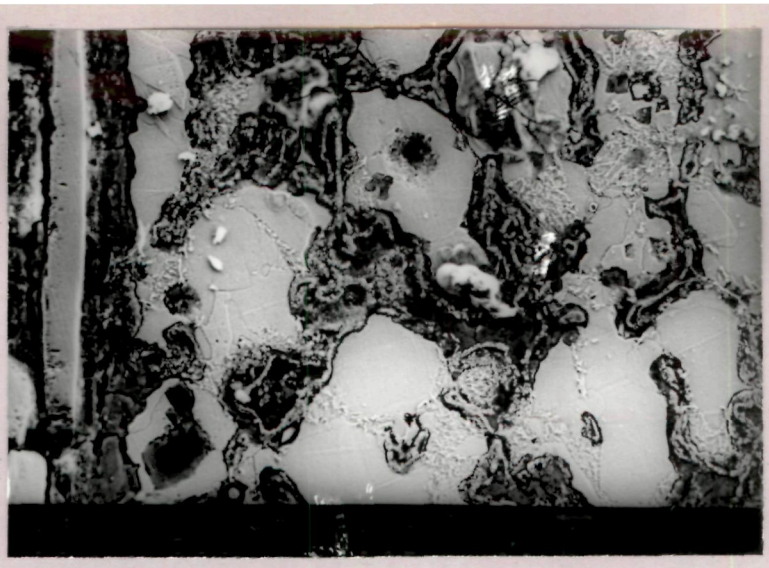

(a)

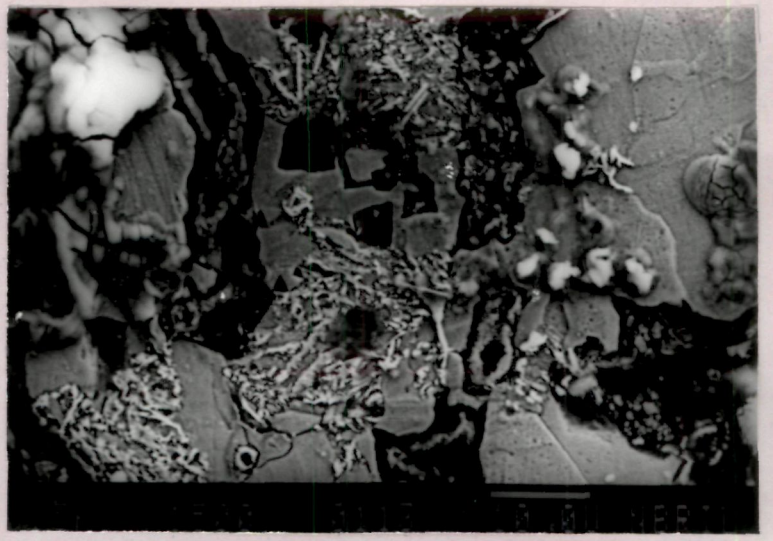

(b)

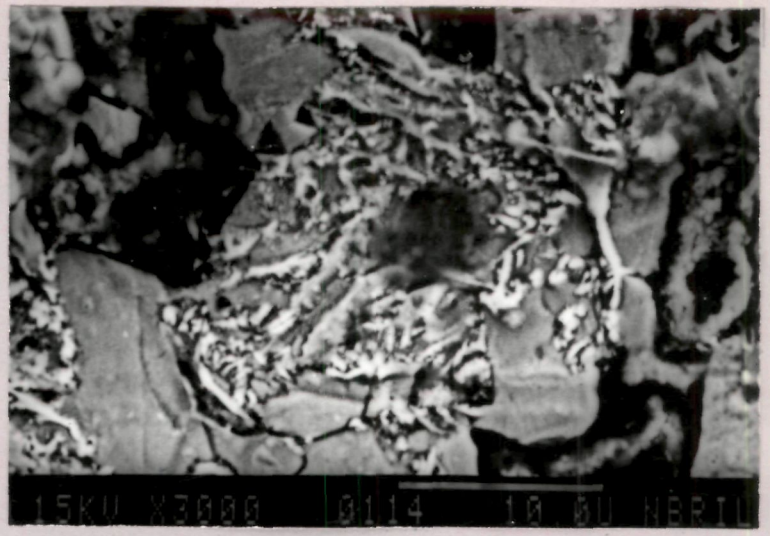

(c)

PASC80 - 0·3C - 2MVM

Fig. 3·152

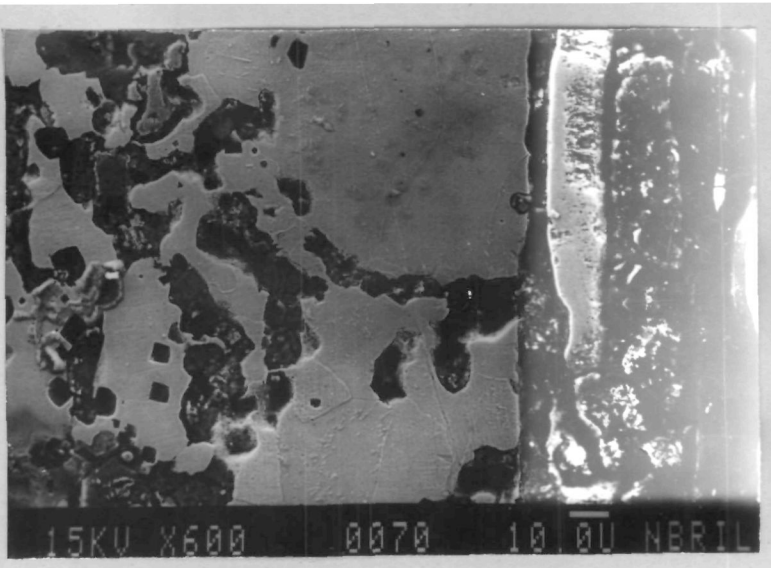

(a)

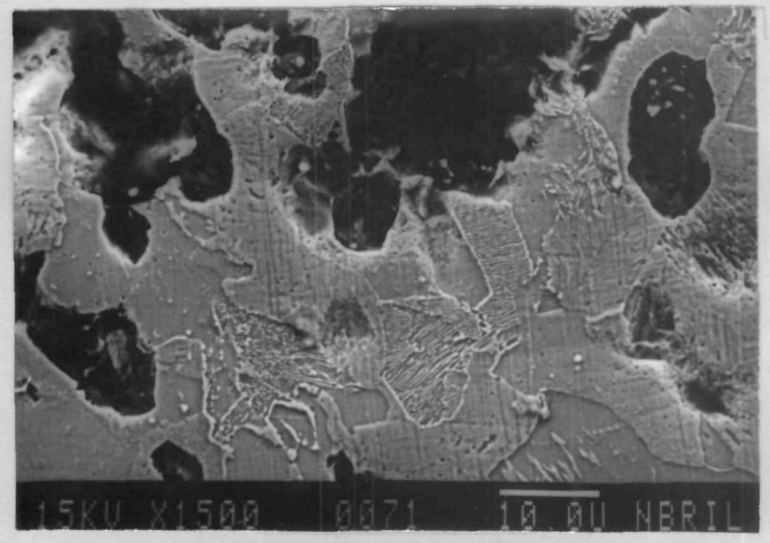

(b)

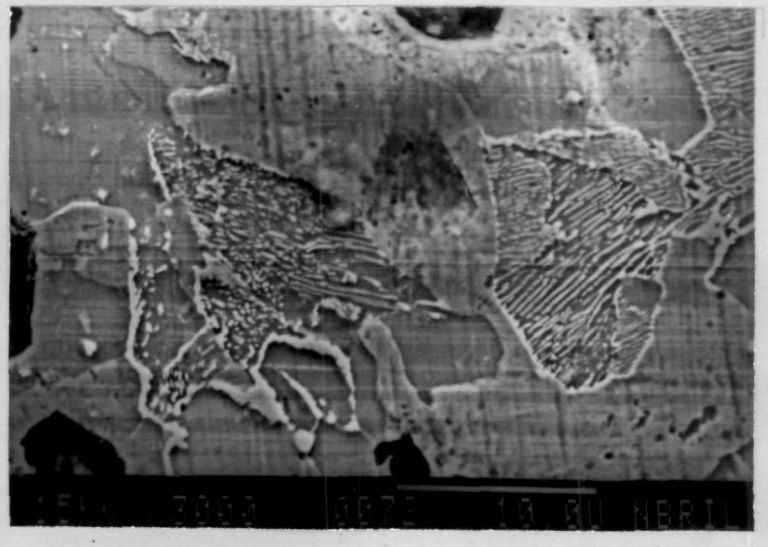

(c)

PA SC30 - 0·6C - 2MVM

Fig. 3·153

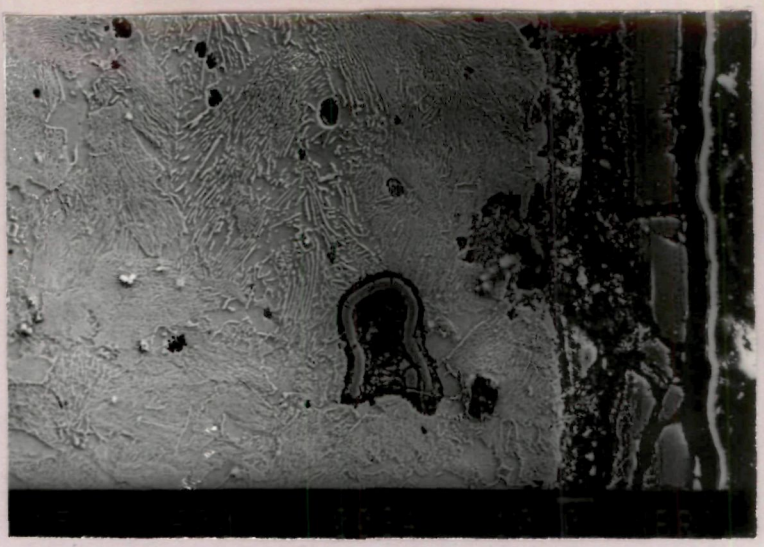

(a)

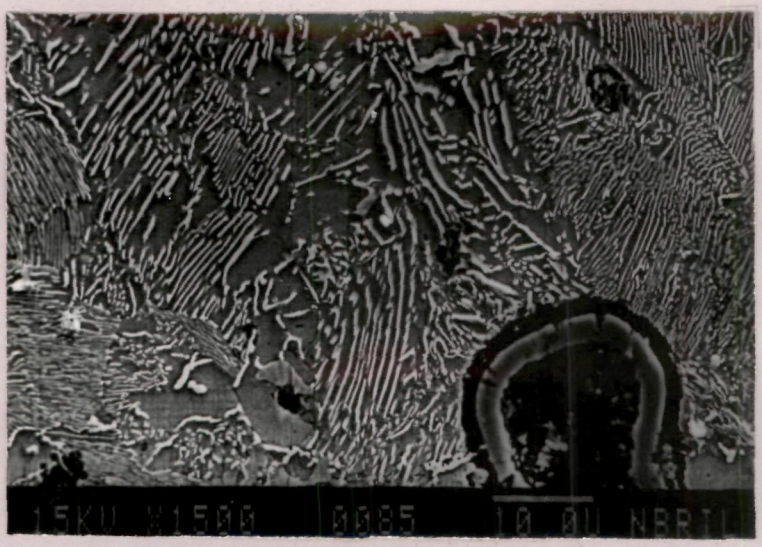

(b)

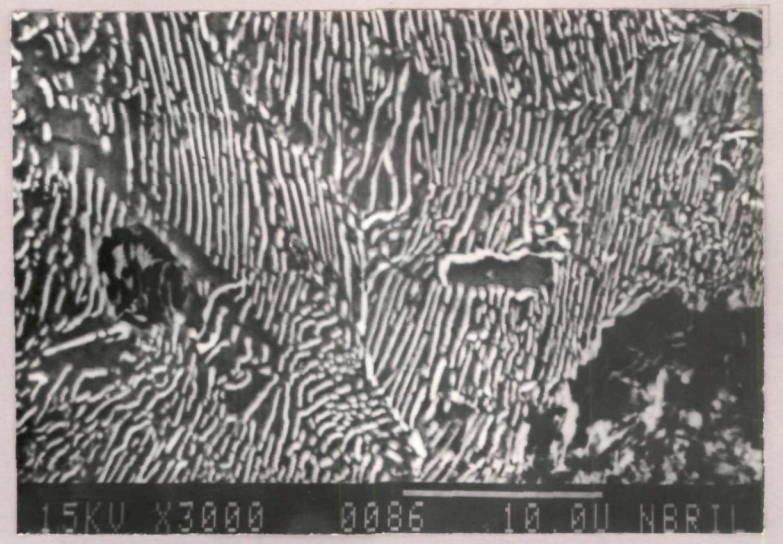

(c)

PASC80 - 0·6C - 2MVM

Fig. 3·154

3.4 MICROHARDNESS VALUES

Microhardness values (Table III.3.3) shows that in case of PASC30 sintered compact steam treated at 527°C for 60 minutes there is hardly any effect of increase of C contents on low load hardness values of oxide layers. However, when Cu-content was increased from 1 to 2 % there is a marginal increase in hardness. Increase of P-content does not give any conclusive effect on microhardness values.

Microhardness values of Ni-containing compacts are slightly higher than that of Cu-containing compacts. However, increase of Ni-content from 1 to 2 % generally decreases microhardness value. Increase of C content from 0.3 to 0.6 % increases microhardness value.

In case of Mo-containing compacts, increasing Mo-content invariably increases microhardness value of scale after steam treatment at 527°C for 60 minutes. Increase of C content from 0.3 to 0.6 % keeping Mo-content constant does not generally affect microhardness values of PASC30-Mo-C compact on steam treatment but increases hardness of PASC80 based oxidized compact significantly. Increase in P-content from 0.3 to 0.8 % keeping other elements constant generally gives significant increase in hardness in case of Mo-containing compacts on subsequent steam oxidation. Micro-

Table III.3.3 Microhardness values of the sintered samples steam treated at 527°C for 60 minutes.

Alloy	Hardness HV0.1	Alloy	Hardness HV0.1
PASC30	411 ± 44	PASC80	268 ± 85
PASC30-0.3C-1Cu	436 ± 22	PASC80-0.3C-1Cu	362 ± 16
PASC30-0.3C-2Cu	488 ± 0	PASC80-0.3C-2Cu	395 ± 28
PASC30-0.6C-1Cu	411 ± 18	PASC80-0.6C-1Cu	423 ± 40
PASC30-0.6C-2Cu	489 ± 12	PASC80-0.6C-2Cu	412 ± 16
PASC30-0.3C-1Ni	474 ± 61	PASC80-0.3C-1Ni	291 ± 88
PASC30-0.3C-2Ni	458 ± 11	PASC80-0.3C-2Ni	385 ± 39
PASC30-0.6C-1Ni	520 ± 42	PASC80-0.6C-1Ni	438 ± 65
PASC30-0.6C-2Ni	495 ± 25	PASC80-0.6C-2Ni	419 ± 56
PASC30-0.3C-1Mo	442 ± 22	PASC80-0.3C-1Mo	431 ± 64
PASC30-0.3C-2Mo	476 ± 54	PASC80-0.3C-2Mo	471 ± 36
PASC30-0.6C-1Mo	449 ± 11	PASC80-0.6C-1Mo	595 ± 42
PASC30-0.6C-2Mo	474 ± 12	PASC80-0.6C-2Mo	558 ±100

Continued ....

Table III.3.3 continued

Alloy	Hardness HV0.1	Alloy	Hardness HV0.1
PASC30-0.3C-1MCM	467 ± 61	PASC80-0.3C-1MCM	331 ± 46
PASC30-0.3C-2MCM	451 ± 41	PASC80-0.3C-2MCM	440 ± 51
PASC30-0.6C-1MCM	386 ± 17	PASC80-0.6C-1MCM	589 ± 64
PASC30-0.6C-2MCM	449 ± 47	PASC80-0.6C-2MCM	606 ± 67
PASC30-0.3C-1MVM	367 ± 45	PASC80-0.3C-1MVM	443 ± 31
PASC30-0.3C-2MVM	336 ± 46	PASC80-0.3C-2MVM	457 ± 28
PASC30-0.6C-1MVM	542 ± 64	PASC80-0.6C-1MVM	483 ± 36
PASC30-0.6C-2MVM	370 ± 58	PASC80-0.6C-2MVM	618 ± 69

hardness values of Mo-containing compacts are generally higher than that of Ni-containing compacts on steam treatment.

Microhardness values of MCM-containing compacts are equivalent or higher than that of Mo-containing compacts particularly at higher carbon content of 0.6 % and P-content of 0.8 %. Microhardness value also increases generally with increasing MCM-content at particular level of C and P. Effect of increase of C-content from 0.3 to 0.6 % maintaining the composition of other alloying elements constant, increases microhardness value of PASC80 based sintered and steam treated compact but hardly affects such values in case of PASC30 based compacts.

After steam treatment, microhardness values of MVM-containing compacts are generally similar to that of MCM-containing compacts. However, magnitude of microhardness value at equivalent composition of alloying element is generally lower in case of MVM containing compact.

In general increase in oxidation period from 45 to 60 minutes, increased microhardness values slightly similar to that observed in case of PNC based sintered compacts.

steels showing oxidized layer and matrix region, treated at 450°C for 45 minutes. Magnification 320X, Nital etched.

Fig. 3.93 Microstructures of sintered and steam treated steels showing oxidized layer and matrix region, treated at 527°C for 45 minutes. Magnification 320X, Nital etched.

Fig. 3.94 Microstructures of sintered and steam treated steels showing oxidized layer and matrix region, treated at 527°C for 120 minutes. Magnification 320X, Nital etched.

Fig. 3.95 Microstructures of sintered and steam treated steels showing oxidized layer and matrix region, treated at 527°C for 45 minutes. Magnification 320X, Nital etched.

Fig. 3.96 Microstructures of sintered and steam treated steels showing oxidized layer and matrix region, treated at 600°C for 45 minutes. Magnification 320X, Nital etched.

Fig. 3.97 Scanning electron microstructures of steam treated alloy, treated at 527°C for 120 minutes.

Fig. 3.98 Scanning electron microstructures of steam treated alloy, treated at 527°C for 120 minutes.

Fig. 3.112 Scanning electron microstructures of steam treated alloy, treated at 527°C for 120 minutes.

Fig. 3.113 Scanning electron microstructures of steam treated alloy, treated at 527°C for 120 minutes.

Fig. 3.114 Microstructures of sintered and steam treated steels showing oxidized layer and matrix region, treated at 450°C for 45 minutes. Magnification 320X, Nital etched.

Fig. 3.115 Microstructures of sintered and steam treated steels showing oxidized layer and matrix region, treated at 450°C for 45 minutes. Magnification 320X, Nital etched.

Fig. 3.116 Microstructures of sintered and steam treated steels showing oxidized layer and matrix region, treated at 450°C for 120 minutes. Magnification 320X, Nital etched.

Fig. 3.117 Microstructures of sintered and steam treated steels showing oxidized layer and matrix region, treated at 527°C for 45 minutes. Magnification 320X, Nital etched.

Fig. 3.118 Microstructures of sintered and steam treated steels showing oxidized layer and matrix region,

Fig. 3.125 Scanning electron microstructures of steam treated alloy, treated at 527°C for 120 minutes.

Fig. 3.126 Scanning electron microstructures of steam treated alloy, treated at 527°C for 120 minutes.

Fig. 3.127 Microstructures of sintered and steam treated steels showing oxidized layer and matrix region, treated at 450°C for 45 minutes. Magnification 320X, Nital etched.

Fig. 3.128 Microstructures of sintered and steam treated steels showing oxidized layer and matrix region, treated at 450°C for 120 minutes. Magnification 320X, Nital etched.

Fig. 3.129 Microstructures of sintered and steam treated steels showing oxidized layer and matrix region, treated at 450°C for 45 minutes. Magnification 320X, Nital etched.

Fig. 3.130 Microstructures of sintered and steam treated steels showing oxidized layer and matrix region, treated at 450°C for 120 minutes. Magnification 320X, Nital etched.

Fig. 3.131 Microstructures of sintered and steam treated steels showing oxidized layer and matrix region,

treated at 527°C for 45 minutes. Magnification 320X, Nital etched.

Fig. 3.132 Microstructures of sintered and steam treated steels showing oxidized layer and matrix region, treated at 527°C for 45 minutes. Magnification 320X, Nital etched.

Fig. 3.133 Microstructure of sintered and steam treated steel showing oxidized layer and matrix region, treated at 527°C for 120 minutes. Magnification 320X, Nital etched.

Fig. 3.134 Microstructure of sintered and steam treated steel showing oxidized layer and matrix region, treated at 600°C for 120 minutes. Magnification 320X, Nital etched.

Fig. 3.135 Microstructure of sintered and steam treated steel showing oxidized layer and matrix region, treated at 600°C for 120 minutes. Magnification 320X, Nital etched.

Fig. 3.136 Microstructure of sintered and steam treated steel showing oxidized layer and matrix region, treated at 600°C for 45 minutes. Magnification 320X, Nital etched.

Fig. 3.137 Microstructures of sintered and steam treated steels showing oxidized layer and matrix region, treated at 600°C for 45 minutes. Magnification 320X, Nital etched.

Fig. 3.138 Scanning electron microstructures of steam treated alloy, treated at 527°C for 120 minutes.

Fig. 3.139 Scanning electron microstructures of steam treated alloy, treated at 527°C for 120 minutes.

Fig. 3.140 Scanning electron microstructures of steam treated alloy, treated at 527°C for 120 minutes.

Fig. 3.141 Scanning electron microstructures of steam treated alloy, treated at 527°C for 120 minutes.

Fig. 3.142 Microstructures of sintered and steam treated steels showing oxidized layer and matrix region, treated at 450°C for 45 minutes. Magnification 320X, Nital etched.

Fig. 3.143 Microstructure of sintered and steam treated steel showing oxidized layer and matrix region, treated at 450°C for 120 minutes, Magnification 320X, Nital etched.

Fig. 3.144 Microstructures of sintered and steam treated steels showing oxidized layer and matrix region,

treated at 450°C for 45 minutes. Magnification 320X, Nital etched.

Fig. 3.145 Microstructures of sintered and steam treated steels showing oxidized layer and matrix regions, treated at 527°C for 45 minutes.

Fig. 3.146 Microstructure of sintered and steam treated steel showing oxidized layer and matrix region, treated at 527°C for 45 minutes. Magnification 320X, Nital etched.

Fig. 3.147 Microstructure of sintered and steam treated steel showing oxidized layer and matrix region, treated at 527°C for 120 minutes. Magnification 320X, Nital etched.

Fig. 3.148 Microstructures of sintered and steam treated steels showing oxidized layer and matrix region, treated at 600°C for 45 minutes. Magnification 320X, Nital etched.

Fig. 3.149 Microstructure of sintered and steam treated steel showing oxidized layer and matrix region, treated at 600°C for 120 minutes. Magnification 320X, Nital etched.

Fig. 3.150 Microstructures of sintered and steam treated

steel showing oxidized layer and matrix region, treated at 600°C for 45 minutes. Magnification 320X, Nital etched.

Fig. 3.151 Scanning electron microstructures of steam treated alloy, treated at 527°C for 120 minutes.

Fig. 3.152 Scanning electron microstructures of steam treated alloy, treated at 527°C for 120 minutes.

Fig. 3.153 Scanning electron microstructures of steam treated alloy, treated at 527°C for 120 minutes.

Fig. 3.154 Scanning electron microstructures of steam treated alloy, treated at 527°C for 120 minutes.

CHAPTER 4

DISCUSSION

This chapter aims at explaining various experimental results. Part I will discuss the results of steam treatment studies on PNC powder compacts. Part II is discussion of results on sintered and mechanical properties of PASC based powder compacts. Part III aims at explaining the various results on steam oxidation of sintered PASC powder compacts containing Cu, Ni, Mo, MCM or MVM with 0.3 or 0.6 % combined C and 0.3 or 0.8 % P.

Part I

4.1 STEAM TREATMENT OF PNC BASED SINTERED COMPACTS

4.1.1 Theoretical and kinetic aspects

According to Wagner's theory (55), if a metal (Fe) is exposed to gas (H_2O) at a proper temperature, gas and metal decompose to ions and electrons as follows :

$$Fe \longrightarrow Fe^{2+} + 2\bar{e}$$

$$H_2O \rightleftharpoons H_2 + 1/2\ O_2 \qquad (1)$$

$$O_2 + 4\bar{e} \longrightarrow 2\ O_2^{-}$$

One molecule of oxygen chemisorbed on the surface of the metal could cause the migration of two Fe^{2+} ions and two electron with formation of two Fe^{2+} vacancies ($^{\square}Fe^{2+}$) and two electron vacancies ($\oplus$) as follows :

$$O_2 = 2Fe^{2+} + 2 \oplus \bar{e} + 2FeO \qquad (2)$$

Iron ions are cations and oxygen ions are anions so they migrate to each other and oxide forms. Thus when iron ions diffuse towards the metal/oxide interface, vacancies diffuse in the opposite direction and they possibly condense at the grain boundaries and pore surfaces. Therefore the vacancy concentration of the matrix decreases.

The principal objective of treatment is to produce a layer of Fe_3O_4 on all surfaces exposed to steam. In industrial practice treatment temperatures of 425 to 600°C (3,5,6) have been used. The basic overall reaction is

$$3Fe + 4H_2O \longrightarrow Fe_3O_4 + 4H_2 \qquad (3)$$

It has been shown that (6) Fe_3O_4 is the only oxide formed at P_{H_2O}/P_{H_2} ratio of 0.1 to 1.0 at reaction temperature of 400-600°C. At lower temperatures (25°C) the only product formed when iron reacts with water vapour free from oxygen is $Fe(OH)_2$. However, if air is present some Fe_3O_4 also forms

(56). At temperature above 60°C Fe_3O_4 forms. FeO does not form at temperatures less than 570°C but within the range 570-700°C both FeO and Fe_3O_4 form and the proportion of FeO produced increases with temperature. The phase diagram for Fe/O_2 system shows that at 570°C, FeO decomposes eutectoidally to α-Fe and Fe_3O_4.

The initial rate of steam oxidation as measured by weight gain is very rapid and more than about 60 % weight gain occurs within 20 minutes. However, this time does not agree with the reported works (2,6) who observed that more than 50 % weight gain occurred within 10 minutes. The reason seems to be the effect of alloying elements giving different density of sintered compacts, phase stabilization, morphology of the pores and affinity of the elements for oxygen etc. (Figs. 3.1-3.5).

Hörnbogen and Glenn (57) reported that in Fe-1.2Cu, clusters of copper grow at a rate that can be explained by the concentration of excess vacancies in the material, which are preferred sites for the nucleation of copper particles within the lattice.

Thus if steam treatment is used as an ageing treatment, most of the preferred sites (vacancies) which would normally be used for nucleation of ε-copper are not available through-

out the matrix as a uniform distribution. Instead, most of the precipitate particles nucleate in those regions (e.g. pore surfaces, grain boundaries) where the vacancy concentration is high. It can be argued that increase of copper content increases resistance to oxidation (58), owing to the smaller number of vacancies for diffusion. As a result fewer nucleation sites for homogenous nucleation of copper particles exist.

Franklin and Davies (1) examined the influence of treatment at 520 and 650°C and demonstrated that at 650°C very rapid oxidation occurred but, because of surface sealing, a lower total oxide content is achieved after long treatment times that is normal at the lower temperature. Our results in general, also show such a behaviour (Figs. 3.1-3.5) as the rate of oxidation decreases with increasing steam treatment times. Oxide layer formed are impervious as is evident through parabolic nature of curve.

4.1.2 Effect of phosphorus

It has been reported that phosphorus due to liquid phase sintering and ferrite stabilization (46) spheroidizes the pores and reduces the amount of interconnected porosity and channels. Thus, there is a corresponding decrease in the amount of open porosity after steam treatment under any

standard set of time/temperature conditions. In specimens having higher sintered density it is reasonable to agree that the channels connecting individual pores will be narrower and that these will become blocked by oxide more rapidly during steam treatment. The apparent residual open porosity in specimens prepared from higher P-containing premixes was lower and this appears to be the reason for lower weight gain with treatment times in such compacts (Fig. 3.1). A maximum in the weight gain occurs at a treatment time of between 45-60 minutes. Oxidation by steam is a diffusion controlled process and the pore closure will occur at a slower rate at longer treatment times because the extent of oxidation, as measured by weight gain, is considerably restricted because of the sealing of surface pores at an early stage during treatment. This is evident from microstructures also which show well-defined oxide layers in specimens containing higher phosphorus contents (Fig. 3.14).

The sintered hardness increases with increasing phosphorus content and this trend is noticed in case of oxidized samples also due to efficient healing and closure of pores (Fig. 3.6). However, the level of increase in steam treated hardness cannot be explained due to oxides

Fe_3O_4 or Fe_2O_3 (minor constituent) alone. X-ray analysis did not show any phosphorus having been oxidized. The major constituent in oxide was found to be hematite Fe_3O_4 which is also evident from parabolic nature of weight gain vs. treatment times curve. Workers in this field (28, 31 etc.) have observed hardness increase of upto 50 % after steam treatment over that of as sintered compacts. Clearly, the increase in hardness seems to be due to some other effect also.

Hörnbogen (45) showed that phosphorus could produce appreciable age-hardening in Fe-P alloys after carrying out experiments on mild steel (0.15C, 1.5Mn). He observed age-hardening to occur in the range 400-550°C, but the maximum effect was observed ~450°C. The intensity of age-hardening increased with increasing P-content. At phosphorus content above 0.5 %, increasing amounts of α-ferrite were observed at the solution treatment temperature with increasing phosphorus contents and at 2 % P, the steel was virtually ferritic. The precipitating phase was Fe_3P but the details of age-hardening process have not been investigated. More recent studies on sintered Fe-P alloys (59) have shown by taking extraction replicas obtained on an electron microscope that upto 0.8 % P content, phosphorus dissolved in the α-Fe and was not segregated in the pure

form or in the form of compounds at the grain boundaries when the specimens were heated and cooled during sintering under laboratory-scale conditions. However, cooling rates have not been mentioned by the author (59) but it is expected that furnace cooling under laboratory conditions should not give higher than 10K/min cooling rate. From the phase diagram of Fe-P system (60) solubility of P in iron was found to be 1.26, 0.83, 0.25 and 0.015 wt. % at 800, 700, 500°C and room temperature, respectively. The results of Amin et al. (61) and Lindskog et al. (46) showed that upto 0.6 wt. % P was completely dissolved and alloyed with iron and was retained in solid solution at room temperature even after as slow cooling as 7K/min. Thus, the increase in hardness in P-containing samples seems to be due to combined action of steam treatment and ageing. This is further confirmed from large increase in hardness when P content was increased from 0.45 to 0.6 wt. % and also due to slight decrease in hardness after reaching maximum at 30 minutes.

4.1.3 Effect of copper

The gain in weight of Fe-Cu sintered alloys with increasing treatment times is, in general, qualitative agreement with the recent results of Phadke, Davies and

his coworkers (25-29) (Fig. 3.2). It has been reported that (21) small addition of copper had little effect on the oxidation of solid iron at 500°C in oxygen-argon atmosphere. Addition of 0.3 % P to Fe-Cu alloy does not change the variation of weight gain with increasing treatment times (Fig. 3.2b) except that the magnitude of weight gain slightly increases. When the P content was increased to 0.45 or 0.6 %, the curves of weight gain vs. treatment time level off at 30 to 60 min. (Figs. 3.2c and 3.2d). Such a behaviour seems to be due to pore-rounding effect of phosphorus which inhibit the diffusion path for oxygen as already described. For diffusion of steam, pores and channels should be interconnected. Such a result is confirmed through microstructures (Fig. 3.15) and scanning electron microstructures (Figs. 3.16-3.19). In fact, longer treatment time appears to have decreased the oxide thickness. However, rounding off of the pores are evident in Fig. 3.19. Some oxygen appears to have diffused inward into the matrix. This may be the reason for lower thickness of oxide with increasing treatment times. For phosphorus free specimens, oxide thickness increases with increasing treatment times and higher copper content (Figs. 3.15 a - 3.15 d).

The variation of hardness with treatment times for

Fe-Cu and Fe-P-Cu specimens is also similar to the earlier results for Fe-Cu alloys (29) (Figs. 3.7 and 3.8). Maximum in hardness is obtained after 30 min. of treatment while Razavizadah and Davies (29) found maximum in hardness after treatment times varying between 25-60 min. However, hardness observed in the present investigation is slightly lower, i.e. 160-190 HV10 while earlier workers (26-29) have reported hardness values of 170-240 HV. Sintered specimens in case of Fe-P-Cu alloy are furnace cooled at an average cooling rate of 13 K/min. It has been reported (26-29) that precipitation hardening was obtained in sintered samples cooled from sintering temperature at a rate of 25°C/min. or higher. The effect due to precipitation hardening appears to be marginal. Scanning pictures also do not show any obvious precipitates (Figs. 3.16-3.19). Microhardness values are shown in Table III.1.2. This is slightly lower than previously reported values of 545 HV (5) for Fe_3O_4 in iron and 460 HV (28) for Fe-2 % Cu alloy. This may be due to either slow cooling of samples from sintering temperature or other constituent in the oxides.

4.1.4 Effect of molybdenum

As is well known if more than 1.2 wt. % Mo is added to iron, the $\alpha(\delta)$ ferrite phase becomes stable at a tempera-

ture of 1050-1200°C (62). Phosphorus, like molybdenum, is also a ferrite stabilizer and iron-phosphorus alloy containing more than 0.65 % P would be fully ferritic at a temperature of 1050-1200°C (46). Thus, because of the additive effect of Mo and P, porosity decreases and becomes rounded.

The variation of weight gain with treatment times is generally similar to that of Cu-containing specimens (Fig. 3.3) reaching a maximum in weight gain at 60 minute of treatment times. The oxidation resistance increases with increasing Mo or P addition (Fig. 3.3). However, the level of weight gain obtained in Fe-P-Mo specimens is less as compared to Cu- or MCM-containing samples (Figs. 3.2, 3.3 and 3.4) due to isolated, smaller and rounded pores and higher sintered density.

The increase in hardness with treatment times reaches a maximum at 60 minute of treatment time. The increase in hardness of as oxidized samples over that of as sintered samples is 120 HV which is difficult to explain by low oxidation rate of such samples because Mo has lower oxygen affinity than iron and the density of the specimens is high. It has been reported (44) that Mo is capable of causing appreciable age-hardening in ferrite.

Little use seems to have been made of molybdenum age-hardening in low alloy steels, apart from a development (63) aimed primarily at high temperature materials. Thus, hardness increase in Fe-P-Mo alloy seems to be due to the combined action of oxidation and precipitation hardening due to the presence of P and Mo. It seems that sufficient amount of P and Mo are retained in solid solution during cooling at 13 K/min. from the sintering temperature of 1120°C.

4.1.5 Effect of transition metal carbide master alloy

MCM addition in iron or iron-phosphorus premixes gives rise to growth as shown in Table III.1.1. Majority of the pores appear to be interconnected as shown in Figs. 3.23 and 3.24. This seems to be the reason for relatively large weight gain with increasing steam oxidation times. The MCM powder added to iron or P-containing iron is upto 4 wt. %. This corresponds to actual alloy contents of upto 0.92 wt. % each of Mn, Cr, and Mo and 0.28 wt. % C. The oxygen affinity for Mn and Cr is higher than that of iron. It is quite probable that these elements also oxidize along with iron. The oxide of Cr is very hard which adds to the bulk hardness of steam treated MCM-containing alloys. However, in general, there is one

difference between hardness variation with treatment times of MCM-containing and Cu-containing compacts, i.e. in this case hardness does not reach maximum (Figs. 3.10 and 3.11). This appears to be due to the fact that surface pores are not healed upto this magnitude of treatment times.

4.1.6 Effect of ternary powder compacts

Of the three alloying constituents, i.e. Mo, Ni and MCM, Mo imparts densification, Ni also imparts densification but at the same time heterogeneity while MCM growth of Fe or Fe-P compacts (64). Copper decreases shrinkage of all such compacts as shown in Table III.1.1.

The effect of increasing copper content on weight gain with treatment times of Mo and MCM-containing compacts is in general to increase oxidation rate (Fig. 3.5) while that of Ni does not give any conclusive results. However, the variation of hardness with increasing copper content of ternary powder compacts with treatment times is in qualitative agreement with such effects on Fe, Fe-P compacts. Such a behaviour is supported by microstructures of oxide plus matrix region which show thicker oxide layer in higher Cu-containing compacts.

Part II

4.2 SINTERED PROPERTIES OF PASC BASED COMPACTS

4.2.1 Copper-containing compacts

Copper addition in P-containing sintered steels gives rise to growth in agreement with earlier reported works (51,65). When carbon content was increased from 0.3 to 0.6 % it changes the role of copper and then compensates growth effect of copper. Berner et al. (66) and others (67-69) reported that C decreases the solubility of Cu in iron and increases the dihedral angle. These effects decrease growth effect. Increase in phosphorus content improves densification in agreement with earlier results (51,65). This result is suported by microstructures which show rounded and smaller number of pores in case of sintered compacts containing 0.8 % phosphorus (Figs. 3.35 a to c). One important point to note is that linear shrinkage shows different behaviour than those exhibited by sintered density or densification parameter variation (Figs. 3.30 a and 3.31 b) due to anisotropic dimensional change in different directions. This fact is confirmed by the fact that volume shrinkage variation is similar to that of densification behaviour (Fig. 3.34a). However, growth in the premixes studied is marginal and dimensionally stable

products can be produced particularly from low P-containing promixes.

At 0.3 % P, both C and Cu increase strength properties due to solid solution hardening effect and formation of pearlitic structure (Fig. 3.35 a) in agreement with earlier results (51,65). Increase in phosphorus content from 0.3 to 0.8 % deteriorates strength properties due to brittle phosphoride formation as is evident through microstructure (Fig. 3.35 b). Presence of brittle iron phosphide is quite probable since maximum solubility of phosphorus in alpha phase is 0.6 % at 1393 K (46) which decreases with decrease or increase in temperature. Thus, even if all the phosphorus present in solid solution at 1393 K is retained after cooling from the sintering temperature, some phosphorus is available for the formation of iron phosphide. Sufficient ductility of 3 to 9 % elongation is confirmed through scanning electron fractographs of PASC30-0.3C-2Cu and PASC30-0.6C-2Cu compacts which show typical dimple like fracture (Fig. 3.36 a and b). Fracture appears to be typically transcrystalline. Pores also deform in cohesion with matrix. Although, graphite additions were 0.5 and 1 %, about 0.2 $\pm$ 0.04 % C was lost during sintering at 1393 K in dissociated ammonia atmosphere of dew point 240 K since no gettering technique was applied.

4.2.2 Nickel-containing compacts

Upto 1 % Ni addition at lower C content of 0.3 % decreases densification in agreement with earlier reported works (49,52) due to the fact that 0.3 % C is not sufficient enough to change the role of Ni. After this composition, both C and Ni improve densification since diffusivity of C in iron is high, although improvement in densification is marginal (Figs. 3.30 b and 3.31 b). Variation of linear dimensional change with composition is slightly different from sintered density or densification parameter variation and this observation can be explained on the basis of anisotropy in dimensional change (Fig. 3.34), similar to that of Cu-containing compacts. However, anisotropy in case of Ni-containing compacts is less than that observed in Cu-containing compacts.

Strength properties improve with C and / or Ni additions while ductility decreases (Figs. 3.32 b and 3.33 b) in agreement with earlier results for C-free Ni-containing Fe-P compacts (2) or PNC-Ni-C compacts (52). Sufficient ductility of 2-9 % elongation is observed which is confirmed through scanning electron fractographs (Figs. 3.37 a and b) which show predominantly ductile fracture at low C and Ni contents. Evidence of some unalloyed particles are observed

in case of PASC30-0.6C-2Ni compacts at high magnification (Fig. 3.37 b).

4.2.3. Molybdenum-containing compacts

At 0.3 % C content, increasing molybdenum content improves densification in agreement with earlier results for C- free Fe-Mo compacts (46) and PNC-Mo-C compacts (53). The reason why at 0.6 % C level, the role of Mo in affecting densification changes is that C is austenite stabilizer while both Mo and P are ferrite stabilizers (46, 62). At higher C content, the amount of austenite probably more than compensates the shrinkage effect produced due to α-phase sintering (Fig. 3.30 c and 3.31 c). Slightly higher densification at higher P-content may be attributed to higher sintering rate due to α-phase stabilization by both P and Mo (46). However the effect of P- and Mo in improving densification of sintered iron compacts in conjunction with carbon does not appear to be additive (Figs. 3.30 c and 3.31 c) and is thus in disagreement with earlier results (46) for C- free alloys. Result showed increased growth for higher P- containing compacts (Fig. 3.31 c) which fact is clarified by volume shrinkage and shrinkage ratio versus composition curves (Fig. 3.34 c).

The effect of Mo on strength properties of PASC

powder compacts is similar to such effects for PNC powder compacts (46,53). Slightly higher ductility of PASC-C-Mo compacts as compared to PASC-C-Ni (Figs. 3.32 b-d and 3.33 b-d) could be explained by slightly better densification of the former. This fact is confirmed through scanning electron fractographs. (Figs. 3.38 a and b) which show typical dimple like fracture which is more pronounced in case of PASC80-0.3C-2Mo test piece. Deformation of pores as well as matrix in cohesion is quite evident here (Fig. 3.38 a and b).

4.2.4 MCM-containing compacts

The decrease in densification produced by MCM addition to PASC-C sintered compacts is in agreement with earlier results of Fe-P (48) and the recent result of PNC-C (54) (Figs. 3.30 d, 3.31 d, and 3.34 d). The strength properties improve upto 2 % MCM at 0.3 % C while upto 1 % MCM at 0.6 % C which is in qualitative agreement with results of a number of workers (70-71) for P-free alloys and P-containing but C- free alloy (48). Fractographs show mixed type of ductile and brittle fracture and often decohesion and tearing of particles(Fig. 3.39 a and b). Pores also seem to have deformed but less than those observed in case of Mo-containing test pieces.

4.2.5 MVM-containing compacts

The behaviour of MVM-containing compacts are similar to that of MCM-containing compacts in respect of densification behaviour and tensile properties variation (Figs. 3.30 e, 3.31 e, 3.32 e and 3.33 e). The proportion of brittle fracture in case of MVM-containing compacts is higher (Figs. 3.40 a and b) particularly at higher MVM and C contents of 2 and 0.6 % , respectively. Micropores are evident in case of PASC30-0.6C-2MVM compacts (Fig. 3.40 a) which are partly minimised or removed with increase in P-content from 0.3 to 0.8 % (Fig. 3.40 b).

One important point to note in all the system studied is that the difference in magnitude of UTS and YS is very small (Figs. 3.32 and 3.33) except in case of Cu-containing compacts at lower C content of 0.3 % (Fig. 3.32 a). This is attributed to the fact that higher hardening and strengthening produced is always associated with the deleterious property of brittleness due to inhomogenous structure, non-uniform distribution of pores with widely different size, shape and morphology.

Part III

4.3 STEAM TREATMENT OF PASC BASED SINTERED COMPACTS

The main difference between steam treatment of PNC based and PASC based powder compact is that in the present case a range of steam oxidation temperature from 450 to 600°C was used and time of oxidation used was begun from 45 minutes instead of 5 minutes since optimum in weight gain was noted only after this period in case of steam treatment of PNC based powder compacts. In case of PNC and PASC based powder compacts, study of the effect of Cu, MCM are common. However, PNC powders contained from 0.3 to 0.6 % P while PASC powder contained from 0.3 to 0.8 % P. All PASC based powder compacts contained 0.3 and 0.6 % combined C while 1 or 2 % of alloying element was used since above this amount of alloying elements, there was hardly any benefit on properties of sintered or steam oxidized compacts made from PNC powders. PNC powder is based on normal compressibility sponge iron powder while PASC powders are purer and based on higher compressibility atomized powders. Thus, the results of steam oxidation shall be discussed in respect of following :

(a) Difference in sintered properties resulting from difference in powder type giving characteristic

microstructure of the matrix and the pore.

(b) Difference in composition, namely presence of C, higher amount of P and other alloying elements and interaction effects due to these on kinetics, hardness values and microstructural features.

4.3.1 Effect of powder type

Weight gain achieved during steam treatment of sintered PNC powder compacts containing copper is between 30 to 40 gm^{-2} (Fig. 3.2), Mo is between 20-30 gm^{-2} (Fig. 3.3) and MCM is of the order of 50 gm^{-2} (Fig. 3.4) at 500°C. If this gain in mass is compared with those of PASC based powder compacts at same temperature much lower weight gain (of the order of 25-37 in case of Cu containing, 17-25 in case of Mo containing and 30-37 gm^{-2} in case of MCM-containing compacts) are observed (Figs. 3.42, 3.52 and 3.57). The reason seems to be slightly higher sintered density obtained due to higher compaction pressure used and also due to higher compressibility of atomized P-containing iron powders. Further, it has been reported (29) that the particles of sponge iron powder are irregular and have rough surfaces while atomized iron powder particles are smoother in outline and approximate more closely to a

spheroidal shape. It has been confirmed by SEM (24) that these differences persisted in sintered specimens. In sponge iron powder, individual pores appear to be smaller (Figs. 3.16-3.19) and channels between pores seem to be narrower in contrast to those observed in case of PASC powders (Figs. 3.97-3.100). Further, the internal surface area is significantly greater. The specimen prepared from sponge powder had gained 1.1 % in weight as a result of treatment for 25 minutes and the residual porosity was 8.2 % whereas the specimen produced from atomized powder was treated for 50 minutes to produce an equivalent weight gain. There was evidence of incomplete pore filling in atomized iron powder compact whereas there was no such evidence in sponge iron powder compact. Internal oxidation was extensive in atomized iron powder compacts but pore closure was incomplete. It was concluded (29) that during steam treatment under any particular set of conditions the pore net work in specimens prepared from sponge powder apparently became blocked more rapidly by oxidation products. Residual open porosity in specimens prepared from sponge powder appear to be less than that it was in specimens prepared from atomized powder even though in the latter case more extensive oxidation had taken place. This explains the lower weight gain in PASC based sintered powder compacts

as compared to PNC based sintered powder compacts (Figs. 3.1-3.4 and 3.41-3.65). However the level of increase in weight gain in the present investigation is much lower than observed in earlier investigations (29, 35). This is because much lower sintered density was used in earlier studies (29,35) as compared to present work. Further, phosphorus spheroidizes and isolates the pores inhibiting the diffusion path for steam through pore net work as already discussed in section 4.1. However, the oxidation and diffusion of oxygen continues similar to that in case of cast and wrought materials.

In a further study (28), it was again found that mass gain increased as the interconnected porosity increased. Higher the amount of interconnected porosity longer was the time required for saturation of oxidation. In that study (28) saturation time required varied between 50 to 90 minutes for porosity of 10.5 to 15 %. The lower saturation time required in the present investigation (Figs. 3.41-3.65) of the order of 45 to 60 minutes is due to lower amount of interconnedted porosity in the present investigation. For continued oxidation, it is necessary that steam should be able to pass freely through the interconnected pore network. With increasing Cu, MCM and MVM (Figs. 3.92 c, 3.93 b,

3.94 b, 3.129 d, 3.130 b and d, 3.132, 3.142 c and d, 3.144 d and 3.147) contents, the volume as well as width of pores increase. Therefore in compacts containing lower amount of such alloying elements (Figs. 3.91 b and c, 3.93 c, 3.96 b, 3.128, 3.130 a and c 3.142 a and b, 3.143 a and 3.145 a and c) or compacts containing higher amount of P, Ni or Mo (Figs. 3.103 b, 3.115 a and 3.118 c) the surface pores will be saturated with Fe_3O_4 easily during oxidation and will isolate the interconnected pores within the compact from coming in contact with steam and the oxidation rate will decrease.

After saturation, it can be assumed that all the surface pores are filled with oxide and oxidation occurs mainly at the external surfaces by outward movement of iron cations and/or inward movement of oxygen anions through the oxide film similar to the case of solid material. In this regime, inspite of increased surface area in compacts containing any of the alloying elements, the oxidation rate is seen to decrease (Figs. 3.41-3.65) and follow the expected trend. Hammer and Vannerberg (21) have explained the decrease in oxidation rate with reference to weakening of the adhesion between the oxide and iron rich in alloying elements.

4.3.2 Effect of temperature

Higher steam oxidation temperature generally gave higher weight gain and higher increase in hardness of steam treated samples (Figs. 3.41-3.90). It has been reported (29) that extent of pore closure and increase in hardness is strongly dependent on temperature. After treatment at 450°C, specimens of high density predominantly attain slightly higher ultimate hardness values than specimens of low density. But at 600°C, low density attain higher hardness than those of higher density. Optimum results in respect of hardness and definition of oxide layers were found in the present case between 500 to 550°C (Figs. 3.67-3.69, 3.72-3.74, 3.77-3.79, 3.82-3.84, 3.87-3.89, 3.93-3.95, 3.104-3.106, 3.47-3.49, 3.131-3.133 and 3.145-3.147). It has been reported (29) about the existence of αFe_2O_3 in the samples treated at higher temperature particularly 600°C. Thus, the slight increase in hardness due to higher steam oxidation temperature used is due to different types of oxides of iron, specific effects of alloying elements on formation of oxides or phase transformations occurring at a particular temperature and precipitation hardening effect to be discussed later. It is already explained in the previous section that oxidation by steam is a diffusion controlled

process and the pore closure will occur at a slower rate at low temperature (450°C) than it does at higher temperature. However at a steam treatment temperature of more than 527°C, little or no benefit in hardness observed in case of Cu, Ni or Mo-containing compacts is perhaps due to conversion of magnetite into other types of oxides of iron during steam treatment on cooling from steam treatment temperature which compensates for improvement in bulk hardness due to higher steam treatment temperature. From iron-oxygen equilibrium diagram (55) it can be seen that only Fe_3O_4 is stable below 570°C. Although, there is a chance for any FeO formed at higher temperature to be converted into Fe_3O_4 during slow cooling from steam treatment temperature (72), this was not the condition in our experiment since samples after steam oxidation was cooled at fast rate. Thus, it is quite likely that some FeO might have remained in steam oxidized samples lowering the hardness which was not compensated for by precipitation hardening or phase transformation reactions. Franklin and Davies (1) have studied the influence of steam treatment at 520 and 650°C and demonstrated that at 650°C very rapid oxidation occurred but, because of surface sealing, a lower total oxide content was achieved after long treatment times than is normal at lower temperature. Such an observation

was noticed indirectly in case of PNC based powder compacts as discussed in section 4.1. This explains the occasional lowering of weight gain and hardness in samples steam treated at higher temperature (Figs. 3.45, 3.50, 3.55, 3.60, 3.65, 3.70, 3.75, 3.80, 3.85 and 3.90). However, the increase in hardness at higher temperature of steam treatment i.e. 550 and 600°C e.g. in case of MCM and MVM- containing compacts is due to transformation of retained austenite into massive martensite (Fig. 3.140 c) and/or oxidation of easily oxidizable alloying elements Mn, Cr and V. However, it is difficult to streamline the individual contribution of each effect and arrive at cummulative benefit because of complexity of composition and the results obtained are only of technological relevance.

4.3.3 Effect of alloying elements

All the systems of sintered alloys contain P and C. The effect of phosphorus in spheroidizing the pores is similar to such effects produced in PNC based powder compacts as already discussed in section 4.1.2. However, higher amount of phosphorus i.e., 0.8 % has been used in the present investigation. From various microstructures (Figs. 3.91 a - 3.95 a) it appears that upto 0.8 % P is dissolved in iron and the structure is single phase ferritic.

Phosphorus was generally found to increase the size of grains (Figs. 3.92 a and 3.95 a) in sintered compacts and the grain size is not affected by steam oxidation in the temperature range of 450-600°C. The increase in grain size of iron-P sintered compact after adding upto 0.8 % P is in agreement with results of Weglinski and Kaczmar (59). The grain size obtained in case of Fe-P sintered compact in the present investigation (Fig. 3.92 a) is in qualitative agreement with recent results of Lund (73). From free energy vs temperature diagram (74) (Fig. 4.1) the free energy of formation of phosphorus oxide (P_2O_5) is slightly more negative (- 104 to -110 kJ/mole) as compared to that of Fe_3O_4 (-100 to -106 kJ/mole). However, the small amount of P in the range of 0.3 to 0.8 % is in the form of solid solution and hence uniformily distributed, chances of oxidation of phosphorus or its loss is negligible. Moreover, after a layer of oxide is formed, passage of steam in the interior of the compact is restricted, particularly because of spheroidal and isolated pores. This was confirmed through chemical analysis of sintered and steam oxidized compacts which showed P-content of 0.27 ± 0.05 and 0.76 ± 0.04 % P in 0.3 and 0.8 % P-containing compacts. Similar change of P-content has been observed in other investigation (59).

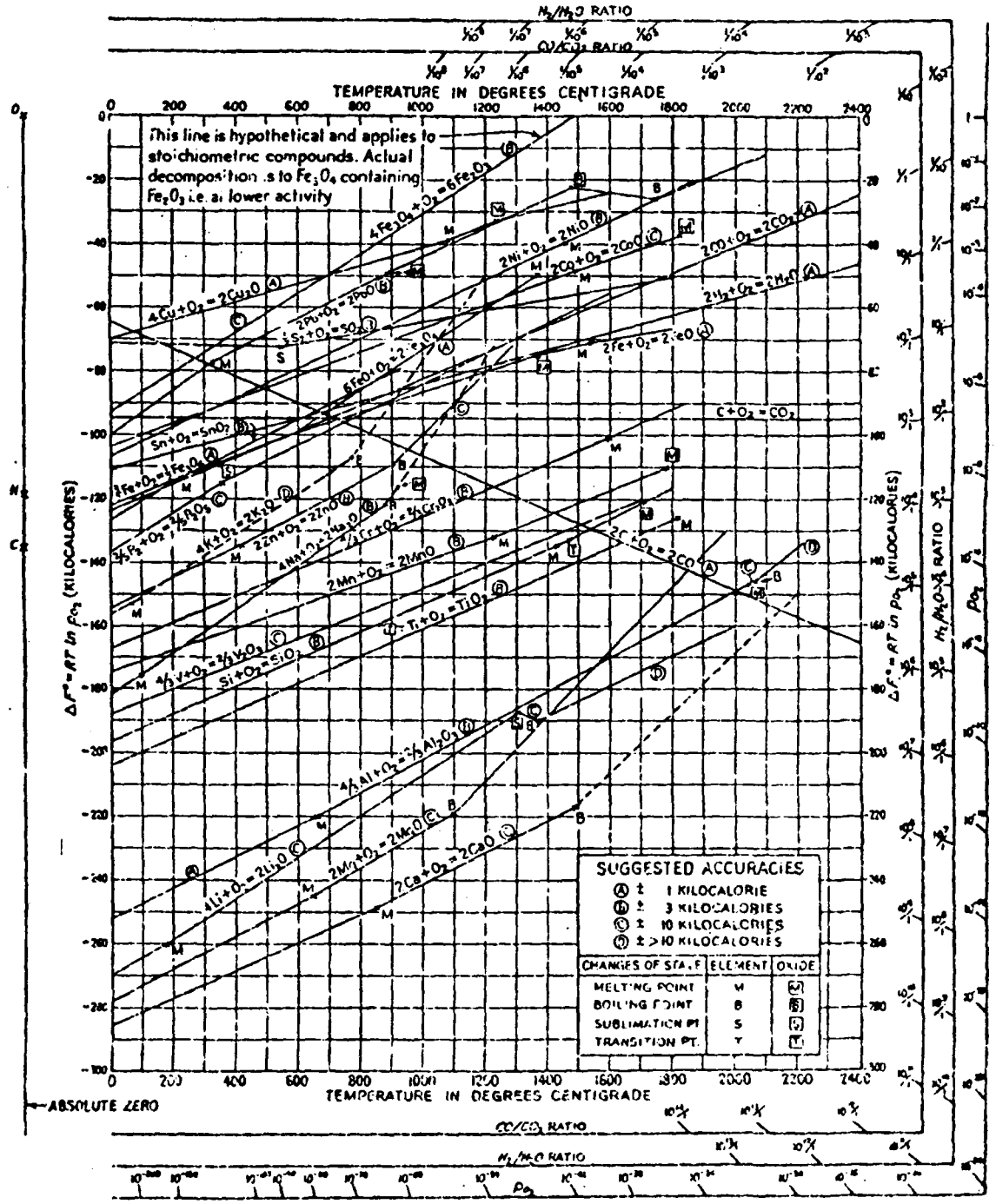

FIG. 4·1 The standard free energy of formation of many metal oxides as a function of temperature. [*From F. D. Richardson and J. H. E. Jeffes, substantially as in J. Iron Steel Inst.* 160, 261 (1948).]

4.3.3.1 Effect of carbon

There should not be any effect of adding or increasing C-content on steam treated weight gain or hardness of compact. The hardness benefit achieved by C-content on sintered specimens should be carried over in case of steam treated samples (Figs. 3.41-3.90). The marginal increase in hardness of steam treated samples is due to austenite stabilization by alloying elements and its consequent transformation into higher hardness constituent during steam oxidation at temperatures of 450-600°C (Figs. 3.66-3.90). This result is particularly more evident in case of MCM and MVM-containing compacts. There is no chance of C- loss during steam oxidation at least in the interior of the compact (Fig. 3.91, 3.96). This is supported by free energy of formation data for CO and CO_2 (-94 to -84 KJ/mole) against for Fe_3O_4 (-106 to -100 KJ/mole (74, Fig. 4.1), at the steam oxidation temperature used. This is in disagreement with the observation of Lund (75) who has stated that due to reaction with iron oxide, some carbon was removed from compacts of Atomet 28 green powder compacts. He (75) found that weight per cent of carbon decreased from 0.105 to 0.086 and 0.062 % after heating in helium at 500 and 600°C respectively. He (75) further found that compacts heated at 600°C actually showed a net weight

decrease of upto 0.1 %. His findings has not been confirmed by any other worker and is not supported by literature (74). Even if his findings are assumed to be correct based on presence of oxides in the powder mass, there is no chance of oxides being present in sintered compacts under D.A. However, oxides do form during steam treatment operation but the possibility of exchange reaction is not supported by thermodynamic consideration (74).

4.3.3.2 Effect of copper

The gain in weight of PASC-Cu-C sintered compact with increasing treatment times, is in general, similar to that observed in case of PNC-Cu compacts (Figs. 3.2, 3.41-3.45). Lower gain in weight is due to higher sintered density and lower amount of interconnected porosity as already discussed in section 4.3.1.

The variation of hardness for such compacts is also similar to PNC-Cu compacts (Figs. 3.7, 3.8 and 3.66-3.70). Maximum in hardness is obtained after 60 minutes at 527°C in contrast to 30 minutes at 500°C for PNC-Cu (Figs. 3.7, 3.8 and 3.68). This is probably due to faster cooling rate achieved under industrial furnace and retention of Cu and P in solid solution which perhaps precipitates on ageing

at steam oxidation temperature. Precipitation reaction requires some time and it is noted that higher is the steam oxidation temperature, generally lower is the time required for saturation in weight gain or hardness (Figs. 3.45 and 3.70). Precipitation reaction is generally enhanced by higher temperature. A large increase in weight gain at 600°C after adding 0.3 % C and 1 % Cu may be due to formation of FeO. The fact that maximum benefit in hardness occurs at steam oxidation temperature of 527°C (Fig. 3.68) and Cu is found to be more effective in enhancing steam treated hardness is in agreement with the results of Phadke (27). Higher hardness of PASC based powder compact (Fig. 3.66-3.70) as compared to PNC based powder compact (Figs. 3.7 and 3.8) is perhaps due to combined action of increase in sintered density, higher cooling rate under industrial sintering atmosphere of dissociated ammonia; about 2-3 times more than the cooling rate recommended by Smith and Palmer (76). However, no precipitates are observed under optical microscope or SEM upto the magnification used (Figs. 3.91-3.100).

Hardness of compacts steam treated at 600°C is lower than at 527°C (Figs. 3.68 and 3.70) and oxide layers were not uniform and well defined and often spalled off.

It has been found (21) that in case of Fe-Cu alloy, at 500°C, oxidation characteristics were same as that of pure iron, but at 625°C the oxide film cracked on cooling. It has been found (77,78) that with the formation of α phase the lattice parameter of bcc Fe-Cu solid solution decreases (79). The resulting volume shrinkage may lead to formation of cracks at the oxide-metal interface and decreases adhesion.

Microhardness value of higher Cu- or P- containing compacts are generally higher than lower P or Cu- free compacts (Table III.3.3) is also because of precipitation hardening effect as already discussed above. This phenomena of age-hardening is further confirmed indirectly by the fact that increase in C content hardly affects steam treated hardness (Figs. 3.66-3.70).

X-ray diffraction of oxides did not show presence of oxides of Cu. This is supported by higher free energy formations of Cu oxide i.e. -55 to -50 KJ/mole (74). Similar phenomena of Cu not affecting chemical nature and the total amount of oxide has been observed by Fedrizzi et al. (90).

4.3.3.3 Effect of nickel

The increase in mass of PASC-Ni-C sintered compact

with increase in steam oxidation period or temperature or with C or P contents are qualitatively similar to such effects observed in case of PASC-Cu-C compacts (Figs. 3.41-3.50). Effect of increasing Ni- content is invariably to decrease the weight gain which is due to densification produced by Ni- addition.

Literature (60) reports that in case of iron-nickel system containing 1 % or more of Ni γ phase forms at about 840°C or at lower temperatures, which is stable upto 1240°C. Thus, at the sintering temperature of 1120°C used in this study, nickel forms with iron austenite and liquid phase is not available (80) since phosphorus has already done its job of spheroidization by transient liquid phase and ferrite stabilization. This fact makes the diffusion of Ni into iron much more difficult, e.g. diffusivity of Ni in iron is $6 \times 10^{-12} cm^2/sec.$ at 1120°C (81, 82). However, the addition of P to binary Fe-Ni alloy stabilizes the ferrite phase and causes an increase in diffusion coefficient (83). This increase in sintered density is the reason for lower gain in mass of PASC-Ni-C steam oxidized compact.

The increase in steam treated hardness due to Ni-content (Figs. 3.71-3.75) is probably due to transformation of retained austenite into massive type of martensite (Figs.

3.101-3.109) which goes on increasing with increase in oxidation temperature to at least 527°C (Figs. 3.117-3.119). Reduction in steam treated hardness of samples oxidized at 600°C seems to be due to tempering effect. There is no reported work (till-to-date) on the steam oxidation of even binary Fe-Ni sintered compact. The results obtained are of industrial importance since it is established that pore sealing and surface hardening of PASC-Ni-C sintered compact is possible without loss of P,C or Ni with improvement in hardness of the order 30-80 HV10 over as sintered hardness. Greater extent of oxidation in Ni-containing compacts as compared to Cu-containing compacts (Figs. 3.97-100 and 3.110-3.113) is perhaps due to irregular and non-spherical nature of pores. Because of more effective austenite stabilization by Ni as compared to Cu and solid state sintering generally heterogenous structures are obtained in case of Ni-containing compacts (Figs. 3.101-3.109). Ni was not oxidized during steam oxidation at the steam treatment temperature used.

4.3.3.4 Effect of molybdenum

Effect of Mo on weight gain and hardness improvement on steam oxidization is in general similar to such effects in C- free PNC based powder compacts (Figs. 3.3, 3.9, 3.51-

3.55 and 3.76-3.80). Higher steam treated hardness is due to more effective age hardening phenomena because of faster cooling rate achieved in industrial furnace and consequent retention of Mo and P in solid solution which precipitates on steam oxidation. The slightly longer saturation time required as compared to Cu or Ni system for attaining maximum hardness is probably due to retention of higher amount of P and Mo in solution due to faster rate of cooling from sintering which requires longer incubation period for precipitation (Figs. 3.76-3.80). However, one significant point to note is that saturation in mass gain and hardness is achieved simultaneously (Figs. 3.51-3.56 and 3.76-3.80) which is advantageous from the point of view of combined effect of oxidation and age-hardening (28). Although there is no data available in literature on the steam oxidation of Fe-Mo system, the results are important from consideration of engineering utility. It is demonstrated from the present study that PASC-Mo-C sintered compacts give best combination of uniformity and definition of oxide layer with hardness. The mixed type of microstructure (Figs. 3.123-3.126) is due to varying effects of P, Mo and C on phase stability at the steam oxidation temperature.

4.3.3.5 Effect of MCM

In case of MCM-containing compacts the higher rate of oxidation as compared to Cu, Ni or Mo- containing compacts, in the initial period of oxidation (Figs. 3.56-3.60) is due to combined effect of lower sintered density and irregular pore morphology (Figs. 3.127-3.137). MCM added in the present investigation is upto 2 mass % which corresponds to actual alloy contents of 0.41 mass % each of Mn, Cr, Mo and 0.14 % C. Of the various constituents in MCM powder, literature (71,65,84-87), report that Mn gives rise to shrinkage in iron compacts, Mo to growth when added in amounts of less than 1 %, Cr to growth at sintering temperatures of 1050-1200°C. However, the overall effect of MCM addition in iron (84-87) and P-containing iron (54) is to produce growth and the pores are generally irregular in shape. This seems to be the reason for higher weight gain in MCM-containing compacts. The effects of P or C in affecting extent of oxidation and on sharpness and definition of oxide layers are not very much different from such effects in other systems as already discussed (Figs. 3.41-3.60 and 3.127-3.137). The decrease in weight gain at steam oxidation temperature of 527°C (Fig. 3.58) is probably due to formation of stoichiometric Fe_3O_4 and oxides of other elements inhibiting the passage of steam further in the

body of the compact. This is further supported by the fact that time required for saturation in weight gain is shorter at higher temperature of oxidation (Figs. 3.57-3.60). From free energy-temperature diagram (Fig. 4.1), Mn and Cr have higher affinity for oxygen. Weak peaks corresponding to oxides of Mn and Cr were observed under X-ray diffraction analysis. Higher values of microhardness obtained in case of MCM-containing compacts may be due to the presence of mixed oxides (Table III.3.3).

There occurs observable increase in hardness of steam treated compacts with increase of C from 0.3 to 0.6 % (Fig. 3.81). This is probably due to austenite stabilization of C in conjunction with Mn and consequent transformation into Bainite and Martensite (Figs. 3.130-3.132 and Figs. 3.135-3.141). The increase in hardness due to formation of some mixed carbides may not however be ruled out. This is supported by the fact that some big pores are observed in case of compacts containing higher MCM and C (Fig. 3.129 d). Some of the hard phases might have been removed during grinding and polishing. Non-uniform and mixed type structures are observed in higher MCM-higher C containing compacts (Figs. 3.131-3.133), particularly at higher steam oxidation temperature (Figs. 3.134).

There is one difference between steam treated hardness of PNC-MCM and PASC-MCM-C sintered compact. There occurs a saturation in hardness values of PASC-MCM-C sintered compact, although time required for saturation is slightly higher as compared to other systems (60-75 minutes) depending on alloy composition and steam oxidation temperature (Figs. 3.81-3.85). This is due to higher sintered density and regular and spheroidal powder particles of atomized powder which persist in sintered structure as already discussed in section 4.3.1 (29).

4.3.3.6 Effect of MVM

The effect of MVM on weight gain and sharpness and definition of oxide layer is more or less similar to the effect of MCM addition (Figs. 3.55-3.60 and 3.61-3.65). This can be understood from the fact that MVM also contains Mn and Mo and V instead of Cr. The effect of increasing C or P on weight gain of MVM- containing compacts is also similar to such effects in case of MCM- containing compacts. The lower level of hardness achieved on steam treatment in case of MVM-containing compacts as compared to MCM- containing compacts may be due to loss of vanadium. The free energy of formation of Vanadium oxide is lowest among all the alloying elements used in the present investigation

(Fig. 4.1). The X-ray diffraction analysis did not show any peak corresponding to any Vanadium oxides which probably supports the loss of V by volatile oxides.

Microstructures and SEM pictures are also similar in terms of heterogeneity and similar type of phases in MVM and MCM- containing compacts (Figs. 3.127-3.154). It appears here also that some of the hard and brittle phases have been removed during grinding and polishing (Fig. 3.151-3.154). The SEM picture have been identically taken on regions of large pores otherwise the structures were similar to those of MCM containing compacts. Microhardness values (Table III.3.3) into two cases are also similar and higher than compacts containing other alloying elements.

4.4 GENERAL DISCUSSION

Out of the various alloy systemsused for steam oxidation in the present study weight gain is Mo → Ni → Cu → MVM → MCM in increasing order. Hardness benefit is Ni → Cu → Mo → MVM → MCM in the increasing order. Sharpness and definition of oxide decreases in the order Mo → Cu → Ni → MCM → MVM. The optimum steam oxidation temperature in respect of hardness benefit, sharpness and definition i.e. uniformity of oxide layer, appears to be generally

527°C with occasional variation to 500 or 550°C. Generally, saturation time required decreases with increase in steam oxidation temperature. However, a reasonably narrow range of 45 to 60 minutes of saturation time required is observed in majority of steam treatment conditions and alloy systems from consideration of weight gain and maximum hardness achieved. Similar behaviour has been observed by Molinari et al. (89) who found little gain in weight of hematite or magnetite at a sintered density of 7.0 Mg m^{-3} when compacts made from pure iron sintered at 1150°C for 90 minutes in endogas were steam treated at 500°C. Type of powder used has not been indicated. In fact, the kinetics curves for all systems studied at the density levels are parabolic in nature (Figs. 3.41-3.65). Precipitation hardening was found to be effective mainly in case of Mo and Cu- containing compacts and the phenomena appeared to increase with increase in temperature. The reasons for all such behaviour has been explained above in various sections. Optimum steam treatment temperature for sintered iron having a density of 6.4 Mg m^{-3} (35) was found to be 527°C. The situation regarding composition, powder type, and the resulting microstructures of the sintered compact is quite complex and any mathematical description is impossible regarding weight gain, hardness, pore sealing, oxide thickness and adherense ; unless only oxide

formed is Fe_3O_4, porosity is all one type particularly interconnected. However some general discription about oxidation of iron which is the main oxide formed can be given.

4.4.1 Adherence of oxide

According to Pilling and Bedworth (F. Mazza - corrosion' Enciclopedia delta chimica vol. 4, USES Firenze 1975), the parameter from which the adhesion depends is given by

$$X = \frac{[Mox].\ \rho m}{n.Mm.\rho ox}$$

where [Mox] is the molecular weight of oxide, ρm is the density of the metal, n is the number of atoms of metal in the oxide molecule, [Mm] is the atomic weight of the metal, ρox is the density of oxide.

When $X < 1$, the oxide is porous, and not protective. If $X > 1$, but not $>> 1$, the layer results to be compact and well adherent, without any strong stresses of compression that otherwise could cause break. In the case of mixed iron oxide, the parameter of Pilling and Bedworth is

$$(X)_{Fe_3O_4} = \frac{231.55 \times 7.86}{3 \times 55.8 \times 5.2} = 2.086$$

and good adherence of oxide is fully demonstrated. In addition, the ratio found is very near that of chromium oxide, from which the resistance to corrosion of stainless steels depends.

It has been stated (82) on the basis of experience acquired in production and of some systematic investigation that parts produced with atomized powders show percentage variations of weight, porosity and hardness greater than those obtained from reduced powders. Small amounts of alloying elements added to metal powders complicates the effect of porosity. Thus, any generalization is possible in specific alloy system only for a particular type of powder and under specific conditions of sintering only.

CHAPTER 5

CONCLUSION

Sintered powder compacts based on PNC have been compacted at 600 MPa pressure and sintered in hydrogen under laboratory conditions using slower heating and cooling rates while those based on PASC powder compacts contain C also and lower amount of alloying elements and were sintered in dissociated ammonia under industrial conditions. Thus, the conclusions can not be general and hence have been divided into three parts similar to the results and discussion.

Part I : Steam oxidation of sintered PNC based powder compacts

1. Air oxidation of sintered ferrous alloys gives non adherent and inhomogenous layer.

2. Steam treatment of PNC, PNC-Cu, PNC-Mo, PNC-MCM, PNC-Ni-Cu, PNC-Mo-Cu and PNC-MCM-Cu sintered compacts can be successfully done at 500°C for times varying between 30 to 75 minutes to seal the surface pores and improve the hardness values by 100-200 HV.

3. In general, weight gain with increasing treatment

times reaches a constant value. However, the variation of weight gain with treatment times is parabolic in nature.

4. Copper addition to iron or PNC powder compacts increases the thickness of oxide layer. Weight gain of the order of 30 to 40 gm^{-2} is obtained after treatment times of 30-60 minutes. An increase in hardness of 120 HV is achieved after steam oxidation for 30 minutes. Variation of hardness with treatment time reaches a maximum at about 30 minutes of treatment times. Increase in hardness of sintered PNC-Cu compacts appears to be due to combined effect of oxidation and age hardening.

5. Molybdenum addition to PNC powder compacts decreases the thickness of oxide layer. Gain in weight of sintered samples is of the order of 20-30 gm^{-2} after treatment times of 60-70 minutes. Hardness increases significantly and an increase in hardness of around 120 HV is obtained after treatment times of 30 to 60 minutes. Such a large increase in hardness also appears to be due to combined effect of steam treatment and age-hardening phenomena due to both molybdenum and phosphorus. Hardness reaches a maximum after 30 to 60 minutes of steam oxidation time.

6. MCM addition in PNC premixes increases weight gain of upto 50 gm^{-2} after treatment times of 60 minutes. In case of lower P-containing compacts the variation of hardness with steam oxidation times reaches a constant value after treatment times of about 60 minutes. However in higher P-containing compacts, hardness in general, increases with increasing steam oxidation time. Hardness increase of 120 to 180 HV is achieved after steam oxidation of upto 120 minutes in PNC-MCM sintered compacts.

7. The effect of copper on steam oxidation behaviour and steam treated properties of PNC-Ni-/Mo/MCM sintered compacts is in general similar to that in case of plain iron or PNC-Cu sintered compacts. Nickel in general produces heterogenosity in sintered ferrous alloys and gives non-uniform oxidation.

8. Phosphorus in sintered ferrous alloys inhibits diffusion path for oxygen and produces relatively uniform and well defined oxide layer. Phosphorus gives rise to age-hardening phenomena in sintered iron alloys at the steam oxidation treatment temperature used i.e. 500°C.

Part II : Sintered properties of PASC powder compacts

1. Higher phosphorus content, generally gives improved densification and mechanical properties after sintering of PASC-C-X (X stands for 1 to 2 % Cu, Ni, Mo, MCM or MVM) powder premixes at 1393 K for 1.8 ks in cracked ammonia. However, improvement in properties are not significant enough to justify the use of higher amount of phosphorus i.e. upto 0.8 % particularly in view of brittle phosphide formation.

2. Higher amount of C, in general, improves strength properties but deteriorates ductility. Graphite loss under the sintering conditions used in the present investigation is more or less constant i.e. 0.2 $\pm$ 0.04 % and is independent of the alloy systems. Like phosphorus, increased amount of C addition to 0.6 % in PASC-X powder compacts cannot be justified for improvement of mechanical properties under the sintering conditions used in the present study.

3. Copper addition to PASC-C sintered compacts improves strength properties but deteriorates ductility.

4. Nickel addition upto 2 % , in general, gives rise to growth in PASC-C compacts after sintering.

5. Molybdenum, in general, improves densification and strength properties but decreases ductility of PASC-C sintered compacts.

6. Both MCM and MVM additions to P-containing sintered steels produce growth but improve strength properties and reduce ductility. By use of phosphorus, it is possible to sinter steels containing MCM and MVM powders at lower sintering temperature of 1393 K for short sintering period of 1.8 ks without much deterioment to mechanical properties.

7. By addition of 1 to 2 mass % Cu, Ni, Mo, MCM or MVM and 0.3 to 0.6 mass % C to PASC30 or PASC80 powder premixes, it is possible to obtain products with UTS, YS and El % values of 330 to 650 MPa, 200 to 450 MPa and 3 to 12 % respectively at sintered density of 7.0 to 7.2 Mg/m^3 after sintering at 1393 K for 1.8 ks in cracked ammonia atmosphere of dew point 240 K. Copper seems to be the best among all the alloying elements added for improving mechanical properties. Apart from Cu, all the other alloying elements are almost of equal value in improving mechanical properties of PASC30 or PASC80 powder compacts containing

0.3 to 0.6 % C under the compaction and sintering parameters used in this study.

Part III: Steam oxidation of sintered PASC powder compacts

1. Steam treatment of PASC-C-X sintered powder compacts can be successfully done at 450 to 600°C for times varying between 45 to 75 minutes to seal the surface pores and improve the hardness values by 100-200 HV10 depending on alloying elements added. Open channels and interconnected pore networks are also blocked.

2. In general, weight gain with increasing treatment times reaches a constant value. However, the variation of weight gain with treatment times is parabolic in nature.

3. With the addition of P the pores becomes spheroidal. Higher amount of P- i.e. 0.8 % dissolved in iron and the structure is single phase ferritic. Phosphorus generally increases the size of grains in sintered compacts and the grain size is not affected by steam oxidation in the temperature range of 450-600°C. Higher amount of phosphorus decreases the propertion of pearlite.

4. With the addition or increasing amount of C-content there is no effect on steam treated weight gain. The hardness achieved by C-content on sintered properties is generally carried over in case of steam treated samples.

5. Copper addition to PASC-C compacts increases the thickness of oxide layer. Weight gain of the order of 25 to 38 gm^{-2} is obtained after treatment times of 45 to 120 minutes at 450 to 600°C. An increase in hardness of upto 200 HV is achieved after steam oxidation times of 45-60 minutes, at 450-600°C. Variation of hardness with treatment time reaches a maximum at about 60 minutes of treatment times.

6. Nickel addition to PASC-C compacts gives a uniform and compact oxide layer. Increasing the steam oxidation time increases the amount of oxidation, and the oxide layer becomes slightly non-uniform. With increasing steam oxidation temperature upto 527°C the oxide layer becomes more uniform, thick, compact and dense. Weight gain of the order of 16 to 28 gm^{-2} is obtained after steam oxidation for 45 to 120 minute at 450-600°C. An increase in hardness of upto 150 HV10 is achieved after steam oxidation for 45-60

minutes at 450° to 600°C. Variation of hardness reaches a maximum at about 60 minutes of the treatment times.

7. Molybdenum addition to PASC-C compacts gives a thin but uniform oxide layer. Increase in oxidation period gives increased oxidation both at the surface and in the interior. Increase in oxidation temperature upto 527°C gives relatively uniform oxide layer. Weight gain of the order of 18 to 25 gm^{-2} is obtained after steam oxidation for 45 to 120 minutes at 450-600°C. An increase in hardness of upto 180 HV10 is achieved after steam oxidation for 45-60 minutes at 450-600°C. Variation of hardness reaches a maximum at about 45-60 minutes of the treatment times.

8. With MCM addition to PASC-C compacts there is considerable oxidation; oxidation also occurs within interior of the sample. Increase in oxidation time also increases the extent of oxidation and makes the oxide layer non-uniform. Increase in temperature of upto 527°C gives uniform structure both in the matrix and the scale. Weight gain of the order of 30 to 38 gm^{-2} is obtained after steam oxidation for 45 to 120 minutes at 450-600°C. An increase in hardness of upto

195 HV10 is achieved after steam oxidation for 45-60 minutes at 450-600°C.

9. MVM addition to PASC-C compacts gives considerable oxidation but the oxide layer formed at the surface is non-uniform. Longer oxidation period results into increased oxidation and the thickness of oxide layer increases. Increase in oxidation temperature brings about heterogeneity in the structure of the matrix as well as oxide layer. Weight gain of the order of 18 to 38 gm^{-2} is obtained after steam oxidation for 45 to 120 minutes at 450-600°C. An increase in hardness of upto 190 HV10 is achieved after steam oxidation for 45-60 minutes at 450-600°C. Variation of hardness reaches a maximum at about 45-60 minutes of the treatment times.

10. The steam treated oxide layers are hard, tenaceous and adherent and do not peel off during grinding and polishing.

11. Optimum steam oxidation temperature in respect of hardness benefit, sharpness and uniformity of oxide layer is generally 527°C with occasional variation to 500 or 550°C. 45 to 60 minutes of saturation

time is required in majority of steam treatment conditions and alloy systems from consideration of weight gain and maximum hardness achieved.

12. By X-ray diffraction studies it is confirmed that the principal product formed during steam treatment at temperature used was Fe_3O_4. Copper and phosphorus were not oxidized. Some weak peaks corresponding to oxides of Cr and Mn were observed in MCM containing compacts.

REFERENCES

1. P. Franklin and B.L. Davies : Powder Metall., Vol. 20, No. 1, 1977, p. 11.
2. F.V. Lenel : Powder Metallurgy (ed., J. Wulff), 1942, P. 512, Metals Park, Ohio (ASM).
3. T.H. Sanderson : Heat Treat. Met., Vol. 4, 1975, p. 109.
4. Steam Treated Properties of Sintered Steel, Technical data sheet 1031. A.O. Smith Inland Inc., Powder Metallurgy Division.
5. J.H. Eggleston and F.L. Spangler : SME Technical paper CM 72-812.
6. F.W. Regal : Engg. Digest, Vol. 24, No. 11, 1963, p. 91.
7. R. Meyer : Treatment Thermique, Vol. 30, 1967, p. 91.
8. Marvin Feir : Post-treatment of P/M parts, SAE Technical Paper Series 800308, 1980.
9. G. Herbsleb : Stahl Eisen, Vol. 81, 1961, p. 1420.
10. I.M. Fedorchenko : Poroshkh, Metall. Vol. 3, No. 6, 1963, p. 78.
11. G. Hoffmann : Anticorros. Methods, Mater., Vol. 16, No. 8, 1969, p. 16.
12. K. Volenik, H. Volrabova, J. Neid, M. Seberini and

J. Cirak : Powder Metallurgy, Vol. 21, No. 3, 1978.

13. S.S. Kurglikov and O.T. Rudyagina : Zasch Met., Vol. 13, 1977, p. 555.

14. W. Zelkowski and W. Miggal : Proceedings of the Fifth Polish Conference on Powder Metallurgy Poznan, Vol. 1, Oct. 1979, p. 317.

15. H. Volrabova et al. : Koroze Oehr, Mater, Vol. 24, No. 1, 1980, p. 10.

16. A. Mechkov, A. Popov and U. Konstantinova : Proceedings of the 6th Int. Conference on Powder Metallurgy : BRNO 10-12, Nov., 1982.

17. B.J. Sunter and B.D. Cosh : Powder Metall., Vol. 17, No. 34, 1974, p. 319.

18. Anon : Ind. Finish Surface Coatings, Vol. 26, No. 31, Oct. 1974, p. 14.

19. R.H. Ketelhohn : Ind. Heat., Vol. 41, No. 7, 1974, p. 36.

20. Anon : Metal Progress, Vol. 10, No. 4, 1972, pp. 72. 74-75.

21. B. Hammer and Vannerberg : Scand. J. Metallurgy, Vol. 3, 1974, p. 123.

22. L. Harrison and R.H.G. Dixon : Powder Metall. Vol. 9, 1962, p. 24.

23. T. Watanabe : Rep. Govt. Ind. Res. Inst. Nagoya, Vol. 7, 1958, p. 105.

24. A. Stern, L. Levin and S.F. Durnfeld, Intl. J. Powder Metallurgy, Vol. 8, 1972, p. 20.

25. V.B. Phadke and B.L. Davies : Powder Met. Int., Vol. 9, No. 2, 1977, p. 64.

26. V.B. Phadke and B.L. Davies : Powder Met. Int., Vol. 9, No. 4, 1977, p. 168.

27. V.B. Phadke : Powder Met., Vol. 24, No. 1, 1981, p. 25.

28. V.B. Phadke : Powder Met. Int., Vol. 13, No. 1, 1981, p. 33.

29. K. Razavizadeh and B.L. Davies : Powder Metallurgy, Vol. 22, No. 4, 1979, p.187.

30. K. Razavizadeh and B.L. Davies : Wear, Vol. 69, 1981, p. 355.

31. K. Razavizadeh and B.L. Davies : Powder Metallurgy, Vol. 25, No. 1, 1982, p. 11.

32. N.G. Schmahl, H. Baumann and H. Schencki, Arch. Eisenhuttenwes, 29, 1958, 83.

33. Met. Powder Rep. Vol. 37, No. 10, Oct. 1982, p. 527, 529-530.

34. E.M. Fainschmidt et al. Izv. Akad Nank SSR, Met. No. 1, 1982, pp. 102-104.

35. G.F. Bocchini, A. Gallo, I. Montevecchi, La Metallurgia Italania, Vol. 75, No. 3, March 1983, 180-187.

36. Hitoshi Sakai, Toshihide Tsuji, and Keiji Naito, Proceedings JIMIS-3 (1983), pp. 127-134.

37. K.H. Davies, M.T. Simnad and C.E. Birchenall : Trans. AIME, 191, 1951, 889.

38. J. Paidassi, Acta Metal., 4, 1956, 227.

39. D. Caplan, M.J. Graham and M. Cohen : Corros. Sci., 10, 1970, 1.

40. L. Jansson and N. Vannerberg : Oxide Metals 3, 1971, 453.

41. A.S. Camara and W. Keune : Corros. Sci., 15, 1975, 441.

42. R.J. Hussey and M. Cohen : Corros. Sci., 11, 1971, 699.

43. R.J. Hussey and M. Cohen : Corros. Sci., 11, 1971, 713.

44. F.B. Pickering : ISI, P 114, 1968, p. 131.

45. A. Hörnbogen : Trans. ASM, Vol. 55, 1962, p. 719.

46. P. Lindskog, J. Tengzelius and S.A. Kvist : Mod. Dev. in Powder Met., Vol. 10, (Eds. H.H. Hausner and P.W. Taubenblatt), MPIF Princeton, N.J., 1977, p. 97.

47. G. Hoffmann and K. Dalal, Powder Met. Int., Vol. 11, No. 4, 1979, p. 177.

48. Md. Hamiuddin and G.S. Upadhyaya : Powder Met. Int., Vol. 12, No. 2, 1980, p. 65.

49. Md. Hamiuddin and G.S. Upadhyaya : Int. J. Powder Met. and Powder Tech., 16, 1, 1980, 57.

50. Md. Hamiuddin and G.S. Upadhyaya : Powder Metallurgy, 23, 3, 1980, 136.

51. Hoganas Iron Powder Information PM 78-6.

52. Md. Hamiuddin : Science of Sintering 15, 2, 1983, 87.

53. Md. Hamiuddin : Powder Met. Int. 15, 3, 1983, 47.

54. Md. Hamiuddin : Int. J. Powder Met. and Powder Tech., 20, 4, 1984, pp. 343-350.

55. O. Kubaschewski and B.F. Hopkins : Vol. 82, 1962, London, Butterworth.

56. V.J. Linnenborn : J. Electrochem., Soc., Vol. 105, 1958, p. 322.

57. A. Hörnbogen and R.C. Glenn : Trans. Am. Inst. Min. Metall., Vol. 218, 1960, p. 1064.

58. K. Razavizadeh : Ph.D. thesis, 1980, Brunnel University.

59. B. Weglinski and J. Kaczmar : Powder Metallurgy, Vol. 23, No. 4, 1980, p. 210.

60. M. Hansen : Constitution of Binary Alloys, Second Ed., 1958, McGraw Hill Book Co. N.Y. 9958, p. 692.

61. M. Amin, Md. Hamiuddin and G.S. Upadhyaya : Praktische Metallographie, Vol. 19, 1982, p. 403.

62. A.K. Sinha, R.A. Buckley and W. Hume-Rothery : J. Iron Steel Inst., Vol. 205, 1967, p. 195.

63. A.P. Coldren et al. : Trans. AIME, Vol. 230, 1964, p. 1236.

64. Md. Hamiuddin and G.S. Upadhyaya : Powder Met. Int., Vol. 14, No. 1, 1982, p. 20.

65. Md. Hamiuddin and G.S. Upadhyaya : Trans. PMAI, 6, 1979, 57.

66. D. Berner, H.E. Exner and G. Petzow: Mod. Dev. in Powder Met. Vol. 6 (Eds. H.H. Hausner and W.E. Smith), MPIF Princeton 237, 1973.

67. G. Bokstiegel, Stahl and Eisen 79 (1959), 1187.

68. T. Ishimara, T. Yonekura and T. Ishisaki: Sci. Rep. Tokilin Imp. Univ. 15 (1926), p. 81.

69. G. Bockstiegel; Metallurgia ISI/4 (1962), 67.

70. G. Hoffmann and K. Dalal : J. of Materials Technology (Z.F. Werkst off technik), 7, (1976), 393.

71. G. Zapf, G. Hoffmann and K. Dalal : Mod. Dev. in Powder Met. Vol. 10 (Eds. H.H. Hausner and P.W. Tanben blatt), MPIF, Princeton (1977), 129.

72. K. Volenik et al.; Powder Metallurgy, 21, 1978, 149.

73. J.A. Lund, Tensile Flow and Fracture of Iron-Phosphorus compacts, Int. J. of Powder Met. and Powder Tech., 1985, Vol. 21, No. 1, pp. 47-55.

74. L.S. Darken and R.W. Gurry, Physical Chemistry of Metals, McGraw Hill, N.Y., 1953, p.

75. J.A. Lund: Origin of Green Strength in Iron P/M compacts, Int. J. of Powder Met. and Powder Tech., Vol. 18, No. 2, 1982, p. 117-127.

76. C.S. Smith and E.W. Palmer : Trans. AIME, Vol. 105, 1933, p. 133.

77. A. Youke and B. Ralph: Metal Sci. J. Vol. 6, 1972, p. 149.

78. L.M. Brown; Acta Met. Vol. 20, 1972, p. 966.

79. E.A. Lund and A.W. Lawson : Trans. Met. Soc. AIME, Vol. 236, 1966, p. 581.

80. J. Bukowiecki and M. Rusinekozga : Prac. Instytutu. Metali Niezelaznch, Vol. IV, 1975, p. 122.

81. F. Thummler and W. Thoma Z. Metallud. Vol. 60, No. 15, 1969, p. 498.

82. L.E. Svensson, Powder Met. Vol. 17, No. 34, 1974, p.271.

83. T.R. Hayward and J.I. Goldstein, Met. Trans. Vol. 4, No. 10, 1973, p. 2335.

84. G. Zapf, G. Hoffmann and K. Kalal, Powder Met. 18 (55), 1975, p. 214.

85. G. Zapf, G. Hoffmann and K. Dalal, Arch. Eisenhuettenwes, 46, 1975, p. 347.

86. H.J. Retelsdorf, Mod. Dev. in Powder Met. (Eds. H.H. Hausner and P.W. Tauben blatt), MPIF, Princeton, Vol. 10, 1977, p. 155.

87. G. Schlieper, Dr. Ing. Thesis, submitted to universitat Karlsruhe, W.G., Aug. 1979 and Kfk Report No. 2855, IMF1, Kerforschungszentrum, Karlsruhe, W.G.

88. G.F. Bocchini : The influence of porosity on the characteristics of sintered materials, Reviews on Powder Metallurgy and Physical Ceramics Vol. 2, No. 4, 1985, p. 313-359.

89. A. Molinari, L. Fedrizzi, P.L. Bonora, S. De Bortoli, A. Tiziani, Study of the oxide layers obtained by steam

treatment on iron sintered to different densities : Paper presented in the International Conference PM 86 at Dusseldorf, 7-11, 7-1986 in the session Theme Zone 8 : Secondary operations.

90. L. Fedrizzi, A. Molinari, E. Ramons, S. De Bortoli, P.L. Bonora : Influence of copper on the corrosion resistance of steam treated sintered iron. Paper presented in the International Conference, PM 86 at Dusseldorf, 7-11, 7-1986 in the session Theme Zone 8 : Secondary Operations.

SUGGESTION FOR FUTURE WORK

1. Individual contribution due to precipitation hardening and oxidation should be studied for Fe-P, Fe-Mo and Fe-Cu sintered compacts.

2. Corrosion resistance of steam oxidized parts should be evaluated under various atmospheres.

3. Wear resistance and coefficient of friction of steam treated samples should be studied.

4. Fatigue strength of the steam treated sintered ferrous materials should be studied for their use in dynamic applications.

5. Higher magnification under SEM should be used till precipitates are observed in case of precipitation hardening alloy systems and the precipitates should be characterized.

LIST OF PUBLICATIONS

Based on a part of the work presented in this thesis following papers have been published:

1. Effects of dopants on oxidation and steam treatment of sintered ferrous alloys.
   Trans. Powd. Met. Ass. of India, Vol. 10, No. 1, 1983, pp 14-18.

2. Steam treatment of sintered iron alloys containing phosphorus and Transition Metal Carbide Master alloy MCM.
   Trans. Powd. Met. Ass. of India., Vol. 11, 1984, pp 41-50.

3. Effect of ageing and steam oxidation on sintered iron and steels containing phosphorus.
   Presented at 1984 Powder Metallurgy Group Meeting at Harrogate, U.K. from 29-31 Oct. 1984, and Powder Metallurgy, Vol. 29, 1986 (in press).

4. Comparative studies of the effect of alloying elements on sintered properties of steels.
   Communicated to International Journal of Powder Metallurgy and Powder Technology, 1986.